ZooKeys 964: 1–30 (2020)
doi: 10.3897/zookeys.964.51554
https://zookeys.pensoft.net

RESEARCH ARTICLE

A peer-reviewed open-access journal
ZooKeys
Launched to accelerate biodiversity research

Heteroonops (Araneae, Oonopidae) spiders from Hispaniola: the discovery of ten new species

Nadine Dupérré[1], Charlotte Francisco[2], Ella Santana-Propper[2], Ingi Agnarsson[3,4], Greta J. Binford[2]

1 *Technical Assistant, Department of Arachnology, Centrum für Naturkunde, Universität de Hamburg, Germany* **2** *Lewis & Clark College, 0615 SW Palatine Hill Rd. Portland, Oregon, 97219, USA* **3** *University of Vermont, Department of Biology, 109 Carrigan Drive, Burlington, VT, 05405-0086, USA* **4** *Department of Entomology, National Museum of Natural History, Smithsonian Institution, Washington, DC, USA*

Corresponding author: Nadine Dupérré (nadineduperre@gmail.com)

Academic editor: Cristina Rheims | Received 28 February 2020 | Accepted 1 June 2020 | Published 27 August 2020

http://zoobank.org/E93FBE23-0057-4DCB-96C8-A56A41300F6C

Citation: Dupérré N, Francisco C, Santana-Propper E, Agnarsson I, Binford GJ (2020) *Heteroonops* (Araneae, Oonopidae) spiders from Hispaniola: the discovery of ten new species. ZooKeys 964: 1–30. https://doi.org/10.3897/zookeys.964.51554

Abstract

The Caribbean biodiversity hotspot harbors vast reserves of undiscovered species. A large-scale inventory of Caribbean arachnids (CarBio) is uncovering new species across the arachnid tree of life, and allowing inference of the evolutionary history that has generated this diversity. Herein we describe ten new species of *Heteroonops* (Oonopidae, or goblin spiders), from Hispaniola: *H. scapula* **sp. nov.**, *H. jurassicus* **sp. nov.**, *H. aylinalegreae* **sp. nov.**, *H. verruca* **sp. nov.**, *H. renebarbai* **sp. nov.**, *H. yuma* **sp. nov.**, *H. carlosviquezi* **sp. nov.**, *H. gabrielsantosi* **sp. nov.**, *H. solanllycarreroae* **sp. nov.** and *H. constanza* **sp. nov.** The occurrence of the pantropical type species *Heteroonops spinimanus* (Simon, 1891) is reported and new localities are given for: *H. validus* (Bryant, 1948), *H. vega* (Platnick & Dupérré, 2009) and *H. castelloides* (Platnick & Dupérré, 2009). Molecular phylogenies indicate substantial genetic divergence separating these taxa. This work adds to evidence that the depth of diversity in the Caribbean biodiversity hotspot is particularly striking for tiny taxa living in leaf litter.

Keywords

biodiversity hotspot, Caribbean biogeography, Goblin spiders, molecular phylogeny

Introduction

The Greater Antilles islands form the most species-rich landmasses in the Caribbean biodiversity hotspot. These islands serve as exceptional systems for studies of species formation and biogeography (Ricklefs and Bermingham 2008). Our ongoing large-scale inventory of Caribbean arachnids (CarBio) is rapidly uncovering new species across the arachnid tree of life and offering new insight into Caribbean biogeography (e.g., Dziki et al. 2015; Agnarsson et al. 2018; Chamberland et al. 2018; Čandek et al. 2019; Tong et al. 2019; Čandek et al. 2020). Yet the biodiversity of many of these islands, including Hispaniola, remains poorly known, especially with respect to tiny cryptic arthropods, such as oonopid spiders. The family Oonopidae currently includes 1846 species distributed in 113 genera, making it the 8th largest spider family (World Spider Catalog 2020). In 2006, the Planetary Biodiversity Inventory (PBI, 2020) project on Oonopidae was launched. At the time only 459 species of Oonopidae were known (PBI, 2020). In eleven years, the PBI project led to the discovery and descriptions of nearly 1300 new oonopid species, increasing our knowledge of the fauna by 300%. Yet, new species continue to be discovered as new areas are more thoroughly sampled, such as during the ongoing Caribbean arachnid biodiversity inventory (project CarBio).

Oonopidae are small (1.0–5.0 mm) yellow, orange to bright red haplogyne spiders. Most members of this family are found living in leaf litter, but some live in canopies (Fannes et al. 2008, Platnick and Dupérré 2011b) or caves (Chamberlin and Ivie 1938), and some are termite nest inquilines (Benoit 1964) or even ant-mimics (Fannes and Jocqué 2008; Platnick and Dupérré 2011b). Oonopids typically have six large contiguous eyes (Ubick 2005), but some species have only two (Platnick 2000), or lack eyes altogether (Chamberlin and Ivie 1938; Benoit 1964; Baehr and Ubick 2010). Oonopids show other striking morphological features, including some with elongated carapace prongs (Abrahim et al. 2012), clypeal prongs (Platnick and Dupérré 2011a) and various cheliceral and endite modifications (e.g., Kranz-Baltensperger 2012; Tong et al. 2018). But an even more peculiar morphological feature is the occurrence of male palpal asymmetry, extremely rare in spiders (Huber et al. 2007), but found in oonopid genera such as *Escaphiella*, *Paradysderina* (Platnick and Dupérré 2009, 2011c). In *Paradysderina* the left and right male palps are so different that if observed independently, even experienced taxonomists would consider them to belong to distinct species (Platnick and Dupérré 2011c).

Platnick and Dupérré (2009) revised the genus *Heteroonops*, including 14 species, of which 10 were new. The type species of the genus, *Heteroonops spinimanus* (Simon, 1892), is pantropical, while the remainder of the group has a circum-Caribbean distribution, occurring from Mexico to Dominica (Platnick and Dupérré 2009). In 2009, four species were known to occur in Dominican Republic: *Heteroonops castelloides* (Platnick & Dupérré, 2009), *H. iviei* (Platnick & Dupérré, 2009), *H. validus* (Bryant, 1948) and *H. vega* (Platnick & Dupérré, 2009). Here we describe ten new species and report for the first time the presence of the pantropical genotype, *H. spinimanus*, as well as new localities for *H. vega*, *H. castelloides* and *H. validus*. We demonstrate substantial genetic divergence between these species and analyze biogeographic patterns within Hispaniola using mitochondrial phylogenies.

Material and methods

Collections examined

All 66 specimens examined are from the 2012 CarBio expedition to Dominican Republic, unless otherwise noted. They were all found in leaf litter samples that were sifted in the field and either hand sorted, or extracted through Berlese funnels. Specimens are stored at the Natural History Museum in Vermont, USA (UVM); type specimens are deposited at the National Museum of Natural History, Smithsonian Institution, Washington, USA (NMNH, USNMENT). Specimens were roughly sorted in-field and stored in 95% ethanol at -20 °C upon return to the laboratory. Species determination was done through morphological assessment, followed by molecular phylogenetic analyses. Genetic divergences guided further morphological assessment and final species delineation.

Morphological assessment

Specimens were collected and examined in 95% ethanol under a SMZ-U Nikon dissection microscope. A Nikon Coolpix 950 digital camera attached to the microscope was used to photograph all the structures to be illustrated. The digital photos were used to trace proportions and the illustrations were detailed and shaded by referring back to the structure under the microscope. Female genitalia were excised using a sharp entomological needle and submerged in lactic acid to clear internal structures. The structures were photographed and illustrated as explained above. All measurements are in millimeters. For complete morphological description of the genus see Platnick and Dupérré (2009: 17–21). Nomenclatural morphology follows Platnick and Dupérré (2009).

Molecular analyses

DNA extraction was done with the QIAGEN DNeasy Tissue Kit (Qiagen, Inc., Valencia, CA). We sequenced fragments of the mitochondrial Cytochrome c oxidase subunit 1 (COI) and 16S ribosomal RNA (16S), which are typically effective phylogenetic markers at low taxonomic levels for spiders. We amplified COI with LCO1490-2776 and 16S with 16SF and 16SR using standard protocols (see e.g., Agnarsson et al. 2007). PCR products were sequenced at the University of Arizona, Beckman Genomics, or the Smithsonian Institution. Sequences were interpreted from chromatograms using Phred and Phrap (Green and Ewing 2002, Green 2009) within the Chromaseq module (Maddison and Maddison 2020) in Mesquite 3.61 (Maddison and Maddison 2019), with default parameters. The sequences were then proofread by examining chromatograms by eye.

The taxon sampling in our final dataset included mitochondrial sequences for 37 of 38 *Heteroonops* from the Dominican Republic in our dataset (Table 1). We obtained COI data for all 37 of these specimens, and 16S for 32 of 37. Neither CO1 nor 16S amplified from the single representative of *H. solanllycarreroae* sp. nov. The concatenated alignment is 1114 nucleotides.

Table 1.

Species (ND 17)	sex	type?	Locality	Latitude / Longitude	elev m	CO1	16s	GenBank Label	Specimen Name
H. spinimanus	f		DR Beach trail to Cueva del Puente, Parque Nacional del Este	18.32902N, 068.80995W	0	MT636140	MT635438	H._spinimanus_f	H. spin 01-1
H. verruca sp. nov.	m	holotype	DR Cachote Biosphere Reserve	18.09786N, 071.18925W	1200	MT636136	MT635434	H._verruca_n_sp_m1	H. verr 37-1
	f	paratype	DR Cachote Biosphere Reserve	18.09786N, 071.18925W	1200	MT636137	MT635435	H._verruca_n_sp_f1	H. verr 37-2
	m		DR Cachote Biosphere Reserve	18.09786N, 071.18925W	1200	MT636139	MT635437	H._verruca_n_sp_m2	H. verr 37-3
	m		DR Cachote Biosphere Reserve	18.09786N, 071.18925W	1200	MT636138	MT635436	H._verruca_n_sp_m3	H. verr 37-4
H. validus	m		DR Inside cueva del puente, Parque Nacional del Este	18.3816N, 068.8017W	25	MT636112	MT635415	H._validus_m1	H. val 02-1
	f		DR Inside cueva del puente, Parque Nacional del Este	18.3816N, 068.8017W	25	MT636113		H._validus_f1	H. val 02-2
	f		DR Inside cueva del puente, Parque Nacional del Este	18.3816N, 068.8017W	25	MT636114	MT635416	H._validus_f2	H. val 02-3
	m		DR Inside cueva del puente, Parque Nacional del Este	18.3816N, 068.8017W	25	MT636115		H._validus_m2	H. val 02-4
	m		DR Inside cueva del puente, Parque Nacional del Este	18.3816N, 068.8017W	25	MT636116		H._validus_m3	H. val 02-5
H. carlosviquezi sp. nov.	f	holotype	DR Loma Quita Espuela	19.34405N, 069.46635W	200	MT636111	MT635414	H._carlosviquezi_n_sp_f	7B11-2
H. castelloides	m		DR Loma Quita Espuela	19.34405N, 069.46635W	200	MT636124	MT635423	H._castelloides_m	H. cast 11-1
H. vega	m		DR Loma Quita Espuela	19.34405N, 069.46635W	200	MT636123		H._vega_m	H. veg 11-3
H. yuma sp. nov.	f	holotype	DR Loma Quita Espuela	19.34405N, 069.46635W	200	MT636122	MT635422	H._yuma_n_sp_f1	H. veg 11-1
	f	paratype	DR Loma Quita Espuela	19.34405N, 069.46635W	200	MT636121	MT635421	H._yuma_n_sp_f2	H. veg 11-2
H. aylinalegreae sp. nov.	m		DR Los Haitises: Cueva la Arena	19.08013N, 069.4649W	17	MT636132	MT635430	H._aylinalegreae_n_sp_m3	H. five 07-1
H. renebarbai sp. nov.	m	holotype	DR Los Haitises: Cueva la Arena	19.08013N, 069.4649W	17	MT636110	MT635413	H._renebarbai_n_sp_m	H. six 07-1
H. aylinalegreae sp. nov.	m	holotype	DR Parque del Este	18.355536N, 068.61825W	46	MT636128	MT635427	H._aylinalegreae_n_sp_m1	H. five 03-1
	f		DR Parque del Este	18.355536N, 068.61825W	46		MT645158	H._aylinalegreae_n_sp_f3	H. five 03-2
	f		DR Parque del Este	18.355536N, 068.61825W	46	MT636131	MT635429	H._aylinalegreae_n_sp_f1	H. five 03-3
	f		DR Parque del Este	18.355536N, 068.61825W	46	MT636129		H._aylinalegreae_n_sp_f2	H. five 03-4
	m		DR Parque del Este	18.355536N, 068.61825W	46	MT636130	MT635428	H._aylinalegreae_n_sp_m2	H. five 03-5

Species (ND 17)	sex	type?	Locality	Latitude / Longitude	elev m	CO1	16s	GenBank Label	Specimen Name
H. constanza sp. nov.	m	holotype	DR Valle Nuevo (Jurassic Park)	18.688N, 070.596W	2100	MT636125	MT635424	H._constanza_n_sp_m	H. cast 24-1
	f	paratype	DR Valle Nuevo (Jurassic Park)	18.688N, 070.596W	2100	MT636126	MT635425	H._constanza_n_sp_f1	H. cast 24-2
	f	paratype	DR Valle Nuevo (Jurassic Park)	18.688N, 070.596W	2100	MT636127	MT635426	H._constanza_n_sp_f2	H. cast 24-3
H. gabrielsantosi sp. nov.	f	paratype	DR Valle Nuevo (Jurassic Park)	18.688N, 070.596W	2100	MT636133	MT635431	H._gabrielsantosi_n_sp_f2	H. one 24-1
	f	holotype	DR Valle Nuevo (Jurassic Park)	18.688N, 070.596W	2100	MT636135	MT635433	H._gabrielsantosi_n_sp_f1	H. one 24-2
	f	paratype	DR Valle Nuevo (Jurassic Park)	18.688N, 070.596W	2100	MT636134	MT635432	H._gabrielsantosi_n_sp_f3	H. one 24-3
H. jurassicus sp. nov.	m		DR Valle Nuevo (Jurassic Park)	18.688N, 070.596W	2100	MT636117	MT635417	H._jurassicus_n_sp_m1	H. jur 24-1
	m		DR Valle Nuevo (Jurassic Park)	18.688N, 070.596W	2100	MT636120	MT635420	H._jurassicus_n_sp_m2	H. jur 24-3
	f		DR Valle Nuevo (Jurassic Park)	18.688N, 070.596W	2100	MT636118	MT635418	H._ jurassicus_n_sp_f1	H. jur 24-4
	f		DR Valle Nuevo (Jurassic Park)	18.688N, 070.596W	2100	MT636119	MT635419	H._ jurassicus_n_sp_f2	H. jur 24-5
H. scapula sp. nov.	f	paratype	DR Valle Nuevo Rd	18.84633N, 070.74064W	2983	MT636109	MT635412	H._ scapula_n_sp_f	H. two 22-2
	m	holotype	DR Valle Nuevo, NP; Valle Nuevo Rd	18.84633N, 070.74064W	2983	MT636108		H._scapula_n_sp_m	H. two 22-1
Oonopidae sp 1	f		DR Los Haitises: Cueva la Arena	19.08013N, 069.4649W	17	MT636142	MT635440	Oonopidae_sp_1_DR_f	H. six 07-2
Oonopidae sp 2	f		PR Mona Island: Bajuga Empalme			MT636141	MT635439	Oonopidae_sp_2_Mona_f	H. mona 1
00392858 *Stenoonops portoricensis*	f		PR Ranger Station, Guanica Dry Forest	17.971472N, 066.86795W	154	MT636143		00392858_S._portoricensis	

For phylogenetic analyses, alignments were done in MAFFT (Katoh 2013) through the online portal EMBL-EBI, using default settings but increasing the tree rebuilding and maxiterate settings to 100. Gaps were treated as missing characters. The aligned sequences for COI, and 16S, were tested for the best fitting substitution model using the program Jmodeltest 2.1.7 (Darriba et al. 2012). The best models for each gene, among the 24 models available in MrBayes, were GTR+G for 16S and GTR+I+G for COI. We conducted Bayesian analyses using MrBayes V3.2.3 through the online portal CIPRES (Miller et al. 2010) on the concatenated mtDNA dataset. The Bayesian analyses ran 10,000,000 generations, sampling every 1000 generations. We used Tracer (Drummond and Rambaut 2007) to verify proper convergence of runs and sufficient sampling of priors.

Abbreviations

Somatic morphology

ALE anterior lateral eye
PLE posterior lateral eye
PME posterior median eye

Genitalia (female)

ar anterior receptaculum
ef epigastric furrow
es epigastric scutum
pr posterior receptaculum
ps postepigastric scutum
wp wing like projections

Genitalia (male)

c bulb
c conductor
e embolus

Results

The ten new species of *Heteroonops* presented in this work are genetically distinct and distinguishable morphologically. They were all collected in leaf litter samples from forest or cave habitats in Hispaniola ranging from near sea level to 2983 m. Mitochondrial genetic divergences and patterns of relationships belie a deep and old history of *Heteroonops* on Hispaniola (Fig. 1).

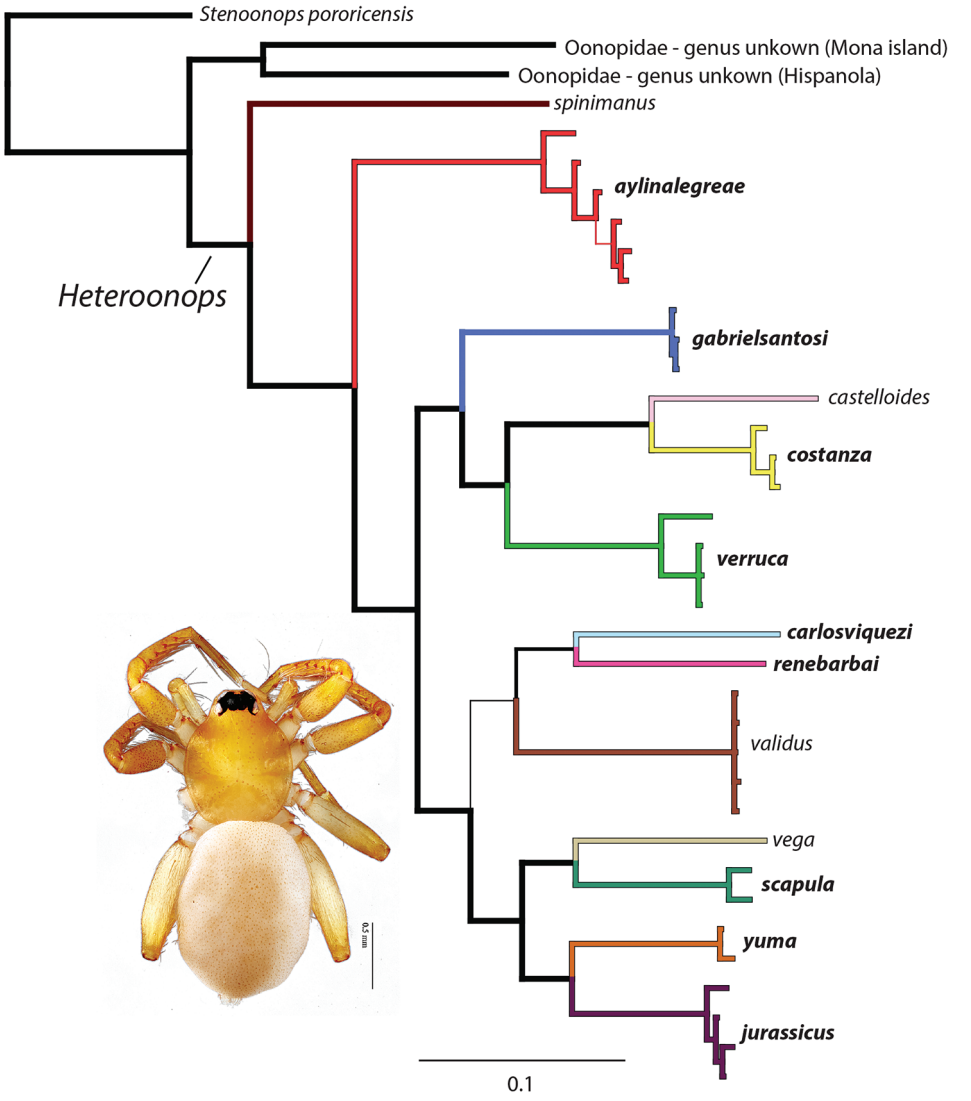

Figure 1. Summary phylogeny of the included species rendering support for the monophyly (multiple samples per species) or exclusivity (single specimens) of each species dealt with here. Species color scheme equals that on map in Figure 40. New species are highlighted in **bold**. Thick branches have >95% posterior probability support, thin branches have >75% posterior probability support. Scale bar indicates the number of expected changes on branches. Inset photo of female *H. jurassicus* sp. nov. For more detailed specimen-level phylogeny see Suppl. material 1.

Taxonomy

Oonopidae

Heteroonops Dalmas, 1916

Composition. *H. andros* Platnick & Dupérré, 2009, *H. aylinalegreae* sp. nov., *H. carlosviquezi* sp. nov., *H. castelloides* Platnick & Dupérré, 2009, *H. castellus* (Chickering, 1971), *H. colombi* Dumitrescu & Georgescu, 1983, *H. constanza* sp. nov., *H. croix* Platnick & Dupérré, 2009, *H. gabrielsantosi* sp. nov., *H. iviei* Platnick & Dupérré, 2009, *H. jurassicus* n. sp, *H. macaque* Platnick & Dupérré, 2009, *H. murphyorum* Platnick & Dupérré, 2009, *H. renebarbai* sp. nov., *H. saba* Platnick & Dupérré, 2009, *H. scapula* sp. nov., *H. singulus* (Gertsch & Davis, 1942), *H. solanllycarreroae* sp. nov., *H. spinigata* Platnick & Dupérré, 2009, *H. spinimanus* (Simon, 1891), *H. toro* Platnick & Dupérré, 2009, *H. validus* (Bryant, 1948), *H. vega* Platnick & Dupérré, 2009, *H. verruca* sp. nov., *H. yuma* sp. nov.

Distribution. Mexico, Costa Rica, Bahama Islands, Cuba, Jamaica, Dominican Republic, Puerto Rico, Virgin Islands, Saba, Montserrat and Dominica (*H. spinimanus* (Simon, 1891) presents a pantropical distribution).

Diagnosis. Males are easily diagnosed from all other Oonopidae by the presence of one or two backward-pointing projections on the male palpal endites (Figs 29–33). Females are easily diagnosed by their elongated, spinose pedipalpi (Platnick and Dupérré 2009, fig. 181).

Heteroonops scapula Dupérré, sp. nov.

http://zoobank.org/00009E22-3BB0-462B-855D-E4B136FEDCB2
Figs 2–5, 34, 40

Type material. Male holotype from Dominican Republic, La Vega Province, Constanza, Valle Nuevo National Park, 18.84633N, 70.74064W, 2983 m, 26.vi.2012, team CarBio (NMNH, USNMENT 01747000). One female paratype, same data.

Etymology. The specific epithet is a noun in apposition meaning wings, in reference to the large wing-like structures of the female internal genitalia.

Diagnosis. Males are diagnosed from all species by the combination of the following characters: constricted tip of palpal bulb and their bent embolus, wider apically, long conductor reaching the tip of the embolus (Figs 2, 3); females are diagnosed by the large, anterior wing-like projections of their internal genitalia and triangular anterior receptaculum (Fig. 5).

Description. Male (holotype): Total length: 1.9; carapace length: 1.0; carapace width: 0.7. ***Cephalothorax*:** Carapace ovoid; shiny, bright orange; pars cephalica flat. Sternum yellow; longer than wide; covered entirely with long dark setae. Endites yellow with one elongated and thin apical backward-pointing projection (Fig. 34); la-

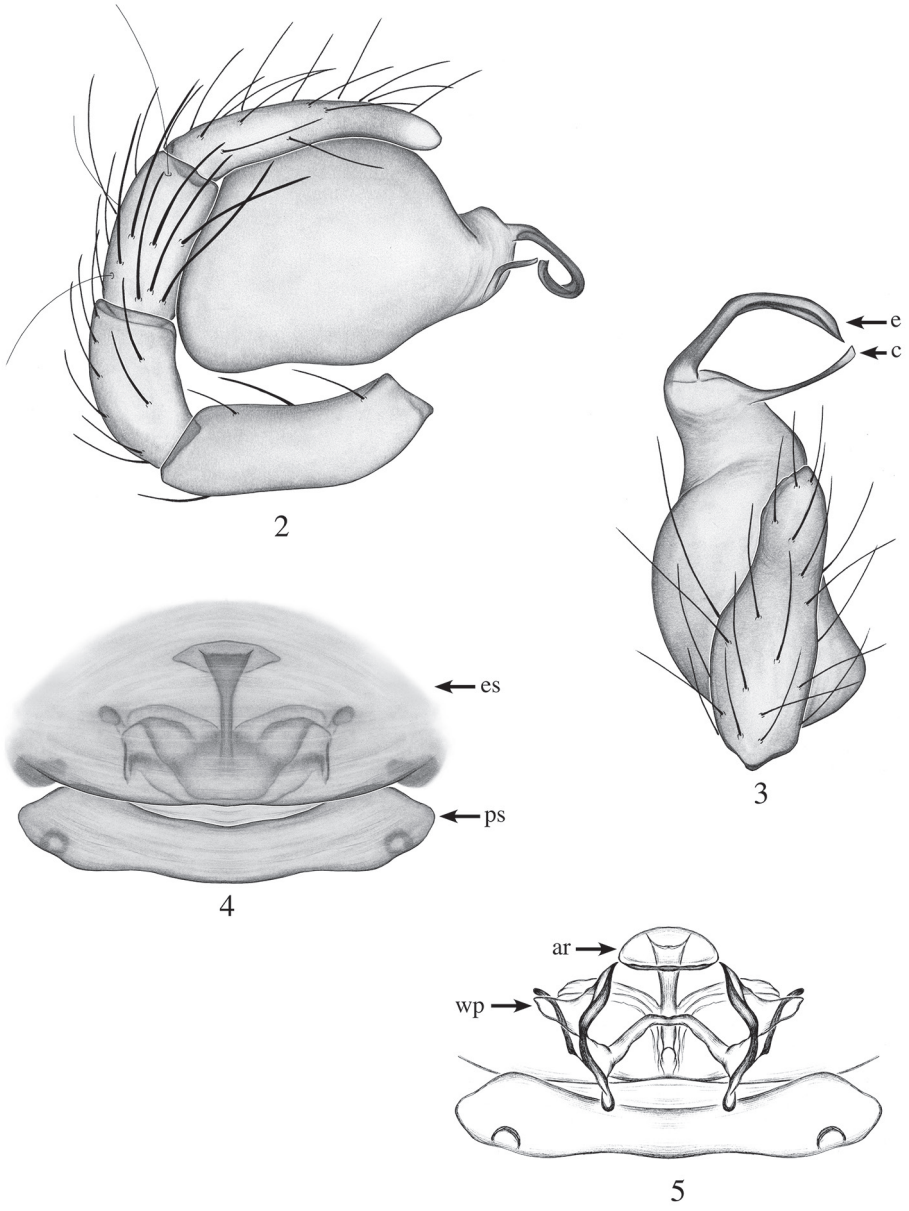

Figures 2–5. *Heteroonops scapula* sp. nov. Male (**2, 3**), female (**4, 5**). **2** Palp, prolateral view **3** palp, apical view **4** epigynal region, ventral view **5** internal genitalia dorsal view.

bium light yellow. Clypeus vertical; short (1/2× radius of ALE). Chelicerae yellow; promargin and retromargin without teeth; fangs normal 1/3 length of chelicerae. ***Eyes*:** Six eyes surrounded by black pigmentation; ALE largest, oval, PME squared; PLE smallest, oval; ALE separated by their radius; ALE-PLE touching; PLE-PME touch-

ing; PME touching. ***Abdomen*:** Oval; light gray covered dorsally with long dark setae; epigastric and postepigastric scuta light orange, well sclerotized. ***Legs*:** Yellow; tibia I with five pairs of ventral spines, metatarsus I with 2 pairs of ventral spines; leg formula undetermined, missing legs II-III-IV. ***Genitalia*:** Palpal segments light yellow; palpal bulb whitish. Palpal femur, patella and tibia with spines prolaterally (Fig. 2). Palpal bulb ovoid constricted at tip (Fig. 2); embolus long, bent medially, wider apically; conductor elongated and thin, wider apically, reaching the tip of the embolus (Fig. 3).

Female (paratype): Total length: 1.98; carapace length: 0.94; carapace width: 0.74. ***Cephalothorax*:** Carapace ovoid; shiny, bright orange; pars cephalica flat. Sternum, labium and chelicerae: as in male. Endites without projection. ***Eyes*:** Same as male. ***Abdomen*:** Oval; gray; epigastric and postepigastric scuta orange, well sclerotized (Fig. 4). ***Legs***: Color as in male; all legs missing; all palpal segments with strong spines. ***Genitalia*:** Epigynal region not protruding, with large structure visible through the epigastric scutum (Fig. 4). Internal genitalia with triangular anterior receptaculum, projecting posteriorly into a plate-like extrusion; posterior receptaculum not observed; wing-like projections well sclerotized, tridimensional (Fig. 5).

Other material examined. None.

Distribution. Dominican Republic, La Vega Province (Fig. 40).

Heteroonops jurassicus Dupérré, sp. nov.

http://zoobank.org/F8D0A1A4-B6CF-438F-BADD-7C5FCAAA995B

Figs 6–9, 35, 40

Type material. Male holotype from Dominican Republic, La Vega Province, Constanza, Valle Nuevo National Park, 'Jurassic Park', 18.688N, 70.596W, 2100 m, 26.vi.2012, team CarBio (NMNH, USNMENT 01747001). Two female paratypes, same data.

Etymology. The specific epithet is a noun in apposition taken from the type locality, Jurassic Park, Dominican Republic.

Diagnosis. Males are distinguished from all species of the genera by the spatula-shaped tip of the embolus (Fig. 7). Females are distinguished by their large funnel-shaped anterior receptaculum (Fig. 9).

Description. Male (holotype): Total length: 1.93; carapace length: 1.03; carapace width: 0.96. ***Cephalothorax*:** Carapace ovoid; shiny, bright orange; pars cephalica slightly elevated. Sternum orange; longer than wide; covered entirely with long dark setae. Endites orange with one very small apical backward-pointing projection (Fig. 35); labium light orange. Clypeus vertical; short (1/2× radius of ALE). Chelicerae orange; promargin and retromargin without teeth; fangs long, 2/3 the length of the chelicerae. ***Eyes*:** Six eyes surrounded by black pigmentation; ALE largest, oval; PME rectangular; PLE smallest, oval; ALE separated by their radius; ALE-PLE touching; PLE-PME touching; PME touching. ***Abdomen*:** Oval; beige dorsally covered with long dark setae; epigastric and postepigastric scuta orange, well sclerotized. ***Legs*:** Orange; tibia I with five pairs of ventral spines, metatarsus I with two pairs of ventral spines; leg formula

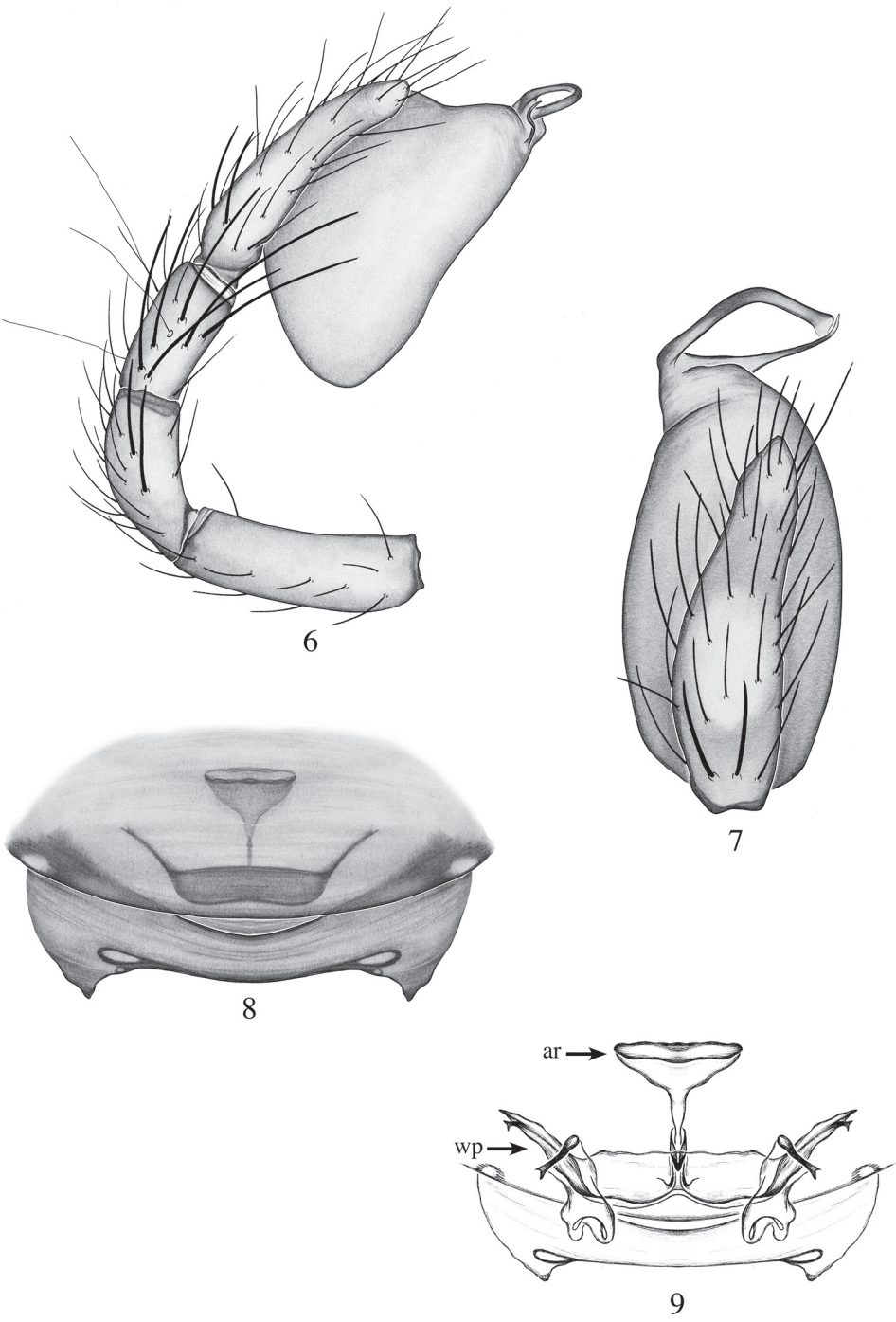

Figures 6–9. *Heteroonops jurassicus* sp. nov. Male (**6, 7**), female (**8, 9**). **6** Palp, prolateral view **7** palp, apical view **8** epigynal region, ventral view **9** internal genitalia, dorsal view.

4123. ***Genitalia*:** Palpal segments yellow; palpal bulb whitish. Palpal patella, tibia and tarsus with spines prolaterally (Fig. 6). Palpal bulb ovoid slightly constricted at tip (Fig. 6); embolus long, bent medially with transparent spatula-shaped tip; conductor long and thin reaching the tip of the embolus (Fig. 7).

Female (paratype): Total length: 2.12; carapace length: 0.92; carapace width: 0.76. ***Cephalothorax*:** Carapace ovoid; shiny, yellow; pars cephalica flat. Sternum and labium light yellow. Chelicerae and endites light yellow, not modified. ***Eyes*:** as in male. ***Abdomen*:** Oval, light beige; epigastric and postepigastric scuta orange, well sclerotized (Fig. 8). ***Legs*:** Light yellow; tibia I with five pairs of ventral spines, metatarsus I with two pairs of ventral spines; leg formula 4123; all palpal segments with strong spines. ***Genitalia*:** Epigynal region not protruding, with funnel-shaped and rectangular structures visible through the epigastric scutum (Fig. 8). Internal genitalia with funnel-shaped anterior receptaculum; posterior receptaculum not observed; wing-like projections well sclerotized, tridimensional (Fig. 9)

Other material examined. Same data as type specimens: 1♂ (USNMENT 00788060), 1♂ (USNMENT 00788048), 1♀ (USNMENT 00788084); 3♂, 4♀ (UVM).

Distribution. Dominican Republic, La Vega Province (Fig. 40).

***Heteroonops aylinalegreae* Dupérré, sp. nov.**
http://zoobank.org/EBB74055-FC21-4252-AD4C-F4628928F811
Figs 10–13, 36, 40

Type material. Male holotype from Dominican Republic, La Alta Gracia Province, Occidental, San Rafael, del Este National Park, 18.355536N, 68.6182518W, 46 m, 7–8.vi.2012, team CarBio (NMNH, USNMENT 01747002). One male and four female paratypes, same data (USNMENT 01747003).

Etymology. The specific epithet is a noun in apposition honoring local arachnologist and CarBio collaborator Aylin Alegre.

Diagnosis. Males are diagnosed from all *Heteroonops* by the combination of the following characters: embolus well sclerotized, not spatulated apically; short conductor not reaching the tip of the embolus (Fig. 11); females are diagnosed by their inverse triangular anterior receptaculum and large posterior receptaculum (Fig. 13).

Description. Male (holotype): Total length: 1.65; carapace length: 0.79; carapace width: 0.67. ***Cephalothorax*:** Carapace ovoid; shiny, light yellow; pars cephalica flat. Sternum light yellow; longer than wide; covered entirely with long dark setae. Endites light yellow with one small apical backward-pointing projection (Fig. 35); labium light yellow. Clypeus vertical; short (1/2× radius of ALE). Chelicerae yellow; promargin and retromargin without teeth; fangs normal, 1/3 length of chelicerae. ***Eyes*:** Six eyes surrounded by black pigmentation; ALE largest, oval; PME squared; PLE smallest, oval; ALE separated by their radius; ALE-PLE touching; PLE-PME touching; PME touching. ***Abdomen*:** Oval; light gray, dorsally covered with long dark setae; epigastric

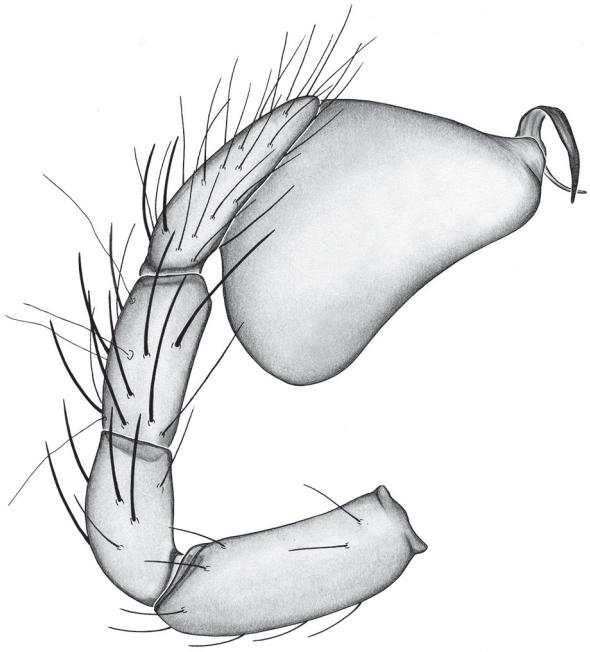

10

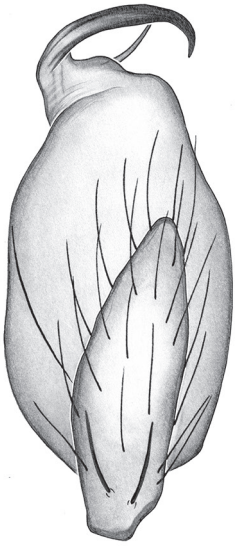

11

12

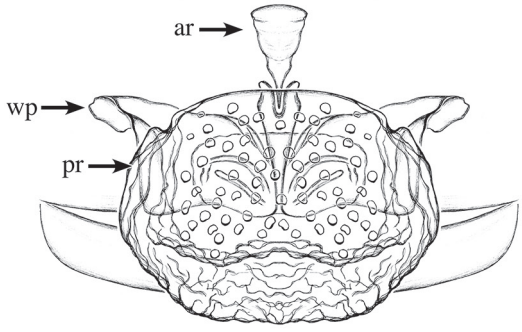

13

Figures 10–13. *Heteroonops aylinalegreae* sp. nov. Male (**10, 11**), female (**12, 13**). **10** Palp, prolateral view **11** palp, apical view **12** epigynal region, ventral view **13** internal genitalia, dorsal view.

and postepigastric scuta light yellow, not well sclerotized. ***Legs*:** Femora whitish; other legs segments light yellow; tibia I with one pair of ventral spines, metatarsus I with two pairs of ventral spines; leg formula 4123. ***Genitalia*:** Palpal segments yellow; palpal bulb whitish. Palpal patella, tibia and tarsus with spines prolaterally (Fig. 10). Palpal bulb ovoid slightly constricted at tip (Fig. 10); embolus well sclerotized, curved with pointed tip; conductor short and pointed not reaching tip of the embolus (Fig. 11).

Female (paratype): Total length: 1.89; carapace length: 0.81; carapace width: 0.67. ***Cephalothorax*:** Carapace, sternum, labium and chelicerae: as in male. Endites without projection. ***Eyes*:** Same as male. ***Abdomen*:** Oval; light gray; epigastric and postepigastric light yellow, not well sclerotized (Fig. 12). ***Legs*:** Color as in male; tibia I with three pairs of ventral spines, metatarsus I with two pairs of ventral spines; leg formula 4123; all palpal segments with strong spines. ***Genitalia*:** Epigynal region not protruding, with tulip-shaped structure visible through the epigastric scutum (Fig. 12). Internal genitalia with inverted triangular anterior receptaculum; posterior receptaculum large, pouch-shaped, wrinkled with pore field; wing-like projections short (Fig. 13).

Other material examined. 1♂ Dominican Republic, Hato Mayor Province, Occidental, San Rafael de Yuma, Parque Nacional los Haitises, Cueva La Arena, 19.08013N 69.4649W, 17♂, 12.vi.2012, team CarBio (UVM); 1♂3♀ Dominican Republic, La Alta Gracia Province, Occidental, San Rafael, del Este National Park, 18.355536N, 68.6182518W, 46 m, 7–8.vi.2012, team CarBio (UVM).

Distribution. Dominican Republic, La Alta Gracia and Hato Mayor provinces (Fig. 40).

***Heteroonops verruca* Dupérré, sp. nov.**
http://zoobank.org/18B6E9E1-0B6C-45C8-B724-85C0A3279651
Figs 14–18, 37, 40

Type material. Male holotype from Dominican Republic, Barahona Province, Cachote Biosphere Reserve, 18.09786N, 71.18925W, 1200 m, 7.vii.2012, team CarBio (NMNH, USNMENT 01747004). One female paratype, same data.

Etymology. The specific epithet is a noun in apposition meaning wart in reference to the male palpal bulb bearing a wart-like projection.

Diagnosis. Males can be diagnosed from all species by the wart-like projection on the prolateral side of the bulb (Fig. 14); females can be diagnosed by their small heart-shaped posterior receptaculum (Fig. 18).

Description. Male (holotype): Total length: 1.9; carapace length: 0.95; carapace width: 0.79. ***Cephalothorax*:** Carapace ovoid; shiny, bright yellow; pars cephalica flat. Sternum yellow; longer than wide; covered entirely with long dark setae. Endites yellow with one large, median backward-pointing projection (Fig. 37); labium yellow. Clypeus vertical; short (1/2× radius of ALE). Chelicerae yellow; promargin and retromargin without teeth; fangs normal, 1/3 the length of the chelicerae. ***Eyes*:** Six eyes

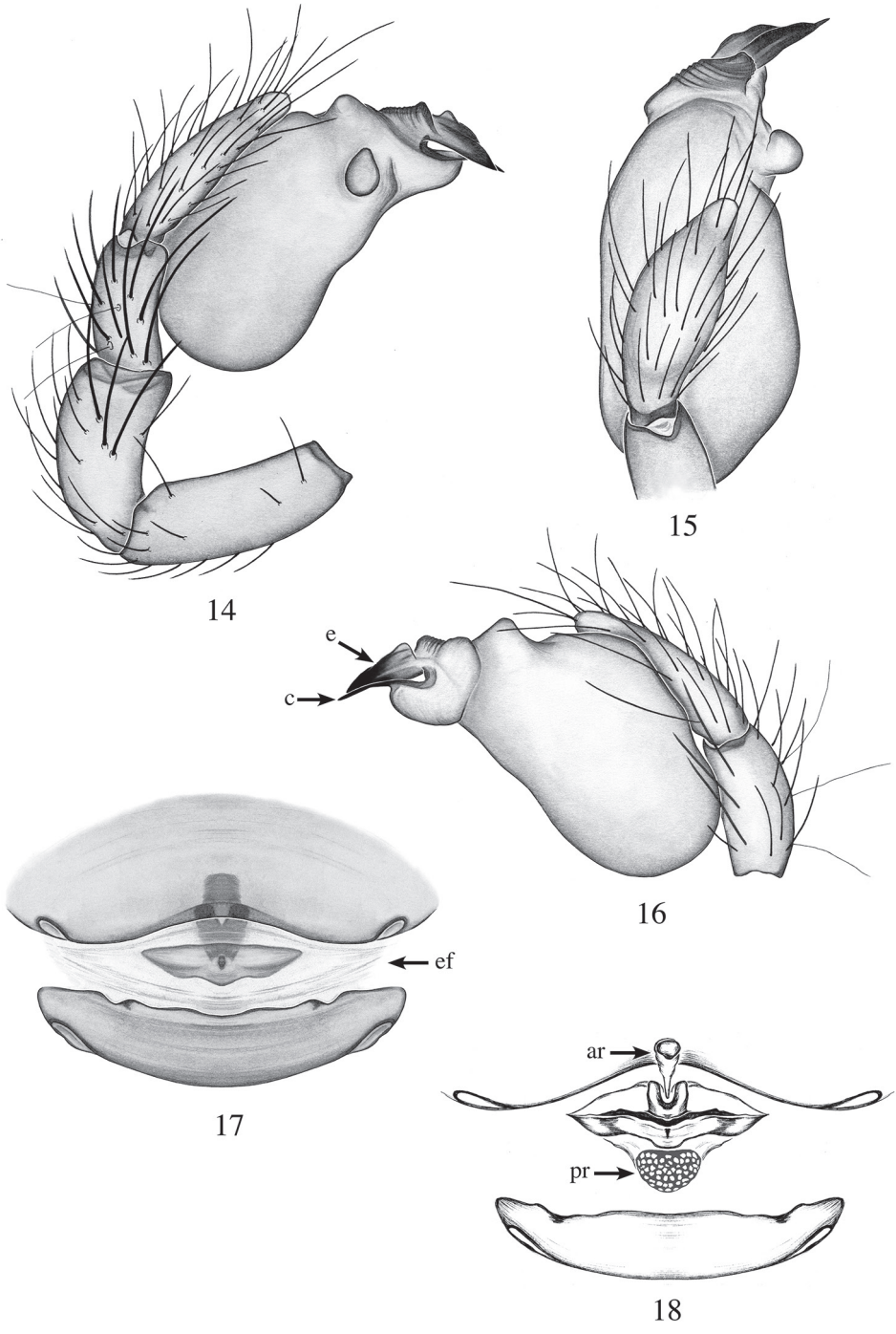

Figures 14–18. *Heteroonops verruca* sp. nov. Male (**14–16**), female (**17, 18**). **14** Palp, prolateral view **15** palp, apical view **16** palp, retrolateral view **17** epigynal region, ventral view **18** internal genitalia, dorsal view.

surrounded by black pigmentation; ALE largest, oval; PME rectangular; PLE smallest, oval; ALE separated by their radius; ALE-PLE touching; PLE-PME touching; PME touching. ***Abdomen*****:** Oval; light beige covered dorsally with long dark setae; epigastric and postepigastric scuta light yellow, well sclerotized. ***Legs*****:** Femora with basal half whitish, apical half-light yellow, other legs segments light yellow; tibia I with three pairs of ventral spines, metatarsus I with two pairs of ventral spines; leg formula 4123. ***Genitalia*****:** Palpal segments yellow; palpal bulb whitish. Palpal patella and tibia with spines prolaterally (Fig. 14). Palpal bulb ovoid with apical triangular bump and prolateral wart-like projection (Figs 13, 14); embolus and conductor set on an oval base with apical ridges (Figs 15, 16); embolus well sclerotized, wide and triangular; conductor spine-like, well sclerotized reaching the tip of the embolus (Fig. 16).

Female (paratype): Total length: 2.04; carapace length: 0.98; carapace width: 0.76. ***Cephalothorax*****:** Carapace, sternum, labium and chelicerae: as in male. Endites without projection. ***Eyes*****:** Same as male. ***Abdomen*****:** Oval, light beige; epigastric and postepigastric scuta orange, well sclerotized (Fig. 17). ***Legs*****:** Color as in male; leg I missing; all palpal segments with strong spines. ***Genitalia*****:** Epigynal region not protruding, with small, squared structure visible through the epigastric scutum, and triangular plate visible through the epigastric furrow (Fig. 17). Internal genitalia with triangular anterior receptaculum, projecting posteriorly; posterior receptaculum small, bulbous with pore field; wing-like projections not observed (Fig. 18).

Other material examined. Same data as type specimens: 2♂ (UVM).

Distribution. Dominican Republic, Barahona Province (Fig. 40).

Heteroonops renebarbai **Dupérré, sp. nov.**
http://zoobank.org/803999F5-7C2D-4CE6-9C83-6264977AA215
Figs 19, 20, 38, 40

Type material. Male holotype from Dominican Republic, Hato Mayor Province, Occidental, San Rafael de Yuma, los Haitises National Park, outside Cueva La Arena, 19.08013N, 69.4649W, 17m, 12.vi.2012, team CarBio (NMNH, USNMENT 01747005).

Etymology. The specific epithet is a noun in apposition honoring local arachnologist and CarBio collaborator René Barba.

Diagnosis. Males are distinguished from most species by their elongated, thin embolus (Fig. 19); from *H. vega* by their long and pointed conductor (Fig. 20), flat and with denticles in the later (Platnick and Dupérré 2009, fig. 194).

Description. Male (holotype): Total length: 1.34; carapace length: 0.71; carapace width: 0.59. ***Cephalothorax*****:** Carapace ovoid; shiny, light yellow; pars cephalica flat. Sternum light yellow; longer than wide; covered entirely with long dark setae. Endites light yellow with an elongated apical backward-pointing projection with rounded tip (Fig. 38); labium light yellow. Clypeus vertical; short (1/2× radius of ALE). Chelicerae yellow; promargin and retromargin without teeth; fangs normal, 1/3 length of

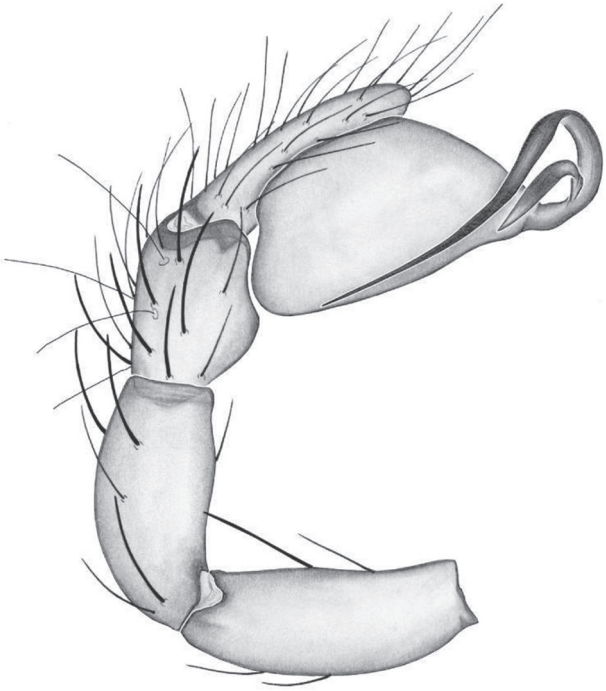

19

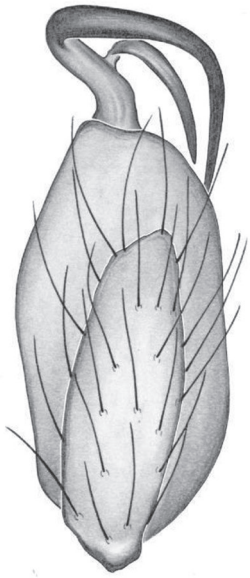

20

Figures 19, 20. *Heteroonops renebarbai* sp. nov. Male. **19** Palp, prolateral view **20** palp, apical view.

chelicerae. ***Eyes*:** Six eyes surrounded by black pigmentation; ALE largest, oval; PME squared; PLE smallest, oval; ALE separated by their radius; ALE-PLE touching; PLE-PME touching; PME touching. ***Abdomen*:** Oval; light beige covered dorsally with long dark setae; epigastric and postepigastric scuta light yellow, not well sclerotized. ***Legs*:** Light yellow; tibia I with two pairs of ventral spines, metatarsus I with one pair of ventral spines; leg formula undertermined, legs II-III-IV missing. ***Genitalia*:** Palpal segments light yellow; palpal bulb whitish. Palpal femur, patella and tibia with spines prolaterally (Fig. 19). Palpal bulb ovoid (Fig. 19); embolus well sclerotized, long and thin; conductor long and pointed, initiating at base of embolus (Figs 19, 20).

Female: Unknown.

Other material examined. None.

Distribution. Dominican Republic, Hato Mayor Province (Fig. 40).

***Heteroonops yuma* Dupérré, sp. nov.**
http://zoobank.org/C9159DF2-1A78-4434-BA1E-65A51DD10D33
Figs 21, 22, 40

Type material. Female holotype from Dominican Republic, Duarte Province, Occidental, San Rafael de Yuma, Loma Quita Espuela, 19.35504N, 70.111W, 200 m, 14.vi.2012, team CarBio (NMNH, USNMENT 01747006). Female paratype, same data (USNMENT 01747007).

Etymology. The specific name is noun in apposition taken from the type locality, San Rafael de Yuma, Dominican Republic.

Diagnosis. Females are distinguished from most species by the anterior receptaculum positioned on a narrow, short stalk; from *H. vega* by their larger anterior receptaculum projecting posteriorly (Fig. 22), not projecting in the later species (Platnick and Dupérré 2009, fig. 211).

Description. Female (holotype) Total length: 1.86; carapace length: 0.76; carapace width: 0.61. ***Cephalothorax*:** Carapace ovoid; shiny, whitish; pars cephalica flat. Sternum whitish; longer than wide; covered entirely with long dark setae. Endites withish, not modified; labium light whitish. Clypeus vertical; short (1/2× radius of ALE). Chelicerae pale yellow; promargin and retromargin without teeth; fangs normal, 1/3 length of chelicerae. ***Eyes*:** Six eyes surrounded by black pigmentation; ALE largest, oval; PME squared; PLE smallest, oval; ALE separated by their radius; ALE-PLE touching; PLE-PME touching; PME touching. ***Abdomen*:** Oval; yellowish; epigastric and postepigastric scuta pale yellow, not well sclerotized (Fig. 21). ***Legs*:** whitish; tibia I with four pairs of ventral spines, metatarsus I with three pairs of ventral spines; leg formula 4123; all palpal segments with strong spines. ***Genitalia*:** Epigynal region not protruding with faint structure visible through the scuta (Fig. 21). Internal genitalia with triangular anterior receptaculum, projecting posteriorly (Fig. 22); posterior receptaculum transparent, W-shaped; wing-like projections golf club-shaped (Fig. 22).

Male: Unknown.

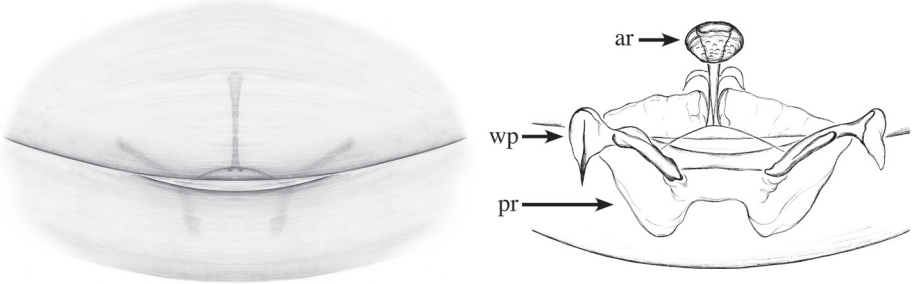

Figures 21, 22. *Heteroonops yuma* sp. nov. Female. **21** Epigynal region, ventral view **22** internal genitalia, dorsal view.

Other material examined. None.

Distribution. Dominican Republic, Duarte Province (Fig. 40).

***Heteroonops carlosviquezi* Dupérré, sp. nov.**

http://zoobank.org/9192A67A-94FD-4CE5-852B-AE9586764724

Figs 23–25, 40

Type material. Female holotype from Dominican Republic, Duarte Province, Occidental, San Rafael de Yuma, Loma Quita Espuela, 19.35504N, 70.111W, 200 m, 14.vi.2012, team CarBio (NMNH, USNMENT 01747008).

Etymology. The specific epithet is a noun in apposition honoring Costa Rican arachnologist and CarBio collaborator Carlos Viquez.

Diagnosis. Females are easily diagnosed by their umbrella-shaped anterior receptaculum (Fig. 24).

Description. Female: Total length: 2.06; carapace length: 0.96; carapace width: 0.8. ***Cephalothorax*:** Carapace ovoid; shiny, light orange; pars cephalica flat. Sternum yellow; longer than wide; covered entirely with long dark setae. Endites yellow, not modified; labium light yellow. Clypeus vertical; short (1/2× radius of ALE). Chelicerae yellow; promargin and retromargin without teeth; fangs normal, 1/3 length of chelicerae. ***Eyes*:** Six eyes surrounded by black pigmentation; ALE largest, oval; PME squared; PLE smallest, oval; ALE separated by their radius; ALE-PLE touching; PLE-PME touching; PME touching. ***Abdomen*:** Oval; dark grayish-blue with pattern, apically whitish (Fig. 25); epigastric and postepigastric scuta light orange, well sclerotized (Fig. 23). ***Legs*:** Orange; tibia I with four pairs of ventral spines, metatarsus I with three pairs of ventral spines; leg formula 4123; all palpal segments with strong spines. ***Genitalia*:** Epigynal region not protruding, with bell-shaped structure visible through the epigastric scutum (Fig. 23). Internal genitalia with umbrella-shaped anterior receptaculum; posterior receptaculum globose with large pore field; wing-like projections large, ear-shaped (Fig. 24).

Male: Unknown.

Other material examined. None.

Distribution. Dominican Republic, Duarte Province (Fig. 40).

***Heteroonops gabrielsantosi* Dupérré, sp. nov.**

http://zoobank.org/33CC4CA3-3B84-43A9-978D-CF5391CEFEAC

Figs 26, 27, 40

Type material. Female holotype from Dominican Republic, La Vega Province, Constanza, Valle Nuevo National Park, 'Jurassic Park', 18.688N, 70.596W, 2100 m, 26.vi.2012, team CarBio (NMNH, USNMENT 01747009). Two female paratypes (USNMENT 01747010, 01747011), same data.

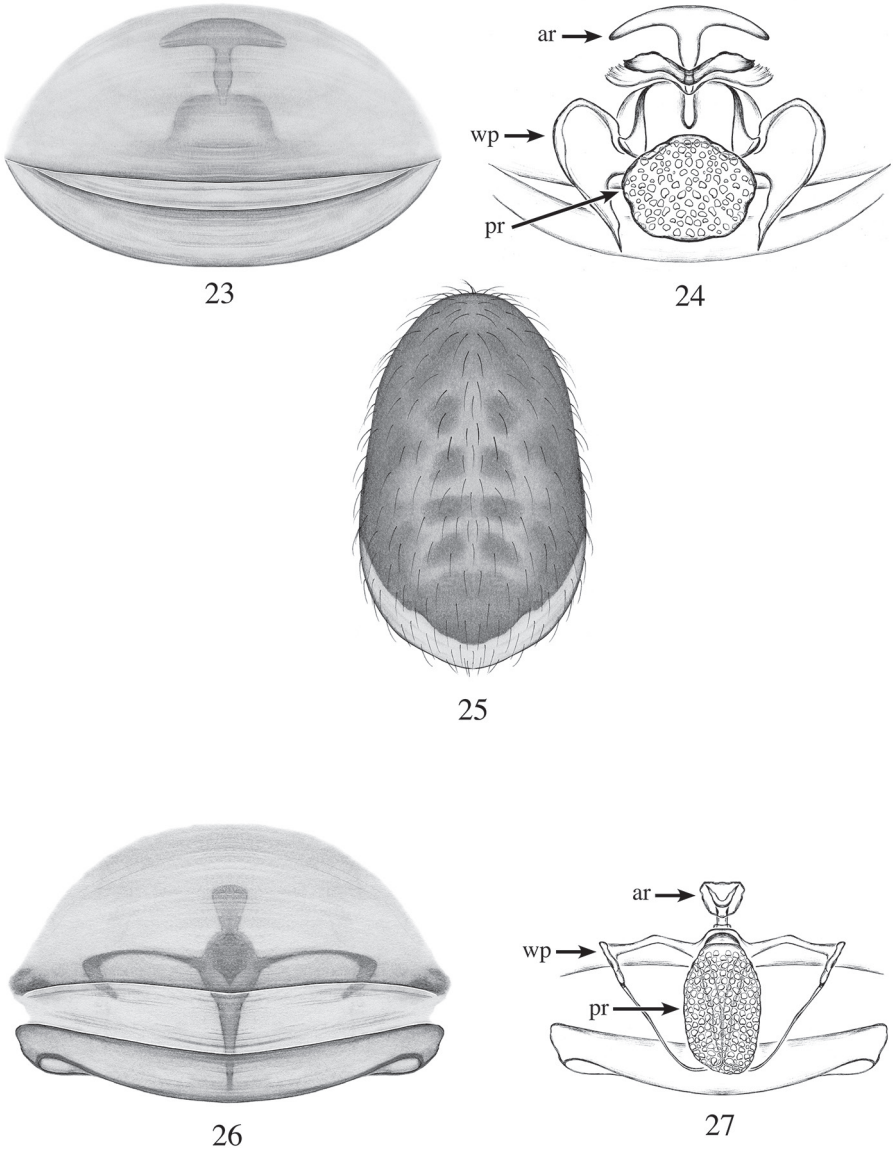

Figures 23–27. *Heteroonops carlosviquezi* sp. nov., female (**23–25**). *Heteroonops gabrielsantosi* sp. nov., female (**27**). **23** Epigynal region, ventral view **24** internal genitalia, dorsal view **25** abdomen, dorsal view **26** epigynal region, ventral view **27** internal genitalia, dorsal view.

Etymology. The specific epithet is a noun in apposition honoring local arachnologist and CarBio collaborator Gabriel Santos.

Diagnosis. Females can be diagnosed from all species by the arch wing-like projections of the internal genitalia and large oval posterior receptaculum (Fig. 27).

Description. Female: Total length: 2.31; carapace length: 0.91; carapace width: 0.84. ***Cephalothorax*:** Carapace ovoid; shiny, light yellow; pars cephalica flat. Sternum light yellow; longer than wide; covered entirely with long dark setae. Endites light yellow, not modified; labium light yellow. Clypeus vertical, short (1/2× radius of ALE). Chelicerae light yellow; promargin and retromargin without teeth; fangs normal, 1/3 length of chelicerae. ***Eyes*:** Six eyes surrounded by black pigmentation; ALE largest, oval; PME squared; PLE smallest, oval; ALE separated by their radius; ALE-PLE touching; PLE-PME touching; PME touching. ***Abdomen*:** Oval; whitish covered dorsally with long dark setae; epigastric and postepigastric scuta light orange, well sclerotized (Fig. 26). ***Legs*:** Femora with basal half whitish, apical half, light yellow; other leg segments light yellow; tibia I with four pairs of ventral spines, metatarsus I with three pairs of ventral spines; leg formula 4123; all palpal segments with strong spines. ***Genitalia*:** Epigynal region not protruding, with crcifix-shaped structure visible through the scutum and the epigastric furrow (Fig. 26). Internal genitalia with triangular anterior receptaculum, projecting posteriorly; posterior receptaculum elongated oval, with large pore field; wing-like projections arched (Fig. 27).

Male: Unknown.

Other material examined. None.

Distribution. Dominican Republic, La Vega Province (Fig. 40).

***Heteroonops solanllycarreroae* Dupérré, sp. nov.**

http://zoobank.org/F190F990-F3D6-4881-B509-382DE2BEA50C

Figs 28, 29, 40

Type material. Female holotype from Dominican Republic, Duarte Province, Occidental, San Rafael de Yuma, Loma Quita Espuela, 19.35504N, 70.111W, 200 m, 14.vi.2012, team CarBio (NMNH, USNMENT 01747012).

Etymology. The specific epithet is a noun in apposition honoring local arachnologist and CarBio collaborator Solanlly Carrrero.

Diagnosis. Females are diagnosed from all species by their posteriorly protruding epigastric scutum and their oval posterior receptaculum with folded bag-like extension (Fig. 29).

Description. Female (holotype). Total length: 1.37; carapace length: 0.61; carapace width: 0.42. ***Cephalothorax*:** Carapace ovoid; shiny, whitish; pars cephalica flat. Sternum whitish; longer than wide; covered entirely with long dark setae. Endites whitish, not modified; labium whitish. Clypeus vertical; short (1/2× radius of ALE). Chelicerae whitish; promargin and retromargin without teeth; fangs normal, 1/3 length of chelicerae. ***Eyes*:** Six eyes surrounded by black pigmentation; ALE largest, oval; PME squared; PLE smallest, oval; ALE separated by their radius; ALE-PLE touching; PLE-PME touching; PME touching. ***Abdomen*:** Oval; light gray covered dorsally with long dark setae; epigastric scutum protruding, postepigastric scutum thin; scuta light yel-

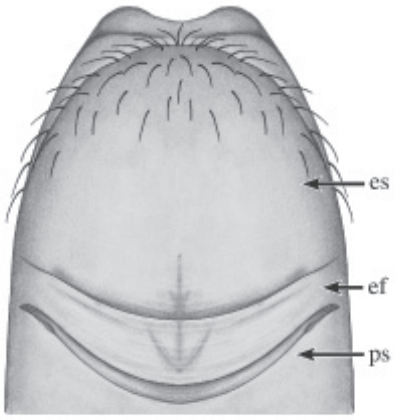

28

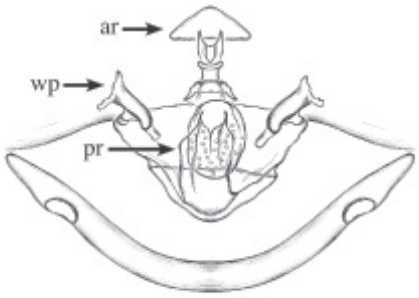

29

Figures 28, 29. *Heteroonops solanllycarreroae* sp. nov.. Female. **28** Epigynal region, ventral view **29** internal genitalia, dorsal view.

low, not well sclerotized (Fig. 28). ***Legs*:** Whitish; tibia I with three pairs of ventral spines, metatarsus I with two pairs of ventral spines; leg formula 4123; all palpal segments with strong spines. ***Genitalia*:** Epigynal region protruding ventrally (not visible on image) with anchor-shaped structure visible through the epigastric scutum and epigastric furrow (Fig. 28). Internal genitalia with hat-shaped anterior receptaculum; posterior receptaculum oval with small pore field region and folded bag-like extension; wing-like projections anvil-shaped (Fig. 29).

Male: Unknown.

Other material examined. None.

Distribution. Dominican Republic, La Duarte Province (Fig. 40).

Heteroonops constanza Dupérré, sp. nov.

http://zoobank.org/C1FAE1A8-EA65-4320-8419-A24E63086580
Figs 30–33, 39, 40

Type material. Male holotype from Dominican Republic, La Vega Province, Constanza, Valle Nuevo National Park, 'Jurassic Park', 18.688N, 70.596W, 2100 m, 26.vi.2012, team CarBio (NMNH, USNMENT 01747013). Two female paratypes (USNMENT 01747014), same data.

Etymology. The specific name is noun in apposition taken from the type locality, Constanza Province, Dominican Republic.

Diagnosis. Both males and females closely resemble *H. castelloides* Platnick & Dupérré, 2009; males are distinguished by the narrow, elongated palpal bulb and palpal tibia 2× longer than patellae (Fig. 30), ovoid in the later species, and palpal tibia 1.5×

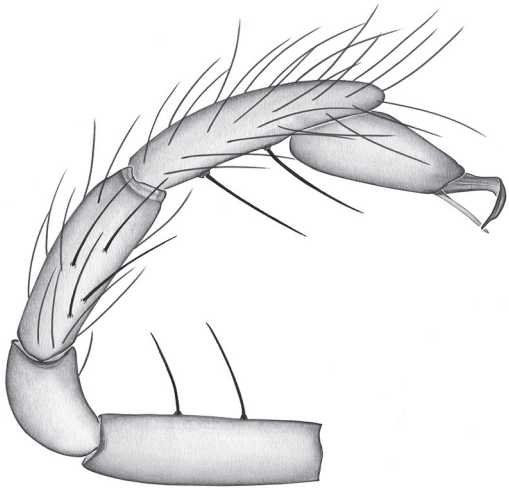

30

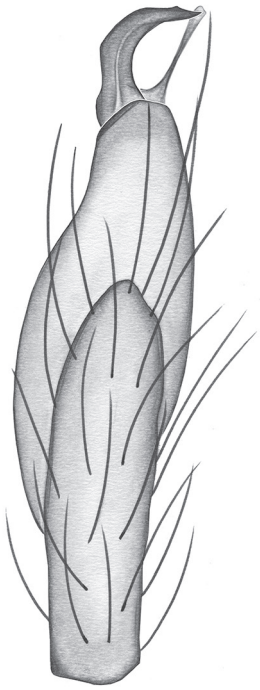

31

32

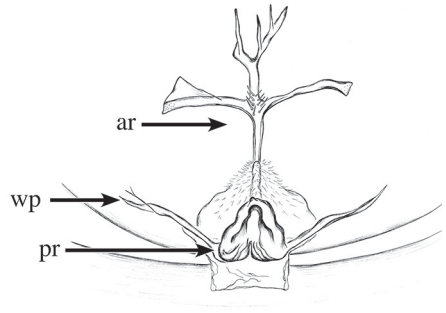

33

Figures 30–33. *Heteroonops constanza* sp. nov. Male (**30, 31**), female (**32, 33**). **30** Palp, prolateral view **31** palp, apical view **32** epigynal region, ventral view **33** internal genitalia, dorsal view.

longer than patellae (Platnick and Dupérré 2009, fig. 242); females are distinguished by their anterior recepetaculum with four branches (Fig. 33), five in *H. castelloides* (Platnick and Dupérré 2009, fig. 259).

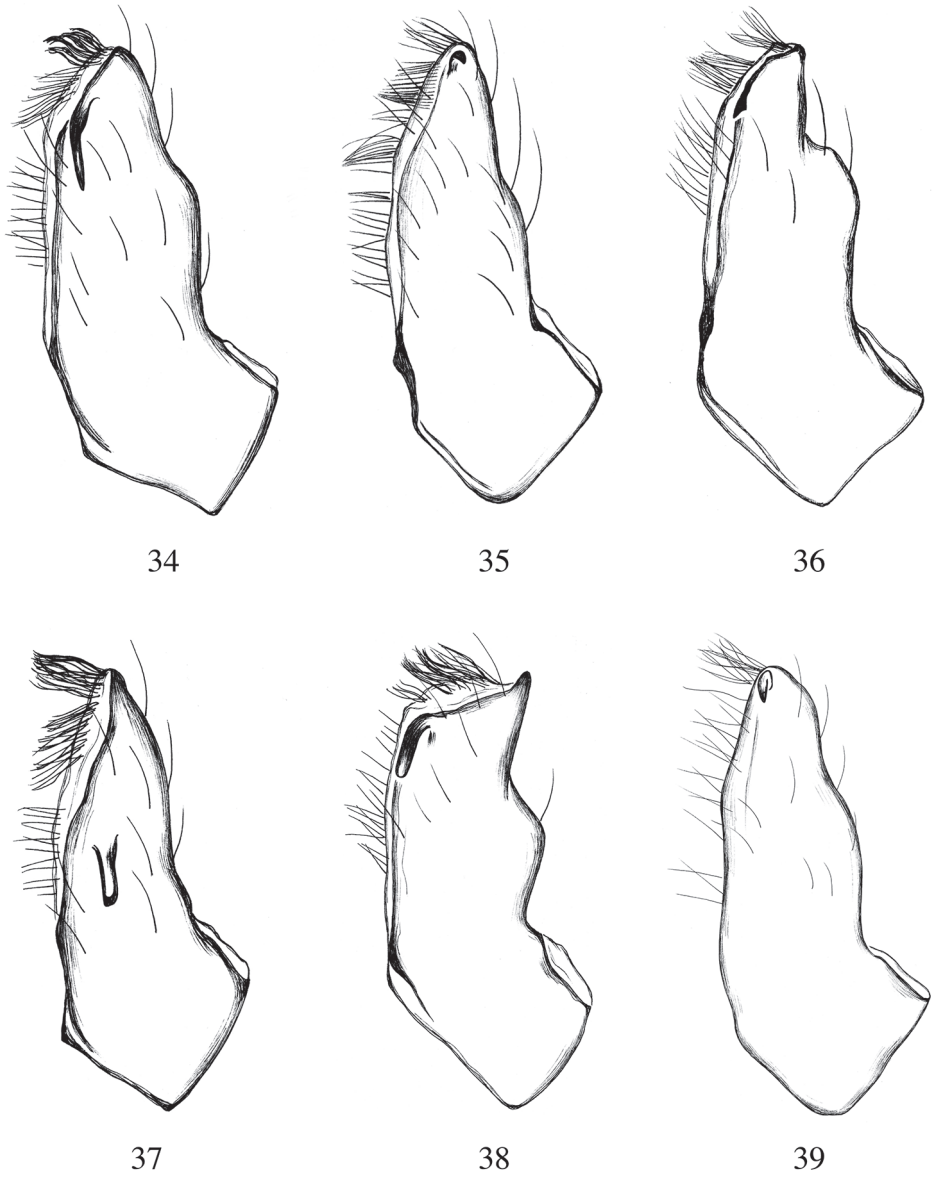

Figures 34–39. Male endites, ventral view. **34** *Heteroonops scapula* sp. nov. **35** *Heteroonops jurassicus* sp. nov. **36** *Heteroonops aylinalegreae* sp. nov. **37** *Heteroonops verruca* sp. nov. **38** *Heteroonops renebarbai* sp. nov. **39** *Heteroonops constanza* sp. nov.

Description. Male (holotype): Total length: 1.79; carapace length: 0.86; carapace width: 0.72. ***Cephalothorax*:** Carapace ovoid; shiny, pale yellow; pars cephalica slightly elevated. Sternum pale yellow; longer than wide; covered entirely with long dark setae. Endites pale yellow, with small apical projection (Fig. 39); labium light yellow. Clypeus sligthly protruding; short (1/2× radius of ALE). Chelicerae yellow; pro-

margin and retromargin without teeth; fangs normal, 1/3 length of chelicerae. ***Eyes*****:** Six eyes surrounded by black pigmentation; ALE largest, oval; PME rounded; PLE smallest, oval; ALE separated by their radius; ALE-PLE touching; PLE-PME touching; PME touching. ***Abdomen*****:** Oval; beige covered dorsally with long setae; epigastric and postepigastric scuta inconspicuous. ***Legs*****:** Legs missing. ***Genitalia*****:** Palpal segments pale yellow; palpal bulb whitish. Palpal femora, tibia and tarsus with spines prolaterally (Fig. 30). Palpal bulb elongated (Fig. 30); embolus strongly bent, pointed apically; conductor long and thin reaching the tip of the embolus (Fig. 31).

Female (paratype): Total length: 2.09; carapace length: 0.85; carapace width: 0.72. ***Cephalothorax*****:** Carapace ovoid; shiny, yellow; pars cephalica flat. Sternum and labium light yellow. Chelicerae and endites light yellow, not modified. ***Eyes*****:** as in male. ***Abdomen*****:** Oval, light beige; epigastric and postepigastric scuta pale yellow, not well sclerotized (Fig. 32). ***Legs*****:** Legs missing; all palpal segments with strong spines. ***Genitalia*****:** Epigynal region not protruding, with tree-shaped structures slightly visible through the epigastric scutum (Fig. 32). Internal genitalia with anterior receptaculum elongated with four main branches; posterior receptaculum triangular well sclerotized; wing-like projections elongated and narrow (Fig. 33).

Other material examined. None.

Distribution. Dominican Republic, La Vega Province (Fig. 40).

New records

Heteroonops spinimanus **(Simon, 1891)**
Fig. 40

Material examined. Dominican Republic, La Alta Gracia Province, Occidental, San Rafael de Yuma, del Este National Park, beach Trail to Cueva del Puente, 18.32902N, 68.80995W, 0 m, 5.vi.2012, team CarBio,1♀ (UVM).

Heteroonops castelloides **Platnick & Dupérré, 2009**
Fig. 40

Material examined. Dominican Republic, La Duarte Province, Occidental, San Rafael de Yuma, Loma Quita Espuela, 19.35504N, 70.111W, 200 m, 14.vi.2012, team CarBio, 1♂ (UVM).

Heteroonops validus **(Bryant, 1948)**
Fig. 40

Material examined. Dominican Republic, La Alta Gracia Province, Occidental, San Rafael de Yuma, del Este National Park, Cueva del Puente, 18.3816N, 68.8017W, 25 m, 6.vi.2012, team CarBio, 3♂4♀ (UVM).

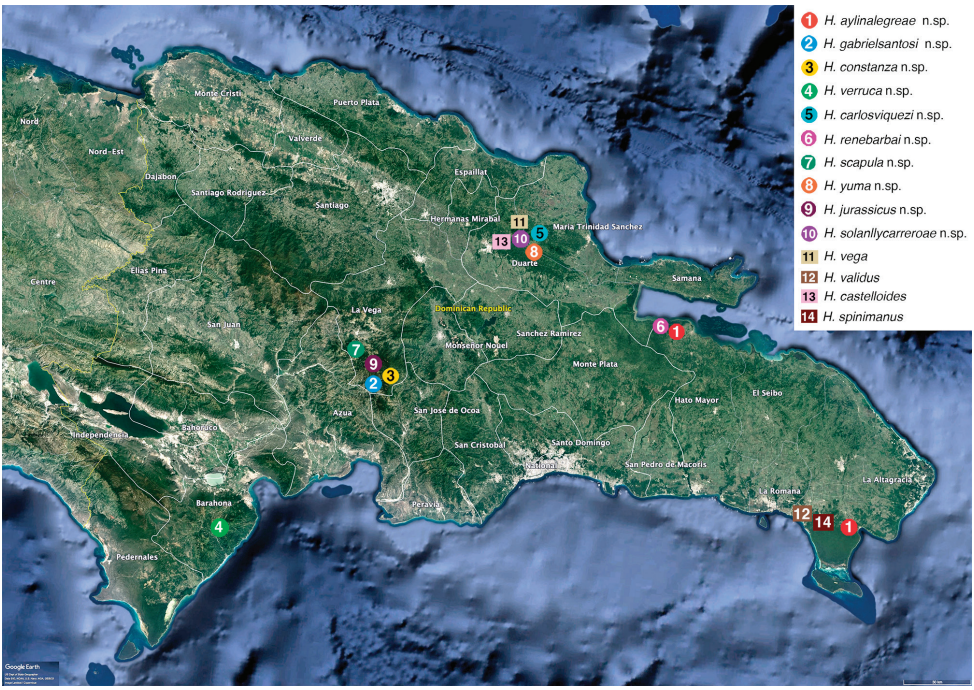

Figure 40. Distribution map of all *Heteroonops* species found in Hispaniola.

Heteroonops vega Platnick & Dupérré, 2009

Fig. 40

Material examined. Dominican Republic, La Duarte Province, Occidental, San Rafael de Yuma, Loma Quita Espuela, 19.35504N, 70.111W, 200m, 14.vi.2012, team CarBio, 1♂ (UVM).

Discussion

Observed patterns in our data are consistent with a high probability that our sampling has only detected a small subset of the *Heteroonops* diversity in Hispaniola. First, we found a total of 66 individuals distributed in 14 *Heteroonops* species, 10 of which were new, from only eight sampling sites. At a single site in Loma Quita (200 m) we found five species including three that are new (*H. yuma*, *H. carlosviquezi*, *H. solanllycarreroae*) and two that represent new records (*H. vega*, *H. castelloides*). Similarly, we found three new species in one locality in a high elevation forest (2100 m) in the Cordillera Central Parque National Valle Nuevo (*H. constanza*, *H. gabrielsantosi*, *H. jurassicus*). Moreover, a fourth new species *H. scapula*, was discovered in the same park at higher elevation (2983 m). Taxa from both of these localities are phylogenetically widespread reflecting an old most recent common ancestor and high levels of subsequent diversification (Fig. 1)). This contrasts with patterns seen in more dispersive Caribbean spiders

that rarely have more than a single species of a given genus in one locality (e.g., Dziki et al. 2015, Agnarsson et al. 2018, Čandek et al. 2019, Tong et al. 2019)

Despite patterns consistent with high local diversity, there is evidence that some *Heteroonops* species are wide ranging. Two taxa that represent new records were collected far from their type localities in the Cordillera Central, *H. castelloides*, and *H. validus.* Interestingly both of these species have been collected in flight intercept traps (Platnick and Dupérré 2009) suggesting the potential for aerial dispersal. Additionally, one species described here, *H. aylinalegreae*, was collected in two separate low elevation localities on the northern and southern sides of Eastern Hispaniola. While it seems that some members of this genus are capable of widespread dispersal, most notably the type species, the high levels of diversity in the Dominican Republic suggest an old presence and much speciation within West Indies, consistent with biologies that are not typically dispersal prone.

Acknowledgements

We thank all the members of the CarBio team, especially those involved in expeditions in the Dominican Republic. We are especially grateful to René Barba Diaz, Aylin Alegre Barosso, Gabriel de los Santos, and Solanlly Carrero Sanchez for help with logistics, organization, and in the field. All material was collected under appropriate collection permits and guidelines: Dominican Republic, Ministerio de Medio Ambiente y Recursos Naturales, no 0577. Funding for this work came from National Science Foundation (DEB-1314749 and DEBs-1050253/1050187) to I. Agnarsson and G. Binford. Additional funds came from the Smithsonian Laboratories of Analytical Biology, a 2013 SI Barcode Network grant to J.A. Coddington and Agnarsson. Thanks to the reviewers Cor Vink and Everton N. L. Rodrigues for positive comments that help improve the manuscript.

References

Abrahim N, Brescovit AD, Rheims CR, Santos AJ, Ott R, Bonaldo AB (2012) A revision of the Neotropical goblin spider genus *Neoxyphinus* Birabén, 1953 (Araneae, Oonopidae). American Museum Novitates 3743: 1–75. https://doi.org/10.1206/3743.2

Agnarsson I, Maddison WP, Avilés L (2007) The phylogeny of the social *Anelosimus* spiders (Araneae: Theridiidae) inferred from six molecular loci and morphology. Molecular Phylogenetics and Evolution 43: 833–851. https://doi.org/10.1016/j.ympev.2006.09.011

Agnarsson I, Van Patten C, Sargeant L, Chomitz B, Dziki A, Binford G (2018) A radiation of the ornate Caribbean 'smiley-faced spiders' – with descriptions of 15 new species (Araneae, Theridiidae, *Spintharus*). Zoological Journal of the Linnean Society 182: 758–790. https://doi.org/10.1093/zoolinnean/zlx056

Baehr BC, Ubick D (2010) A review of the Asian goblin spider genus *Camptoscaphiella* (Araneae: Oonopidae). American Museum Novitates 3697: 1–65. https://doi.org/10.1206/3697.2

Benoit PLG (1964) La découverte d'Oonopidae anophthalmes dans des termitières africaines (Araneae). Revue de Zoologie et de Botanique Africaines 70: 174–187.

Bryant EB (1948) The spiders of Hispaniola. Bulletin of the Museum of Comparative Zoololgy, Harvard 100: 331–459.

Čandek K, Agnarsson I, Binford G, Kuntner M (2019) Biogeography of the Caribbean Cyrtognatha spiders. Scientific Reports 9: 397. https://doi.org/10.1038/s41598-018-36590-y

Čandek K, Agnarsson I, Binford GJ, Kuntner M (2020) Caribbean golden orbweaving spiders maintain gene flow with North America. Zoologica Scripta 49: 210–221. https://doi.org/10.1111/zsc.12405

Chamberland L, McHugh A, Kechejian S, Binford GJ, Bond J, Coddington JA, Dolman G, Hamilton C, Harvey MS, Kuntner M, Agnarsson I (2018) From Gondwana to GAARlandia: global biogeography of ogre-faced spiders (Deinopidae) mirrors geologic history. Journal of Biogeography 45: 2442–2457. https://doi.org/10.1111/jbi.13431

Chamberlin RV, Ivie W (1938) Araneida from Yucatan. Publications of the Carnegie Institute 491: 123–136.

Dalmas R (1916) Révision du genre *Orchestina* E.S., suive de la description de nouvelles espèces du genre *Oonops* et d'une étude sur les Dictynidae du genre *Scotolathys*. Annales de la Société Entomologique de France 85: 203–258.

Darriba D, Taboada GL, Doallo R, Posada D (2012) jModelTest 2: more models, new heuristics and parallel computing. Nature Methods 9: 772. https://doi.org/10.1038/nmeth.2109

Drummond AJ, Rambaut A (2007) BEAST: Bayesian evolutionary analysis by sampling trees. BMC Evolutionary Biology 7: 1–8. https://doi.org/10.1186/1471-2148-7-1

Dumitrescu M, Georgescu M (1983) Sur les Oonopidae (Araneae) de Cuba. Résultats des Expéditions Biospéologiques Cubano-Roumaines à Cuba: 65–114.

Dziki A, Binford GJ, Coddington JA, Agnarsson I (2015) *Spintharus flavidus* in the Caribbean – a 30 million year biogeographical history and radiation of a 'widespread species'. PeerJ 3: e1422. https://doi.org/10.7717/peerj.1422

Fannes W, Jocqué R (2008) Ultrastructure of *Antoonops*, a new, ant-mimicking genus of Afrotropical Oonopidae (Araneae) with complex internal genitalia. American Museum Novitates 3614: 1–30. https://doi.org/10.1206/563.1

Fannes W, Bakker DD, Loosveldt K, Jocqué R (2008) Estimating the diversity of arboreal oonopid spider assemblages (Araneae, Oonopidae) at Afrotropical sites. Journal of Arachnology 36: 322–330. https://doi.org/10.1636/CT07-128.1

Gertsch WJ, Davis LI (1942) Report on a collection of spiders from Mexico. IV. American Museum Novitates 1158: 1–19.

Green P (2009) PHRED, 1.090518 edn. http://www.phrap.org

Green P, Ewing B (2002) PHRED, 0.020425c edn. http://www.phrap.org

Huber BA, Sinclair BJ, Schmitt M (2007) The evolution of asymmetric genitalia in spiders and insects. Biological reviews of the Cambridge Philosophical Society 82: 647–698. https://doi.org/10.1111/j.1469-185X.2007.00029.x

Katoh S (2013) MAFFT multiple sequence alignment software version 7: improvements in performance and usability. Molecular Biology and Evolution 30: 772–780. https://doi.org/10.1093/molbev/mst010

Katoh K, Kuma K, Toh H, Miyata T (2005) MAFFT version 5: improvement in accuracy of multiple sequence alignment. Nucleic Acids Research 33: 511–518. https://doi.org/10.1093/nar/gki198

Kranz-Baltensperger, Y (2012) Three new species of the oonopid spider genus *Ischnothyreus* (Araneae: Oonopidae) from Tioman Island (Malaysia). Zootaxa 3161: 37–47. https://doi.org/10.11646/zootaxa.3161.1.3

Maddison WP, Maddison DR (2019) Mesquite: a modular system for evolutionary analysis. Version 3.61 http://www.mesquiteproject.org

Maddison DR, Maddison WP (2020) Chromaseq: a Mesquite package for analyzing sequence chromatograms. Version 1.52. http://chromaseq.mesquiteproject.org

Miller MA, Pfeiffer W, Schwartz T (2010) Creating the CIPRES science gateway for inference of large phylogenetic trees. In: Proceedings of the Gateway Computing Environments Workshop (GCE); 2010 Nov 14; New Orleans (LA). Institute of Electrical and Electronics Engineers (IEEE): 1–8. https://doi.org/10.1109/GCE.2010.5676129

Planetary Biodiversity Inventory (2020) The Goblin Spider PBI. The American Museum of Natural History. https://research.amnh.org/oonopidae/ [accessed on 12.v.2020]

Platnick NI (2000) On *Coxapopha*, a new genus of the spider family Oonopidae from Panama (Araneae Haplogynae). Memorie della Societa Entomologica Italiana 78: 403–410.

Platnick NI, Dupérré N (2009) The goblin spider genus *Heteroonops* (Araneae, Oonopidae), with notes on *Oonops*. American Museum Novitates 3672: 1–72. https://doi.org/10.1206/690.1

Platnick NI, Dupérré N (2011a) The Andean goblin spiders of the new genus *Scaphidysderina* (Araneae, Oonopidae), with notes on *Dysderina*. American Museum Novitates 3712: 1–51. https://doi.org/10.1206/3712.2

Platnick NI, Dupérré N (2011b) The goblin spider genus *Pescennina* (Araneae, Oonopidae). American Museum Novitates 3716: 1–64. https://doi.org/10.1206/3716.2

Platnick NI, Dupérré N (2011c) The Andean goblin spiders of the new genera *Paradysderina* and *Semidysderina* (Araneae, Oonopidae). Bulletin of the American Museum of Natural History 364: 1–121. https://doi.org/10.1206/771.1

Ricklefs R, Bermingham E (2008) The West Indies as a laboratory of biogeography and evolution. Philosophical Transactions of the Royal Society B-Biological Sciences 363: 2393–2413. https://doi.org/10.1098/rstb.2007.2068

Simon E (1891) On the spiders of the island of St. Vincent. Part 1. Proceedings of the Zoological Society, London 1891: 549–575.

Tong Y, Binford G, Agnarsson I (2019). Huntsmen of the Caribbean: multiple tests of the GAARlandia hypothesis. Molecular Phylogenetics and Evolution 130: 259–268. https://doi.org/10.1016/j.ympev.2018.09.017

Tong YF, Chen H F, Liu SJ, Li SQ (2018) A new genus of oonopid spiders from Myanmar (Araneae, Oonopidae). ZooKeys 794: 31–43. https://doi.org/10.3897/zookeys.794.29156

Ubick D (2005) Oonopidae. In: Ubick D, Paquin P, Cushing, P, Roth V (Eds) Spiders of North America, an identification Manual. American Arachnological Society, 181–182.

World Spider Catalog (2020) World Spider Catalog. Natural History Museum Bern. http//wsc.nmbe.ch [version 15.5, accessed on 23.iv.2017]

Supplementary material 1

Phylogeny in Figure 1 with full taxon labeling

Authors: Nadine Dupérré, Charlotte Francisco, Ella Santana-Propper, Ingi Agnarsson, Greta J. Binford

Data type: Tree topology inferred using Bayesian analyses of mtDNA with each terminal taxon labeled

Explanation note: This tree is the same phylogeny as in Figure 1, however each terminal taxon is labeled with details that links that taxon with information in Table 1. Each label includes the name of the species, the sex (f/m), whether the specimen represents a holotype (h) or paratype (p), and a secondary label used to track the specimen through our analysis process. These labels connect the terminals with locality information and GenBank accession numbers detailed in Table 1. Values at nodes indicate posterior probabilities (and correspond to branch width).

Link: https://doi.org/10.3897/zookeys.964.51554.suppl1

ZooKeys 964: 31–40 (2020)
doi: 10.3897/zookeys.964.48655
https://zookeys.pensoft.net

RESEARCH ARTICLE

A peer-reviewed open-access journal
ZooKeys
Launched to accelerate biodiversity research

Two new species of the leafhopper genus *Mitjaevia* Dworakowska from China (Hemiptera, Cicadellidae, Typhlocybinae)

Xiaoxiao Chen[1], Yuehua Song[1]

1 *School of Karst Science, Guizhou Normal University / State Key Laboratory Cultivation Base for Guizhou Karst Mountain Ecology Environment of China, Guiyang, Guizhou 550001, China*

Corresponding author: Yuehua Song (songyuehua@163.com)

Academic editor: Mick Webb | Received 21 November 2019 | Accepted 30 July 2020 | Published 27 August 2020

http://zoobank.org/63EFF2A4-4B7D-46B4-B31F-C3D2C543A924

Citation: Chen X, Song Y, Webb MD (2020) Two new species of the leafhopper genus *Mitjaevia* Dworakowska from China (Hemiptera, Cicadellidae, Typhlocybinae). ZooKeys 964: 31–40. https://doi.org/10.3897/zookeys.964.48655

Abstract

In the present paper, two new species of the leafhopper genus *Mitjaevia* Dworakowska, 1970 from Guizhou Province China are described and illustrated, i.e., *Mitjaevia shibingensis* **sp. nov.** and *Mitjaevia dworakowskae* **sp. nov.** A checklist to species of the genus and a key to distinguish the Chinese species of the genus are given and the female valvulae are described and figured for the first time.

Keywords

Checklist, distribution, Homoptera, identification key, morphology, taxonomy

Introduction

The leafhopper genus *Mitjaevia* Dworakowska, 1970 belongs to the tribe Erythroneurini of Typhlocybinae, with *Erythroneura amseli* Dlabola, 1961 as its type species; seventeen species are known, seven from China (see Checklist). Two new species from Guizhou Province, China are described and illustrated in this paper together with a checklist and key to species from China.

Materials and methods

Specimens for this study were collected by sweep-net. Morphological terminology used follows Dietrich (2005) and Song and Li (2013) and observations and drawings were made using Olympus SZX16 and BX53 microscopes. Habitus photos were taken using a KEYENCE VHX-5000 digital microscope. Body measurements are from the apex of the vertex to the tip of the forewing. All specimens examined are deposited in the collection of the School of Karst Science, Guizhou Normal University, China (**GZNU**).

Taxonomy

Mitjaevia Dworakowska, 1970

Mitjaevia Dworakowska, 1970: 763.

Type species. *Erythroneura amseli* Dlabola, 1961, by original designation.

Diagnosis. Species with distinctive dark brown markings; head distinctly narrower than pronotum; male pygofer with simple dorsal appendage and sometimes ventral appendage; subgenital plate with a series of lateral peg-like setae basally or subbasally and a few macrosetae centrally at midlength; style elongate with subapical extension and variably developed lateral lobe; aedeagus with shaft cylindrical or laterally compressed, with or without processes, with ventral gonopore, basal apodeme variably developed and preatrium distinct.

Distribution. Palaearctic and Oriental Regions.

Remarks. Dworakowska (1970: 763–765) gave a detailed description of this genus based on the three included species known at that time; based on subsequently included species a modified description was given by Song et al. (2011: 26–27) and Dmitriev (2020). In addition, the female valvulae are described and figured here for the first time. Although a diagnosis is given above, clearly further studies are needed to elucidate fully the diagnostic characters of the genus and to test if the genus is monophyletic in the light of the observed variation in male genitalia between species.

Checklist to species of the genus *Mitjaevia*

1 *Mitjaevia amseli* (Dlabola, 1961: 297, figs 137–141, *Erythroneura*. Uzbekistan); Dlabola 1964: 248, Afghanistan; Dworakowska 1970: 765, figs 33–44, transferred to *Mitjaevia*. Kazakhstan; Korolevskaya, 1976: 42–43, figs 7, 8.

2 *Mitjaevia atropictila* (Ahmed, 1970a: 35; fig. 5: A–F, *Erythroneura*. Pakistan); Sharma 1984: 33, figs 19–29, transferred to *Mitjaevia*. India.

3 *Mitjaevia aurantiaca* (Mitjaev, 1969: 1045; figs 1, 2, *Erythroneura*. Kazakhstan); Dworakowska 1970: 765, transferred to *Mitjaevia*; Korolevskaya 1976: 42, figs 9, 10.
4 *Mitjaevia aurea* Dworakowska, 1994: 118; figs 407–414. India.
5 *Mitjaevia bibichanae* (Dlabola, 1961: 296, figs 131–135, *Erythroneura*. Uzbekistan); Korolevskaya 1976: 43–44, figs 11–13, transferred to *Mitjaevia*. Tadzhikistan.
6 *Mitjaevia callosa* Dworakowska, 1980: 179; figs 263–272. India.
7 *Mitjaevia diana* (Distant, 1918: 100, *Typhlocyba*. India); Dworakowska 1970: 765; 1980: 179, figs 252–262, transferred to *Mitjaevia*. India, Kazakhstan.
8 *Mitjaevia elegantula* Dworakowska, 1994: 119; figs 415–425. India.
9 *Mitjaevia korolevskayae* Dworakowska, 1979: 44; figs 349–358. Vietnam.
10 *Mitjaevia maculata* (Ahmed, 1970b: 175; fig. 6: A–H, *Helionidia*. Pakistan); Dworakowska and Viraktamath 1975: 529, transferred to *Mitjaevia*. India.
11 *Mitjaevia nanaoensis* Chiang & Knight, 1990: 223; fig. 18: 1–7. China.
12 *Mitjaevia narzikulovi* Korolevskaya, 1976: 43; figs 1–6. Tadzhikistan.
13 *Mitjaevia notata* (Ahmed & Khokhar, 1971: 70; fig. 4a–f, *Helionidia*. Pakistan); Dworakowska 1980: 179, transferred to *Mitjaevia*. India.
14 *Mitjaevia protuberanta* Song, Li & Xiong, 2011: 27; figs 1–10. China.
15 *Mitjaevia shibingensis* sp. nov. China.
16 *Mitjaevia sikkimensis* Dworakowska, 1994: 119; figs 426–434. India.
17 *Mitjaevia dworakowskae* sp. nov. China.
18 *Mitjaevia tappana* Chiang & Knight, 1990: 224; fig. 19: 1–7. China.
19 *Mitjaevia wangwushana* Song, Li & Xiong, 2011: 29; figs 11–19. China.

Key to species of *Mitjaevia* from China (males)

1 Aedeagus with process.....**2**
– Aedeagus without process **3**
2 Processes arising from aedeagal shaft subbasally (Figs 42, 43) ...***M. protuberanta***
– Processes arising from aedeagal shaft subapically (Figs 44, 45) ....***M. wangwushana***
3 Aedeagus with shaft cylindrical, evenly tapered from base to apex (Figs 20, 34) **4**
– Aedeagus with shaft laterally compressed, abruptly tapered subapically to apex (Figs 45, 49) **5**
4 Style lateral lobe small (Fig. 18); aedeagal shaft tapered to narrowly rounded apex in lateral view (Fig. 20) .....***M. shibingensis* sp. nov.**
– Style lateral lobe large (Fig. 31); aedeagal shaft tapered to acute apex in lateral view (Fig. 34)..... ***M. dworakowskae* sp. nov.**
5 Subgenital plate with few long macrosetae; aedeagus as in Figs 48, 49 ....***M. nanaoensis***
– Subgenital plate with several long macrosetae; aedeagus as in Figs 46, 47..... .....***M. tappana***

***Mitjaevia shibingensis* sp. nov.**
http://zoobank.org/A8734F83-DBCD-4741-92C5-F2CF7AA083AC
Figs 1–7, 15–27

Description. Vertex pale yellow, with pair of small black apical spots and two irregular markings at sides of coronal suture (Figs 1, 3). Face pale brownish yellow, anteclypeus with apical half dark brown; frontoclypeus with brownish black patches at sides basally (Fig. 4). Pronotum mostly dark brown, with pair of symmetrical brownish yellow oval impressed patches medially, showing brownish yellow near anterior margin (Figs 1, 3). Scutellum orange yellow, with brown irregular elliptical spot at base medially (Figs 1, 3). Forewing with orangey and gray patches (Fig. 6).

Abdominal apodemes small, not extended to hind margin of 3rd sternite (Fig. 15). Male genitalia with subgenital plate relatively short, broadened basally, provided with two long macrosetae at midlength on lateral surface and numerous peg-like setae along dorsal margin basally to near midlength; several microsetae scattered on apical portion (Fig. 17). Style elongate, with subapical extension laterally, lateral lobe moderately large (Fig. 18). Aedeagal shaft narrow tapered to narrowly rounded apex in lateral view, gonopore arising near midlength on ventral surface; basal apodeme reduced; preatrium well developed (Figs 19, 20). Connective moderately broadly Y-shaped, central lobe well developed (Fig. 21). Female 7th sternite as in Fig. 24. Valvula I elongate, curved dorsad and evenly tapered from base to apex, finely strigate along dorsal margin of apical 1/5 (Fig. 25). Valvulae II elongate, slightly expanded blade-like to near apex, thereafter tapered to down-turned apex, with few dorsal roundish teeth distally on right branch (Fig. 26). Valvula III tapered distally to narrowly rounded apex (Fig. 27).

Measurement. Body length, males 2.6–2.8 mm, females 2.7–2.8 mm.

Specimen examined. ***Holotype*** ♂: China, Guizhou Prov., Shibing, 27 V 2019, coll. Zhouwei Yuan, Chao Tan and Xiaowei Yuan. ***Paratypes***: 14♂♂, 55♀♀, same data as holotype.

Remarks. This species has a similar shaped aedeagus to *M. korolevskayae* but the style has a preapical extension ("heel") and a smaller lateral lobe.

Etymology. The new species is named after its type locality: "Shibing", Guizhou Province.

***Mitjaevia dworakowskae* sp. nov.**
http://zoobank.org/AE8B70FC-D3C5-4F7E-ACA6-1B23044AAB49
Figs 8–14, 28–41

Description. Vertex light yellow, with two pairs of irregular black preapical spots distributed symmetrically (Figs 8, 10). Face milky yellow, anteclypeus with central area brownish; frontoclypeus with brownish black patches at sides basally (Fig. 11). Pronotum mostly black, with pair of symmetrical pale-yellow oval impressed patches medially, also showing pale yellow near anterior margin (Figs 8, 10). Scutellum milky

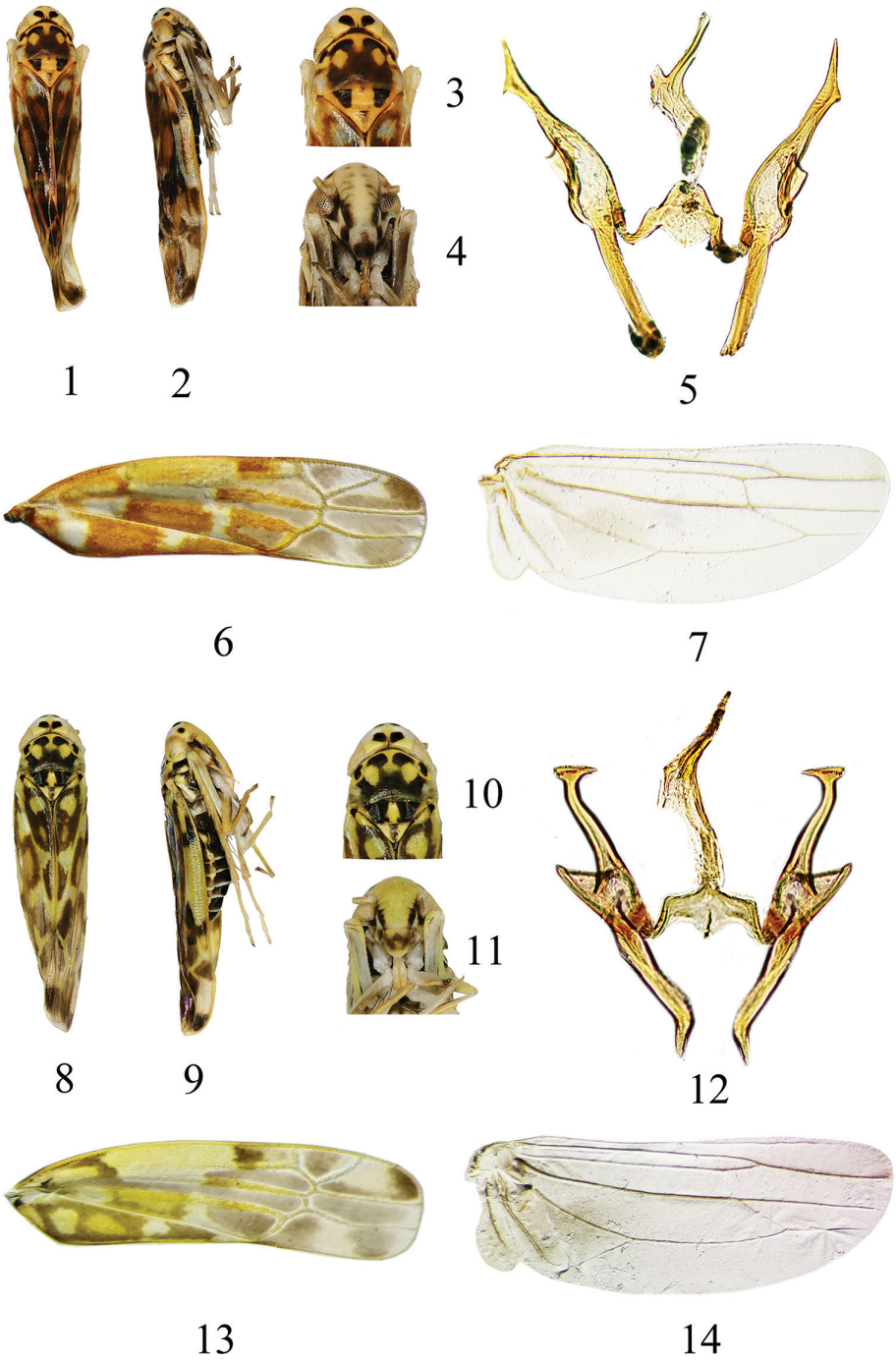

Figures 1–14. Species of *Mitjaevia* **1–7** *Mitjaevia shibingensis* sp. nov. **1** habitus, dorsal view **2** habitus, lateral view **3** head and thorax, dorsal view **4** face **5** style and connective, ventral view, aedeagus lateral view **6** forewing **7** hindwing **8–14** *Mitjaevia dworakowskae* sp. nov. **8** habitus, dorsal view **9** habitus, lateral view **10** head and thorax, dorsal view **11** face **12** style and connective, ventral view, aedeagus lateral view **13** forewing **14** hindwing.

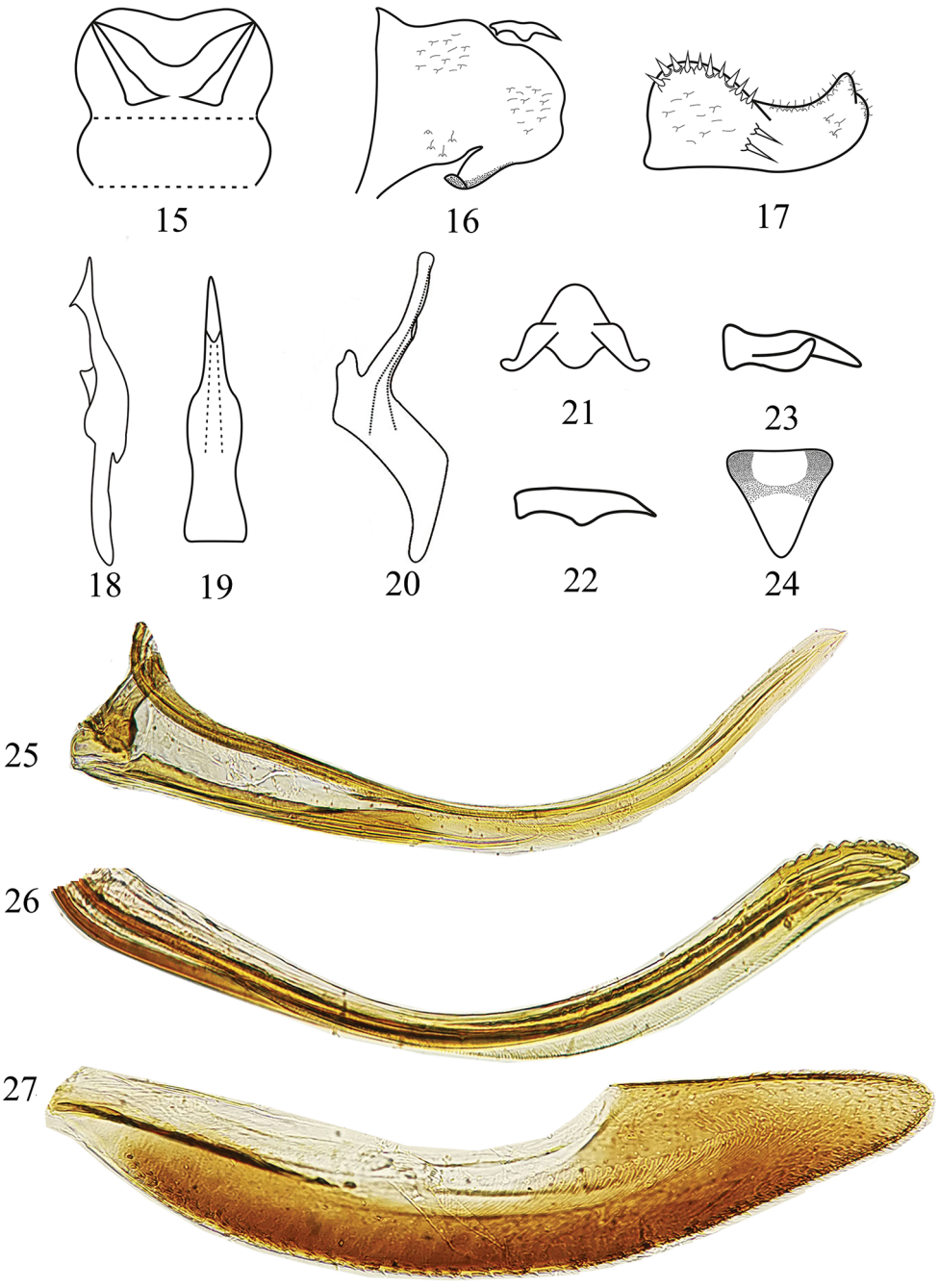

Figures 15–27. *Mitjaevia shibingensis* sp. nov. **15** abdominal apodemes **16** male pygofer, lateral view **17** subgenital plate, lateral view **18** style **19** aedeagus, ventral view **20** aedeagus, lateral view **21** connective **22** male pygofer dorsal appendage **23** male pygofer dorsal appendage **24** female 7th sternite **25** valvula I **26** valvulae II **27** valvula III.

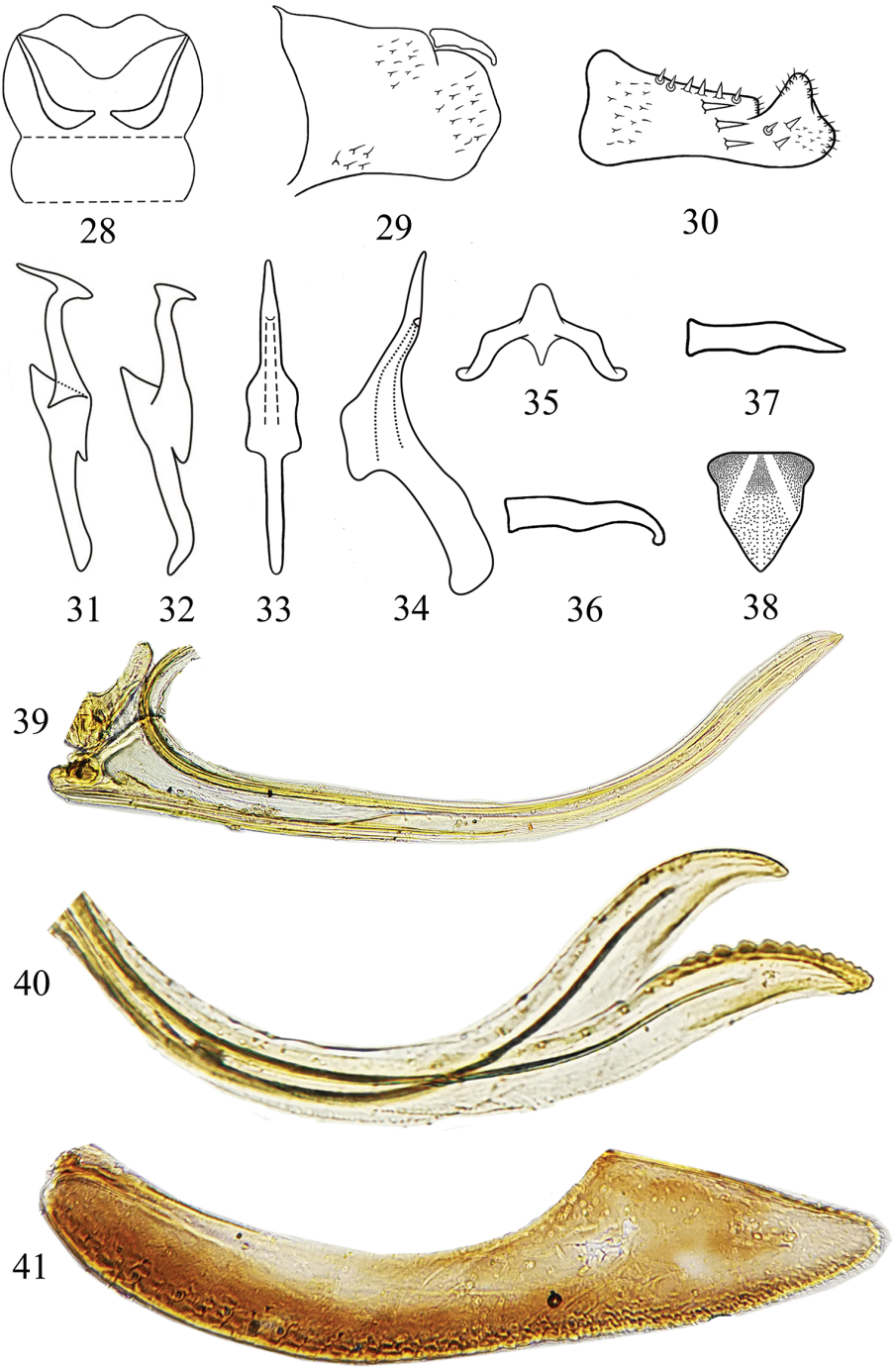

Figures 28–41. *Mitjaevia dworakowskae* sp. nov. **28** abdominal apodemes **29** male pygofer lobe, lateral view **30** subgenital plate **31** style **32** style **33** aedeagus, ventral view **34** aedeagus, lateral view **35** connective **36** pygofer dorsal appendage **37** pygofer dorsal appendage **38** female 7th sternite **39** valvula I **40** valvulae II **41** valvula III.

yellow, with longitudinal black stripe between scutellar suture and apex (Figs 8, 10). Forewing with brown and brownish yellow patches (Fig. 13).

Abdominal apodemes small, not extended beyond hind margin of 3rd sternite (Fig. 28). Male genitalia with subgenital plate laterally with 3 macrosetae at midlength and three more distal shorter macrosetae, dorsal peg-like setae restricted to central part (Fig. 30). Style elongate with preapical extension on inner surface, lateral lobe large (Figs 31, 32). Aedeagal shaft narrow slightly sinuate and tapered to acute apex in lateral view with gonopore arising near midlength of ventral surface; basal apodeme reduced (Figs 33, 34). Connective broadly Y-shaped, central lobe slender (Fig. 35). Female 7th as in Fig. 38. Valvulae as in previous species (Figs 39–41).

Measurement. Body length, males 2.3–2.4 mm, females 2.4–2.5 mm.

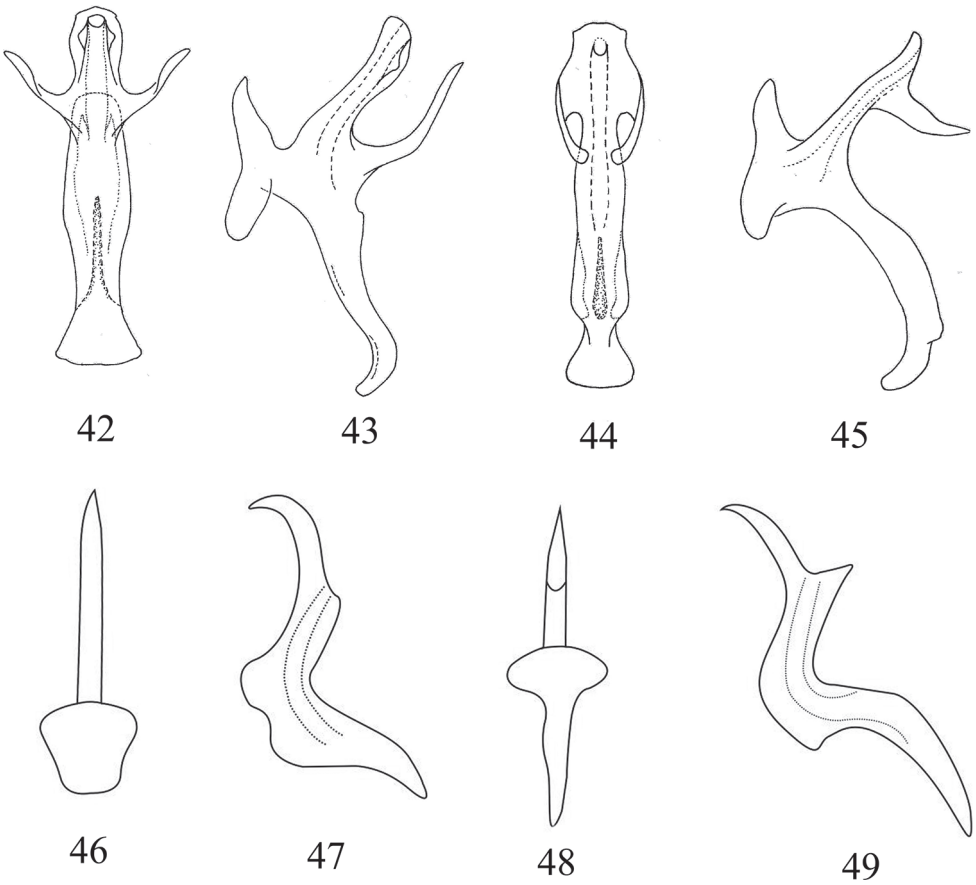

Figures 42–49. Species of Chinese *Mitjaevia* **42, 43** *M. protuberanta* Song, Li & Xiong **42** aedeagus, ventral view **43** aedeagus, lateral view **44, 45** *M. wangwushana* Song, Li & Xiong **44** aedeagus, ventral view **45** aedeagus, lateral view **46, 47** *M. tappana* Chiang & Knight **46** aedeagus, ventral view **47** aedeagus, lateral view **48, 49** *M. nanaoensis* Chiang & Knight **48** aedeagus, ventral view **49** aedeagus, lateral view (Figs **42–45**, from original; Figs **46–49**, redrawn from Chiang and Knight 1990).

Specimen examined. ***Holotype*** ♂: China, Guizhou Prov., Shibing, 27.V.2019, coll. Zhouwei Yuan, Chao Tan and Xiaowei Yuan. ***Paratypes***: 14♂♂, 19♀♀, same data as holotype.

Remarks. This species can be distinguished by the narrow and slightly sinuate aedeagal shaft in lateral view and the style with a subapical extension on the inner surface with a greatly enlarged lateral lobe.

Etymology. This species is named for Dr Irina Dworakowska in recognition of her immense contribution to taxonomy of World Typhlocybinae.

Acknowledgements

We thank Chandra Viraktamath for critically reading an early draft of the ms. The study was partly supported by the Guizhou Provincial Science and Technology Foundation ([2018]1411), the Guizhou Science and Technology Support Project ([2019]2855), the Science and Technology Project of Guiyang City ([2020]7–18), the Training Program for High-level Innovative Talents of Guizhou Province ([2016]4020), the Program for Academician Workstation in Guiyang University ([2019]5605), The World Top Discipline Program of Guizhou Province: Karst Ecoenvironment Sciences (No.125 2019 Qianjiao Keyan Fa) and the Project for Regional Top Discipline Construction of Guizhou Province: Ecology in Guiyang University (Qian Jiao Keyan Fa [2017]85).

References

Ahmed M (1970a) Studies of the genus *Erythroneura* Fitch (Erythroneurini: Cicadellidae) in West Pakistan. Pakistan Journal of Zoology 2(1): 29–42.

Ahmed M (1970b) Further studies on the leafhoppers of tribe Erythroneurini (Cicadellidae: Typhlocybinae) from West Pakistan. Pakistan Journal of Zoology 2(2): 167–184.

Ahmed M, Khokhar KF (1971) Genus *Helionidia* Zachvatkin (Erythroneurini-Cicadellidae) with four new species from West Pakistan. Sind University Research Journal 5(1): 63–72.

Chiang CC, Knight WJ (1990) Studies on Taiwanese Typhlocybinae (Homoptera: Cicadellidae) (IV) tribe Erythroneurini. Bulletin of the National Museum of Natural Science Number 2: 223–225.

Dietrich CH (2005) Keys to the families of Cicadomorpha and subfamilies and tribes of Cicadellidae (Hemiptera: Auchenorrhyncha). Florida Entomologist 88: 502–517. https://doi.org/10.1653/0015-4040(2005)88[502:KTTFOC]2.0.CO;2

Distant WL (1918) Rhynchota. VII. Homoptera: appendix. Heteroptera: addenda. The fauna of British India, including Ceylon and Burma. London, Taylor & Francis [VIII+] 210 pp.

Dlabola J (1961) Zikaden von Zentralasien, Dagestan und Transkaukasien (Homopt. Auchenorrhyncha). Acta Entomologica Musei Nationalis Pragae 34: 241–358.

Dlabola J (1964) Die Zikaden Afghanistans (Homoptera, Auchenorrhyncha II. Teil). Ergebnisse der Sammelreisen von Dr. H.G. Amsel, G. Ebert, Dr. Erichson, J. Klapperich und Dr. K. Lindberg. Mitteilungen der Münchner Entomologischen Gesellschaft 54: 237–255.

Dmitriev D (2020) An online interactive key and searchable database of Auchenorrhyncha (Hemiptera). http://dmitriev.speciesfile.org/

Dworakowska I (1970) On the genera *Asianidia* Zachv. and *Singapora* Mahm. with the description of two new genera (Auchenorrhyncha, Cicadellidae, Typhlocybinae). Bulletin de l'Academie Polonaise des Sciences, Serie des Sciences Biologiques 18(12): 759–765.

Dworakowska I (1979) On some Erythroneurini from Vietnam (Typhlocybinae, Cicadellidae). Annotationes Zoologicae et Botanicae 131: 44–45.

Dworakowska I (1980) On some Typhlocybinae from India (Homoptera, Auchenorrhyncha, Cicadellidae). Entomologische Abhandlungen Staatliches Museum für Tierkunde in Dresden 43(8): 151–201.

Dworakowska I (1994) Typhlocybinae (Auchenorrhyncha: Cicadellidae) of Sikkim, a preliminary survey. Folia Entomologica Hungarica Rovartani K zlem ények 55: 93–215.

Dworakowska I, Viraktamath CA (1975) On some Typhlocybinae from India (Auchenorrhyncha, Cicadellidae). Bulletin de l'Academie Polonaise des Sciences. (Serie des Sciences Biologiques) 23(8): 521–530.

Korolevskaya LL (1976) Leafhoppers of the genus *Mitjaevia* Dworakowska, I 1970 (Homoptera, Typhlocybinae) from Tadzhikistan. Izvestiia Akademii nauk Tadzhikskoi SSR (Otdelenie biologicheskikh nauk) 3(64): 41–44.

Mitjaev ID (1969) New species of leaf-hoppers (Homoptera, Cicadinea) from Tien Shan and Karatau. Zoologicheskii zhurnal 48(7): 1041–1047.

Sharma B (1984) On some Typhlocybinae from Kishtwar, Jammu & Kashmir (India), with description of five new species (Homoptera, Auchenorrhyncha, Cicadellidae). Reichenbachia 22(3): 31–40.

Song YH, Li ZZ (2013) Two new species of *Empoascanara* Distant (Hemiptera: Cicadellidae:Typhlocybinae) from Yunnan Province, China. Zootaxa 3637(1): 089–093. https://doi.org/10.11646/zootaxa.3637.1.11

Song YH, Li ZZ, Xiong KN (2011) Two new species of the genus *Mitjaevia* Dworakowska from China (Hemiptera: Cicadellidae: Typhlocybinae). Zootaxa 2805: 26–30. https://doi.org/10.11646/zootaxa.2805.1.2

ZooKeys 964: 41–107 (2020)
doi: 10.3897/zookeys.964.56131
https://zookeys.pensoft.net

REVIEW ARTICLE

A peer-reviewed open-access journal
ZooKeys
Launched to accelerate biodiversity research

A revision of the *Aleiodes bakeri* (Brues) species subgroup of the *A. seriatus* species group with the descriptions of 18 new species from the Neotropical Region

Scott R. Shaw[1], Eduardo M. Shimbori[2], Angélica M. Penteado-Dias[3]

1 *Department of Ecosystem Science and Management, University of Wyoming, Laramie, Wyoming 82071-3354, USA* **2** *ESALQ/USP, Departamento de Entomologia e Acarologia – LEA, Avenida Pádua Dias, 11 Piracicaba/SP, CEP 13418-900, Brazil* **3** *Universidade Federal de São Carlos, Rodovia Washington Luiz, km 235, CEP 13 565-905, São Carlos, SP, Brazil*

Corresponding author: Eduardo M. Shimbori (shimbori@usp.br)

Academic editor: Kees van Achterberg | Received 3 July 2020 | Accepted 22 July 2020 | Published 27 August 2020

http://zoobank.org/C84F8638-5169-4006-9E64-2CF6F560F4EE

Citation: Shaw SR, Shimbori EM, Penteado-Dias AM (2020) A revision of the *Aleiodes bakeri* (Brues) species subgroup of the *A. seriatus* species group with the descriptions of 18 new species from the Neotropical Region. ZooKeys 964: 41–107. https://doi.org/10.3897/zookeys.964.56131

Abstract

The *Aleiodes bakeri* (Brues) species subgroup of the *A. seriatus* species group is defined based on two previously described species, *A. bakeri* and *A. nigristemmaticum* (Enderlein), and is greatly expanded in this paper with an identification key, descriptions, and illustrations of 18 new species from the Neotropical Region: *A. andinus* Shaw & Shimbori, **sp. nov.**; *angustus* Shimbori & Shaw, **sp. nov.**; *asenjoi* Shimbori & Shaw, **sp. nov.**; *bahiensis* Shimbori & Shaw, **sp. nov.**; *barrosi* Shimbori & Shaw, **sp. nov**.; *brevicarina* Shimbori & Shaw, **sp. nov.**; *coariensis* Shimbori & Shaw, **sp. nov.**; *goiasensis* Shimbori & Shaw, **sp. nov**.; *gonodontivorus* Shaw & Shimbori, **sp. nov.**; *hyalinus* Shimbori & Shaw, **sp. nov.**; *inga* Shimbori & Shaw, **sp. nov.**; *joaquimi* Shimbori & Shaw, **sp. nov.**; *lidiae* Shimbori & Shaw, **sp. nov.**; *mabelae* Shimbori & Shaw, **sp. nov.**; *maculosus* Shimbori & Shaw, **sp. nov.**; *ovatus* Shimbori & Shaw, **sp. nov.**; *santarosensis* Shaw & Shimbori, **sp. nov.**; and *taurus* Shimbori & Penteado-Dias, **sp. nov.** It is hypothesized that the *A. bakeri* species subgroup is a monophyletic lineage within the larger and probably artificial *A. seriatus* species group (those *Aleiodes* with a comb of flat setae at the apex of the hind tibia), and can be distinguished from other members of the *seriatus* group by having the hind wing vein r present, although weakly indicated; the hind wing marginal cell suddenly widened at junction of veins RS and r; the subbasal cell of the fore wing mostly glabrous but often with two rows of short setae subapically; glabrous regions of the wings also commonly found in the first subdiscal, discal, and basal cells of the fore wing, and the basal cell of hind wing; ocelli quite large, with the width of a lateral ocellus being distinctly larger than the ocellar-

ocular distance; and being relatively large *Aleiodes* species with body almost entirely brownish yellow or reddish brown. In addition, a new replacement name, *Aleiodes buntikae* Shimbori & Shaw, **nom. nov.**, is proposed for the species formerly called *Aleiodes* (*Hemigyroneuron*) *bakeri* Butcher & Quicke, 2011.

Keywords
Aleiodini, Erebidae, koinobionts, parasitoid wasps, taxonomy

Introduction

Aleiodes Wesmael (Hymenoptera: Braconidae: Rogadinae; tribe Aleiodini) is the most common and species-rich rogadine genus worldwide (S.R. Shaw et al. 1997; Areekul-Butcher and Quicke 2011; Shimbori and S.R. Shaw 2014; van Achterberg et al. 2020). *Aleiodes* species are sometimes commonly called "mummy wasps" (S.R. Shaw 2006) because of their peculiar and distinctive habit of pupating inside the remains of the host caterpillar, which shrinks and dries into a distinctive caterpillar "mummy" (M.R. Shaw 1983, 1994; M.R. Shaw and Huddleston 1991; S.R. Shaw et al.1997; S.R. Shaw 2006; Zaldívar–Riverón et al. 2008; Shimbori and S.R. Shaw 2014). There are at least 212 named *Aleiodes* species described from the New World Region, of which at least 143 occur in the Nearctic Region and 108 in the Neotropical Region (Yu et al. 2012; Garro et al. 2017). The larger number of named species in Nearctic Region is most likely due to more research effort in this region (S.R. Shaw et al. 1997, 1998a, 1998b, 2006, 2013; Marsh and S.R. Shaw 1998, 1999, 2001, 2003; Fortier 2009), rather than any particular biological process (Quicke 2012). However, the number of known *Aleiodes* species from the Neotropical Region has been rising with increasing discovery and focus of studies of the tropical fauna (S.R. Shaw 1993; Townsend and S.R. Shaw 2009; Shimbori and Penteado-Dias 2011; Shimbori and S.R. Shaw 2014; Shimbori et al. 2015; Garro et al. 2017).

Due to the high diversity of species in this genus, revisionary studies of *Aleiodes* have progressed in recent years by defining and examining species groups (S.R. Shaw et al.1997, 1998a, 1998b, 2006, 2013; S.R. Marsh and Shaw 1998, 1999, 2001, 2003; Fortier 2009; Townsend and S.R. Shaw, 2009; Shimbori and S.R. Shaw 2014). S.R. Shaw et al. (1997) divided *Aleiodes* into 15 species groups, with two additional groups proposed after additional phylogenetic analyses (Fortier and S.R. Shaw 1999) plus one subgenus (Shimbori et al. 2016). One of these, the *A. seriatus* species group, was the initial focus for this study. Marsh and S.R. Shaw (1998) defined the *A. seriatus* species group as comprising those *Aleiodes* species with a row (or comb) of flattened setae at the apex of the hind tibia on the inner side (Fig. 3). Marsh and S.R. Shaw (1998) circumscribed the *A. seriatus* species group as including *Aleiodes seriatus* (Herrich-Schäffer), eight other named species, and five new species from the Nearctic Region. Subsequently, studies by Townsend and S.R. Shaw (2009) Shimbori and S.R. Shaw (2014) proposed additional new species of the *A. seriatus* species group, and indicated that the group may be particularly diverse in the neotropics. Phylogenetic research by Fortier (1999) supports the hypothesis that the *A. seriatus* species group

is a monophyletic group as defined by Marsh and S.R. Shaw (1998) and Fortier and S.R. Shaw (1999), although some subsequent studies suggest that similarly appearing combs of flat setae may have evolved independently in some other lineages within Aleiodini (Areekul-Butcher and Quicke 2012; van Achterberg and M.R. Shaw 2016). For example, a molecular phylogeny for Thai species of *Aleiodes*, based solely on the DNA barcoding region of the gene COI, recovered at least two separate lineages where the specialized comb of setae is present, one of which is paraphyletic (Areekul-Butcher and Quicke 2012). Additionally, the Neotropical subgenus *Athacryvac* (Braet & van Achterberg), which is morphologically distinct from any of the species groups previously defined, and is clearly independent from the *A. seriatus* species group, also exhibits a distinct comb of specialized setae on hind tibia reinforcing the homoplasious nature of this character (Shimbori et al. 2016). For the Palearctic fauna, van Achterberg and M.R. Shaw (2016) adopted a different system of division, including overall less species groups when compared with the division based on the Nearctic fauna (S.R. Shaw et al. 1997). Further supported by a molecular phylogeny, also based on DNA barcoding, the system circumscribes six or seven species groups, comprising most of the Palearctic species, but with several species left outside species groups because their relationships are not yet resolved (van Achterberg et al. 2020).

Some confusion could result since a similar comb of flat hind tibial setae has also evolved in some genera of the tribe Rogadini such as *Rogas* Nees, *Triraphis* Ruthe, *Cystomastax* Szepligeti, and *Macrostomion* Szeplegeti. It is therefore important that specimens are carefully identified as belonging to the genus *Aleiodes* first, using identification keys such as those of van Achterberg (1991) or S.R. Shaw (1997), before applying the species-group concepts used within *Aleiodes.* Additional care must be taken when examining specimens for the presence or absence of the comb of flattened setae on the hind tibia, not only because this feature is microscopically small but also because it only occurs on the inner side, and on the hind tibia only (not on the middle tibia). Despite these challenges, the row of flattened setae along the inner margin of the hind tibia has proven to be a consistently valuable characteristic for recognizing members of the *A. seriatus* species group from the Neotropical Region, where the group appears to be quite diverse (but see Braet and van Achterberg (2011) and Shimbori et al. (2016) for a distinction between the *A. seriatus* species group and the subgenus *Athacryvac*).

During our studies we discovered that many of the more commonly encountered specimens of the *A. seriatus* species group from the Neotropical Region fall into a particular presumed lineage characterized by having the hind wing vein r present (as in Figs 1, 23); the marginal cell suddenly widened at junction of veins RS and r (as in Figs 1, 2, 23), the subbasal cell of the fore wing mostly glabrous (as in Figs 2, 27) and usually with two rows of short setae subapically (as in Figs 2, 32), glabrous areas in the first subdiscal, discal, and basal cells of the fore wing (as in Fig. 2) and the basal cell of hind wing (as in Figs 2, 28), ocelli large to enormous (as in Figs 7, 9, 15, 20, 24, 26, 30, 36, 38, 45, 49, 52, 57, 61, 65, 67, 70, 74, 77, 80), with the width of lateral ocellus being distinctly larger than the ocellar-ocular distance (at least 1.8–9.0 × larger), tarsi with well-developed apical spines (as in Fig. 40), and being relatively large specimens with body almost entirely

brownish yellow (as in Figs 18, 22, 34, 41, 51, 59, 64, 69, 81) or reddish brown (as in Figs 29, 48, 55, 73). The oldest available name for a species in this distinctive lineage is *Aleiodes bakeri* (Brues), therefore in this paper we propose to call this presumed lineage the *Aleiodes bakeri* (Brues) species subgroup of the *A. seriatus* species group. A technical argument might be made that since "species groups" are informal constructs that merely designate groups of similar or related species, this lineage might be equally well called a "species group" but we prefer the term "subgroup" to remind the reader that this is a cluster of species within a previously named species group (the *A. seriatus* species group).

Although *Aleiodes bakeri* (Brues) was described and named more than a century ago, and is among the commonest of species covered in this manuscript, its identity and relationships to other species have remained largely obscure. A closely related species, *Aleiodes nigristemmaticum* (Enderlein) is the only other previously named species in this subgroup, and the only one to extend its range into the southern parts of the Nearctic Region (Marsh and S.R. Shaw 1998). Otherwise the species subgroup is found exclusively in the neotropics. In this paper, we describe and name 18 other new species of the *Aleiodes bakeri* (Brues) species subgroup of the *A. seriatus* species group.

Materials and methods

For identification of the braconid subfamily Rogadinae see van Achterberg (1993) or Sharkey (1997). For recognition of rogadine genera refer to the identification keys of van Achterberg (1991) or S.R. Shaw (1997). The definition of *Aleiodes* adopted here follows that of van Achterberg (1991), S.R. Shaw (1993, 1997, 2006), and S.R. Shaw et al. (1997). Species groups within *Aleiodes* have been defined and clarified by S.R. Shaw et al. (1997), Marsh and S.R. Shaw (1998), Fortier and S.R. Shaw (1999), Zaldívar–Riverón et al. 2008, and Townsend and S.R. Shaw (2009); although for the Western Palearctic fauna van Achterberg and M.R. Shaw (2016) and van Achterberg et al. (2020) divided the genus along different lines.

Morphological terminology for descriptions follows that of Sharkey and Wharton (1997), S.R. Shaw et al. (1997), Shimbori et al. (2015, 2016), and Garro et al. (2017). Microsculpture terminology follows that of Harris (1979). Wing vein terminology follows the system adopted by Sharkey and Wharton (1997) (see Figs 1, 2). The term "inclivous" is applied to describe the orientation of the vein fore wing 2CUa, where the more transverse (= vertical) veins are considered less inclivous. Measurements were taken following Shimbori et al. (2016), except for the pronotal collar length, which refers to the median length of pronotum in dorsal view. We follow Karlsson and Ronquist (2012) in defining the mesosomal area just lateral to the mesoscutellar disc (or scutellum) as the "mesoscutellar trough". The occipital carina in this group of species (and in *Aleiodes* in general) is either complete (as in Fig. 7) or interrupted mid-dorsally (as in Fig. 15). In some cases, among other species of the *A. seriatus* species group not treated in this paper, the interruption in the occipital carina is accompanied by a deviation of the carina toward the ocelli and/or an indentation on the occiput, therefore the

descriptions use the terms "occiput indented"(or not) medially, and "occipital carina curved" (or not) towards the ocelli. Abbreviations used throughout the descriptions are as follows:

OOL distance between eye and lateral ocellus
OD diameter of lateral ocellus
POL distance between lateral ocelli
T1 metasomal tergite 1
T2 metasomal tergite 2
T3 metasomal tergite 3

A number of specimens from Área de Conservación Guanacaste (ACG) in Costa Rica had sequences of the COI DNA barcoding region generated by standard protocols for the ACG barcode inventory, which are described in detail by Smith et al. (2007, 2008). All sequences are deposited in the Barcode of Life Data System (BOLD, http://www.boldsystems.org; Ratnasingham and Hebert 2007), and access codes are provided for each barcoded specimen.

Examined specimens and types are deposited at the following collections:

CNCI Canadian National Collection, Ottawa, Canada
DCBU Coleção Entomológica do Departamento de Ecologia e Biologia Evolutiva da Universidade Federal de São Carlos, São Carlos, Brazil
DZUP Coleção Entomológica Padre Jesus S. Moure, Departamento de Zoologia da Universidade Federal do Paraná, Curitiba, Brazil
INBIO Instituto Nacional de Biodiversidad, Santo Domingo de Heredia, Costa Rica
MCZC Museum of Comparative Zoology, Harvard University, Cambridge, USA
MUSM Colección de Entomologia del Museo de Historia Natural de La Universidad Nacional Mayor de San Marcos, Lima, Peru
MZUSP Museu de Zoologia da Universidade de São Paulo, São Paulo, Brazil
PASW Polish Academy of Sciences, Warsaw, Poland
UFES Coleção de Insetos do Departamento de Ciências Biológicas da Universidade Federal do Espírito Santo, Vitória, Brazil
UPP University of Pennsylvania, Philadelphia, USA
UWIM University of Wyoming Insect Museum, University of Wyoming, Laramie, USA

Aleiodes bakeri species subgroup of the *seriatus* species group

Included species

Aleiodes bakeri (Brues, 1912); *nigristemmaticum* (Enderlein, 1920); *andinus* Shaw & Shimbori, sp. nov.; *angustus* Shimbori & Shaw, sp. nov.; *asenjoi* Shimbori & Shaw, sp. nov.;

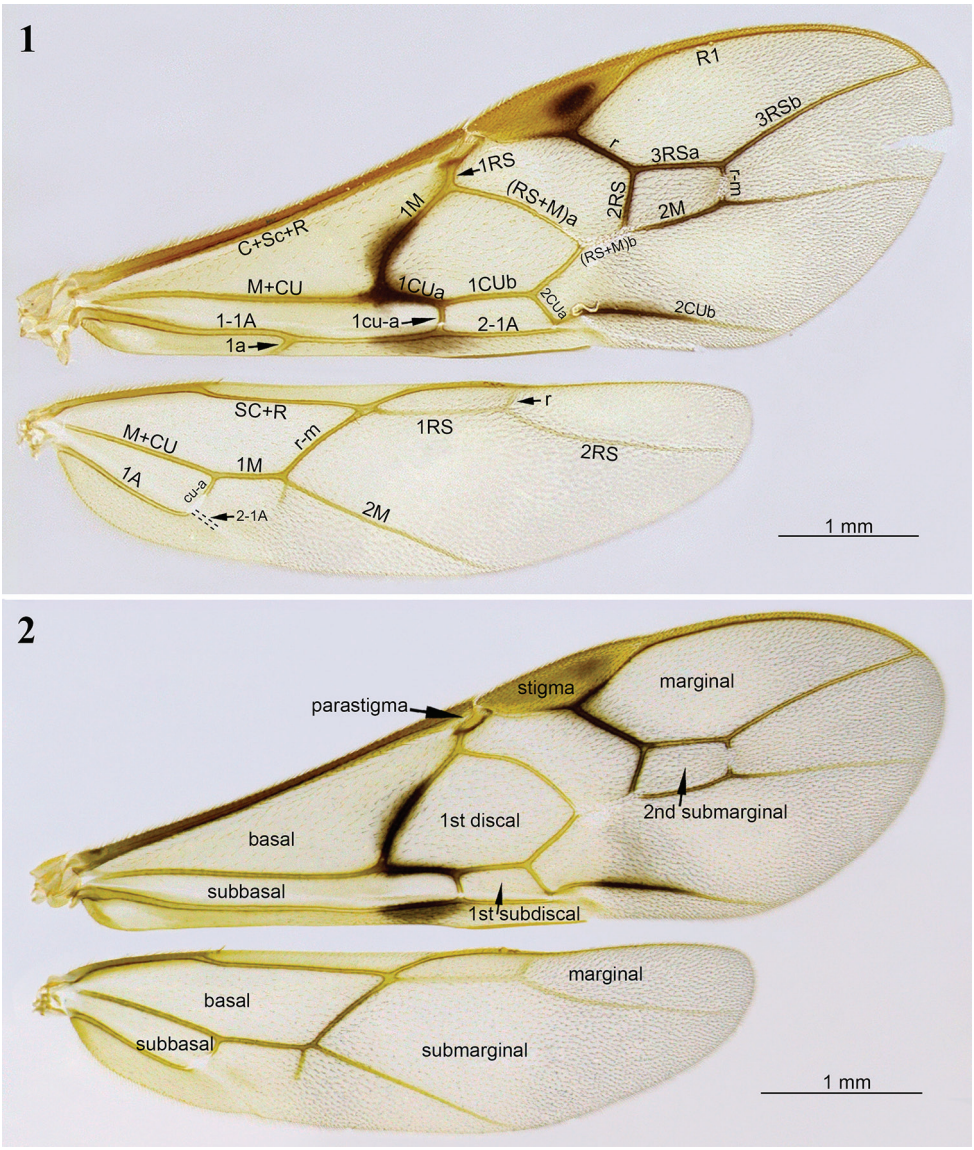

Figures 1, 2. *Aleiodes bakeri* (Brues) species subgroup. **1** Wings with principal veins labelled **2** wings with principal cells labelled.

bahiensis Shimbori & Shaw, sp. nov.; *barrosi* Shimbori & Shaw, sp. nov.; *brevicarina* Shimbori & Shaw, sp. nov.; *coariensis* Shimbori & Shaw, sp. nov.; *goiasensis* Shimbori & Shaw, sp. nov.; *gonodontivorus* Shaw & Shimbori, sp. nov.; *hyalinus* Shimbori & Shaw, sp. nov.; *inga* Shimbori & Shaw, sp. nov.; *joaquimi* Shimbori & Shaw, sp. nov.; *lidiae* Shimbori & Shaw, sp. nov.; *mabelae* Shimbori & Shaw, sp. nov.; *maculosus* Shimbori & Shaw, sp. nov.; *ovatus* Shimbori & Shaw, sp. nov.; *santarosensis* Shaw & Shimbori, sp. nov.; and *taurus* Shimbori & Penteado-Dias, sp. nov.

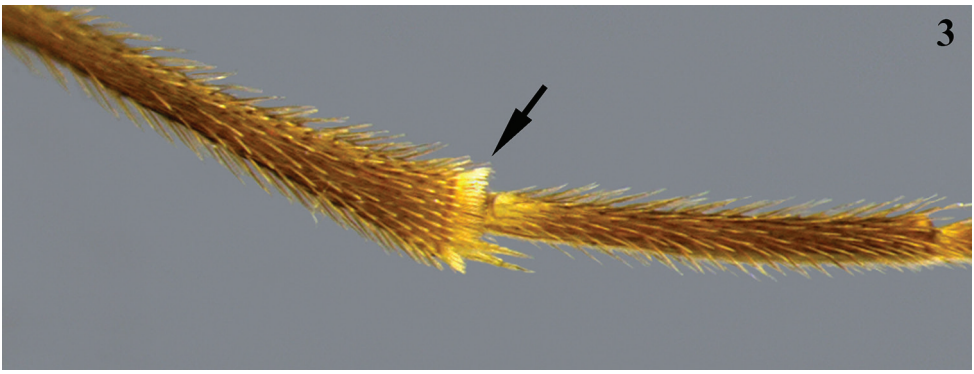

Figure 3. Inner side of hind tibia showing the comb of specialized setae apically (arrow) – *Aleiodes* sp.

Species subgroup diagnosis

Hind tibia with row of flattened setae along inner margin (as in Fig. 3). Hind wing vein r present, usually weakly indicated (Figs 1, 23); marginal cell suddenly widened at junction of veins RS and r (Figs 1, 2, 23). Subbasal cell of fore wing mostly glabrous (Figs 2, 27, 47, 50, 54, 63, 75), usually with two rows of short setae subapically (Figs 2, 32). Glabrous regions on the wings are also commonly found in the first subdiscal, discal and basal cells of the fore wing (Fig. 2) and the basal cell of hind wing (Figs 2, 28). Ocelli large to enormous (Figs 7, 9, 15, 20, 24, 27, 30, 36, 38, 45, 49, 52, 57, 61, 65, 67, 70, 77, 80), with the width of lateral ocellus being distinctly larger than the ocellar-ocular distance (at least 1.8–9.0 × larger). Tarsi with well-developed apical spines (as in Fig. 40). Relatively large specimens with body almost entirely brownish yellow (as in Figs 18, 22, 34, 41, 51, 59, 64, 69, 81) or reddish brown (as in Figs 29, 48, 55, 73).

Distribution

Known only from the New World with most species occurring in the Neotropical parts of South America and Central America. The northern limits of the group are set by a few species that occur in Mexico, parts of the Caribbean, and southern Florida. Species of this group have been recorded from the following countries: Bolivia, Brazil, Colombia, Costa Rica, Cuba, Dominican Republic, Ecuador, Honduras, Mexico, Panama Peru, southeastern USA (Florida), Suriname, and Venezuela.

Biology

As far as known, species of this group are koinobiont endoparasitoids of Noctuoidea caterpillars, with all confirmed hosts of three of the treated species being from the family Erebidae (subfamilies Calpinae, Eulepidotinae and Erebinae). They have been reared from mummified caterpillars of several erebid species including hosts of economical relevance (i.e., *Mocis latipes* (Guenée), an occasional pest of pasture).

Comments

We propose that the presence of the vein r on hind wing is a putative synapomorphy of this monophyletic group of species within the larger *seriatus* species group.

Results

Key to species of the *Aleiodes bakeri* species subgroup

1 Occipital carina interrupted mid-dorsally (as in Figs 24, 65); subbasal cell of fore wing usually with sparse setae basally (as in Figs 2, 23) **2**

– Occipital carina complete dorsally (as in Figs 7, 36, 57); subbasal cell of fore wing rarely with setae basally (as in Figs 32, 75) **5**

2 Fore wing vein 1a absent (as in Figs 2, 23); hind femur honey yellow to orange-brown (as in Fig. 22) **3**

– Fore wing vein 1a present and tubular (as in Figs 1, 12); hind femur orange-brown with infuscate apex (as in Figs 8, 14) **4**

3 Fore wing second submarginal cell comparatively short (Figs 2, 23), vein 3RSa approx. as long as vein r; flagellum entirely the same color, varying from yellow to light brownish orange (Figs 21, 22) ..... ***A. bakeri*** **Brues**

– Fore wing second submarginal cell longer (Fig. 64), vein 3RSa more than 2.0 × longer than vein r; flagellum black at base, gradually lightening toward yellow apex (Fig. 64) ..... ***A. mabelae*** **sp. nov.**

4 Basal polished triangular area of T1 long, distinctly extending over dorsal surface (Fig. 7). Females with large ovipositor, sheaths 1.4 × longer than hind basitarsus (Figs 8, 11); division of T2 and 3 weak, T3 weakly granulate and without longitudinal carina (Fig. 10) ..... ***A. angustus*** **sp. nov.**

– Basal triangular area of T1 short, not extending dorsally (Fig. 16). Females with ovipositor sheaths 0.5–0.7 × longer than hind basitarsus (Figs 14, 17); T2 and T3 divided by deep and crenulate sulcus, T3 striate and with longitudinal carina on basal 0.75 (Fig. 16) ..... ***A. asenjoi*** **sp. nov.**

5 Hind tibia whitish yellow basally and dark brown or black apically, fore and mid tibia basally or entirely whitish yellow; all tarsomeres 1–4 whitish yellow (Figs 29, 55, 77); body reddish brown or brownish orange (Figs 29, 55–57, 73) **6**

– Hind tibia and tarsi usually entirely brownish yellow, if tibia basally and tarsomeres 1–4 whitish yellow, then apex of hind tibia not dark brown and body brownish yellow (Fig. 25) **9**

6 Thorax mottled light pale yellow and brown (Fig. 66), mesoscutum pale yellow contrasting with brown tegula and scutellum (Fig. 67) ..... ***A. maculosus*** **sp. nov.**

– Thorax entirely dark reddish brown (Fig. 55) or brownish orange; mesoscutum, scutellum and tegula of similar dark color (Figs 57, 74) **7**

7 Fore wing with distinct, rounded infuscate spot around veins 1M and 1CUa (Fig. 75); head light yellow, but brown at lower face and dark brown at vertex and around occipital carina (Fig. 74); palpi dark brown (Fig. 74) ..***A. ovatus* sp. nov.**

– Fore wing without distinct infuscate spot but basal half of vein 1M infuscate (Fig. 32); head entirely dark reddish brown to yellowish brown, including palpi (Fig. 29) **8**

8 Fore wing first discal cell evenly, rather densely setose (Fig. 32); basal cell mostly setose but less densely than first discal cell (Fig. 32). Hind tibia and femur dark brown apically (Fig. 29). Fore wing with distinct infuscate area present at basal half of vein 1M (Fig. 32). Hind wing vein 2-1A absent (Fig. 31) ..... ***A. brevicarina* sp. nov.**

– Fore wing discal cell with distinct glabrous spot along veins 1M and 1CU; basal cell mostly glabrous, setose below costal vein and anteriorly near vein 1M. Fore wing without infuscate spots (Fig. 55). Hind wing vein 2-1A present, although short (Fig. 58) ..... ***A. joaquimi* sp. nov.**

9 First subdiscal cell of fore wing widening apically and relatively long (Fig. 28); vein 1CUb ~ 1.7–2.2 × longer than 1CUa. Vein 2CUa strongly inclivous, vein 1CUa 0.9–1.2 × longer than 2CUa (Figs 27–28) .....***A. barrosi* sp. nov.**

– First subdiscal cell of fore wing not widening apically and shorter; vein 1CUb 1.00–1.25 × longer than 1CUa. Vein 2CUa less inclivous, vein 1CUa 1.5–2.0 × longer than vein 2CUa **10**

10 Antenna entirely yellowish (as in Fig. 18)..... **11**

– Antenna dark brown basally, apically light brown to yellow (as in Figs 33, 34); rarely flagellum mostly yellowish with few basal segments slightly darker, but at least pedicel dark brown and scape with lateral brown patch **13**

11 All wing veins evenly brown, membrane hyaline without distinct infuscate patches around veins (Fig. 51) ..... ***A. hyalinus* sp. nov.**

– Veins 1M, 1CUa, and part of 2CUb dark brown, darker than remaining veins, membrane around these veins, and below vein 1-1A apically, at least weakly infuscate (as in Figs 19, 78) **12**

12 All legs with tarsomeres 1–4 and at least base of tibiae whitish yellow, contrasting with brownish orange femur (Fig. 76) ..... ***A. santarosensis* sp. nov.**

– Legs honey yellow (Fig. 18) ..... ***A. bahiensis* sp. nov.**

13 All femora dark brown apically (Fig. 34). Stigma mostly dark brown, yellow at basal and apical tips (Fig. 35) ..... ***A. coariensis* sp. nov.**

– Fore and mid femora yellow, hind femur sometimes mostly dark brown. Stigma mostly or entirely yellow (Fig. 4) **14**

14 Flagellum with two colors, black basally and yellow apically, not gradually lighter, usually with one "transitional" flagellomere, lighter than basal and darker than apical flagellomeres (Fig. 4). Ovipositor sheaths variable, most species with rounded apex and apical point (Figs 46, 62, 82) but some with sheaths truncated apically, without point **15**

– Flagellum gradually lightening toward apex. Ovipositor sheaths truncated apically, without point (as in Fig. 40)..... **18**

15 Basal cell of fore wing evenly, rather densely setose, without large glabrous spots (Fig. 6). Ovipositor sheaths truncated apically, without point (Fig. 5)... .....***A. andinus* sp. nov.**

– Basal cell of fore wing largely glabrous (Fig. 59), with few sparse setae. Ovipositor sheaths with distinct point apically (Figs 62, 82).....**16**

16 Frons entirely rugulose (Fig. 80); second submarginal cell long and rectangular (Fig. 83), vein 3RSa 2.1 × longer than 2RS; median carina of propodeum defined at basal 0.3, effaced in posterior 0.7 (Fig. 84) .....***A. taurus* sp. nov.**

– Frons shiny coriaceous (Figs 60, 61), sometimes with longitudinal rugae medially; second submarginal cell shorter and trapezoidal (Fig. 59), vein 3RSa ~ 1.4–1.7 × longer than 2RS; median carina of propodeum complete or nearly so.....**17**

17 Hind femur mostly dark brown (Fig. 59); dark markings around veins 1M/1CUa and vein r conspicuous (Fig. 63), veins dark brown and wing membrane clearly infuscate around veins. Diameter of lateral ocellus 2.4–2.5 × distance between ocelli (Fig. 61). Scape shorter, 1.7–1.9 × longer than pedicel (Fig. 60).....***A. lidiae* sp. nov.**

– Hind femur brownish yellow (Fig. 41); veins 1M/1CUa and vein r faintly darker, membrane around veins not distinctly infuscate (Figs 44, 47). Diameter of lateral ocellus 2.9–3.8 × distance between ocelli (Fig. 45). Scape longer, 2.5–2.6 × longer than pedicel (Figs 42–43) ....***A. gonodontivorus* sp. nov.**

18 Second submarginal cell of fore wing long, vein 3RSa ~ 2.0 × longer than 2RS (Fig. 54). Frons without distinct lateral carina (Fig. 52) .....***A. inga* sp. nov.**

– Second submarginal cell short, vein 3RSa 1.3–1.5 × longer than vein 2RS (Figs 39, 71). Frons with distinct lateral carina (Figs 38, 70).....**19**

19 Occipital carina in dorsal view distinctly curved medially, carina weaker mid-dorsally (Fig. 38). Vertex rugose-granular (Fig. 38). Fore wing vein r ~ 1.5 × longer than vein 2RS (Fig. 39) ..... ***A. goiasensis* sp. nov.**

– Occipital carina straight or weakly bent mid-dorsally (Fig. 70). Vertex weakly granular-coriaceous (Fig. 70). Fore wing vein r 1.0–1.1 × longer than vein 2RS (Fig. 71) .....***A. nigristemmaticum* Enderlein**

Species descriptions

***Aleiodes andinus* Shaw & Shimbori, sp. nov.**
http://zoobank.org/095E7E57-B313-4549-BFC8-97F655CD97AA
Figs 4–7

Type material. Holotype, female (MUSM) "PERU: CUSCO, La Convención, Echarate, C. Segakiato. 11°45'38.6"S, 73°14'57.7"W 908m. 01.ii.2011. M. Alvarado & E Rázuri."

Description. Body length 8.1 mm. Fore wing length 6.4 mm.

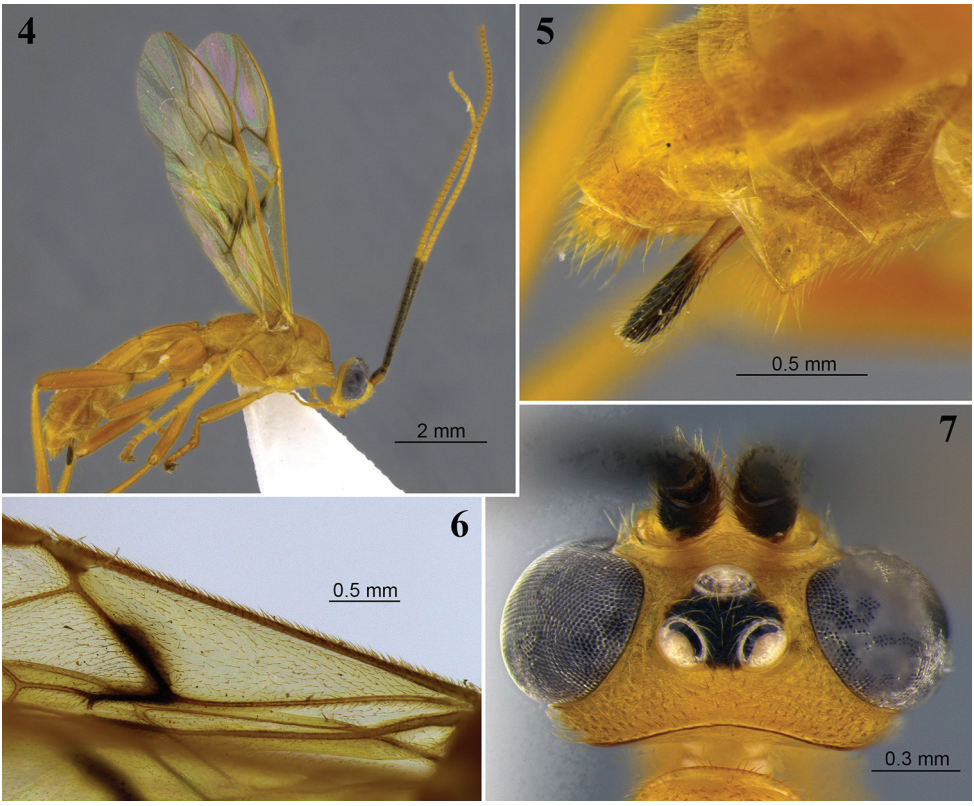

Figures 4–7. *Aleiodes andinus* sp. nov. **4** lateral habitus **5** apex of metasoma and ovipositor, lateral view **6** basal cell of fore wing showing dense setae **7** head, dorsal view.

Head. In dorsal view eye length/temple 4.0. Eye height/head width 0.4. Eye height/minimum distance between eyes 1.1. OD/POL 2.2. OD/OOL 2.4. Frons excavated. Frons lateral carina present. Occipital carina dorsally complete, weakly curved. Occiput in dorsal view nearly straight, not indented medially. Occipital carina ventrally meeting hypostomal carina. Mid-longitudinal crest at upper face present. Hypoclypeal depression/face width 0.33. Malar space/eye height 0.19. Face height/width 0.7. Clypeus height/width 0.66. Clypeus convex, granulate. Sculpture of head mostly shiny granulate. Face weakly rugose, transversely rugose-striate around median crest.

Antenna. Antennal segments 55. Antenna/body length 1.2. Scape/pedicel length 2.3. Length of first/second flagellomere 1.2. Fourth flagellomere length/apical width 1.7. Tip of apical segment of antenna pointed.

Mesosoma. Length/height ~ 1.6. Width of mesoscutum/width of head 0.7. Mesoscutum length/width ~ 1.1. Pronotal collar/vertex 0.7. Prescutellar sulcus with complete median carina, rugose laterally without distinct lateral carinae. Mesoscutum posterior border with distinct complete carina. Metanotum with mid-longitudinal carina complete, connecting to a carinate pit posteriorly, carina bisecting posterior pit, although weaker posteriorly. Metanotum mid-pit present, delimited by carinae.

Mid-longitudinal carina of propodeum present at basal 0.7, absent posteriorly. Ventral mid-line of mesopleuron set within shallow smooth sulcus; pit at ventral mid-line absent. Notauli weakly indicated anteriorly, indistinctly crenulate. Sternaulus weakly indicated anteriorly, rugose. Sculpture of mesosoma mostly granulate. Pronotum rugose laterally, or granulate ventrally, pronotal groove crenulate anteriorly, short subventral longitudinal carina present. Mesopleuron rugose below subalar groove. Subalar groove crenulate. Mid-posterior region of mesoscutum rugose. Mesoscutellar trough entirely costate. Metanotum mostly smooth and weakly crenulate. Propodeum mostly rugose.

Wings. Fore wing: Stigma length/height 3.4. Vein r/2RS 1.3. Vein r/RS+Mb 1.2. Vein 3RSa/2RS 1.8. Vein 3RSa/2M 0.83. Vein 3RSa/3RSb 0.46. Vein 1CUa/1CUb 1.0. Vein 1CUa/2CUa 2.1. Vein 1cu-a weakly inclivous. Vein 1M nearly straight. Vein RS+Ma virtually straight. Vein M+CU weakly sinuate. Vein 1-1A very weakly sinuate apically. Vein 1a absent. Second submarginal cell trapezoidal. Subbasal cell glabrous, with two parallel rows of short setae subapically, a row of setae just below of vein 1CUa and M+CU apically, a row of setae apically just above vein 1-1A, and sparsely setose at base. Basal cell evenly setose. Hind wing: Vein RS bent at basal 0.3, with vein r. Marginal cell narrowest at base. Vein M+CU/1M 1.6. Vein M+CU/r-m 1.3. Vein m-cu present, spectral. Vein m-cu position relative to vein r-m antefurcal. Vein 2-1A absent. Basal cell sparsely setose, bare posteriorly.

Hind legs. Femur length/width 5.0. Length of tibia/tarsi ~ 0.9. Length of basitarsus/tarsi 2–4 ~ 0.7. Sculpture of hind coxa dorsally mostly shiny granular-coriaceous, finely striate apically. Tarsal claws not pectinate.

Metasoma. T1 length/apical width ~ 1.3. T2 length/apical width ~ 0.9. T3 length/apical width 0.7. Mid-longitudinal carina extending until near apex of T3. Metasoma sculpture T1 rugose, T2 and most of T3 striate-rugose, remainder metasoma smooth. Ovipositor sheath/hind basitarsus 0.5. Ovipositor sheaths narrow, with truncate apex; apical point absent.

Color. Brownish yellow. Antenna with basal 12–13 flagellomeres black, apical segments yellow. Wings tinged yellow; stigma and most veins yellow; vein 1M at basal 0.7 and vein 1CUa black, veins r, 2RS, and apex of and 2CUb brown; distinctly infuscate area around base of vein 1M and vein 1CUa, faintly infuscate spots below apex of vein 1-1A and around vein 2CUb.

Male. Unknown.

Diagnosis. *Aleiodes andinus* is similar to three other new species described in this paper, *A. gonodontivorus*, *A. lidiae*, and *A. taurus*, which also have a distinctly bicolored flagellum with rapid transition from dark to light color (Figs 4, 41, 59, 79). However, those three species have a fore wing basal cell that is largely glabrous (Figs 47, 63, 83) and ovipositor sheath with an apical point (Figs 46, 62, 82), whereas the basal cell of *A. andinus* is evenly setose (Fig. 6) and the the ovipositor sheath lacks an apical point (Fig. 5).

Distribution. Known only from the type-locality in Cusco, Peru.

Etymology. The name refers to the Andes Mountains, which are prominent features of the Cusco region of Peru where the holotype specimen was collected.

***Aleiodes angustus* Shimbori & Shaw, sp. nov.**
http://zoobank.org/D0B5D8EA-E4B0-4795-BE9D-7E16376A895C
Figs 8–13

Type material. Holotype, female (CNCI), top label: "Avispas, 400m. PERU Madre de Dios Dept. Sept. 12–20, 1962 L.E. Pena.", bottom label: "divided Radiellan + Interanal New Genus [hand written] Det. W.R.M. Mason 75."

Paratypes. 1 female, 1 male (CNCI), same as holotype; 1 male (CNCI) "BRAZIL: Mato Grosso Sinop, X.1974, 350m 12°31'S, 55°37'W malaise, M. Alvarenga"; 1 female (MUSM) "PERU: CUSCO, La Convención, Echarate, C.C. Timpia. 72°49'34.56"/ 12°06'47.04" 519m. 20–21.x.2009. Light. M. Alvarado & Rázuri"; 1 female (MUSM), same data except "... C.C. Pomareni. 72°50'8.89"/ 12°15'28.38" 477m. 08.xi.2009 Light C. Carranza y C. Rossi"; 5 females (MUSM) "PERU: MD, Rio Los Amigos, CICRA, Aeródromo, 276m, 12°33'36"S, 70°06'17.5"W 22–28. vii.2006, Light trap, A. Asenjo"; 3 females (MUSM) "PERU: JU, Pachitea River-System Stat. Panguana am. Rio Llullapichis, trop. Tiefland-Regenwald. 260m, 9°37'S, 74°56'W 2–20.x.2009, G. Riedel."

Description. Body length 7.3–8.0 mm. Fore wing length 5.9–6.3 mm.

Head. In dorsal view eye length/temple 3.5–4.0. Eye height/head width 0.41–0.43. Eye height/minimum distance between eyes 1.1–1.2. OD/POL 2.4–2.6. OD/OOL 2.5–3.2. Frons excavated. Frons lateral carina weakly indicated. Occipital carina dorsally incomplete. Occiput in dorsal view weakly indented medially. Occipital carina not curved toward ocelli. Occipital carina ventrally meeting hypostomal carina. Mid-longitudinal crest at upper face present. Hypoclypeal depression/face width 0.35–0.45. Malar space/eye height 0.2. Face height/width 0.6–0.7. Clypeus height/width 0.56–0.60. Clypeus convex, granulate. Sculpture of head shiny granular-coriaceous. Face transversely rugose-striate, medially granular-coriaceous below crest.

Antenna. Antennal segments 47–48. Antenna/body length 0.94–0.96. Scape/pedicel length 2.0–2.1. Length of first/second flagellomere 1.2–1.3. Fourth flagellomere length/apical width 1.3–1.4. Tip of apical segment of antenna pointed.

Mesosoma. Length/height 1.5–1.6. Width of mesoscutum/width of head 0.76–0.83. Mesoscutum length/width ~ 1.1. Pronotal collar/vertex 0.6–0.8. Prescutellar sulcus with complete mid-longitudinal carina, and a few irregular and incomplete carinae laterally. Mesoscutum posterior border with distinct complete carina. Metanotum with mid-longitudinal carina present anteriorly. Metanotum mid-pit present, delimited by carinae. Mid-longitudinal carina of propodeum complete. Ventral mid-line of mesopleuron smooth, without distinct sulcus; pit at ventral mid-line present, shallow. Notauli weakly indicated anteriorly, indistinctly crenulate. Sternaulus weakly indicated anteriorly, rugose. Sculpture of mesosoma mostly granulate. Pronotum rugose laterally, pronotal groove curvedly crenulate anteriorly. Mesopleuron rugose below subalar groove. Subalar groove crenulate. Mid-posterior region of mesoscutum rugose. Mesoscutellar trough entirely costate. Metanotum mostly smooth, with one or two pairs of lateral carinae. Propodeum mostly shiny granular-coriaceous, with a few carinae radiating from mid-posterior knob.

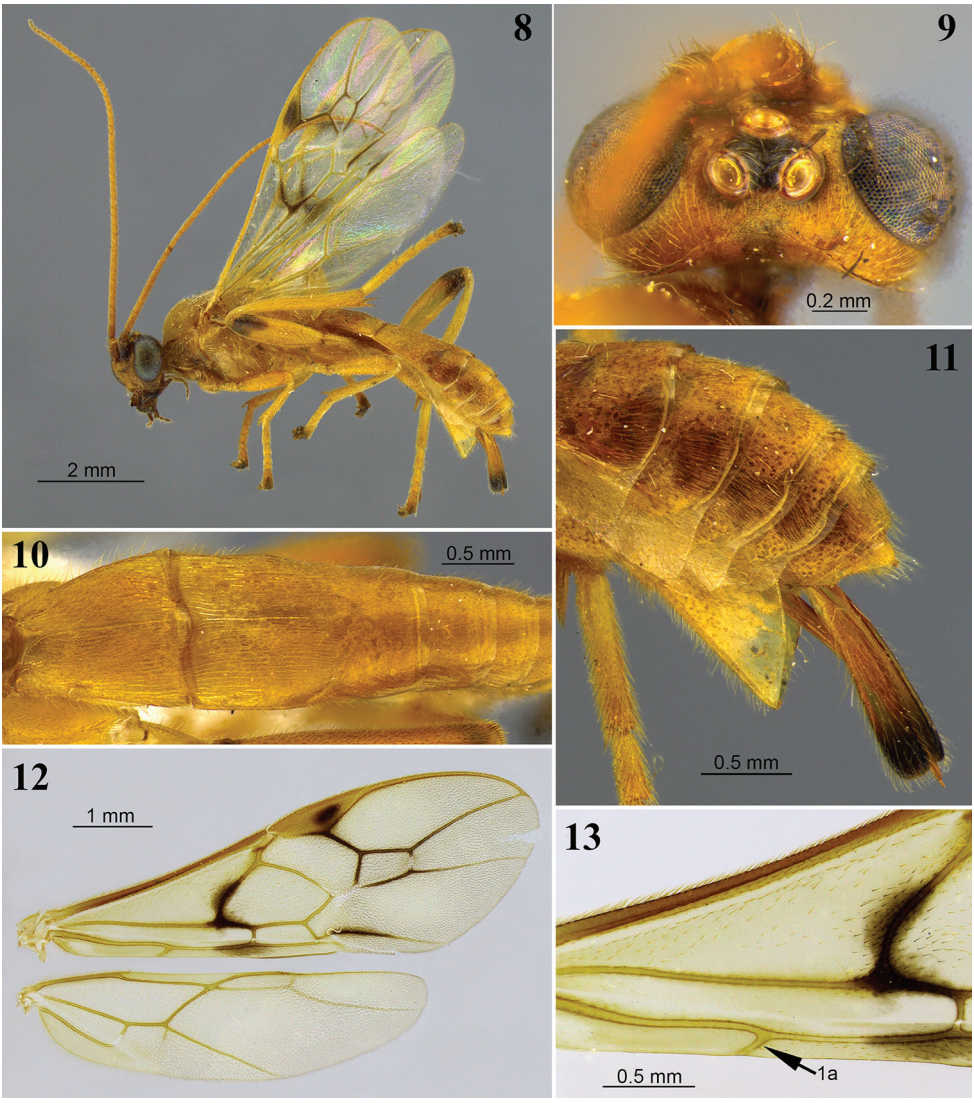

Figures 8–13. *Aleiodes angustus* sp. nov. **8** lateral habitus **9** head, dorsal view **10** metasoma, dorsal view **11** apex of metasoma and ovipositor sheaths, lateral view **12** wings **13** fore wing basally showing tubular and distinct vein 1a.

Wings. Fore wing: Stigma length/height 3.0–3.2. Vein r/2RS 1.1–1.3. Vein r/RS+Mb 1.4–1.6. Vein 3RSa/2RS 1.2–1.5. Vein 3RSa/2M 0.8–0.9. Vein 3RSa/3RSb 0.32–0.43. Vein 1CUa/1CUb ~ 0.8. Vein 1CUa/2CUa 1.65–1.75. Vein 1cu-a vertical. Vein 1M strongly curved at base. Vein RS+Ma weakly curved. Vein M+CU virtually straight. Vein 1-1A distinctly sinuate basally. Vein 1a present and tubular. Second submarginal cell trapezoidal. Subbasal cell mostly glabrous, with sparse setae basally, a small setose patch at the infuscate region bellow vein 1CUa, and two or three ir-

regular rows of short setae subapically above vein 1-1A. Basal cell with more or less large glabrous region posteriorly, sometimes with sparse setae; costal and apical regions evenly setose. Hind wing: Vein RS bent at basal 0.3, with vein r present. Marginal cell narrowest at base. Vein M+CU/1M 2.3–2.5. Vein M+CU/r-m 1.7–1.8. Vein m-cu present, spectral. Vein m-cu position relative to vein r-m interstitial, or just postfurcal. Vein 2-1A absent. Basal cell sparsely setose, bare posteriorly.

Hind legs. Femur length/width 3.7–4.0. Length of tibia/tarsi 1.2–1.3. Length of basitarsus/tarsi 2–4 ~ 0.7. Sculpture of hind coxa dorsally mostly shiny granular-coriaceous, finely striate apically. Tarsal claws not pectinate.

Metasoma. T1 length/apical width ~ 1.0. T2 length/apical width 0.8–0.9. T3 length/apical width 0.7. Mid-longitudinal carina extending until T2. Metasoma sculpture T1 and T2 costate, basal 0.2 of T3 finely costate, remainder terga granular-coriaceous. Ovipositor sheath/hind basitarsus 1.4. Ovipositor sheaths unusually long and with, with truncate apex; apical point absent

Color. Brownish yellow. Hind femur dark brown at apical 0.2; all fifth tarsomeres light brown. Wings faintly tinged yellow; most veins yellow, infuscate spots at fore wing veins 1M/1CUa, apex of 1CUa, 2CUb, and veins enclosing second submarginal cell. Ovipositor sheaths honey brown with dark brown apex.

Male. Essentially as in female, but metasoma not laterally compressed apically. Body length 5.6–6.2 mm, fore wing length 4.2–5.4 mm; 42–44 antennomeres.

Diagnosis. *Aleiodes angustus* is the only species in this study with long and wide ovipositor sheaths that are distinctly longer than hind basitarsus (Fig. 11). It is most similar to *A. asenjoi* but has the ovipositor sheaths very long and large (Figs 8, 11); the division between T2/T3 is very weak and T3 is mostly smooth and without a longitudinal carina (Fig. 10); the metasoma is compressed laterally beyond T2 (Figs 10, 11); and the scutellum is entirely yellow. By contrast, in *A. asenjoi* the ovipositor sheaths are much shorter (Figs 14, 17); a division between T2/T3 is present and distinct (Fig. 16); and the scutellum is usually dark brown apically. Males are more difficult to separate; however, males of *A. angustus* have a longer basal triangular polished area that clearly extends dorsally, as compared with strictly basally in *A. asenjoi*.

Distribution. Known from several localities in Peru, and in Mato Grosso state in Brazil.

Etymology. The name *angustus* is from the Latin word for narrow or slender, being a reference to the compressed and narrow apex of the metasoma in this species (Fig. 10).

Aleiodes asenjoi Shimbori & Shaw, sp. nov.

http://zoobank.org/382E1219-318C-43D0-80F9-80AA4D6F3AC4
Figs 14–17

Type material. Holotype, female (MUSM) "PERU: MD, Rio Los Amigos, CICRA, Aeródromo, 276m, 12°33'36"S, 70°06'17.5"W 22–28.vii.2006, Light trap, A. Asenjo."

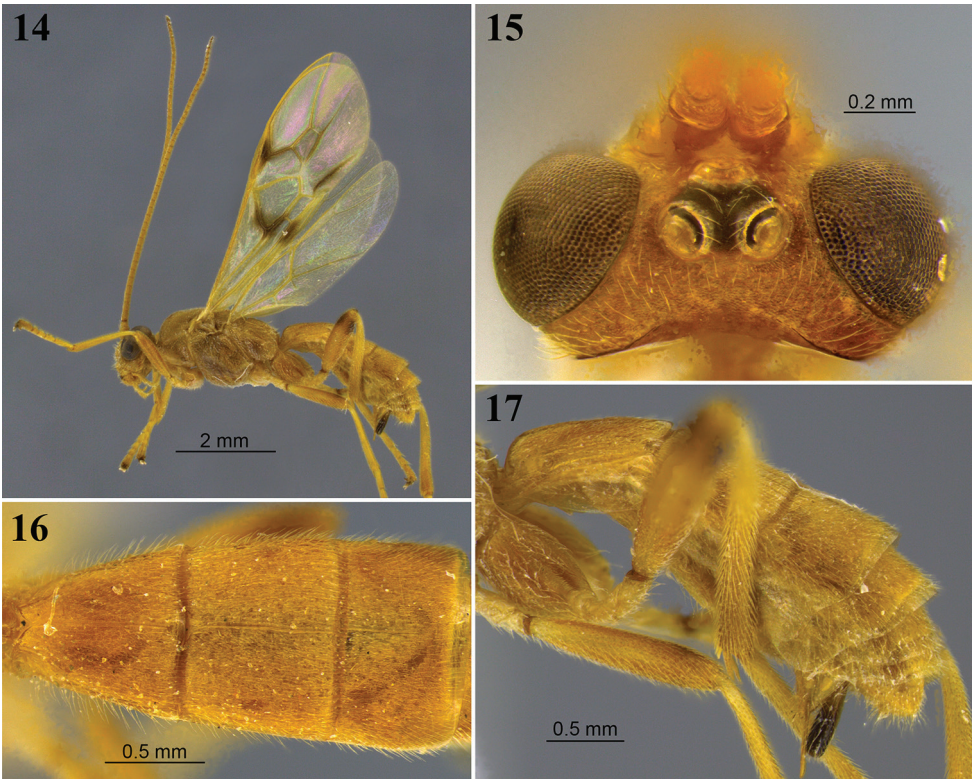

Figures 14–17. *Aleiodes asenjoi* sp. nov. **14** lateral habitus **15** head, dorsal view **16** metasoma, dorsal view **17** metasomal, lateral view.

Paratypes. 2 females (MUSM), same as holotype; 1 female, 1 male (CNCI) "Avispas, 400m. PERU Madre de Dios Dept. Sept. 12–20, 1962 L.E. Pena"; 3 females (CNCI) "BRAZIL: Bahia, Encruzilhada, XI.1972, M. Alvarenga"; 1 male (DCBU 29634) "Piracuruca, PI, Brasil Parque Nacional Sete Cidades Adm. – Cerrado/Caatinga 04°06'03"S, 41°41'32"W Armadilha Luminosa 22.III.2013 A.S. Soares & E.M. Shimbori cols."

Description. Body length 5.4–6.2 mm. Fore wing length 4.9–5.4 mm.

Head. In dorsal view eye length/temple 4.1–5.3. Eye height/head width 0.43–0.45. Eye height/minimum distance between eyes 1.1–1.2. OD/POL 1.8–2.5. OD/OOL 1.8–2.5. Frons excavated. Frons lateral carina present in addition to W-shaped carina. Occipital carina dorsally incomplete. Occiput in dorsal view weakly indented medially. Occipital carina not curved toward ocelli. Occipital carina ventrally meeting hypostomal carina. Mid-longitudinal crest at upper face present. Hypoclypeal depression/face width 0.36–0.42. Malar space/eye height 0.18–0.20. Face height/width 0.6–0.7. Clypeus height/width 0.5–0.6. Clypeus convex, strongly bulging, granulate. Sculpture of head shiny granular-coriaceous. Face transversely rugose-striate, medially granular-coriaceous below crest.

Antenna. Antennal segments 45. Antenna/body length 1.0–1.1. Scape/pedicel length 2.0–2.1. Length of first/second flagellomere 1.0–1.1. Fourth flagellomere length/apical width 1.7–1.8. Tip of apical segment of antenna pointed.

Mesosoma. Length/height 1.6–1.7. Width of mesoscutum/width of head 0.71–0.76. Mesoscutum length/width 1.0–1.1. Pronotal collar/vertex 0.6. Prescutellar sulcus with complete mid-longitudinal carina, and 2–4 pairs of rather incomplete carinae laterally. Mesoscutum posterior border with distinct complete carina. Metanotum with mid-longitudinal carina present anteriorly, and with carinate pit mid-posteriorly. Metanotum mid-pit present, delimited by carinae. Mid-longitudinal carina of propodeum complete, or nearly complete. Ventral mid-line of mesopleuron set within shallow smooth sulcus; pit at ventral mid-line absent. Notauli present anteriorly and indistinctly crenulate. Sternaulus absent. Sculpture of mesosoma mostly granulate. Pronotum granulate-rugose laterally, pronotal groove crenulate anteriorly, crenulation curved posteriorly into ventral curved striation. Mesopleuron rugose below subalar groove. Subalar groove sparsely crenulate. Mid-posterior region of mesoscutum rugose. Mesoscutellar trough entirely costate. Metanotum costate. Propodeum mostly rugose.

Wings. Fore wing: Stigma length/height 2.8–3.0. Vein r/2RS 1.1–1.3. Vein r/RS+Mb 1.4–1.7. Vein 3RSa/2RS 1.2–1.5. Vein 3RSa/2M 0.8–0.9. Vein 3RSa/3RSb 0.34–0.42. Vein 1CUa/1CUb 0.75–0.95. Vein 1CUa/2CUa 1.6–1.8. Vein 1cu-a vertical. Vein 1M weakly curved basally. Vein RS+Ma weakly sinuate. Vein M+CU virtually straight. Vein 1-1A distinctly sinuate basally. Vein 1a present and tubular. Second submarginal cell trapezoidal. Subbasal cell mostly glabrous, with sparse setae basally, a small setose patch at the infuscate region bellow vein 1CUa, and two or three irregular rows of short setae subapically above vein 1-1A. Basal cell with more or less large glabrous region posteriorly, sometimes with sparse setae; costal and apical regions evenly setose. Hind wing: Vein RS Bent at basal 0.3, with vein r present. Marginal cell narrowest at base. Vein M+CU/1M 1.8–2.1. Vein M+CU/r-m 1.5–1.7. Vein m-cu present, spectral. Vein m-cu position relative to vein r-m interstitial. Vein 2-1A absent. Basal cell sparsely setose, bare posteriorly.

Hind legs. Femur length/width 4.0–4.3. Length of tibia/tarsi 1.1–1.2. Length of basitarsus/tarsi 2–4 0.73–0.77. Sculpture of hind coxa dorsally mostly shiny granular-coriaceous, finely striate apically. Tarsal claws not pectinate.

Metasoma. T1 length/apical width 1.0–1.1. T2 length/apical width 0.75–0.80. T3 length/apical width 0.6–0.7. Mid-longitudinal carina extending until basal 0.5 of T3. Metasoma sculpture T1, T2 and basal 0.7 of T3 rugose-costate, sculpture weaker at T3, or remainder terga granular-coriaceous. Ovipositor sheath/hind basitarsus 0.5–0.7. Ovipositor sheaths relatively narrow, with roughly rounded apex; apical point absent.

Color. Brownish yellow to light brown, including antenna. With more or less distinct brown spots at apex of hind femur and apex of scutellum, sometimes also at apex of mid femur. Wings moderately tinged yellow, vein yellow with typical darker regions on vein 1M, 1CUa and apex of 1-1A and at vein r, 2RS and 2CUb, stigma with a round brown spot mid-apically. Ovipositor sheaths dark brown.

Male. Essentially as in female, but fore wing vein 1a shorter. Body length 4.8–5.1 mm; fore wing length 3.8–4.4 mm; antenna with 41 segments.

Diagnosis. *Aleiodes asenjoi* is most similar to *A. angustus* (they are the only two species in this study that have a distinct and tubular fore wing vein 1a) but these two can be separated by the characters discussed in the diagnosis for *A. angustus* (above). *Aleiodes asenjoi* is also very similar to *A. bakeri* but it has the occipital carina more widely absent dorsally (Fig. 15), fore wing vein 1a present (absent in *A. bakeri*); vein (RS+M)a only weakly curved and almost straight (Fig. 14), fore wing stigma with an infuscate dot centrally (Fig. 14), and female with longer and wider ovipositor sheaths (Figs 14, 17).

Distribution. Known from localities in Brazil and Peru.

Etymology. The name is a patronym for Angelico Asenjo, the collector of the holotype specimen.

***Aleiodes bahiensis* Shimbori & Shaw, sp. nov.**
http://zoobank.org/078FA6CA-5C55-443F-A0E6-7A5471AEA860
Figs 18–20

Type material. Holotype, female (CNCI) "BRAZIL: Bahia, Encruzilhada, XI.1972 M. Alvarenga."

Paratype, female (CNCI), same as holotype.

Description. Body length 6.2–6.4 mm. Fore wing length 5.0–5.3 mm.

Head. In dorsal view eye length/temple 4.0–5.0. Eye height/head width 0.43–0.45. Eye height/minimum distance between eyes 1.3–1.4. OD/POL 2.8–3.2. OD/OOL 3.2–3.3. Frons excavated. Frons lateral carina present. Occipital carina dorsally complete and nearly straight. Occiput in dorsal view nearly straight, not indented medially. Occipital carina ventrally meeting hypostomal carina. Mid-longitudinal crest at upper face present. Hypoclypeal depression/face width 0.36–0.37. Malar space/eye height 0.2. Face height/width 0.70–0.75. Clypeus height/width 0.70–0.75. Clypeus convex, granulate. Sculpture of head shiny granular-coriaceous. Face transversely rugose-striate around median crest.

Antenna. Antennal segments 48–49. Antenna/body length 1.1. Scape/pedicel length 1.7–1.8. Length of first/second flagellomere 1.2. Fourth flagellomere length/apical width 1.7–1.8. Tip of apical segment of antenna nipple-shaped.

Mesosoma. Length/height ~ 1.7. Width of mesoscutum/width of head 0.65. Mesoscutum length/width 1.2. Pronotal collar/vertex 0.9–1.0. Prescutellar sulcus with five distinct carinae. Mesoscutum posterior border with distinct complete carina. Metanotum with mid-longitudinal carina complete, connecting to a carinate pit posteriorly. Metanotum mid-pit present, delimited by carinae. Mid-longitudinal carina of propodeum present at basal 0.7, absent posteriorly. Ventral mid-line of mesopleuron set within shallow smooth sulcus. Pit at ventral mid-line weakly indicated. Notauli weakly indicated anteriorly, indistinctly crenulate. Sternaulus weakly indicated anteriorly, ru-

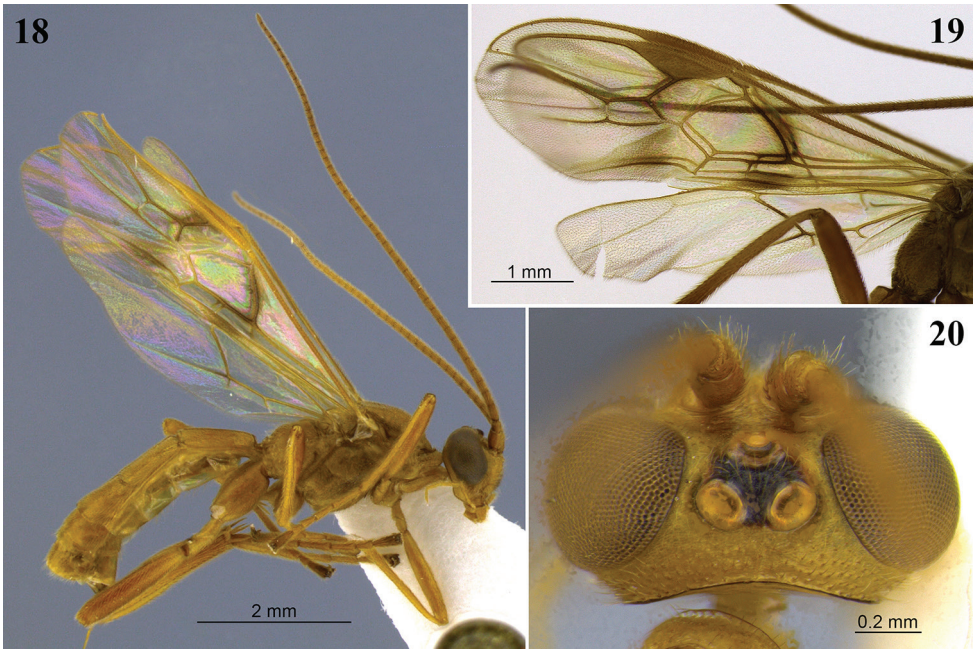

Figures 18–20. *Aleiodes bahiensis* sp. nov. **18** Lateral habitus **19** wings **20** head, dorsal view.

gose. Sculpture of mesosoma mostly granulate. Pronotum granulate ventrally, pronotal groove mostly crenulate, short subventral longitudinal carina present. Mesopleuron mostly rugose. Subalar groove crenulate. Mid-posterior region of mesoscutum rugose, with a short mid-longitudinal carina posteriorly. Mesoscutellar trough entirely costate. Metanotum mostly smooth, with one or two pairs of lateral carinae. Propodeum mostly rugose.

Wings. Fore wing: Stigma length/height 3.5. Vein r/2RS 1.1–1.2. Vein r/RS+Mb 1.5. Vein 3RSa/2RS 1.5–1.8. Vein 3RSa/2M 0.75–0.80. Vein 3RSa/3RSb 0.34–0.42. Vein 1CUa/1CUb 0.85–0.90. Vein 1CUa/2CUa 1.9. Vein 1cu-a weakly inclivous. Vein 1M weakly curved basally. Vein RS+Ma weakly curved. Vein M+CU virtually straight. Vein 1-1A nearly straight. Vein 1a absent. Second submarginal cell trapezoidal. Subbasal cell glabrous, with two parallel rows of short setae subapically, and a narrow patch of setae just below vein 1CUa. Basal cell mostly evenly setose, sparsely setose posteriorly. Hind wing: Vein RS bent at basal 0.3, with vein r present. Marginal cell narrowest at base. Vein M+CU/1M 1.5–1.6. Vein M+CU/r-m 1.3. Vein m-cu present, spectral. Vein m-cu position relative to vein r-m interstitial, or antefurcal. Vein 2-1A absent. Basal cell evenly, rather sparsely setose, posteriorly with small bare area.

Hind legs. Femur length/width 4.7–5.5. Length of tibia/tarsi ~ 1.0. Length of basitarsus/tarsi 2–4 ~ 0.7. Sculpture of hind coxa dorsally mostly shiny granular-coriaceous, finely striate apically. Tarsal claws not pectinate.

Metasoma. T1 length/apical width 1.2–1.3. T2 length/apical width ~ 0.9. T3 length/apical width 0.6. Mid-longitudinal carina extending until basal 0.7 of T3.

Metasoma sculpture T1 rugose, T2 and most of T3 striate-rugose, remainder terga granular-coriaceous. Ovipositor sheath/hind basitarsus ~ 0.4. Apex of ovipositor sheaths truncate; apical point absent.

Color. Entirely yellowish brown, except for stemmaticum black. Wings weakly tinged brownish yellow; veins and stigma yellow except 1M, 1CUa, apex of 1-1A, r, 2RS, 3RS, 2M and part of 2CUb brown; faintly infuscate areas around veins 1M, r and 2CUa, and bellow apex of vein 1-1A.

Male. Unknown

Diagnosis. *Aleiodes bahiensis* is similar to *A. hyalinus* and *A. santarosensis.* These three species have the antenna entirely yellow (as in Fig. 18). *Aleiodes hyalinus* is easily distinguished by its entirely clear wings and evenly brown wing venation, while both *A. bahiensis* and *A. santarosensis* share similar wing markings: veins 1M, 1CUa, and part of 2CUb dark brown, darker than remaining veins, and the wing membrane around these veins, and below vein 1-1A apically, is weakly to distinctly infuscate (as in Fig. 19). *Aleiodes bahiensis* can be distinguished from *A. santarosensis* by having entirely yellow legs (Fig. 18), while in *A. santarosensis* the legs have tarsomeres 1–4 and at least the base of the tibia whitish yellow, contrasting with a brownish orange femur.

Distribution. Known only from the type-locality in Bahia, Brazil.

Etymology. The name *bahiensis* refers to Bahia State in northeastern Brazil, the type-locality of this species.

Aleiodes bakeri (Brues, 1912)

Figs 21–24

Rhogas bakeri Brues, 1912: 222, fig 21.
Aleiodes bakeri Shenefelt, 1975: 1166.
not *Aleiodes* (*Hemigyroneuron*) *bakeri* Butcher & Quicke, 2011: 1417.

Type material examined. Holotype, female (MCZ-Harvard). 7 labels: 1. "Rio Madeira, Brazil Mann & Baker." 2. "Madeira-mamoré R.R. Co. Camp 39." 3. "TYPE." 4. "M.C.Z. H Type 29923." 5. "*Rhogas bakeri* Brues." 6. "MCZ Image Database." 7 "MCZ-ENT 00029923."

Non-type material examined. BRAZIL: 2 females (CNCI), Encruzilhada, Bahia; 6 males (CNCI), Sinop, Mato Grosso; 25 females and 2 males (DCBU), PARNA Serra das Confusões, Caracolândia, Piauí; 3 females and 1 male (DCBU), PARNA Serra da Capivara, Coronel José Dias, Piauí; 3 females and 2 males (DCBU), PARNA Sete Cidades, Piracuruca, Piauí; 1 female (MZUSP), Buritis, Minas Gerais; 1 female (MZUSP), Cabeceiras, Goiás. PERU: 1 female (MUSM), CICRA, Madre de Dios.

Re-description of holotype. Holotype in fair condition. All but the left front leg detached from body, two hind and two mid legs glued in a separate card, metasoma loose but still attached to body, both antennae broken before middle.

Body length 7.0 mm. Fore wing length 6.0 mm.

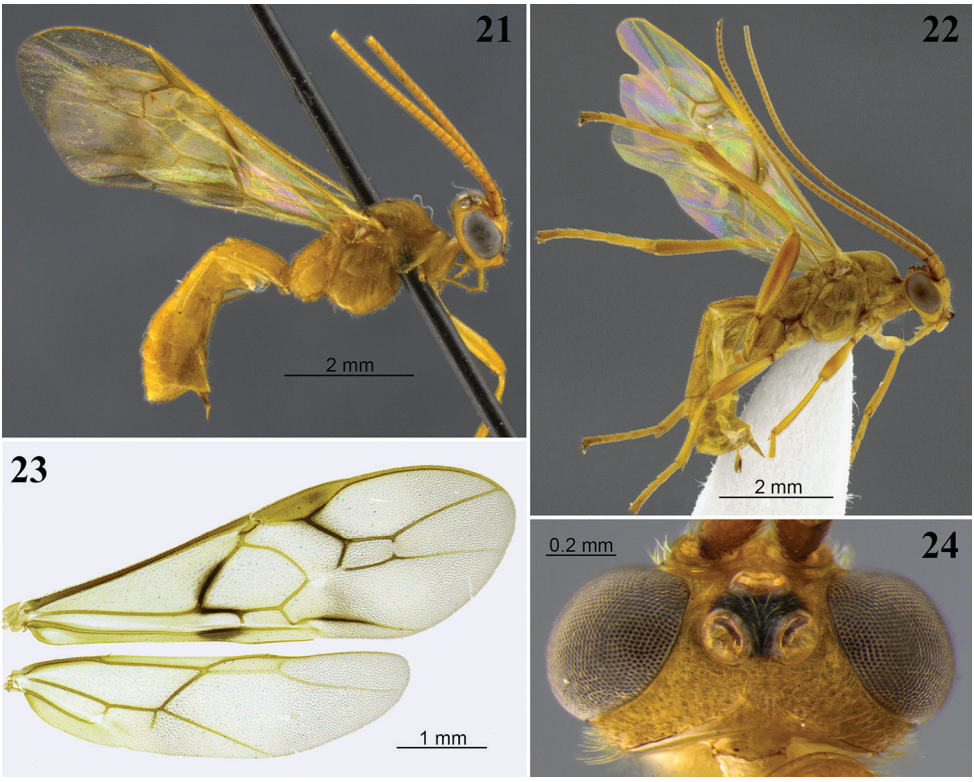

Figures 21–24. *Aleiodes bakeri* (Brues). **21** Holotype female, lateral view **22** non-type female, lateral view **23** wings **24** head, dorsal view.

Head. In dorsal view eye length/temple 3.2. Eye height/head width 0.36. Eye height/minimum distance between eyes 1.1. OD/POL 2.5. OD/OOL 2.5. Frons excavated. Frons lateral carina present. Occipital carina dorsally incomplete. Occiput in dorsal view nearly straight, not indented medially. Occipital carina not curved toward ocelli. Occipital carina ventrally meeting hypostomal carina. Mid-longitudinal crest at upper face present. Hypoclypeal depression/face width 0.35. Malar space/eye height 0.2. Face height/width 0.65. Clypeus height/width ~ 0.6. Clypeus convex, granulate. Sculpture of head shiny granular-coriaceous. Face weakly rugose, with bulging granulate area below crest, transversely rugose-striate around median crest.

Antenna. Antennal segments (antenna broken). Antenna/body length unknown (antenna broken). Scape/pedicel length 2.0. Length of first/second flagellomere 1.3. Fourth flagellomere length/apical width 1.3.

Mesosoma. Length/height 1.5–1.6. Width of mesoscutum/width of head 0.55. Mesoscutum length/width ~ 1.0. Pronotal collar/vertex 0.5. Prescutellar sulcus with complete mid-longitudinal carina, and a few irregular and incomplete carinae laterally. Mesoscutum posterior border with distinct complete carina. Metanotum with mid-longitudinal carina complete, connecting to a carinate pit posteriorly. Metanotum

mid-pit present, delimited by carinae. Mid-longitudinal carina of propodeum present at basal 0.7, absent posteriorly. Ventral mid-line of mesopleuron smooth, without distinct sulcus; pit at ventral mid-line present, shallow. Notauli present anteriorly, shallow and weakly crenulate. Sternaulus absent. Sculpture of mesosoma mostly granulate. Metapleuron rugose posteriorly. Pronotum rugose laterally, pronotal groove curvedly crenulate anteriorly. Mesopleuron mostly rugose. Subalar groove crenulate. Mid-posterior region of mesoscutum destroyed by pin. Mesoscutellar trough entirely costate. Metanotum mostly smooth and weakly crenulate. Propodeum rugose posteriorly.

Wings. Fore wing: Stigma length/height 3.6–3.9. Vein r/2RS 1.3. Vein r/RS+Mb 1.4. Vein 3RSa/2RS 1.3. Vein 3RSa/2M 0.8. Vein 3RSa/3RSb 0.3. Vein 1CUa/1CUb 0.9. Vein 1CUa/2CUa 1.8. Vein 1cu-a weakly inclivous. Vein 1M weakly curved basally. Vein RS+Ma distinctly curved. Vein M+CU virtually straight. Vein 1-1A weakly sinuate at apex. Vein 1a absent. Second submarginal cell short and trapezoidal. Subbasal cell glabrous, with two parallel rows of short setae subapically. Basal cell with more or less large glabrous region posteriorly, sometimes with sparse setae; costal and apical regions evenly setose. Hind wing: Vein RS bent at basal 0.3, with vein r present. Marginal cell narrowest at base. Vein M+CU/1M 1.9. Vein M+CU/r-m 1.6. Vein m-cu present, spectral. Vein m-cu position relative to vein r-m interstitial. Vein 2-1A absent. Basal cell evenly setose.

Hind legs. Femur length/width 4.3. Length of tibia/tarsi ~ 1.0. Length of basitarsus/tarsi 2–4 0.75. Sculpture of hind coxa dorsally shiny granular-coriaceous. Tarsal claws not pectinate.

Metasoma. T1 length/apical width ~ 1.1. T2 length/apical width ~ 0.8. T3 length/apical width 0.6. Mid-longitudinal carina extending until basal 0.7 of T3. Metasoma sculpture of T1, T2, and basal 0.7 of T3 rugose-costate, sculpture weaker at T3, remainder metasoma smooth. Ovipositor sheath/hind basitarsus 0.3. Apex of ovipositor sheaths roughly rounded; apical point relatively long and curved.

Color. Mostly pale honey yellow; all coxa, trochanter and trochantellus, and base of femur whitish (fore legs lighter than hind, hind coxa light yellow); stemmaticum and mandible tips brown; wings weakly tinged yellow, with two infuscate regions on fore wing, one around vein 1M, extending to a infuscate region below apex of subbasal cell, and another at stigma level, including the second submarginal cell and part of vein 2CUb (in original description the infuscate regions are described as cross-bands, maybe specimen lost color during the past 100 years; in holotype and in younger specimens the infuscate regions do not form cross bands. Instead there are infuscate regions around vein 1M, below apex of vein 1-1A, around vein r and veins forming the second submarginal cell, and around vein 2CUb medially); stigma brownish yellow without any dark spot; veins yellow, brown in the infuscate regions: veins 1M at basal ¾, 1CUa, apex of 1-1A, r, 2RS, 3RS, and 2CUb subapically.

Description of non-type specimens. Body length 6.3–7.5 mm. Fore wing length 5.3–6.0 mm.

Head. In dorsal view eye length/temple 3.2–4.1. Eye height/head width 0.36–0.42. Eye height/minimum distance between eyes 1.1–1.3. OD/POL 2.5–3.7. OD/

OOL 2.5–4.0. Frons excavated. Frons lateral carina present. Occipital carina dorsally incomplete. Occiput in dorsal view weakly indented medially. Occipital carina not curved toward ocelli. Occipital carina ventrally meeting hypostomal carina. Mid-longitudinal crest at upper face present. Hypoclypeal depression/face width 0.32–0.37. Malar space/eye height 0.14–0.20. Face height/width 0.6–0.7. Clypeus height/width 0.57–0.67. Clypeus convex, granulate. Sculpture of head shiny granular-coriaceous. Face weakly rugose, with bulging granulate area below crest, transversely rugose-striate around median crest.

Antenna. Antennal segments 46–51. Antenna/body length 1.1. Scape/pedicel length 2.0. Length of first/second flagellomere 1.2–1.3. Fourth flagellomere length/apical width 1.3–1.4. Tip of apical segment of antenna pointed.

Mesosoma. Length/height 1.7–1.8. Width of mesoscutum/width of head 0.65–0.68. Mesoscutum length/width 1.1–1.2. Pronotal collar/vertex 0.6–0.7. Prescutellar sulcus with complete mid-longitudinal carina, and a few irregular and incomplete carinae laterally. Mesoscutum posterior border with distinct complete carina. Metanotum with mid-longitudinal carina complete, connecting to a carinate pit posteriorly. Metanotum mid-pit present, delimited by carinae. Mid-longitudinal carina of propodeum present at basal 0.7, absent posteriorly. Ventral mid-line of mesopleuron smooth, without distinct sulcus; pit at ventral mid-line present, shallow. Notauli present anteriorly, shallow and weakly crenulate. Sternaulus absent. Sculpture of mesosoma mostly granulate, metapleuron rugose posteriorly. Pronotum rugose laterally, pronotal groove sparsely crenulate anteriorly. Mesopleuron mostly rugose. Subalar groove crenulate. Mid-posterior region of mesoscutum rugose with long and irregular mid-longitudinal carina. Mesoscutellar trough entirely costate. Metanotum mostly smooth and weakly crenulate. Propodeum rugose posteriorly.

Wings. Fore wing: Stigma length/height 3.7–4.0. Vein r/2RS 1.3–1.5. Vein r/RS+Mb 1.5–1.7. Vein 3RSa/2RS 1.4–1.6. Vein 3RSa/2M 0.82–0.85. Vein 3RSa/3RSb 0.37–0.40. Vein 1CUa/1CUb 0.9–1.0. Vein 1CUa/2CUa 1.6–2.0. Vein 1cu-a weakly inclivous, or nearly vertical. Vein 1M weakly curved basally. Vein RS+Ma distinctly curved. Vein M+CU virtually straight. Vein 1-1A weakly sinuate at apex. Second submarginal cell short and trapezoidal. Subbasal cell mostly glabrous, with two parallel rows of short setae subapically, and few scattered setae medially. Basal cell mostly evenly, rather sparsely setose, with narrow glabrous anal spot. Hind wing: Vein RS bent at basal 0.3, with vein r present. Marginal cell narrowest at base. Vein M+CU/1M 1.6–1.7. Vein M+CU/r-m 1.3–1.4. Vein m-cu present, spectral. Vein m-cu position relative to vein r-m interstitial, or antefurcal. Vein 2-1A absent. Basal cell evenly, rather sparsely setose, posteriorly with small bare area.

Hind legs. Femur length/width 4.4–4.6. Length of tibia/tarsi 0.9–1.0. Length of basitarsus/tarsi 2–4 0.72–0.74. Sculpture of hind coxa dorsally shiny granular-coriaceous. Tarsal claws not pectinate.

Metasoma. T1 length/apical width 1.0–1.1. T2 length/apical width 0.8–0.9. T3 length/apical width 0.6–0.7. Mid-longitudinal carina extending until near apex of T3, or extending until basal 0.7 of T3. Metasoma sculpture T1, T2 and basal 0.7 of T3 rugose-

costate, remainder metasoma smooth. Ovipositor sheath/hind basitarsus 0.27–0.45. Apex of ovipositor sheaths roughly rounded; apical point relatively long and curved.

Color. Essentially as in holotype. Body color varying from brownish yellow to pale yellow. Some specimens have a brown subapical spot on the pterostigma.

Male. Essentially as in female. Body length 5.6–6.6 mm; fore wing length 4.3–5.4 mm; antenna with 48–50 segments.

Diagnosis. The color patterns, body proportions, and other features of *Aleiodes bakeri* are similar to those in *A. nigristemmaticum* (Enderlein). The most useful characters to distinguish them are the occipital carina, which is incomplete at the vertex in *bakeri* (Fig. 24) but is complete in *nigristemmaticum*, and the hind wing venation, with vein M+CU being more than 2 × longer than 1M in *bakeri* (Fig. 23), as compared with ~ 1.5 × longer in *nigristemmaticum*. Specimens of *A. nigristemmaticum* have the antenna dark brown basally, lightening toward apex, as compared with entirely honey yellow in *A. bakeri* (Fig. 22). Three of the new species, *A. angustus*, *A. asenjoi*, and *A. mabelae*, also have a dorsally incomplete occipital carina. Two of these, *A. angustus* and *A. asenjoi*, are easily distinguished by having the fore wing vein 1a present (as in Fig. 1), while this vein is absent in *A. bakeri* (Fig. 2). *Aleiodes mabelae* can be distinguished by its longer fore wing second submarginal cell (Fig. 64) and the flagellum which is black at the base (Fig. 64). The second submarginal cell is comparatively shorter in *A. bakeri* (Figs 2, 23), and the flagellum is entirely the same color, yellow or orange, without being black basally (Fig. 22).

Distribution. *Aleiodes bakeri* is known from localities in Brazil and Peru.

Nomenclatural note. Butcher and Quicke (2011) synonymized *Hemigyroneuron* Baker as a junior synonym of *Aleiodes* but retained *Hemigyroneuron* as a subgenus. The species *Aleiodes* (*Hemigyroneuron*) *bakeri* Butcher & Quicke, 2011 is not the same species as *Aleiodes bakeri* (Brues, 1912). Despite its assignment to a different subgenus, *Aleiodes bakeri* Butcher & Quicke, 2011 is a junior homonym of *Aleiodes bakeri* (Brues, 1912) and a replacement name is needed. There we hereby propose the new name, *Aleiodes buntikae* Shimbori & Shaw, nom. nov., for the species formerly called *Aleiodes* (*Hemigyroneuron*) *bakeri* Butcher & Quicke, 2011: p. 1417. The new name is a patronym in honor of Buntika Areekul-Butcher, author of the species formerly called *Aleiodes* (*Hemigyroneuron*) *bakeri.*

Aleiodes barrosi Shimbori & Shaw, sp. nov.

http://zoobank.org/AF3B7B7D-C358-4F18-97CE-B38EE202F433
Figs 25–28

Type material. Holotype, female (DCBU #21889) "Faz. Sto. Antônio do Paraíso, Itiquira, MT Armadilha Malaise 1.IX.1999 M.M. Barros & J.C.M. Lutz cols."

Paratypes. 1 female (DCBU #22357) "Luís Antônio, SP, Brasil Estação Ecológica do Jataí, Luz 24.IV.2001 L.A. Joaquim col."; 1 female (DCBU #21906), same data except "... Mata Ciliar 21°36'54"S, 47°47'02"W 04.I.2007 Armadilha Malaise 2 N.W.

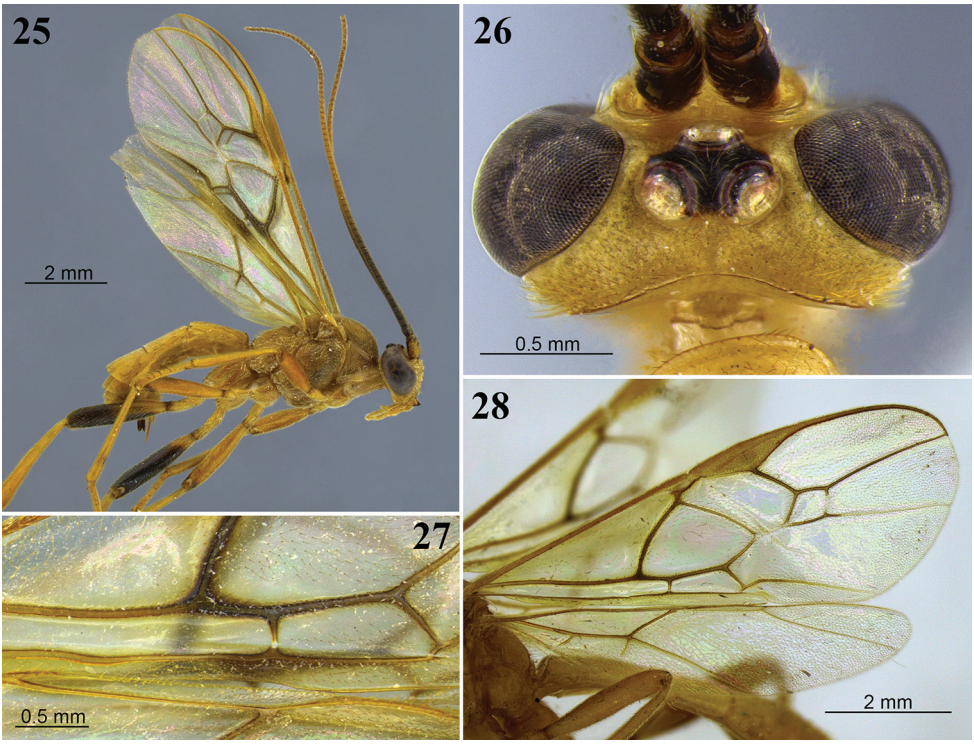

Figures 25–28. *Aleiodes barrosi* sp. nov. **25** lateral habitus **26** head, dorsal view **27** fore wing close-up basomedially **28** wings.

Perioto col.", 1 female (DCBU #21907), same data except "01.III.2007"; 1 female (DCBU #28167) "Rio Branco, AC, Brasil, 09°59'30"S, 67°48'36"W Armadilha Malaise 01.I.2010 A.S. Soares col."; 1 female (MUSM) " PERU: MD, Parque Nacional Bahuaha – Sonene 70°0758.2"W, 13°11'38.7"S 347m 03–19.vi.2013 J. Grados Leg"; 1 female (MUSM) "PERU: MD, Rio Los Amigos, CICRA, Aeródromo, 276m, 12°33'36"S, 70°06'17.5"W 22–28.vii.2006, Light trap, A. Asenjo"; 1 male (MUSM) "PERU: CUSCO, La Convención, Echarate, C. Segakiato. 11°45'38.6"S, 73°14'57.7"W 908m. 01.ii.2011. M. Alvarado & E Rázuri."; 1 female (INBIO) "Rancho Quemado, 200m, Peninsula de Osa, Prov. Puntarenas, Costa Rica Set 1992. F. Quesada L-S 292500, 51000"; 1 female (INBIO), same data except "Nov 1992"; 2 females (INBIO), same data except "… Oct 1992, M. Segura …"

Description. Body length 7.6–9.4 mm. Fore wing length 7.0–8.6 mm.

Head. In dorsal view eye length/temple 3.4–4.5. Eye height/head width 0.38–0.43. Eye height/minimum distance between eyes 1.1–1.3. OD/POL 3.0–5.0. OD/OOL 3.1–4.2. Frons excavated. Frons lateral carina present. Occipital carina dorsally complete, weakly curved. Occiput in dorsal view nearly straight, not indented medially. Occipital carina ventrally nearly touching hypostomal carina, or meeting hypostomal carina. Mid-longitudinal crest at upper face present. Hypoclypeal

depression/face width 0.36–0.42. Malar space/eye height 0.11–0.19. Face height/width 0.8–0.9. Clypeus height/width 0.6–0.7. Clypeus convex, granulate. Sculpture of head shiny granular-coriaceous. Face transversely rugose-striate, medially granular-coriaceous below crest.

Antenna. Antennal segments 58–67. Antenna/body length 1.1–1.2. Scape/pedicel length 2.3–2.9. Length of first/second flagellomere 1.0–1.2. Fourth flagellomere length/apical width 1.1–1.3. Tip of apical segment of antenna pointed.

Mesosoma. Length/height 1.47–1.51. Width of mesoscutum/width of head 0.7–0.8. Mesoscutum length/width 1.0–1.2. Pronotal collar/vertex 0.5–0.7. Prescutellar sulcus with 3–5 distinct carinae. Mesoscutum posterior border with distinct complete carina. Metanotum with mid-longitudinal carina complete, connecting to a carinate pit posteriorly. Metanotum mid-pit present, delimited by carinae. Mid-longitudinal carina of propodeum complete, or nearly complete. Ventral mid-line of mesopleuron without sulcus anteriorly, shallow smooth sulcus present posteriorly; pit at ventral mid-line absent. Notauli weakly indicated anteriorly, indistinctly crenulate. Sternaulus absent. Sculpture of mesosoma mostly granulate. Pronotum rugose laterally, granulate ventrally, pronotal groove crenulate anteriorly, short subventral longitudinal carina present. Mesopleuron mostly rugose. Subalar groove sparsely crenulate. Mid-posterior region of mesoscutum rugose, with irregularly carinate notauli. Mesoscutellar trough entirely costate. Metanotum mostly smooth, with one or two pairs of lateral carinae. Propodeum mostly granulate, rugose posteriorly.

Wings. Fore wing: Stigma length/height 3.6–3.8. Vein r/2RS 1.3–1.6. Vein r/RS+Mb 1.4–1.7. Vein 3RSa/2RS 1.1–1.3. Vein 3RSa/2M 0.76–0.85. Vein 3RSa/3RSb 0.24–0.29. Vein 1CUa/1CUb 0.45–0.60. Vein 1CUa/2CUa 0.9–1.1. Vein 1cu-a vertical. Vein 1M weakly curved basally, or nearly straight. Vein RS+Ma virtually straight. Vein M+CU weakly sinuate. Vein 1-1A strongly sinuate. Vein 1-1A distinctly changing thickness along apical half. Vein 1a absent. Second submarginal cell short and trapezoidal. Subbasal cell glabrous, with a narrow patch of setae subapically just below vein 1CUa. Basal cell with more or less large glabrous region posteriorly, sometimes with sparse setae; costal and apical regions evenly setose. Hind wing: Vein RS bent at basal 0.3, with vein r present. Marginal cell narrowest at base. Vein M+CU/1M 1.3–1.6. Vein M+CU/r-m 1.2–1.4. Vein m-cu present, partly tubular. Vein m-cu position relative to vein r-m interstitial, or antefurcal. Vein 2-1A absent. Basal cell sparsely setose, bare posteriorly.

Hind legs. Femur length/width 4.5–5.0. Length of tibia/tarsi 0.9–1.0. Length of basitarsus/tarsi 2–4 0.7–0.8. Sculpture of hind coxa dorsally mostly shiny granular-coriaceous, finely striate apically. Tarsal claws not pectinate.

Metasoma. T1 length/apical width 1.0–1.2. T2 length/apical width 0.6–0.8. T3 length/apical width 0.5–0.7. Mid-longitudinal carina extending until basal 0.5 or 0.7 of T3. Metasoma sculpture T1 rugose, T2 and most of T3 striate-rugose, sculpture weaker at T3, remainder terga granular-coriaceous. Ovipositor sheath/hind basitarsus 0.36–0.56. Apex of ovipositor sheaths truncate; apical point very short, not distinctly visible in some paratypes.

Color. Brownish yellow or pale honey yellow. Antenna dark brown basally, gradually lightening toward brown or brownish yellow apex. Legs with same color as body, rarely hind femur mostly dark brown. Wings tinged brown, stigma and most veins light brown; fore wing veins 1M, 1CU, apex of 1-1A, 2CUb medially, r, and veins of second submarginal cell dark brown. Ovipositor sheaths dark brown.

Male. The only male paratype is very similar to the females with dark brown hind femur. Body length 7.8 mm; fore wing length 6.7 mm; antenna with 44 antennomeres.

Diagnosis. *Aleiodes barrosi* is similar to *A. joaquimi* in that both species have the first subdiscal cell relatively long and widening apically (Figs 27, 28), and both have the vein 1CUb 1.7–2.1 × longer than 1CUa (0.9–1.3 × in other species). These two species are easily separated by the mainly yellow body color in *A. barrosi* (deep reddish brown in *A. joaquimi*), yellow palpi and tegula (dark brown in *A. joaquimi*), and entirely yellow tibia and tarsi (tibia basally and tarsi 1–4 white in *A. joaquimi*). Additionally, the hind wing vein 2-1A is absent in *A. barrosi* (Fig. 28), but present in *A. joaquimi* (Fig. 58).

Distribution. Known from localities in Brazil, Costa Rica, and Peru.

Etymology. The name is a patronym for Marina Moraes Barros Lutz, one of the collectors of the holotype specimen.

Aleiodes brevicarina Shimbori & Shaw, sp. nov.

http://zoobank.org/CC5929A9-D8ED-4EBE-AB4C-B4502DA8CC3E
Figs 29–32

Type material. Holotype, female (DCBU #20780) top label: "FAZ. CANCHIM SÃO CARLOS – SP 29.III.1985 A.S. Soares col.", bottom label "Mata (Luz) [handwritten]."

Paratypes. 3 females, 4 male (DCBU #s: 20778, 20779, 20781-20784, 20787), same as holotype; 1 male (DCBU #20785), same data except "11.II.1983"; 1 male (DCBU #20786), same data except "... cerrado, Varredura, 23.I.1981 N.W. Perioto col."

Description. Body length 7.8–8.1 mm. Fore wing length 6.4–7.0 mm.

Head. In dorsal view eye length/temple 3.9–4.1. Eye height/head width 0.41. Eye height/minimum distance between eyes 1.2–1.3. OD/POL 3.7–5.0. OD/OOL 3.1–4.2. Frons excavated. Frons lateral carina present. Occipital carina dorsally complete and nearly straight. Occiput in dorsal view nearly straight, not indented medially. Occipital carina ventrally meeting hypostomal carina. Mid-longitudinal crest at upper face present. Hypoclypeal depression/face width 0.35–0.37. Malar space/eye height 0.16–0.17. Face height/width 0.72–0.77. Clypeus height/width 0.63–0.73. Clypeus convex, granulate. Sculpture of head shiny granular-coriaceous. Face transversely rugose-striate around median crest.

Antenna. Antennal segments 55–56. Antenna/body length 1.1. Scape/pedicel length 2.0–2.1. Length of first/second flagellomere 1.2–1.3. Fourth flagellomere length/apical width 1.7–1.8. Tip of apical segment of antenna pointed.

Mesosoma. Length/height 1.5–1.6. Width of mesoscutum/width of head 0.73–0.75. Mesoscutum length/width 1.0–1.1. Pronotal collar/vertex 0.7–0.8. Prescutellar

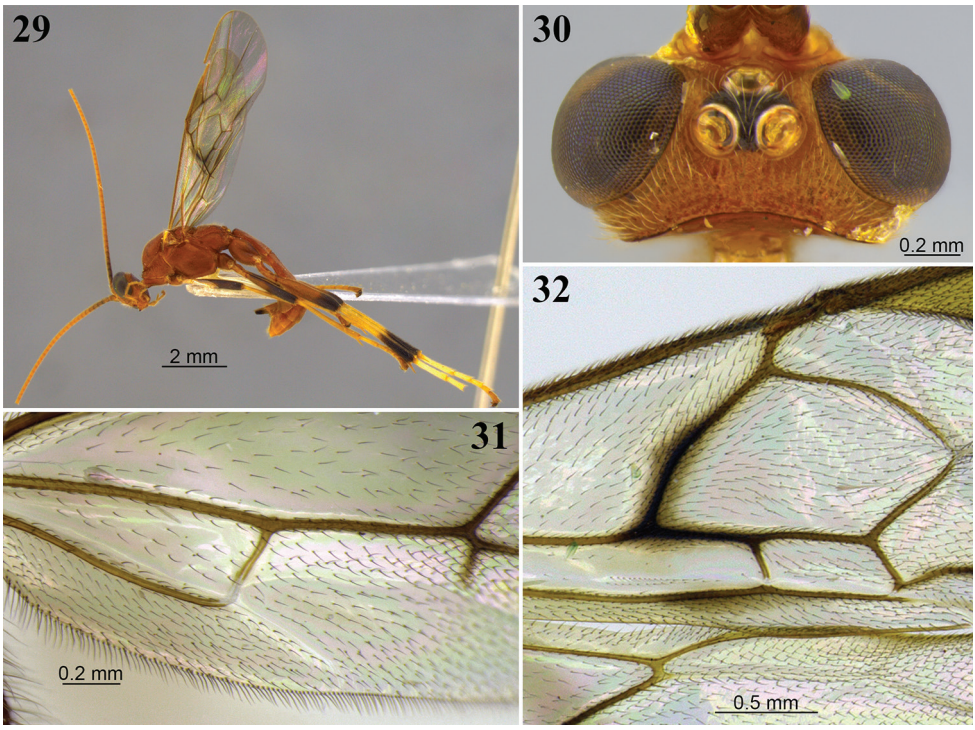

Figures 29–32. *Aleiodes brevicarina* sp. nov. **29** lateral habitus **30** head, dorsal view **31** hind wing close-up basally **32** wings medially.

sulcus with complete mid-longitudinal carina, and 2–4 pairs of rather incomplete carinae laterally. Mesoscutum posterior border with distinct complete carina. Metanotum with mid-longitudinal carina complete, connecting to a carinate pit posteriorly. Metanotum mid-pit present, delimited by carinae. Mid-longitudinal carina of propodeum present at basal 0.5 or less. Ventral mid-line of mesopleuron set within shallow smooth sulcus; pit at ventral mid-line absent. Notauli weakly indicated anteriorly, indistinctly crenulate. Sternaulus absent. Sculpture of mesosoma mostly granulate. Pronotum rugose laterally, pronotal groove sparsely crenulate anteriorly, short subventral longitudinal carina present. Mesopleuron mostly rugose. Subalar groove crenulate. Mid-posterior region of mesoscutum rugose, with irregular mid-longitudinal carina and a pair of irregular carinae along notauli. Mesoscutellar trough entirely costate. Metanotum mostly smooth and weakly crenulate, costate laterally. Propodeum mostly rugose.

Wings (Figs 31, 32). Fore wing: Stigma length/height 3.6–3.7. Vein r/2RS 1.1–1.2. Vein r/RS+Mb 1.4. Vein 3RSa/2RS ~ 1.6. Vein 3RSa/2M 0.8. Vein 3RSa/3RSb ~ 0.4. Vein 1CUa/1CUb 0.9. Vein 1CUa/2CUa 1.8–1.9. Vein 1cu-a weakly inclivous. Vein 1M weakly curved basally. Vein RS+Ma sinuate. Vein M+CU virtually straight. Vein 1-1A nearly straight. Vein 1a absent. Second submarginal cell trapezoidal. Subbasal cell glabrous, with two parallel rows of short setae subapically, and a narrow patch of setae just below vein 1CUa. (Fig. 32). Basal cell mostly evenly setose, sparsely setose

posteriorly. Hind wing: Vein RS bent at basal 0.3, with vein r present. Marginal cell narrowest at base. Vein M+CU/1M 1.5–1.8. Vein M+CU/r-m 1.2–1.4. Vein m-cu present and pigmented, although not tubular. Vein m-cu position relative to vein r-m interstitial or nearly so. Vein 2-1A absent. Basal cell evenly, rather sparsely setose, posteriorly with small bare area (Fig. 31).

Hind legs. Femur length/width 4.8–5.5. Length of tibia/tarsi ~ 0.9. Length of basitarsus/tarsi 2–4 0.65–0.75. Sculpture of hind coxa dorsally granulate. Tarsal claws not pectinate.

Metasoma. T1 length/apical width 1.3–1.4. T2 length/apical width 0.8–1.0. T3 length/apical width 0.5–0.6. Mid-longitudinal carina extending until near apex of T3. Metasoma sculpture T1 rugose, T2 and most of T3 striate-rugose, sculpture weaker at T3, T4 granular-coriaceous, remainder of metasoma smooth. Ovipositor sheath/hind basitarsus ~ 0.37. Apex of ovipositor sheaths truncate; apical point absent.

Color (Figs 29, 30). Brownish orange. Palpi yellow. Antenna mostly brownish orange, but basally brown and tip slightly darker. Wings weakly infuscate, veins brown, stigma yellow. Fore and middle legs with femur dark brown, tibia and tarsi brownish yellow or pale yellow; fifth tarsomeres light brownish orange. Hind legs with femur mostly dark brown apically, tibia pale yellow with apical ~ 0.3 dark brown, tarsi 1–4 mostly pale yellow, fifth tarsomeres light brown. Ovipositor sheaths dark brown.

Male. Essentially as in female except body length 7.0–8.1 mm; fore wing length 6.0–6.8 mm; antenna with 51–53.

Diagnosis. *Aleiodes brevicarina* is one of a small group of species with similarly colored, distinctively banded hind legs (Fig. 29), including *A. joaquimi*, *A. maculosus*, and *A. ovatus*. This species differs from these other species with similarly banded hind legs in having propodeum with a very short longitudinal carina, less than half of its length.

Distribution. Known only from type locality at Canchim Farm (Embrapa Pecuária Sudeste), São Paulo state, Brazil.

Etymology. The name *brevicarina* is Latin for short ridge, being a reference to the short median carina on the propodeum in this species.

Aleiodes coariensis Shimbori & Shaw, sp. nov.

http://zoobank.org/41AEFC83-8976-4A5E-B0C6-1620FF5CA038
Figs 33–36

Type material. Holotype, female (DCBU #20788) "BR, AM, Coari, rio Urucu, Petrobras, ROC-29, 5–10/II/1992, P. Bührnneim. N.O. Aguiar & N.Fé col."

Paratypes. 1 female (CNCI) "BRAZIL, Mato Grosso, Sinop, XI.1975 M. Alvarenga, Mal. Trap"; 1 female, 1 male (MUSM) "PERU: MD, Rio Los Amigos, CICRA, Aeródromo, 276m, 12°33'36"S, 70°06'17.5"W 22–28.vii.2006, Light trap, A. Asenjo"; 1 female (MUSM), same data except "… 380m … 2009, Manual, S. Carbonel"; 1 female (MUSM) "PERU: PU, Sandia, San Pedro de Putina Punco, P.N. Bahuaja Sonene 13°23'29.4"S, 69°29'00.1"W 322m 11–24.ix.2011 E. Guilhermo y E. Razuri."

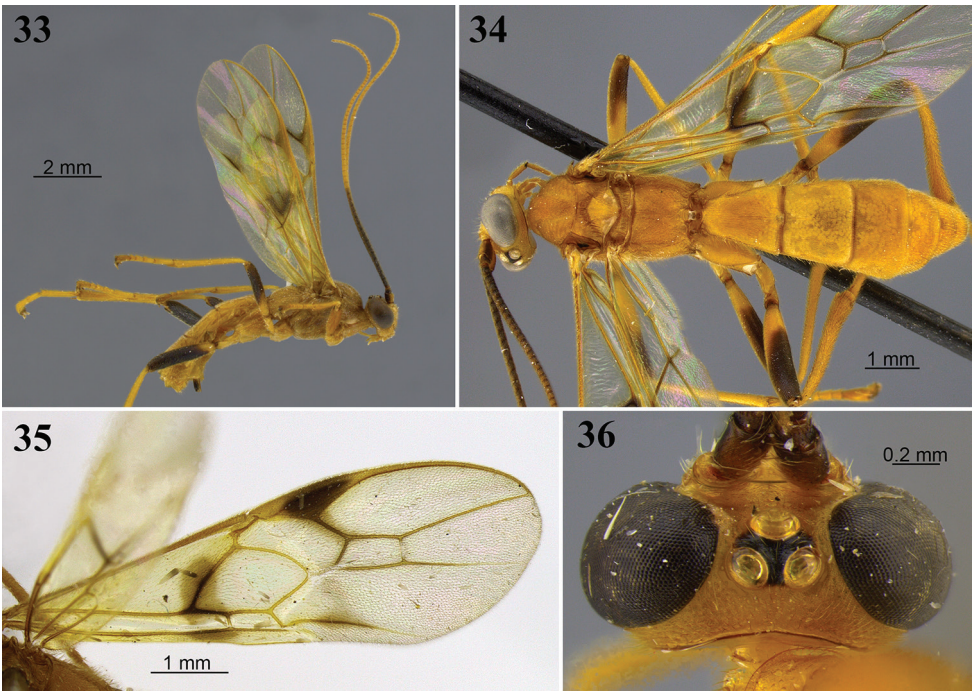

Figures 33–36. *Aleiodes coariensis* sp. nov. **33** lateral habitus **34** dorsal habitus **35** fore wing **36** head, dorsal view.

Description. Body length 7.5–9.2 mm. Fore wing length 6.7–7.7 mm.

Head (Fig. 36). In dorsal view eye length/temple 4.6–4.9. Eye height/head width 0.40–0.42. Eye height/minimum distance between eyes 1.2–1.4. OD/POL 2.4–3.4. OD/OOL 2.8–3.4. Frons excavated. Frons lateral carina present. Occipital carina dorsally complete, weakly curved. Occiput in dorsal view nearly straight, not indented medially. Occipital carina ventrally meeting hypostomal carina. Mid-longitudinal crest at upper face present. Hypoclypeal depression/face width 3.7–3.9. Malar space/eye height 0.18–0.19. Face height/width 0.84–0.87. Clypeus height/width 0.6–0.7. Clypeus convex, granulate. Sculpture of head shiny granular-coriaceous. Face transversely rugose-striate, medially granular-coriaceous below crest.

Antenna. Antennal segments 57–59. Antenna/body length 1.3. Scape/pedicel length 2.2–2.5. Length of first/second flagellomere 1.1. Fourth flagellomere length/apical width 1.5–1.6. Tip of apical segment of antenna pointed.

Mesosoma. Length/height ~ 1.7. Width of mesoscutum/width of head 0.7. Mesoscutum length/width ~ 1.0. Pronotal collar/vertex 0.8. Prescutellar sulcus with 5–7 distinct carinae. Mesoscutum posterior border with distinct complete carina. Metanotum with mid-longitudinal carina complete, connecting to a carinate pit posteriorly, or carina bisecting posterior pit, although weaker posteriorly. Metanotum mid-pit present, delimited by carinae. Mid-longitudinal carina of propodeum complete, or nearly complete. Ventral mid-line of mesopleuron without sulcus anteriorly, shallow smooth sulcus present posteri-

orly; pit at ventral mid-line absent. Notauli weakly indicated anteriorly, indistinctly crenulate. Sternaulus weakly indicated anteriorly, rugose. Sculpture of mesosoma mostly granulate. Metapleuron rugose posteriorly. Pronotum rugose laterally, pronotal groove sparsely crenulate anteriorly, short subventral longitudinal carina present. Mesopleuron rugose below subalar groove. Subalar groove crenulate. Mid-posterior region of mesoscutum rugose, with a short mid-longitudinal carina posteriorly. Mesoscutellar trough entirely costate. Metanotum costate, or mostly smooth and weakly crenulate. Propodeum mostly rugose.

Wings (Fig. 35). Fore wing: Stigma length/height 3.6–3.7. Vein r/2RS 1.2–1.4. Vein r/RS+Mb 1.3–1.4. Vein 3RSa/2RS 1.5–1.7. Vein 3RSa/2M 0.8. Vein 3RSa/3RSb 0.3–0.4. Vein 1CUa/1CUb 0.85. Vein 1CUa/2CUa 1.6. Vein 1cu-a weakly inclivous. Vein 1M weakly curved basally. Vein RS+Ma distinctly curved. Vein M+CU virtually straight. Vein 1-1A very weakly sinuate apically. Vein 1a absent. Second submarginal cell trapezoidal. Subbasal cell glabrous, with two parallel rows of short setae subapically, and a row of setae just below vein 1CUa and M+CU apically, plus a row of setae apically just above vein 1-1A. Basal cell mostly evenly setose, although setae sparser posteriorly, rarely with more or less large glabrous region posteriorly. Hind wing: Vein RS bent at basal 0.3, with vein r present. Marginal cell narrowest at base. Vein M+CU/1M 1.7–1.8. Vein M+CU/r-m 1.3–1.4. Vein m-cu present and pigmented, although not tubular. Vein m-cu position relative to vein r-m interstitial, or just antefurcal. Vein 2-1A absent. Basal cell evenly, rather sparsely setose, posteriorly with small bare area.

Hind legs. Femur length/width 5.0–5.3. Length of tibia/tarsi 0.85–0.95. Length of basitarsus/tarsi 2–4 0.75. Sculpture of hind coxa dorsally shiny granular-coriaceous. Tarsal claws not pectinate.

Metasoma. T1 length/apical width 1.1–1.2. T2 length/apical width 0.8–0.9. T3 length/apical width 0.65. Mid-longitudinal carina extending until basal 0.7 of T3. Metasoma sculpture T1 rugose, T2 and most of T3 striate-rugose, sculpture weaker at T3, remainder terga granular-coriaceous. Ovipositor sheath/hind basitarsus 0.3–0.5. Apex of ovipositor sheaths truncate; apical point absent.

Color. Body entirely brownish yellow, including palpi and tegula. Antenna dark brown basally, gradually lightening toward light brown apex. All three femora apically dark brown, dark region larger at hind femur. Wings tinged yellow; most veins yellow, except vein 1M basally and 1CUa dark brown, apex of 1-1A brown, and veins r, 2RS, 3RS, 2M and part of 2CUb light brown; distinct infuscate spot around vein 1M, more faintly infuscate areas around veins r and 2CUa, and bellow apex of vein 1-1A; stigma varying from entirely yellow to mostly dark brown expect basal 0.3 yellow. Ovipositor sheaths dark brown.

Male. Essentially as in female with stigma mostly dark brown, although dark spot at stigma smaller. Body length 8.0–8.6 mm; fore wing 6.7–7.0 mm; antenna with 61 segments.

Diagnosis. *Aleiodes coariensis* is the only species in the *A. bakeri* species subgroup with all femora at least partially marked with dark brown color (Fig. 34). There is also a distinctive infuscate spot on the fore wing near the base of vein 1M (Fig. 35). See the key for additional diagnostic characters.

Distribution. This species is known from localities in Brazil and Peru (Amazonian region).

Etymology. The name *coariensis* refers to the municipality of Coari, in Amazonas State in northwestern Brazil, the type-locality of this species.

Aleiodes goiasensis Shimbori & Shaw, sp. nov.

http://zoobank.org/D64CAA48-0F68-4784-87CE-AF235F500FE4
Figs 37–40

Type material. Holotype, female (MZUSP) "Cabeceiras (Lagôa Formosa) Goiás 24–27.X.1964 Exp. Dep. Zool."

Paratypes. 5 females (MZUSP), same as holotype; 1 female (DCBU #21878) "Brasil Pará Serra Norte N-1C. Pedra 5-IX-1983."

Description. Body length 7.2–8.8 mm. Fore wing length 6.3–7.6 mm.

Head. In dorsal view eye length/temple 3.6–3.8. Eye height/head width 0.39–0.43. Eye height/minimum distance between eyes 1.1–1.3. OD/POL 2.6–2.8. OD/OOL 3.2–3.5. Frons excavated. Frons lateral carina present. Occipital carina dorsally complete and curved. Occiput in dorsal view weakly indented medially. Occipital carina ventrally meeting hypostomal carina. Mid-longitudinal crest at upper face present. Hypoclypeal depression/face width 0.34–0.38. Malar space/eye height 0.16–0.17. Face height/width 0.7. Clypeus height/width ~ 0.6. Clypeus convex, granulate. Sculpture of head mostly granulate, vertex granular-rugose, frons shiny granular-coriaceous. Face mostly transversely rugose-striate, granulate medially.

Antenna. Antennal segments 54–61. Antenna/body length 1.1. Scape/pedicel length 2.4–2.6. Length of first/second flagellomere 1.2–1.3. Fourth flagellomere length/apical width 1.3–1.5. Tip of apical segment of antenna pointed.

Mesosoma. Length/height 1.56–1.67. Width of mesoscutum/width of head 0.67–0.70. Mesoscutum length/width 1.2. Pronotal collar/vertex 0.7. Prescutellar sulcus with complete mid-longitudinal carina, and 2–4 pairs of rather incomplete carinae laterally. Mesoscutum posterior border with distinct complete carina. Metanotum with mid-longitudinal carina complete, connecting to a carinate pit posteriorly, sometimes bisecting posterior pit. Metanotum mid-pit present, delimited by carinae. Mid-longitudinal carina of propodeum present at basal 0.8, or complete. Ventral mid-line of mesopleuron set within shallow smooth sulcus; pit at ventral mid-line present, shallow. Notauli weakly indicated anteriorly, indistinctly crenulate. Sternaulus absent. Sculpture of mesosoma mostly granulate. Pronotum rugose laterally, pronotal groove curvedly crenulate anteriorly, short subventral longitudinal carina present. Mesopleuron mostly rugose. Subalar groove crenulate. Mid-posterior region of mesoscutum rugose with long and irregular mid-longitudinal carina. Mesoscutellar trough costate near scutellum. Metanotum mostly smooth, with one or two pairs of lateral carinae. Propodeum mostly rugose.

Wings. Fore wing: Stigma length/height 3.2–3.6. Vein r/2RS 1.5. Vein r/RS+Mb 1.4–1.5. Vein 3RSa/2RS 1.4–1.5. Vein 3RSa/2M 0.8. Vein 3RSa/3RSb 0.31–0.34.

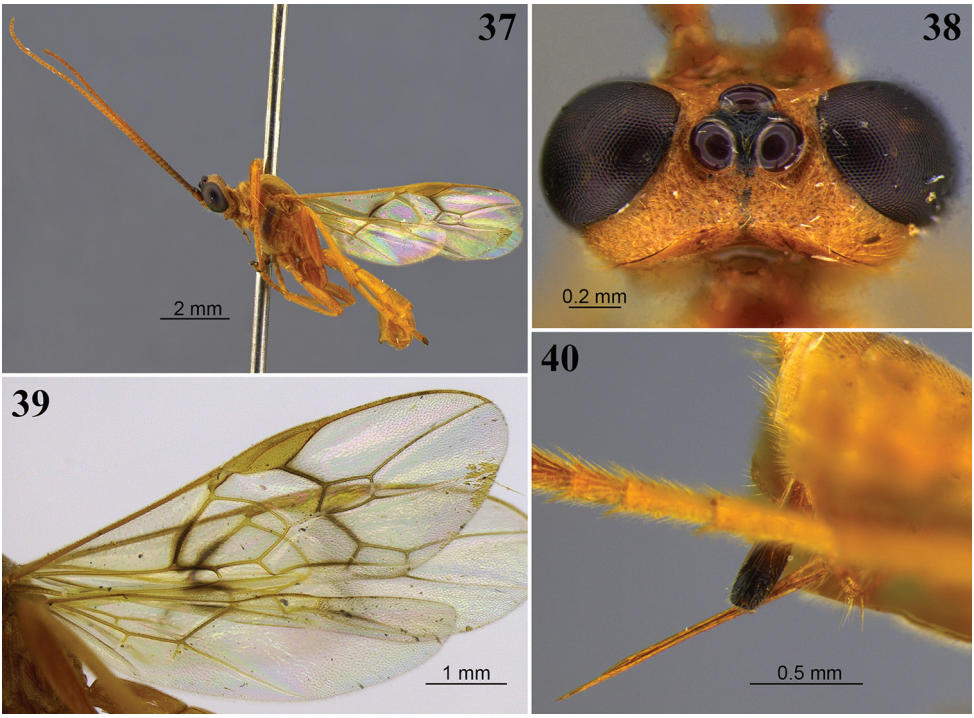

Figures 37–40. *Aleiodes goiasensis* sp. nov. **37** lateral habitus **38** head, dorsal view **39** wings **40** apex of metasoma showing ovipositor and sheath.

Vein 1CUa/1CUb 0.8–0.9. Vein 1CUa/2CUa 1.6–1.7. Vein 1cu-a inclivous. Vein 1M weakly curved basally. Vein RS+Ma distinctly curved. Vein M+CU virtually straight. Vein 1-1A sinuate. Vein 1a absent. Second submarginal cell short and trapezoidal. Subbasal cell glabrous, with two parallel rows of short setae subapically, and a narrow patch of setae just below vein 1CUa. Basal cell with more or less large glabrous region posteriorly, sometimes with sparse setae; costal and apical regions evenly setose. Hind wing: Vein RS bent at basal 0.3, with vein r present. Marginal cell narrowest at base. Vein M+CU/1M 1.6–1.7. Vein M+CU/r-m 1.4. Vein m-cu present, spectral. Vein m-cu position relative to vein r-m interstitial, or antefurcal. Vein 2-1A absent. Basal cell sparsely setose, bare posteriorly.

Hind legs. Femur length/width 4.7–4.8. Length of tibia/tarsi ~ 1.0. Length of basitarsus/tarsi 2–4 0.75. Sculpture of hind coxa dorsally granulate. Tarsal claws not pectinate.

Metasoma. T1 length/apical width ~ 1.1. T2 length/apical width 0.75. T3 length/apical width 0.6. Mid-longitudinal carina extending until basal 0.5 of T3. Metasoma sculpture T1 rugose, T2 and most of T3 striate-rugose, sculpture weaker at T3, remainder terga granular-coriaceous. Ovipositor sheath/hind basitarsus 0.1–0.2. Apex of ovipositor sheaths truncate; apical point absent.

Color. Brownish orange. Stemmaticum black. Antenna dark brown basally, gradually lightening toward brownish yellow apex; pedicel dark brown; scape dark brown,

ventrally yellow. Wings weakly tinged yellow; stigma and most veins yellow but veins 1M at basal 0.7, 1CUa, apex of 1-1A and of 2CUb, and sometimes vein r brown to dark brown; infuscate areas around base of vein 1M and below apex of vein 1-1A. Ovipositor sheaths dark brown.

Male. Unknown

Diagnosis. *Aleiodes goiasensis* is similar to *A. nigristemmaticum* (Enderlein) but differs by having the fore wing vein r distinctly longer than 2RS (Fig. 39), the occipital carina distinctly curved mid-dorsally (Fig. 38), and the hind femur relatively shorter (4.7–4.8 × longer than wide). In contrast, in *A. nigristemmaticum* specimens the fore wing vein r is approximately equal to vein 2RS length, the occipital carina dorsally is mostly straight or only slightly bent, and the hind femur is 5.5–5.7 × longer than wide.

Distribution. *Aleiodes goiasensis* is known only from central Brazil.

Etymology. The name refers to Goiás, a state in mid-west Brazil, and the type locality for this new species.

Aleiodes gonodontivorus Shaw & Shimbori, sp. nov.

http://zoobank.org/F7196D5E-362C-46CD-9E34-DB554180CC54
Figs 41–47

Type material. Holotype, female (UWIM) "COSTA RICA: Puntarenas Pen. Osa, 23 km N. Pto. Jimenez, La Palma, 10m viii.ix.1991, P. Hanson Malaise, in large trees."

Paratype data: 1 female (CNCI) Voucher: D.H. Janzen & W. Hallwachs, DB http://janzen.sas.upenn.edu, Area de Conservacion Guanacaste, COSTA RICA, 08-SRNP-56870, DHJPAR0029068. 17 females (pinned) with same data as except database code numbers as follows: 02-SRNP-15182; 02-SRNP-16572; 04-SRNP-22853; 05-SRNP-21738, DHJPAR0009352; 05-SRNP-57663, DHJPAR0009351; 06-SRNP-33504, DHJPAR0016434; 07-SRNP-21855, DHJPAR0021131; 07-SRNP-55246, DHJPAR0016925;07-SRNP-55995,DHJPAR0021153;07-SRNP-57169,DHJPAR0021156; 07-SRNP-55235, DHJPAR0016919; 07-SRNP-56915, DHJPAR0021154; 08-SRNP-21657, DHJPAR0028027; 08-SRNP-21975, DHJPAR0028034; 08-SRNP-21658, DHJPAR0028026; 08-SRNP-21742, DHJPAR0028035; 08-SRNP-56872, DHJPAR0028025 [BOLD ID: ASHYE262-08; additional data: Sector Mundo Nuevo, Vado Huacas, 10.755 -85.391, 490 m, ex. *Gonodonta fulvangula* (Erebidae), 3.viii.2008, J. Cortez col.] (CNCI). 6 males (pinned) with same data except code numbers as follows: 90-SRNP-1226; 94-SRNP-6152; 07-SRNP-56881, DHJPAR0021155; 08-SRNP-21758, DHJPAR0028028; 08-SRNP-21980, DHJPAR0028029 (CNCI). 5 females (in alcohol vials) with same data except code numbers as follows: 05-SRNP-58906, DHJPAR0021181; 06-SRNP-22766, DHJPAR0029041; 08-SRNP-57558, DHJPAR0029063; 08-SRNP-56966, DHJPAR0029060; 08-SRNP-57556, DHJPAR0029062 (CNCI). 4 males (in alcohol vials) with same data except code numbers as follows: 06-SRNP-32956, DHJPAR0029042; 06-SRNP-32931, DHJPAR0029049; 08-SRNP-56881, DHJPAR0029066 [BOLD ID: ASHYF744-09; additional data: Sector Mundo Nuevo, Vado

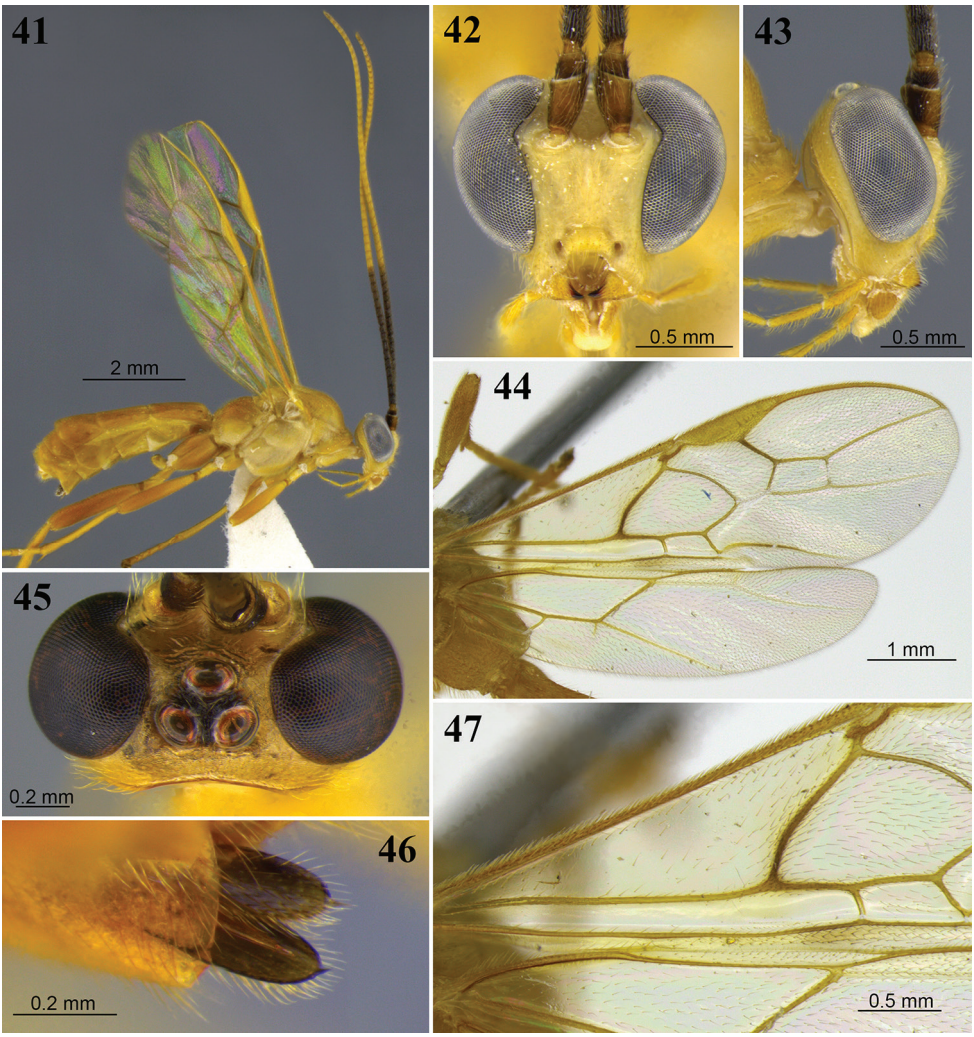

Figures 41–47. *Aleiodes gonodontivorus* sp. nov. **41** lateral habitus **42** head, anterior view **43** head, lateral view **44** wings **45** head, dorsal view **46** apex of metasoma showing ovipositor and sheath with apical point **47** fore wing basally.

Huacas, 10.755 -85.391, 490 m, ex. *Gonodonta fulvangula* (Erebidae), 4.viii.2008, D. Guadamuz col.]; 08-SRNP-56740, DHJPAR0029065 (CNCI). 1 female, Mexico, Campeche, Escárcega, El Tormento, 18°36'30.1"N, 90°48'45.7"W, ex. *Gonodonta nitidimacula* on *Piper amalago*, 25. 8. 2018, D. Campos. 1 male (INBIO) "P.N. Manuel Antonio, 80 m, Quepos, Prov. Punt., COSTA RICA, May 1993. G. Varela. L-S 370900, 448800"; 1 male (MZUSP) "Brasil: BA: Andarai, Mata Carrasco (Castanha), 13–14.XII.1990 Brandão, Diniz & Oliveira"; 1 female (DCBU #21872) "BIOTA – FAPESP Recife, PE, Brasil Pque. Estadual de Dois Irmãos 21.VII.2002 Varredura – Amostra 1 S.T.P. Amarante e equipe col."; 1 female (DCBU #21873), same data except "... 22.VII.2002 ... Amostra 7."

Description. Body length 6.5–8.1 mm. Fore wing length 5.6–6.2 mm.

Head (Figs 42, 43, 45). In dorsal view eye length/temple 3.6–4.5. Eye height/head width 0.41–0.43. Eye height/minimum distance between eyes 1.2–1.4. OD/POL 2.9–3.8. OD/OOL 2.3–3.8. Frons excavated. Frons lateral carina present; W-shaped carina present or absent, usually poorly defined. Occipital carina dorsally complete and curved (Fig. 45). Occiput in dorsal view weakly indented medially. Occipital carina ventrally meeting hypostomal carina. Mid-longitudinal crest at upper face present. Hypoclypeal depression/face width 0.35–0.39. Malar space/eye height 0.15–0.19. Face height/width 0.68–0.76. Clypeus height/width 0.67–0.69. Clypeus convex, granulate. Sculpture of head mostly granulate. Face transversely rugose-striate around median crest.

Antenna. Antennal segments 52–54. Antenna/body length 1.1–1.2. Scape/pedicel length 2.3–2.6. Length of first/second flagellomere 1.0–1.2. Fourth flagellomere length/apical width 1.5–1.6. Tip of apical segment of antenna pointed, or nipple-shaped.

Mesosoma. Length/height ~ 1.6. Width of mesoscutum/width of head 0.7–0.8. Mesoscutum length/width ~ 1.1. Pronotal collar/vertex 0.9. Prescutellar sulcus with complete mid-longitudinal carina plus two or three pairs of lateral carinae more or less defined, or entirely costate, lateral carina oblique and nearly reaching anterior border. Mesoscutum posterior border with distinct complete carina. Metanotum with complete mid-longitudinal carina, sometimes interrupted at middle; carinate posterior pit sometimes bisected by carina. Metanotum mid-pit present, delimited by carinae. Mid-longitudinal carina of propodeum nearly complete. Ventral mid-line of mesopleuron set within shallow smooth sulcus; pit at ventral mid-line present, shallow. Notauli weakly indicated anteriorly, indistinctly crenulate. Sternaulus weakly indicated anteriorly, rugose. Sculpture of mesosoma mostly granulate. Pronotum granulate-rugose laterally, pronotal groove curvedly crenulate anteriorly, short subventral longitudinal carina present. Mesopleuron rugose below subalar groove. Subalar groove crenulate. Mid-posterior region of mesoscutum rugose, with a short mid-longitudinal carina posteriorly. Mesoscutellar trough entirely costate. Metanotum costate. Propodeum mostly rugose.

Wings (Figs 44, 47). Fore wing: Stigma length/height 3.4–3.6. Vein r/2RS 1.2–1.3. Vein r/RS+Mb 1.2–1.4. Vein 3RSa/2RS 1.4–1.7. Vein 3RSa/2M 0.79–0.86. Vein 3RSa/3RSb 0.32–0.43. Vein 1CUa/1CUb 0.9–1.0. Vein 1CUa/2CUa 1.6–1.9. Vein 1cu-a weakly inclivous. Vein 1M weakly curved basally. Vein RS+Ma distinctly curved. Vein M+CU virtually straight. Vein 1-1A sinuate. Vein 1a absent. Second submarginal cell trapezoidal. Subbasal cell glabrous, with two parallel rows of short setae subapically, and a narrow patch of setae just below vein 1CUa. Basal cell with more or less large glabrous region posteriorly, sometimes with sparse setae; costal and apical regions evenly setose. Hind wing: Vein RS bent at basal 0.3, with vein r present. Marginal cell narrowest at base. Vein M+CU/1M 1.5–1.7. Vein M+CU/r-m 1.3–1.4. Vein m-cu present, spectral. Vein m-cu position relative to vein r-m interstitial, or antefurcal. Vein 2-1A absent. Basal cell sparsely setose, bare posteriorly.

Hind legs. Femur length/width 5.0–5.3. Length of tibia/tarsi 0.9–1.0. Length of basitarsus/tarsi 2–4 0.70–0.75. Sculpture of hind coxa dorsally shiny granulate, apically striate. Tarsal claws not pectinate.

Metasoma. T1 length/apical width 1.1–1.2. T2 length/apical width 0.7–0.9. T3 length/apical width 0.5–0.6. Mid-longitudinal carina extending until basal 0.7 of T3. Metasoma sculpture T1, T2 and basal 0.7 of T3 rugose-costate, or sculpture weaker at T3, remainder terga granular-coriaceous. Ovipositor sheath/hind basitarsus 0.3–0.5. Apex of ovipositor sheaths roughly rounded with distinct apical point (Fig. 46).

Color. Brownish yellow. Stemmaticum black. Antenna with basal 14–16 flagellomeres black, apical segments yellow; pedicel black; scape black, ventrally brownish yellow. Wings weakly tinged yellow; stigma pale yellow, most veins yellow but veins 1M at basal half, apex of 2CUb, and sometimes vein r brown; faint infuscate areas around base of vein 1M and below apex of vein 1-1A. Ovipositor sheaths dark brown.

Male. Essentially as in female, 10–16 black basal flagellomeres. Body length 6.6–7.3 mm; fore wing length 5.4–5.6 mm; antenna with 50 segments.

Diagnosis. *Aleiodes gonodontivorus* resembles *A. nigristemmaticum* (Enderlein) but is readily recognizable by the distinctly and abruptly contrasting bicolored antenna (Fig. 41). In *A. nigristemmaticum* specimens the flagellum is dark basally but becomes gradually lighter over many flagellomeres. *Aleiodes gonodontivorus* may also be easily distinguished by the short second submarginal cell (Fig. 44), and the fore wing vein r being distinctly longer than vein 2RS (Fig. 44). In *A. nigristemmaticum* the veins r and 2RS are of similar length. *Aleiodes gonodontivorus* is also similar to *A. lidiae* but these two species can be easily separated by the characters given in couplet 17 of the key and they are also discussed in the diagnosis for *A. lidiae*.

Biology. Parasitoids of caterpillars of *Gonodonta bidens* (Geyer) [8-SRNP-57556, 57558], *G. correcta* Walker [06-SRNP-32931], *G. fulvangula* (Geyer) [4-SRNP-22853; 7-SRNP-21855, 5691557169; 8-SRNP-21738, 21742, 21758, 21975, 21980, 56740, 56870, 56872, 56881, 56966], *G. immacula* (Guenée) [8-SRNP-58906; 90-SRNP-1226], *G. incurva* (Sepp) [2-SRNP-15182; 5-SRNP-57663; 6-SRNP-22766, 33504; 7-SRNP-55235, 55246, 55995; 8-SRNP-21657, 21658; 94-SRNP-6152], *G. maria* (Guenée) [7-SRNP-56881], *G. nitidimacula* Guenée, *G. pyrgo* (Cramer) [2-SRNP-16752], and *G. uxor* (Cramer) [6-SRNP-32956] (Erebidae, Calpinae), which feed on species of *Piper* (Piperaceae), *Annona* (Annonaceae) and on *Ocotea veraguensis* (Lauraceae).

Distribution. *Aleiodes gonodontivorus* is known from localities in Costa Rica and Brazil.

Etymology. The name is from *Gonodonta* Hubner, 1818 (a genus of moths in the family Erebidae and a recorded host for this new species), and the Latin word *vorus* meaning to eat or devour.

Aleiodes hyalinus Shimbori & Shaw, sp. nov.

http://zoobank.org/5D2F5A96-801A-481A-9609-17C89C3BD377
Figs 48–50

Type material. Holotype, female (DCBU #21839) "Rio Mogi Guaçu Luís Antônio-SP luz, 28.XII.1989 L.A. Joaquim, col."

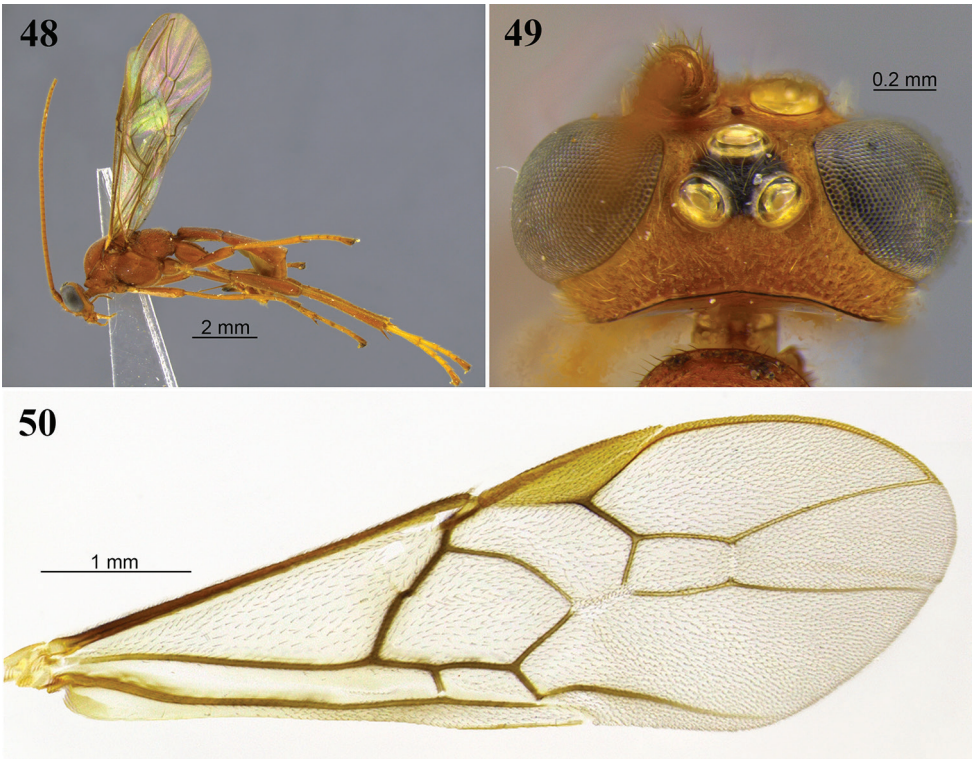

Figures 48–50. *Aleiodes hyalinus* sp. nov. **48** lateral habitus **49** head, dorsal view **50** fore wing.

Paratypes. 1 female (DCBU #21838), same as holotype; 1 male (DCBU #21840), same data except "18.II.1988"; 1 female (DCBU #21812) "Faz. Jacutinga São Carlos – SP 28.IX.1987, luz, U. Fernandes col."; 1 male (DCBU #21815) "Faz. Canchim São Carlos – SP 29.III.1985 A.S. Soares, col."; 1 male (DCBU #21813), same data except "3.II.1987"; 3 females, 1 male (CNCI) "BRAZIL, 960m Bahia, Encruzilhada XI.1972 M. Alvarenga"; 1 female (CNCI) "Brazil, Pedra Azul, M. Gerais XI.1972"; 1 female (DZUP) "Jundiaí do Sul, PR, Brasil Fazenda Monte Verde 30.XI.1986 Luminosa, Lev. Ent. PROFAUPAR."

Description. Body length 5.8–8.3 mm. Fore wing length 5.0–6.9 mm.

Head. In dorsal view eye length/temple 4.6–6.0. Eye height/head width 0.41–0.43. Eye height/minimum distance between eyes 1.3–1.4. OD/POL 2.0–3.6. OD/OOL 3.7–9.0. Frons excavated. Frons lateral carina weakly indicated. Occipital carina dorsally complete, weakly curved. Occiput in dorsal view nearly straight, not indented medially. Occipital carina ventrally meeting hypostomal carina. Mid-longitudinal crest at upper face present. Hypoclypeal depression/face width 0.33–0.36. Malar space/eye height 0.15–0.19. Face height/width 0.72–0.77. Clypeus height/width 0.6–0.7. Clypeus convex, granulate. Sculpture of head mostly granular-coriaceous, vertex granular-rugose, frons shiny granular-coriaceous. Face transversely rugose-striate, medially granular-coriaceous below crest.

Antenna. Antennal segments 47–54. Antenna/body length 1.1. Scape/pedicel length 1.8–2.1. Length of first/second flagellomere 1.1–1.2. Fourth flagellomere length/apical width 1.6–1.7. Tip of apical segment of antenna nipple-shaped.

Mesosoma. Length/height 1.5–1.6. Width of mesoscutum/width of head 0.68–0.78. Mesoscutum length/width 1.0–1.1. Pronotal collar/vertex 0.67–0.75. Prescutellar sulcus with complete mid-longitudinal carina, and a few irregular and incomplete carinae laterally. Mesoscutum posterior border with distinct complete carina. Metanotum with mid-longitudinal carina complete, connecting to a carinate pit posteriorly, or with complete mid-longitudinal carina, sometimes interrupted at middle. Metanotum mid-pit present, delimited by carinae. Mid-longitudinal carina of propodeum present and basal 0.5 or less, or nearly complete. Ventral mid-line of mesopleuron set within shallow smooth sulcus. Pit at ventral mid-line present, or weakly indicated. Notauli weakly indicated anteriorly, indistinctly crenulate. Sternaulus absent. Sculpture of mesosoma mostly granulate. Pronotum granulate ventrally, pronotal groove mostly crenulate, short subventral longitudinal carina present. Mesopleuron mostly rugose. Subalar groove crenulate. Mid-posterior region of mesoscutum rugose, with a short mid-longitudinal carina posteriorly. Mesoscutellar trough costate near scutellum. Metanotum mostly smooth and weakly crenulate. Propodeum mostly rugose.

Wings. Fore wing (Fig. 50): Stigma length/height 3.4–3.6. Vein r/2RS 1.1–1.3. Vein r/RS+Mb 1.2–1.4. Vein 3RSa/2RS 1.5–1.9. Vein 3RSa/2M 0.77–0.87. Vein 3RSa/3RSb 0.37–0.44. Vein 1CUa/1CUb 0.8–0.9. Vein 1CUa/2CUa 1.6–1.8. Vein 1cu-a inclivous. Vein 1M weakly, evenly curved. Vein RS+Ma distinctly curved. Vein M+CU weakly sinuate. Vein 1-1A weakly sinuate at apex. Second submarginal cell trapezoidal. Vein 1a absent. Subbasal cell glabrous, with two parallel rows of short setae subapically, and a line of setae just below most part of veins M+CU/1CUa. Basal cell mostly evenly setose, more sparsely setose posteriorly. Hind wing: Vein RS bent at basal 0.3, with vein r present. Marginal cell narrowest at base. Vein M+CU/1M 1.5. Vein M+CU/r-m 1.2–1.3. Vein m-cu present, spectral, or partly tubular. Vein m-cu position relative to vein r-m distinctly antefurcal. Vein 2-1A absent. Basal cell sparsely setose, bare posteriorly.

Hind legs. Femur length/width 4.4–4.8. Length of tibia/tarsi ~ 0.9. Length of basitarsus/tarsi 2–4 ~ 0.7. Sculpture of hind coxa dorsally granulate. Tarsal claws not pectinate.

Metasoma. T1 length/apical width 1.1–1.2. T2 length/apical width 0.75–0.80. T3 length/apical width 0.45–0.60. Mid-longitudinal carina extending until basal 0.7 of T3. Metasoma sculpture T1 rugose, T2 and most of T3 striate-rugose, remainder terga granular-coriaceous. Ovipositor sheath/hind basitarsus 0.42–0.54. Apex of ovipositor sheaths truncate, without apical point.

Color (Fig. 48). Body reddish brown. Stemmaticum black (Fig. 49). Tegula dark brown. Wings subhyaline, veins light brown and stigma honey yellow (Fig. 50). Ovipositor sheaths dark brown.

Male. Essentially as in female. Body length 5.9–6.8 mm; fore wing length 4.9–5.7 mm; antenna with 45–51 segments.

Diagnosis. *Aleiodes hyalinus* is most similar to *A. santarosensis*, but its wings are entirely subhyaline with all veins honey yellow to light brown, without distinct darker regions (Fig. 50). By contrast, the wings are tinged with yellow and with dark markings in *A. santarosensis* (Figs 76, 78). The body is brownish orange or reddish brown in *A. hyalinus* (Fig. 48), as opposed to being entirely yellow in *A. santarosensis* (Figs 76, 77). The ovipositor sheath is mostly dark brown to black in *A. hyalinus* (Fig. 48), as opposed to being light brown in *A. santarosensis* (Fig. 76), and the basal cell is evenly setose in *A. hyalinus* (Fig. 50), while in *A. santarosensis* the basal cell has a large bare area entirely lacking setae (Fig. 78).

Distribution. *Aleiodes hyalinus* is known only from localities in Brazil.

Etymology. The name *hyalinus* is Latin for glass-like or clear being a reference to the lack of coloration in the wings of this species.

Aleiodes inga Shimbori & Shaw, sp. nov.

http://zoobank.org/82072909-4984-4D62-A11C-EA89327F75CD
Figs 51–54

Type material. Holotype data: Female (CNCI). Voucher: D.H. Janzen & W. Hallwachs, DB http://janzen.sas.upenn.edu, Area de Conservacion Guanacaste, COSTA RICA, 07-SRNP-42836, DHJPAR0029056.

Paratype: 1 female (pinned) with same data as holotype except database code number as follows: 07-SRNP-42756, DHJPAR0023529 [BOLD ID: ASHYM281-08; additional data: Sector Rincon Rain Forest, Puente Rio Negro, 10.904 -85.303, 340 m, ex. *Rosema deolis* (Notodontinae), 15.xi.2007, J. Perez col.] (CNCI); 6 males (in alcohol vials) with same data as holotype except database code numbers as follows: 07-SRNP-43021, DHJPAR0029053; 07-SRNP-42801, DHJPAR0029052; 07-SRNP-34415, DHJPAR0029057 [BOLD ID: ASHYE936-09; additional data: Sector Pitilla, Pasmompa, 11.019 -85.41, 440 m, ex. *Epitausa dilina* (Erebidae), 22.i.2008, C. Moraga and M. Rios col.]; 07-SRNP-42751, DHJPAR0029050 [BOLD ID: ASHYE929-09; additional data: Sector Rincon Rain Forest, Puente Rio Negro, 10.904 -85.303, 340 m, ex. *Helia argentipes* (Erebidae), 21.xi.2007, M. Carmona col.]; 07-SRNP-66111, DHJPAR0028755; 07-SRNP-42758, DHJPAR0029055 [BOLD ID: ASHYE934-09; additional data: Sector Rincon Rain Forest, Puente Rio Negro, 10.904 -85.303, 340 m, ex. *Helia argentipes* (Erebidae), 22.xi.2007, J. Perez col.] (CNCI).

Description. Body length 6.6–6.7 mm. Fore wing length 5.3–5.5 mm.

Head (Fig. 52). In dorsal view eye length/temple 4.8–5.1. Eye height/head width 0.44–0.46. Eye height/minimum distance between eyes 1.4–1.5. OD/POL 2.5. OD/OOL 3.3. Frons excavated. Frons lateral carina absent. Occipital carina dorsally complete, weakly curved. Occiput in dorsal view nearly straight, not indented medially. Occipital carina ventrally meeting hypostomal carina. Mid-longitudinal crest at upper face present. Hypoclypeal depression/face width 0.37. Malar space/eye height 0.18–0.19. Face height/width 0.81–0.85. Clypeus height/width 0.70–0.75. Clypeus

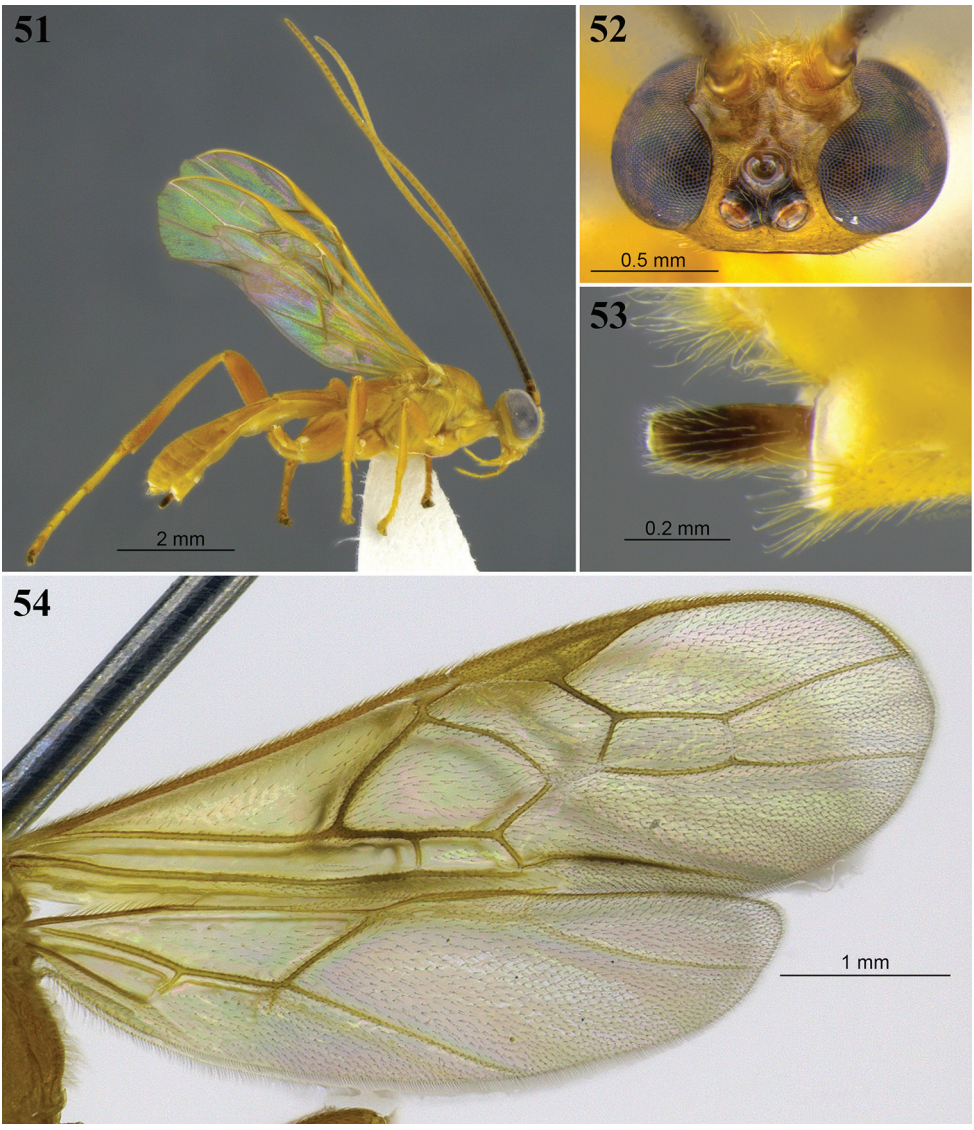

Figures 51–54. *Aleiodes inga* sp. nov. **51** lateral habitus **52** head, dorsal view **53** apex of metasoma showing ovipositor and truncate sheath without apical point **54** wings.

convex, granulate. Sculpture of head shiny granular-coriaceous. Face mostly granular-coriaceous, transversely rugose-striate around median crest.

Antenna. Antennal segments 51–54. Antenna/body length 1.1–1.2. Scape/pedicel length 2.1–2.4. Length of first/second flagellomere 1.1. Fourth flagellomere length/apical width 1.6. Tip of apical segment of antenna pointed.

Mesosoma. Length/height 1.6–1.7. Width of mesoscutum/width of head 0.66–0.69. Mesoscutum length/width ~ 1.1. Pronotal collar/vertex 0.78–0.83. Prescutellar sulcus

with complete mid-longitudinal carina, and a few irregular and incomplete carinae laterally. Mesoscutum posterior border with distinct complete carina. Metanotum with mid-longitudinal carina complete, connecting to a carinate pit posteriorly, sometimes bisecting posterior pit. Metanotum mid-pit present, delimited by carinae. Mid-longitudinal carina of propodeum nearly complete. Ventral mid-line of mesopleuron without sulcus anteriorly, shallow smooth sulcus present posteriorly; pit at ventral mid-line weakly indicated. Notauli weakly indicated anteriorly, indistinctly crenulate. Sternaulus weakly indicated anteriorly, rugose. Sculpture of mesosoma mostly granulate. Pronotum with pronotal groove mostly crenulate, short subventral longitudinal carina present. Mesopleuron rugose below subalar groove. Subalar groove sparsely crenulate. Mid-posterior region of mesoscutum rugose. Mesoscutellar trough entirely costate. Metanotum mostly smooth, with one or two pairs of lateral carinae. Propodeum mostly rugose.

Wings. Fore wing: Stigma length/height 3.5–3.7. Vein r/2RS 1.1–1.3. Vein r/RS+Mb 1.2–1.3. Vein 3RSa/2RS 1.9–2.0. Vein 3RSa/2M 0.83. Vein 3RSa/3RSb 0.5. Vein 1CUa/1CUb 0.8–0.9. Vein 1CUa/2CUa 1.8–1.9. Vein 1cu-a nearly vertical. Vein 1M weakly curved basally. Vein RS+Ma weakly curved. Vein M+CU virtually straight. Vein 1-1A weakly sinuate at apex. Vein 1a absent. Second submarginal cell long and trapezoidal. Subbasal cell glabrous, with two parallel rows of short setae subapically, and a narrow patch of setae just below vein 1CUa. Basal cell mostly evenly setose, sparsely setose posteriorly, with a bare spot posteriorly. Hind wing: Vein RS bent at basal 0.3, with vein r present. Marginal cell narrowest at base. Vein M+CU/1M 1.4–1.6. Vein M+CU/r-m 1.4–1.5. Vein m-cu present, spectral. Vein m-cu position relative to vein r-m antefurcal. Vein 2-1A absent. Basal cell sparsely setose, bare posteriorly.

Hind legs. Femur length/width 4.3–4.4. Length of tibia/tarsi ~ 0.9. Length of basitarsus/tarsi 2–4 0.70–0.75. Sculpture of hind coxa dorsally granulate. Tarsal claws not pectinate.

Metasoma. T1 length/apical width 1.2–1.3. T2 length/apical width 0.85. T3 length/apical width 0.60–0.65. Mid-longitudinal carina extending until basal 0.5 of T3. Metasoma sculpture T1 rugose, T2 and most of T3 striate-rugose, remainder terga granular-coriaceous. Ovipositor sheath/hind basitarsus 0.3. Apex of ovipositor sheaths truncate; apical point absent.

Color. (Figs 51–53) Brownish yellow. Stemmaticum black. Antenna dark brown basally, gradually lightening toward brownish yellow apex; pedicel dark brown; scape dark brown, ventrally yellow. Wings weakly tinged yellow; stigma yellow; most veins yellow but veins 1M at basal half, apex of 2CUb, and sometimes vein r brown; faint infuscate areas around base of vein 1M and below apex of vein 1-1A. Ovipositor sheaths dark brown (Fig. 53).

Male. Essentially as in female. Body length 6.5–6.7 mm; fore wing 5.2 mm; antenna with 51–52 segments.

Diagnosis. *Aleiodes inga* is unique within the subgroup in having the fore wing vein r longer than 2RS and much shorter than 3RSa, the second submarginal cell rectangular and comparatively long (Fig. 54) and the frons without lateral carina (Fig. 52). Other characters are similar to *A. nigristemmaticum*.

Biology. The most common host caterpillar for this species is *Helia argentipes* (Walker) (Erebidae, Erebinae) [7-SRNP-42758, 42751, 42801, 42836], but there are also records from *Epitausa dilina* (Herrich-Schäffer) (Erebidae, Eulepidotinae) [7-SRNP-34415], feeding on *Inga edulis* and *I. oerstediana* (Fabaceae), and *Letis mycerina* (Cramer) [10-SRNP-65094] (Erebidae) feeding on *Inga oerstediana*. A database record from caterpillars of the Área de Conservación Guanacaste (http://janzen.sas.upenn.edu) of *Rosema deolis* (Cramer) (Notodontidae) [7-SRNP-42756] is refuted based on the morphology of the accompanying mummy.

Distribution. This species is only known from northwest Costa Rica.

Etymology. The name is a reference to *Inga*, a genus of small tropical trees in the Fabaceae family and the recorded host plant for some Erebidae host caterpillars of this new species.

Aleiodes joaquimi Shimbori & Shaw, sp. nov.

http://zoobank.org/3C90EA2C-3A02-4C98-812D-040FA74537D0
Figs 55–58

Type material. Holotype, female (DCBU #20794) "Sta. Maria Madalena, RJ, Brasil. P.E. Desengano 18.IV.2002 (luz) L.A. Joaquim & S.A. Soares cols."

Paratype, female (CNCI) "BRAZIL: Bahia, Encruzilhada, XI.1972 M. Alvarenga."

Description. Body length 8.6–9.0 mm. Fore wing length 7.0–7.2 mm.

Head. In dorsal view eye length/temple 4.1. Eye height/head width 0.39–0.43. Eye height/minimum distance between eyes 1.1–1.3. OD/POL 3.2–3.4. OD/OOL 2.6–3.4. Frons excavated. Frons lateral carina present in addition to W-shaped carina. Occipital carina dorsally complete and curved. Occiput in dorsal view weakly indented medially. Occipital carina ventrally nearly touching hypostomal carina. Mid-longitudinal crest at upper face present. Hypoclypeal depression/face width 0.4. Malar space/eye height 0.11–0.14. Face height/width 0.85. Clypeus height/width 0.69. Clypeus convex, granulate. Sculpture of head shiny granular-coriaceous. Face transversely rugose-striate, medially granular-coriaceous below crest.

Antenna. Antenna with 59 antennomeres. Antenna/body length 1.0–1.1. Scape/pedicel length 2.5. Length of first/second flagellomere 1.1. Fourth flagellomere length/apical width 1.1. Tip of apical flagellomere pointed.

Mesosoma. Length/height 1.45–1.50. Width of mesoscutum/width of head 0.7–0.8. Mesoscutum length/width ~ 1.0. Pronotal collar/vertex 0.6–0.7. Prescutellar sulcus with complete mid-longitudinal carina, and a few irregular and incomplete carinae laterally. Mesoscutum posterior border with distinct complete carina. Metanotum with mid-longitudinal carina complete, connecting to a carinate pit posteriorly. Metanotum mid-pit present, delimited by carinae. Mid-longitudinal carina of propodeum complete. Ventral mid-line of mesopleuron smooth, without distinct sulcus; pit at ventral mid-line weakly indicated. Notauli weakly indicated anteriorly, indistinctly crenulate. Sternaulus absent. Sculpture of mesosoma mostly granulate. Pronotum pronotal groove strongly

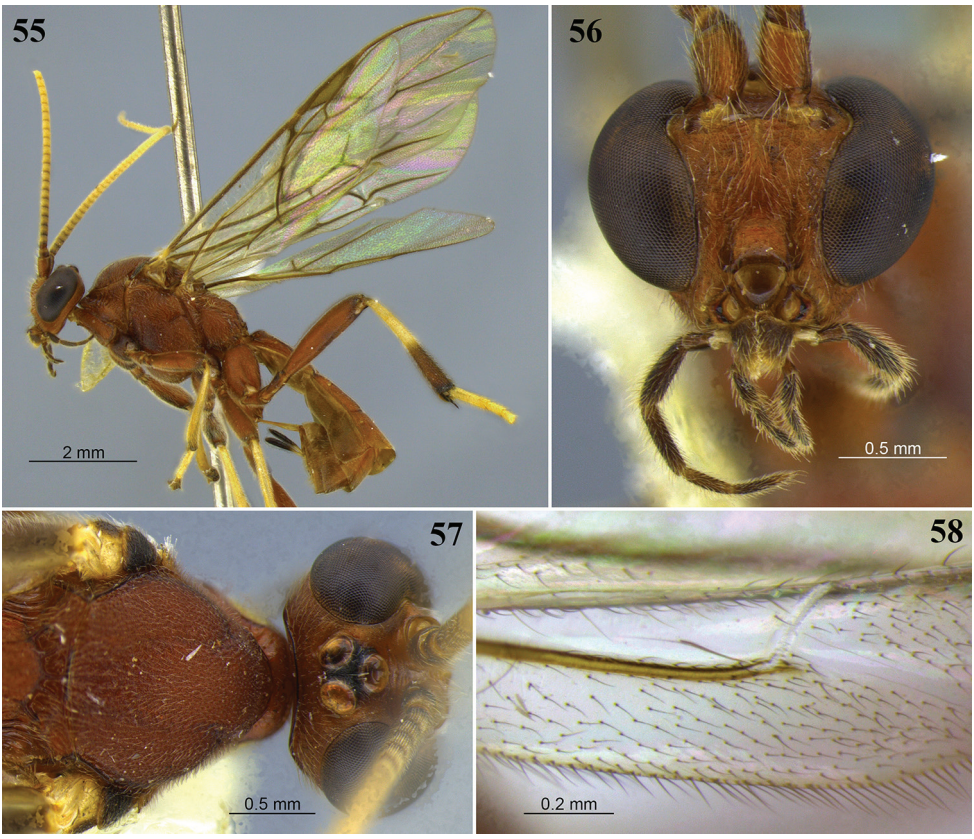

Figures 55–58. *Aleiodes joaquimi* sp. nov. **55** lateral habitus **56** head, anterior view **57** head, dorsal view **58** hind wing, posteriorly.

crenulate anteriorly, short subventral longitudinal carina present. Mesopleuron mostly rugose. Subalar groove crenulate. Mid-posterior region of mesoscutum rugose with long and irregular mid-longitudinal carina. Mesoscutellar trough entirely costate. Metanotum mostly smooth, with one or two pairs of lateral carinae. Propodeum mostly rugose.

Wings. Fore wing: Stigma length/height 3.3–3.5. Vein r/2RS 1.6. Vein r/RS+Mb 1.4–1.5. Vein 3RSa/2RS 1.2–1.3. Vein 3RSa/2M 0.71–0.75. Vein 3RSa/3RSb 0.24. Vein 1CUa/1CUb 0.6. Vein 1CUa/2CUa 1.1–1.2. Vein 1cu-a vertical. Vein 1M weakly, evenly curved. Vein RS+Ma virtually straight. Vein M+CU weakly sinuate. Vein 1-1A strongly sinuate. Vein 1a absent. Second submarginal cell short and trapezoidal. Subbasal cell glabrous, with a row of setae just below vein 1CUa and a row of setae apically just above vein 1-1A. Basal cell with more or less large glabrous region posteriorly, sometimes with sparse setae; costal and apical regions evenly setose. Hind wing: Vein RS bent at basal 0.3, with vein r present. Marginal cell narrowest at base. Vein M+CU/1M 1.6. Vein M+CU/r-m 1.4–1.5. Vein m-cu present and pigmented, although not tubular. Vein m-cu position relative to vein r-m interstitial. Vein 2-1A present, although very short (Fig. 58). Basal cell sparsely setose, bare posteriorly.

Hind legs. Femur length/width 4.8–5.3. Length of tibia/tarsi ~ 1.0. Length of basitarsus/tarsi 2–4 ~ 0.8. Sculpture of hind coxa dorsally granulate. Tarsal claws not pectinate.

Metasoma. T1 length/apical width ~ 1.2. T2 length/apical width 0.7. T3 length/apical width 0.55. Mid-longitudinal carina extending until T2 or basal 0.5 of T3. Metasoma sculpture: T1–2 rugose-striate, T3 granulate, remainder metasoma smooth. Ovipositor sheath/hind basitarsus 0.5–0.6. Apex of ovipositor sheaths roughly rounded; apical point present, although very short.

Color (Figs 55–57). Dark reddish brown. Palpi and tegula dark brown. Antenna mostly pale yellow, apex and base brown. All tibiae pale yellow with dark reddish brown apex, dark region larger in posterior legs; tarsi 1–4 whitish yellow, fifth tarsomere dark brown. Wings weakly tinged brown, veins brown, no infuscate regions. Ovipositor sheaths dark brown.

Male. Unknown

Diagnosis. *Aleiodes joaquimi* differs from similar species with banded hind legs by its deep reddish brown color (Figs 55–57), absence of infuscate spots on wings (Fig. 55), hind wing vein 2-1A present, although short (Fig. 58), and vein 1CUb relatively long, ~ 1.7 times longer than vein 1CUa (no more than 1.25 times in other species). It is most similar to *A. barrosi*, and the differences between these two species are discussed in the diagnosis for *A. barrosi*.

Distribution. The Atlantic Forest in Bahia and Rio de Janeiro states in Brazil

Etymology. The name is an honorary patronym for Luiz A. Joaquim, one of the collectors of the holotype specimen.

Aleiodes lidiae Shimbori & Shaw, sp. nov.

http://zoobank.org/0120A76E-85EC-4F3E-B5A8-E61704045AB1
Figs 59–63

Type material. Holotype, female (MUSM) "PERU: MD, Madama, 12°29'3846"S, 65°1'34"W, 182m [19–20], vii.2009, M. Alvarado."

Paratypes, 1 female (MUSM) "PERU: CU, La Convención, Echarate, CC. Timpia. 72°49'34.56"S, 12°06'47.04"W 519m. 20–21.x.2009. Light. M. Alvarado y E Rázuri." 1 female (MUSM) "PERU: JU, Pachitea River-System, Stat. Panguana am. Rio Llullapichis, trop. Tiefland-Regenwald. 260m. 9°37'S, 74°56'W, 2020.x.2009, G. Riedel."

Description. Body length 6.7–7.8 mm. Fore wing length 6.5–7.0 mm.

Head (Figs 60, 61). In dorsal view eye length/temple 4.0–5.0. Eye height/head width 0.41–0.43. Eye height/minimum distance between eyes 1.2–1.4. OD/POL 2.5–3.0. OD/OOL 2.5–4.0. Frons excavated. Frons lateral carina present. Occipital carina dorsally complete, weakly curved. Occiput in dorsal view nearly straight, not indented medially. Occipital carina ventrally meeting hypostomal carina. Mid-longitudinal crest at upper face present. Hypoclypeal depression/face width 0.35–0.39. Malar space/eye height 0.16–0.17. Face height/width 0.76–0.82. Clypeus height/width 0.7. Clypeus

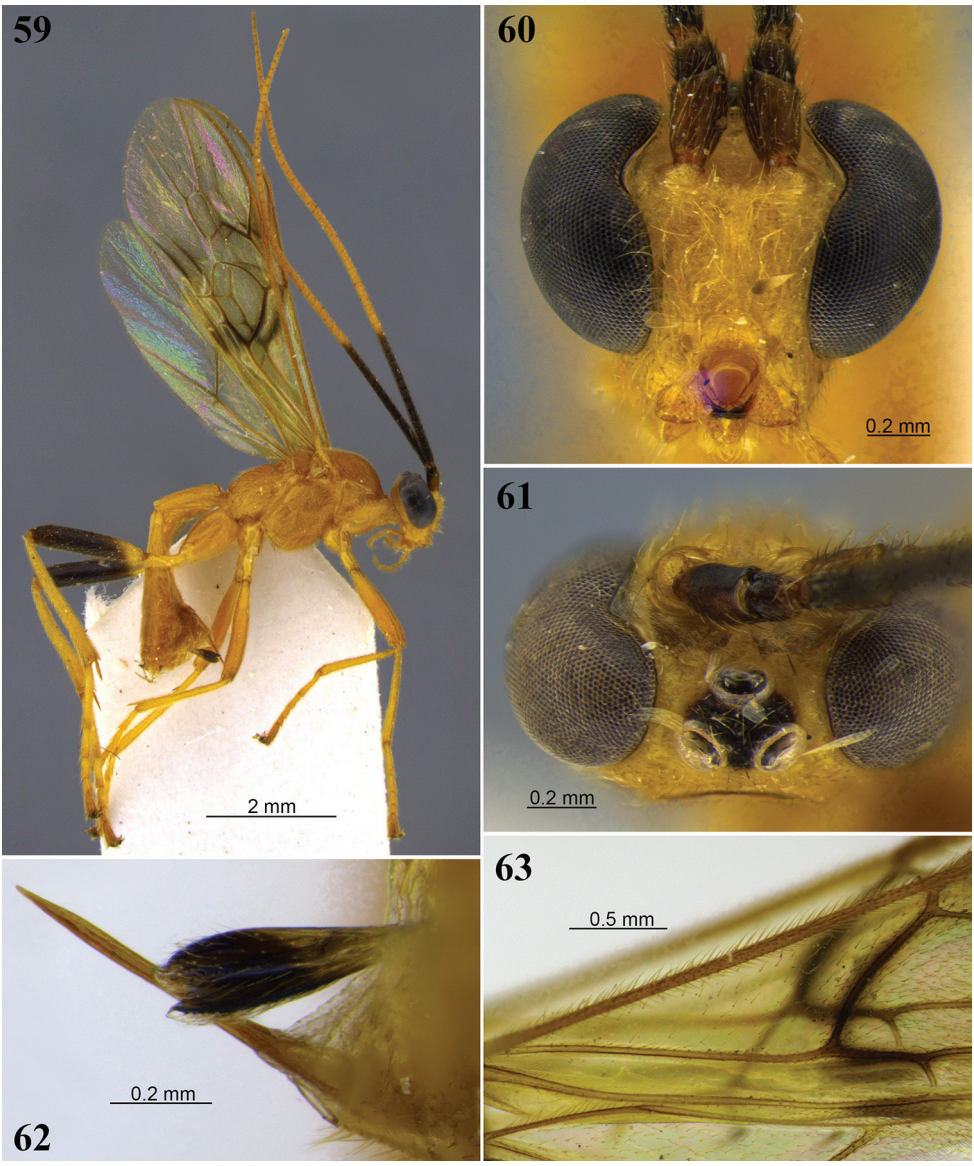

Figures 59–63. *Aleiodes lidiae* sp. nov. **59** lateral habitus **60** head, anterior view **61** head, dorsal view **62** Apex of metasoma showing ovipositor and sheath with apical point **63** wings, basally.

convex, granulate. Sculpture of head shiny granular-coriaceous. Face weakly rugose, transversely rugose-striate around median crest.

Antenna. Antennal segments 53–56. Antenna/body length 1.2. Scape/pedicel length 1.9–2.0. Length of first/second flagellomere 1.1–1.2. Fourth flagellomere length/apical width 1.3–1.5. Tip of apical segment of antenna pointed.

Mesosoma. Length/height 1.7–1.8. Width of mesoscutum/width of head 0.7. Mesoscutum length/width 1.2. Pronotal collar/vertex 0.8. Prescutellar sulcus with 3–5 distinct carinae. Mesoscutum posterior border with distinct complete carina. Metanotum with mid-longitudinal carina complete, connecting to a carinate pit posteriorly, carina bisecting posterior pit, although weaker posteriorly. Metanotum mid-pit present, delimited by carinae. Mid-longitudinal carina of propodeum present at basal 0.7, absent posteriorly, or nearly complete. Ventral mid-line of mesopleuron set within shallow smooth sulcus; pit at ventral mid-line present, shallow. Notauli weakly indicated anteriorly, indistinctly crenulate. Sternaulus weakly indicated anteriorly, rugose. Sculpture of mesosoma mostly granulate. Metapleuron rugose posteriorly. Pronotum rugose laterally, pronotal groove sparsely crenulate anteriorly, short subventral longitudinal carina present. Mesopleuron rugose below subalar groove. Subalar groove crenulate. Mid-posterior region of mesoscutum rugose, with a short mid-longitudinal carina posteriorly. Mesoscutellar trough entirely costate. Metanotum mostly smooth, with one or two pairs of lateral carinae. Propodeum mostly rugose.

Wings. Fore wing: Stigma length/height 3.3. Vein r/2RS 1.2–1.4. Vein r/RS+Mb 1.3–1.4. Vein 3RSa/2RS ~ 1.7. Vein 3RSa/2M 0.86–0.88. Vein 3RSa/3RSb 0.40–0.44. Vein 1CUa/1CUb 1.0. Vein 1CUa/2CUa 1.7–1.9. Vein 1cu-a weakly inclivous. Vein 1M weakly curved basally. Vein RS+Ma distinctly curved. Vein M+CU virtually straight. Vein 1-1A nearly straight. Vein 1a absent. Second submarginal cell trapezoidal. Subbasal cell glabrous, with two parallel rows of short setae subapically, a row of setae just below of vein 1CUa and M+CU apically, plus a row of setae apically just above vein 1-1A. Basal cell mostly glabrous, setose below costal vein and around dark spot near vein 1M. Hind wing: Vein RS bent at basal 0.3, with vein r present. Marginal cell narrowest at base. Vein M+CU/1M 1.3–1.4. Vein M+CU/r-m 1.2. Vein m-cu present, spectral. Vein m-cu position relative to vein r-m antefurcal. Vein 2-1A absent. Basal cell sparsely setose, bare posteriorly.

Hind legs. Femur length/width 4.8–5.0. Length of tibia/tarsi 0.96. Length of basitarsus/tarsi 2–4 ~ 0.7. Sculpture of hind coxa dorsally shiny granular-coriaceous. Tarsal claws not pectinate.

Metasoma. T1 length/apical width 1.0–1.1. T2 length/apical width 0.7–0.9. T3 length/apical width 0.5–0.6. Mid-longitudinal carina extending until basal 0.7 of T3. Metasoma sculpture T1 rugose, T2 and most of T3 striate-rugose, sculpture weaker at T3, remainder terga granular-coriaceous. Ovipositor sheath/hind basitarsus 0.3–0.5. Apex of ovipositor sheaths roughly rounded; apical point present, distinct (Fig. 62).

Color (Figs 59–61). Brownish yellow. Stemmaticum black. Antenna with basal 11–13 flagellomeres black, apical segments yellow; pedicel black; scape black, ventrally brownish yellow. Wings tinged yellow; stigma and most veins orange to yellow; veins 1M, 1CUa, apex of 1-1A and r dark brown, veins 2RS, 3RS and 2M sometimes brown, apex of 2CUb brown; infuscate areas around base of vein 1M and below apex of vein 1-1A. Hind femur mostly dark brown, roughly basal 0.2 ventrally and 0.25 dorsally brownish orange. Ovipositor sheaths dark brown.

Male. Essentially as in female. Body length 6.8 mm; fore wing length 5.6 mm; antenna broken.

Diagnosis. *Aleiodes lidiae* is most similar to *A. gonodontivorus*, but differing by having the hind femur mostly dark brown (Fig. 59) and conspicuous infuscate spots on the fore wing (Figs 59, 63). It also resembles *A. andinus*. The differences between these two species are discussed in the diagnosis given for *A. andinus.*

Distribution. This species in known only from localities in Peru.

Etymology. The name is an honorary patronym for our friend and fellow braconidologist, Lidia Sulca.

***Aleiodes mabelae* Shimbori & Shaw, sp. nov.**

http://zoobank.org/70539E94-7397-4489-8377-CAB3FCEAFD8A

Figs 64, 65

Type material. Holotype, female (MUSM) "PERU: CUSCO, La Convención, Echarate, C. Segakiato. 11°45'38.6"S, 73°14'57.7"W 908m. 01.ii.2011. M. Alvarado & E Rázuri."

Paratypes. 2 females (MUSM) same as holotype except "28.ii.92011"; 1 female (MUSM), same as holotype except "… C.C. Timpia. 72°49'34.56"/ 12°06'47.04" 519m. 20–21.x.2009. Light …"; 1 female (MUSM) "PERU: JU, Satipo, San Andres, 11.33056S, 074.68665W, 975 m. 24.x.2012; UV&MV lights; E. Nearms & S. Carbonel"; 1 male (MUSM) "PERU: UC, Coronel Portillo, Puerto Alegre 19.vii.2008 08°44'7"S, 74°09'5"W 196m M. Alvarado; 1 male (MUSM) "PERU: MD, Rio Los Amigos, CICRA, 270m 1–16.ix.2007 12°34'8"S, 70°06'0"W Manual collect. S. Carbonel".

Description. Body length 6.9–7.5 mm. Fore wing length 6.1–6.8 mm.

Head. In dorsal view eye length/temple 3.3–3.6. Eye height/head width 0.39–0.43. Eye height/minimum distance between eyes 1.1–1.2. OD/POL 2.0–2.7. OD/OOL 2.0–2.2. Frons weakly excavated. Frons lateral carina absent, or very weakly indicated. Occipital carina dorsally incomplete. Occiput in dorsal view nearly straight, not indented medially. Occipital carina not curved toward ocelli. Occipital carina ventrally meeting hypostomal carina. Mid-longitudinal crest at upper face present. Hypoclypeal depression/face width 0.31–0.35. Malar space/eye height 0.21–0.23. Face height/width 0.70–0.75. Clypeus height/width 0.63–0.69. Clypeus convex, granulate. Sculpture of head shiny granular-coriaceous. Face transversely rugose-striate, medially granular-coriaceous below crest.

Antenna. Antennal segments 51–53. Antenna/body length 1.2. Scape/pedicel length 2.5–2.6. Length of first/second flagellomere 1.1–1.3. Fourth flagellomere length/apical width 1.6–1.7. Tip of apical segment of antenna pointed.

Mesosoma. Length/height ~ 1.6. Width of mesoscutum/width of head 0.72–0.77. Mesoscutum length/width 1.0–1.1. Pronotal collar/vertex 0.7–0.8. Prescutellar sulcus with complete mid-longitudinal carina, and a few irregular and incomplete carinae laterally. Mesoscutum posterior border with distinct complete carina. Metanotum with complete mid-longitudinal carina, sometimes interrupted at middle. Metanotum mid-pit pre-

Figures 64, 65. *Aleiodes mabelae* sp. nov. **64** lateral habitus **65** head, dorsal view showing interrupted occipital carina.

sent, delimited by carinae. Mid-longitudinal carina of propodeum complete, sometimes irregular apically. Ventral mid-line of mesopleuron without sulcus anteriorly, shallow smooth sulcus present posteriorly; pit at ventral mid-line absent. Notauli weakly indicated anteriorly, indistinctly crenulate. Sternaulus weakly indicated anteriorly, rugose. Sculpture of mesosoma mostly granulate. Pronotum mostly smooth, granulate ventrally, pronotal groove entirely crenulate. Mesopleuron rugose below subalar groove. Subalar groove crenulate. Mid-posterior region of mesoscutum rugose, with a short mid-longitudinal carina posteriorly. Mesoscutellar trough weakly costate laterally. Metanotum mostly smooth, with one or two pairs of lateral carinae. Propodeum mostly granulate, rugose posteriorly.

Wings. Fore wing: Stigma length/height 3.5–3.8. Vein r/2RS 0.75–0.85. Vein r/RS+Mb 1.0–1.2. Vein 3RSa/2RS 1.7–1.8. Vein 3RSa/2M 0.86–0.94. Vein 3RSa/3RSb 0.43–0.48. Vein 1CUa/1CUb 0.9–1.1. Vein 1CUa/2CUa 1.65–1.75. Vein 1cu-a vertical or weakly reclivous. Vein 1M nearly straight. Vein RS+Ma virtually straight. Vein M+CU virtually straight. Vein 1-1A nearly straight. Vein 1a absent. Second submarginal cell rectangular. Subbasal cell mostly glabrous, with sparse setae basally, a small setose patch at the infuscate region bellow vein 1CUa, and two or three irregular rows of short setae subapically above vein 1-1A. Basal cell evenly setose. Hind wing: Vein RS bent at basal 0.3, with vein r present. Marginal cell narrowest at base. Vein M+CU/1M 1.4–1.5. Vein M+CU/r-m 1.6–1.8. Vein m-cu present and pigmented, although not tubular. Vein m-cu position relative to vein r-m distinctly antefurcal. Vein 2-1A absent. Basal cell evenly and rather sparsely setose, with a small bare spot posteriorly.

Hind legs. Femur length/width 4.7–5.1. Length of tibia/tarsi ~ 1.0. Length of basitarsus/tarsi 2–4 0.81–0.88. Sculpture of hind coxa dorsally shiny granular-coriaceous. Tarsal claws not pectinate.

Metasoma. T1 length/apical width 1.1–1.2. T2 length/apical width 0.8–0.9. T3 length/apical width 0.6–0.7. Mid-longitudinal carina extending until basal 0.5 of T3. Metasoma sculpture T1 rugose, T2 and most of T3 striate-rugose, remainder metasoma smooth. Ovipositor sheath/hind basitarsus 0.36–0.56. Ovipositor sheaths relatively narrow and truncate at apex; apical point very short, in most specimens hardly visible.

Color (Fig. 64). Brownish yellow. Antenna dark brown basally, gradually lightening toward yellow to light brown apex; scape ventrally lighter. Apex of hind tibia darker apically, varying from dark brown to only faintly darker; hind femur, and sometimes of mid femur, dark brown in some specimens. Tarsal claws brown. Wings tinged yellow; most veins yellow, infuscate spots at fore wing veins 1M/1CUa, r, apex of 1-1A and 2CUb, membrane around these veins distinctly infuscate; stigma mostly dark brown or entirely brownish yellow. Ovipositor sheaths dark brown.

Male. Essentially as in females with dark stigma and apex of hind femur and tibia dark brown. Body length 7.0 mm, fore wing length 5.5 mm; antenna broken, with 33+ segments.

Diagnosis. *Aleiodes mabelae* is similar to *A. bakeri* in having the occipital carina interrupted mid-dorsally (Fig. 65), and the vein 1a absent from the fore wing. However, these two species are readily separated by the color of the antenna, which is dark brown basally in *A. mabelae* (Fig. 64) but entirely brownish yellow in *A. bakeri* (Figs 21, 22). Also, the longitudinal carina of the propodeum is complete in *A. mabelae*, whereas it is incomplete in *A. bakeri*.

Comments. Specimens collected at higher elevations (~ 900–1000 m) have the stigma and all legs yellow, while specimens from lower elevations (~ 200–500 m) have the stigma mostly dark brown, and the apex of the hind tibia and femur dark brown.

Distribution. This species is known only from localities in Peru.

Etymology. This species is named in honor to our friend, and fellow entomologist, Mabel Alvarado, collector of most of the type specimens of this new species.

***Aleiodes maculosus* Shimbori & Shaw, sp. nov.**
http://zoobank.org/D8493855-F91E-49AB-A512-733343B00DFD
Figs 66–68

Type material. Holotype, female (CNCI) "BRAZIL, Encruzilhada, 980m, Bahia, XI.1975, M. Alvarenga"

Paratypes. 1 female (CNCI), same as holotype; 2 males (DCBU #s: 20789, 20793) "FAZ. CANCHIM SÃO CARLOS – SP luz 3.II.1984 A.S. Soares col."; 1 male (DCBU #20790), same data except "29.III.1985"; 1 male (DCBU #20791), same data except "... cerrado, Varredura, 23.I.1981 N.W. Perioto col"; 1 male (DZUP) "Fênix, PR, Brasil Res. Est. ITCF Arm. Luminosa 3.X.1986 Projeto PROFAUPAR"; 1 male (CNCI) "Nova Teutonia 27°11'S, 52°23'W Brazil, 300–500m 3-IX-1948 Fritz Plaumann."

Description. Body length 8.0–8.1 mm. Fore wing length 6.4–6.9 mm.

Head (Figs 67, 68). In dorsal view eye length/temple 4.6–5.0. Eye height/head width 0.39–0.43. Eye height/minimum distance between eyes 1.3. OD/POL 5.5–6.5. OD/OOL 3.7–4.3. Frons excavated. Frons lateral carina present in addition to W-shaped carina. Occipital carina dorsally complete and nearly straight, or weakly bent mid-dorsally. Occiput in dorsal view nearly straight, not indented medially. Occipital carina (complete). Occipital carina ventrally nearly touching hypostomal carina. Mid-longitudinal crest at upper face present. Hypoclypeal depression/face width 0.35. Malar space/eye height 0.16–0.18. Face height/width 0.77. Clypeus height/width 0.67–0.69. Clypeus convex, granulate. Sculpture of head shiny granular-coriaceous. Face weakly rugose, with bulging granulate are above clypeus and below crest, transversely rugose-striate around median crest.

Antenna. Antennal segments 55. Antenna/body length 1.1. Scape/pedicel length 2.1. Length of first/second flagellomere 1.1. Fourth flagellomere length/apical width 1.9–2.0. Tip of apical segment of antenna nipple-shaped.

Mesosoma. Length/height ~ 1.7. Width of mesoscutum/width of head 0.71–0.75. Mesoscutum length/width ~ 1.1. Pronotal collar/vertex 0.7–0.9. Prescutellar sulcus with complete median carina plus 3 pairs of distinct but weaker lateral carinae. Mesoscutum posterior border with distinct complete carina. Metanotum with mid-longitudinal carina complete, connecting to a carinate pit posteriorly, bisecting the posterior pit in paratype. Metanotum mid-pit present, delimited by carinae. Mid-longitudinal carina of propodeum complete. Ventral mid-line of mesopleuron set within shallow smooth sulcus; pit at ventral mid-line absent. Notauli weakly indicated anteriorly, indistinctly crenulate. Sternaulus absent. Sculpture of mesosoma mostly granulate. Pronotum rugose laterally, short subventral longitudinal carina present. Mesopleuron mostly rugose. Subalar groove crenulate. Mid-posterior region of mesoscutum rugose, with a short mid-longitudinal carina posteriorly. Mesoscutellar trough entirely costate. Metanotum mostly smooth and weakly crenulate. Propodeum mostly rugose.

Wings. Fore wing: Stigma length/height 3.3–3.5. Vein r/2RS 1.0–1.1. Vein r/RS+Mb 1.2–1.3. Vein 3RSa/2RS 1.8–1.9. Vein 3RSa/2M 0.80–0.85. Vein 3RSa/3RSb 0.41–0.45. Vein 1CUa/1CUb 0.80–0.85. Vein 1CUa/2CUa 1.7. Vein 1cu-a weakly

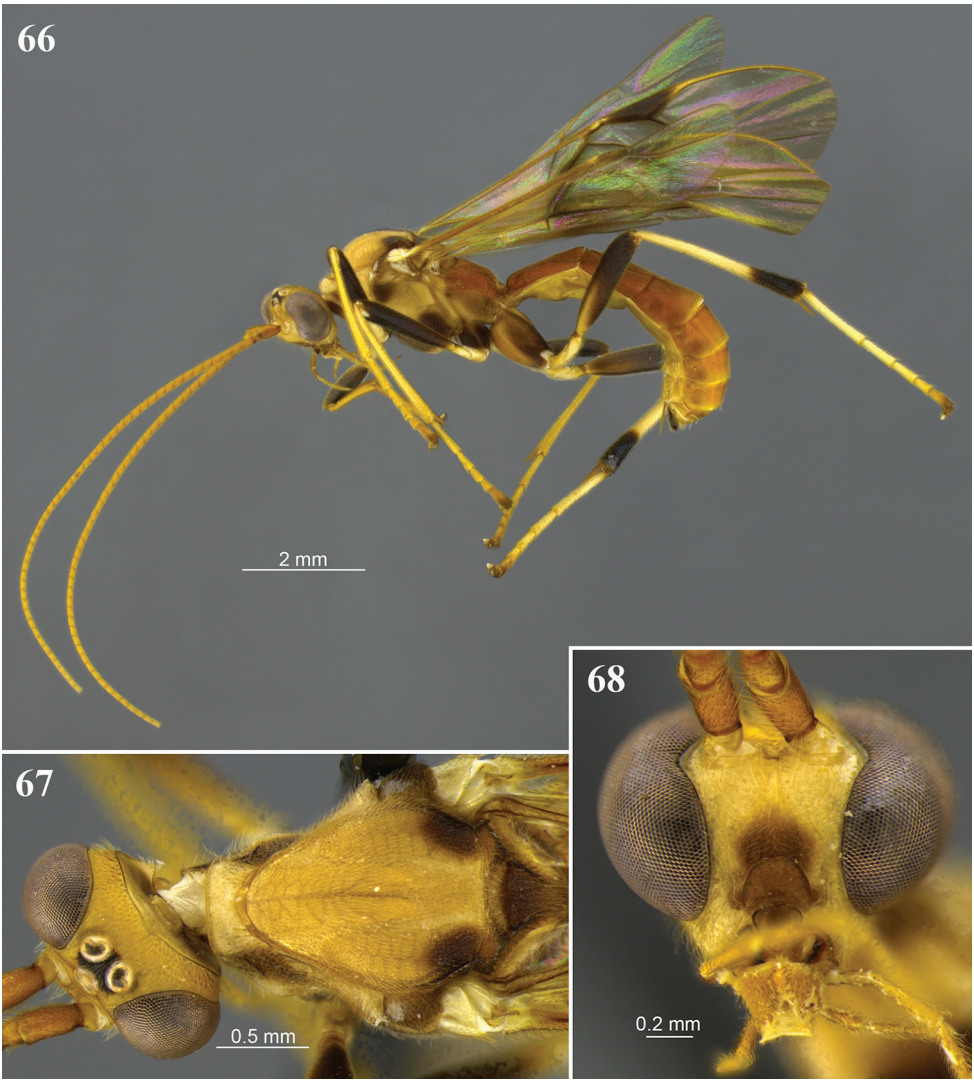

Figures 66–68. *Aleiodes maculosus* sp. nov. **66** lateral habitus **67** head and anterior mesosoma, dorsal view **68** head, anterior view.

inclivous. Vein 1M weakly curved near middle. Vein RS+Ma sinuate. Vein M+CU virtually straight. Vein 1-1A very weakly sinuate apically. Vein 1a absent. Second submarginal cell trapezoidal. Subbasal cell glabrous, with two parallel rows of short setae subapically, and a narrow patch of setae just below vein 1CUa. Basal cell mostly setose but glabrous region just above vein M+CU. Hind wing: Vein RS Bent at basal 0.3, with vein r present. Marginal cell narrowest at base. Vein M+CU/1M 1.4–1.5. Vein M+CU/r-m 1.4. Vein m-cu present and tubular. Vein m-cu position relative to vein r-m interstitial, or antefurcal. Vein 2-1A absent. Basal cell evenly setose with a small bare spot posteriorly.

Hind legs. Femur length/width 4.8–5.0. Length of tibia/tarsi ~ 1.0. Length of basitarsus/tarsi 2–4 0.65. Sculpture of hind coxa dorsally granulate. Tarsal claws pectinate basally.

Metasoma. T1 length/apical width 1.3–1.4. T2 length/apical width ~ 0.8. T3 length/apical width 0.5–0.6. Mid-longitudinal carina extending until basal 0.7 of T3. Metasoma sculpture T1 rugose, T2 and most of T3 striate-rugose, or remainder terga granular-coriaceous. Ovipositor sheath/hind basitarsus ~ 0.4. Apex of ovipositor sheaths truncate; apical point absent.

Color (Fig. 66). Body mottled pale yellow, orange and dark brown. Head pale yellow, clypeus and part of face just above clypeus brown, mandibles pale brown with dark brown teeth. Antenna yellow. Mesosoma mostly pale yellow except propodeum orange; dark brown markings at propleuron and pronotum anteriorly, mesopleuron below subalar groove and ventrally, posterior corners of mesoscutum, and scutellum; metanotum and part of metapleuron pale brown. Metasoma orange, pale yellow ventrally. Wings slightly infuscate, most veins dark brown, costal vein brownish orange, basal veins yellow; stigma mostly dark brown with both tips whitish yellow; tegula brown or dark brown. Legs with trochanter, trochantellus, tibia and tarsi 1–4 whitish yellow; coxae and femora dark brown, but light yellow at base; fifth tarsomeres yellow; exceptions: hind coxa mostly brown, hind tibia with apical 0.25 dark brown.

Male. Very similar to female but fifth tarsomeres usually dark brown. Body length 7.1–7.9 mm, fore wing length 5.8–6.3; 49–52 antennomeres.

Diagnosis. *Aleiodes maculosus* can be easily distinguished by its mottled pale yellow, orange and dark brown body colors (Figs 66–68). It is most similar to *A. brevicarina*, but differs in having the fore coxa dark brown, stigma dark brown (Fig. 66), palpi yellow to pale brown (Figs 66, 68), face light yellow with mid-ventral brown spot which extends to clypeus and mandibles (Fig. 68), tegula infuscate (Fig. 67), and antenna entirely yellow (Fig. 66) (the antenna is basally dark brown in *A. brevicarina*). *Aleiodes maculosus* has a complete longitudinal carina on the propodeum, whereas the propodeal carina of *A. brevicarina* is quite short, extending over less than half the length of the propodeum.

Distribution. This species is known only from localities in Brazil.

Etymology. The specific epithet *maculosus* is Latin for dappled or spotted, a reference to the mottled color pattern in this species (Figs 66–68).

Aleiodes nigristemmaticum (Enderlein, 1920)

Figs 69–72

Rhogas nigristemmaticum Enderlein, 1920: 156.

Aleiodes nigristemmaticum: Marsh & S.R. Shaw, 1998: 400. New combination, lectotype designation, and distribution.

Type material. Lectotype, female. Mexico, Chiapas (PASW). Examined by SRS (see Marsh and S.R. Shaw, 1998).

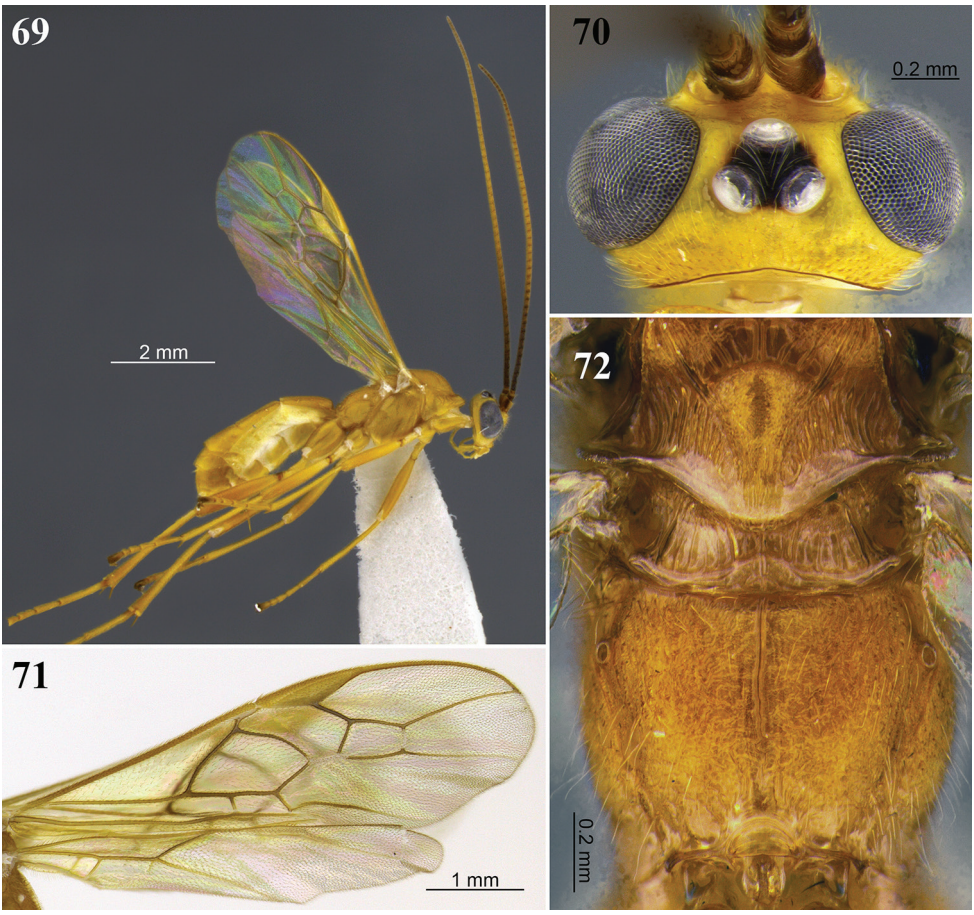

Figures 69–72. *Aleiodes nigristemmaticum* (Enderlein). **69** Lateral habitus **70** head, dorsal view **71** wings **72** mesosoma and propodeum, dorsal view.

Non-type material examined. In addition to the specimens studied by Marsh and S.R. Shaw (1998), which were re-examined, the following specimens were studied: 1 female, BOLIVIA: Santa Cruz, Nuflo de Chavez, xi.1963 (CNCI). 30 females, BRAZIL: Encruzilhada, 960m, light culls, xi.1972, M. Alvarenga (CNCI). 1 female, BRAZIL: M. Gerais, Pedra Azul, xi.1972 (CNCI). 15 females and 2 males, BRAZIL: Mato Grosso do Sul [MS], Aquidauana, 20°25'54"S, 55°39'21"W, Malaise trap, 26.x.2011, Lamas & Nihei cols. (DCBU). 1 female, BRAZIL: Ceará [CE], Crato, Chapada do Araripe, 07°13'56"S, 39°26'16.5"W, light trap, 10.ii.2013, A.S. Soares & E.M. Shimbori cols. (DCBU). 1 female, BRAZIL: Bahia [BA], Morro do Chapéu, Pq. Est. Morro do Chapéu, 11°24'44"S, 41°19'55"W, light trap, 19.iv.2013 (DCBU). 6 females and 3 males, BRAZIL: Piauí [PI], Coronel José Dias, PARNA Serra da Capivara, Pedra Furada, 08°50'11"S, 42°32'55"W, light trap, 20.iii.2013, A.S. Soares & E.M. Shimbori cols. (DCBU). 2 males, BRAZIL: Pernambuco [PE], Agrestina, Fazenda Amapá, 11–

17.vi.1971, Exp[edition] ABC-MZUSP (MZUSP). 6 females, BRAZIL: Goiás [GO], Cabeceiras (Lagoa Formosa), 24–27.x.1964, Exp[edition] Dep. Zool. (MZUSP). 5 females, BRAZIL: São Paulo [SP], Luiz Antônio, Mogi Guaçu River, light: 1 female, 27.iii.1987, L.A. Joaquim col., 1 female, 18.ii.1988, L.A. Joaquim col., 3 females, 2.iii.1994, A.S. Soares col. (DCBU); 1 female, BRAZIL: São Paulo [SP], Caraguatatuba, 40m, (Res. Flor.), 2.iv.1962, K. Lenko col. (MZUSP). 1 female, COLOMBIA: Vichada PNN, El Tupparo Bosque Sabana, 5°21'N, 67°51'W, 100m, Malaise, 15–19. vii.2000, W. Villalba leg. M511 (IHCB). 1 male, CUBA: Soledad, 25.ii.1925, Geo. Salt (CNCI). 1 male, DOMINICAN REPUBLIC: La Vega Province, Bonao, 05.ix.1997, UV light, hotel courtyard, Baranowski R. (CNCI). 1 female, REP. DOMINICANA: La Cumbre, 600m, L. Masner (CNCI). 1 male, HONDURAS: Comayagua, along road north of Meambar, 13 December 1987, R.D. Cave, col. (UWIM). 1 female, MEXICO: Chiapas, 16°58'N, 91°47'W, 6–9.xi.1978, J. Rawlins (CNCI). 1 female, 2 males, VENEZUELA: Cagua Edo. Aragua, i.1974, light trap (UWIM).

Description of non-type specimens. Body length 5.9–7.5 mm. Fore wing length 4.8–6.3 mm.

Head. In dorsal view eye length/temple 3.0–4.0. Eye height/head width 0.39–0.44. Eye height/minimum distance between eyes 1.0–1.3. OD/POL 2.0–3.3. OD/OOL 2.0–2.8. Frons excavated. Frons lateral carina present. Occipital carina dorsally complete and nearly straight, or weakly bent mid-dorsally. Occiput in dorsal view nearly straight, not indented medially. Occipital carina ventrally meeting hypostomal carina. Mid-longitudinal crest at upper face present. Hypoclypeal depression/face width 0.33–0.36. Malar space/eye height 0.20–0.24. Face height/width 0.7–0.8. Clypeus height/width 0.7–0.8. Clypeus convex, granulate. Sculpture of head shiny granular-coriaceous. Face transversely rugose-striate at dorsal half, or mostly transversely rugose-striate, medially granular-coriaceous below crest.

Antenna. Antennal segments 51–55. Antenna/body length ~ 1.2. Scape/pedicel length 1.8–1.9. Length of first/second flagellomere 1.1–1.2. Fourth flagellomere length/apical width 1.8–2.0. Tip of apical segment of antenna nipple-shaped.

Mesosoma. Length/height 1.7–1.8. Width of mesoscutum/width of head 0.6–0.7. Mesoscutum length/width 1.0–1.2. Pronotal collar/vertex 0.6–0.9. Prescutellar sulcus with complete mid-longitudinal carina plus two or three pairs or lateral carinae more or less defined. Mesoscutum posterior border with distinct complete carina. Metanotum with mid-longitudinal carina present anteriorly. Metanotum mid-pit present, delimited by carinae. Mid-longitudinal carina of propodeum complete or nearly complete, usually irregular posteriorly. Ventral mid-line of mesopleuron set within smooth sulcus; pit at ventral mid-line absent, or weakly indicated. Notauli weakly indicated anteriorly, indistinctly crenulate. Sternaulus absent. Sculpture of mesosoma mostly granulate. Pronotum mostly rugose-costate laterally, short subventral longitudinal carina present. Mesopleuron rugose centrally and anteriorly. Subalar groove sparsely crenulate. Mid-posterior region of mesoscutum rugose, with a short mid-longitudinal carina posteriorly. Mesoscutellar trough entirely costate. Metanotum mostly smooth, with one or two pairs of lateral carinae. Propodeum rugose posteriorly, or mostly rugose.

Wings. Fore wing: Stigma length/height 3.1–3.4. Vein r/2RS 0.9–1.1. Vein r/RS+Mb 1.2–1.5. Vein 3RSa/2RS 1.3–1.6. Vein 3RSa/2M 0.76–0.85. Vein 3RSa/3RSb 0.36–0.44. Vein 1CUa/1CUb 0.8–0.9. Vein 1CUa/2CUa 1.4–1.8. Vein 1cu-a weakly inclivous, or nearly vertical. Vein 1M weakly curved basally. Vein RS+Ma distinctly curved. Vein M+CU virtually straight. Vein 1-1A very weakly sinuate apically. Vein 1a absent. Second submarginal cell trapezoidal. Subbasal cell glabrous, with two parallel rows of short setae subapically, and a narrow patch of setae just below vein 1CUa, very few scattered setae may be present medially. Basal cell mostly evenly setose, sparsely setose posteriorly, with a bare spot posteriorly. Hind wing: Vein RS bent at basal 0.3, with vein r present. Marginal cell narrowest at base. Vein M+CU/1M 1.3–1.6. Vein M+CU/r-m 1.2–1.7. Vein m-cu present, spectral. Vein m-cu position relative to vein r-m antefurcal, or nearly interstitial. Vein 2-1A absent. Basal cell evenly, rather sparsely setose, posteriorly with small bare area.

Hind legs. Femur length/width 5.3–5.6. Length of tibia/tarsi 0.9–1.0. Length of basitarsus/tarsi 2–4 0.7–0.8. Sculpture of hind coxa dorsally granulate. Tarsal claws not pectinate.

Metasoma. T1 length/apical width 1.1–1.3. T2 length/apical width 0.8–0.9. T3 length/apical width 0.5–0.7. Mid-longitudinal carina extending until basal 0.7 of T3. Metasoma sculpture T1, T2 and basal 0.7 of T3 rugose-costate, remainder terga granular-coriaceous. Ovipositor sheath/hind basitarsus 0.3–0.5. Apex of ovipositor sheaths truncate; apical point absent.

Color (Figs 69–72). Body entirely pale yellow to brownish yellow (variation among specimens); antenna varying from mostly yellow to entirely dark brown, usually dark brown basally gradually lighter to apically pale yellow, but commonly darker at apex (lighter only at middle); scape yellow or honey yellow with brown lateral stripe, pedicel brown or dark brown. Wings hyaline, veins and stigma yellow, but vein r and 1M darker, stigma rarely with a nearly central infuscate dot. Legs mostly brownish yellow, usually trochanter and trochantellus slightly lighter and femur slightly darker than remainder legs; all fifth tarsomeres mostly brown, darker than remainder tarsi.

Male. Essentially as in female. Body length 5.5–7.0 mm; fore wing length 4.3–5.4 mm; antenna with 48–50 segments.

Diagnosis. Traditionally this very common and widespread species has been recognized by the predominantly yellow body color, yellow stigma, and sharply contrasting black ocellar triangle (hence the name *nigristemmaticum*) (Figs 69, 70). The following characters are also useful for distinguishing this species from others treated in this paper: fore wing vein r approximately as long as 2RS and shorter than 3RSa, second submarginal cell trapezoidal (Fig. 71); antenna brown basally, gradually lightening to light brown apically, scape and pedicel mostly honey yellow with brown lateral stripe (Fig. 69); fourth flagellomere 1.8–1.9 × longer than wide; occiput not receding middorsally (Fig. 70); fifth tarsomeres darker than remainder of tarsi in all legs (Fig. 69).

Biology. Parasitoid of *Mocis latipes* (Guenée.) and *Mocis* spp (Erebidae, Erebinae), mostly feeding on grasses (Poaceae), including several crops. Additional details regarding biological information are given by Marsh and S.R. Shaw (1998).

Distribution. USA (Florida and Mississippi); Mexico; Honduras; Cuba; Costa Rica; Venezuela; Peru, Brazil, Bolivia, Ecuador, Dominican Republic, Panama, Puerto Rico, Honduras, Colombia, and Suriname. Its widespread distribution may be a reflection of the distribution and pest status of the host, which feeds on grasses, as well as crops such as corn and rice. This species is recorded from Florida to Southern Brazil.

***Aleiodes ovatus* Shimbori & Shaw, sp. nov.**

http://zoobank.org/5E0F8CE2-4982-4F19-BAF5-FE78706B0537

Figs 73–75

Type material. Holotype, female (UEFS #33424) "Brasil, BA, Seabra, 12°27'S, 41°44'W 15.XI.2007 Leg. Alvim, E."

Paratypes. 2 females, 1 male (UEFS #s:33396, 33406, 33404), same as holotype; 1 male (DCBU #20792) "FAZ. CANCHIM SÃO CARLOS – SP luz 11.II.1983 A.S. Soares col."

Description. ***Body*** length 6.8–7.0 mm. Fore wing length 5.9–6.3 mm.

Head. In dorsal view eye length/temple 4.2–4.5. Eye height/head width 0.43–0.45. Eye height/minimum distance between eyes 1.4–1.5. OD/POL 2.9–3.1. Ocelli exceptionally large, OD/OOL 3.7–4.6 (Fig. 74). Frons excavated. Frons lateral carina present. Occipital carina dorsally complete and nearly straight. Occiput in dorsal view nearly straight, not indented medially. Occipital carina ventrally meeting hypostomal carina. Mid-longitudinal crest at upper face present. Hypoclypeal depression/face width 0.35. Malar space/eye height 0.16–0.17. Face height/width 0.83–0.86. Clypeus height/width 0.6–0.7. Clypeus convex, granulate. Sculpture of head mostly shiny granulate, vertex granulate-rugose, frons shiny granular-coriaceous. Face mostly transversely rugose-striate, granulate medially.

Antenna. Antennal segments 54. Antenna/body length 1.3. Scape/pedicel length 2.0. Length of first/second flagellomere 1.2–1.3. Fourth flagellomere length/apical width 1.7. Tip of apical flagellomere pointed.

Mesosoma. Length/height ~ 1.7. Width of mesoscutum/width of head 0.67–0.72. Mesoscutum length/width ~ 1.1. Pronotal collar/vertex 0.7–0.8. Prescutellar sulcus with 5–7 distinct carinae. Mesoscutum posterior border with distinct complete carina. Metanotum with mid-longitudinal carina present anteriorly, with carinate pit mid-posteriorly. Metanotum mid-pit present, delimited by carinae. Mid-longitudinal carina of propodeum present at basal 0.7, absent posteriorly. Ventral mid-line of mesopleuron set within shallow smooth sulcus; pit at ventral mid-line weakly indicated. Notauli present anteriorly, shallowly and weakly crenulate. Sternaulus absent. Sculpture of mesosoma mostly granulate. Pronotum rugose laterally, short subventral longitudinal carina present. Mesopleuron mostly rugose. Subalar groove crenulate. Mid-posterior region of mesoscutum rugose with long and irregular mid-longitudinal carina. Mesoscutellar trough entirely costate. Metanotum mostly smooth and weakly crenulate. Propodeum mostly rugose.

Wings (Fig. 75). Fore wing: Stigma length/height 3.3. Vein r/2RS 0.9–1.0. Vein r/RS+Mb 1.2–1.3. Vein 3RSa/2RS 1.6–1.7. Vein 3RSa/2M 0.85–0.89. Vein 3RSa/3RSb

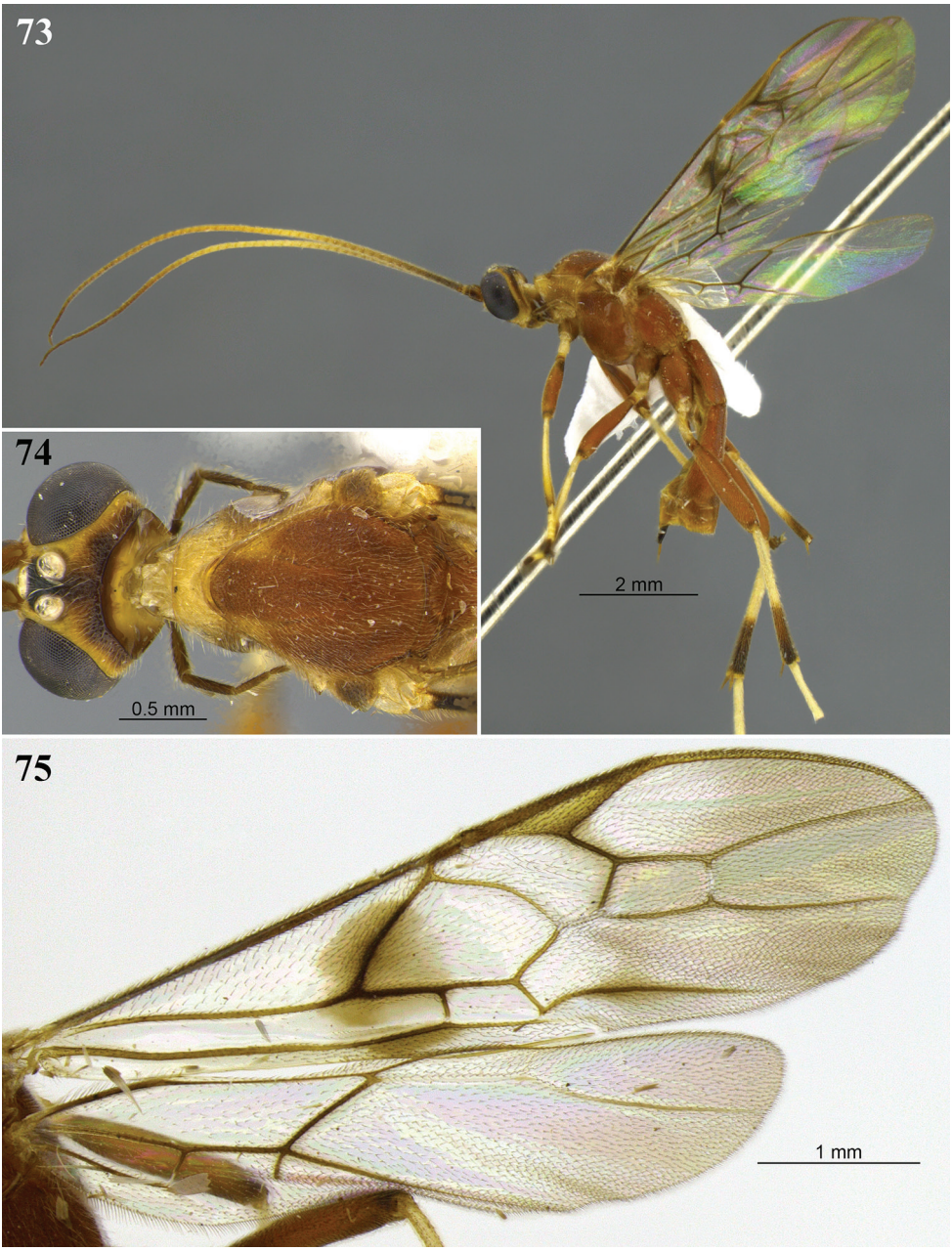

Figures 73–75. *Aleiodes ovatus* sp. nov. **73** lateral habitus **74** head and anterior mesosoma, dorsal view **75** wings.

0.41–0.45. Vein 1CUa/1CUb 0.9–1.0. Vein 1CUa/2CUa 1.9–2.0. Vein 1cu-a weakly inclivous. Vein 1M weakly curved basally. Vein RS+Ma sinuate. Vein M+CU virtually straight. Vein 1-1A weakly sinuate at apex. Vein 1a absent. Second submarginal cell trapezoidal. Subbasal cell glabrous, with two parallel rows of short setae subapically,

and a narrow patch of setae just below vein 1CUa. Basal cell mostly evenly setose, sparsely setose posteriorly. Hind wing: Vein RS Bent at basal 0.3, with vein r present. Marginal cell narrowest at base. Vein M+CU/1M 1.6–1.7. Vein M+CU/r-m 1.3–1.4. Vein m-cu present and pigmented, although not tubular. Vein m-cu position relative to vein r-m postfurcal, or interstitial. Vein 2-1A absent. Basal cell evenly, rather sparsely setose, posteriorly with small bare area.

Hind legs. Femur length/width 4.8–5.0. Length of tibia/tarsi 0.9–1.0. Length of basitarsus/tarsi 2–4 ~ 0.7. Sculpture of hind coxa dorsally mostly shiny granular-coriaceous, finely striate apically. Tarsal claws pectinate basally.

Metasoma. T1 length/apical width ~ 1.3. T2 length/apical width 0.8–1.0. T3 length/apical width 0.6–0.7. Mid-longitudinal carina extending until basal ~ 0.7 of T3. Metasoma sculpture T1, T2, and basal ~ 0.7 of T3 rugose-costate, remainder metasoma smooth. Ovipositor sheath/hind basitarsus 0.25–0.40. Apex of ovipositor sheaths truncate and narrow; apical point absent.

Color (Figs 73–75). Brownish orange. Head light yellow with a dark brown spot dorsally from stemmaticum and along occipital carina on vertex (Fig. 74), and a brown spot on face, covering clypeus and part of face on each side of the clypeus; palpi dark brown. Antenna brown basally, lightening to light yellow medially, then darkening to brown apex. Pronotum mostly pale yellow except laterally brownish orange; anterior corner of mesopleuron pale yellow; propleuron mostly brown with light yellow borders. Legs with trochanter, trochantellus, most of tibia, and tarsomeres 1–4 whitish yellow; all fifth tarsi dark brown; all tibiae dark brown apically, dark region smaller in frontal and mid legs; hind trochanter and trochantellus with brown lateral spots. Wings weakly tinged brown, veins and stigma brown; fore wing with an infuscate oval spot around junction of veins 1M and 1CU (Fig. 75). Ovipositor sheaths black.

Male. Essentially as in female. Body length 6.8–7.0 mm, fore wing length 5.5 mm.

Diagnosis. *Aleiodes ovatus* is similar to *A. brevicarina* and *A. maculosus* in having a whitish yellow hind tibia with dark brown apex (as in Figs 29, 66, 73). *Aleiodes ovatus* can be distinguished from both species by the oval infuscate spot on fore wing (Fig. 75). In the other two species dark coloration is present only along the veins (Figs 32, 66) and does not form a large spot. Also distinctive for *A. ovatus* is the mostly light yellow head with a dark brown vertex (except for orbits) (Fig. 74), whereas in *A. brevicarina* and *A. maculosus* the vertex does not have any dark brown markings (Figs 30, 67).

Distribution. This species is known only from localities in Brazil.

Etymology. The name *ovatus* is Latin for oval or egg-shaped, being a reference to the distinctive oval marking on the fore wing in this species (Fig. 77).

Aleiodes santarosensis Shaw & Shimbori, sp. nov.

http://zoobank.org/0DB7477F-54D6-46EB-885E-410E5826A6F2
Figs 76–78

Type material. Holotype, female (UWIM) "Costa Rica, Guanacaste, Pr. Guan. Conservation Area Santa Rosa hdq. 200m lighttrap, 7-VII-1997 L. J. van der Ent."

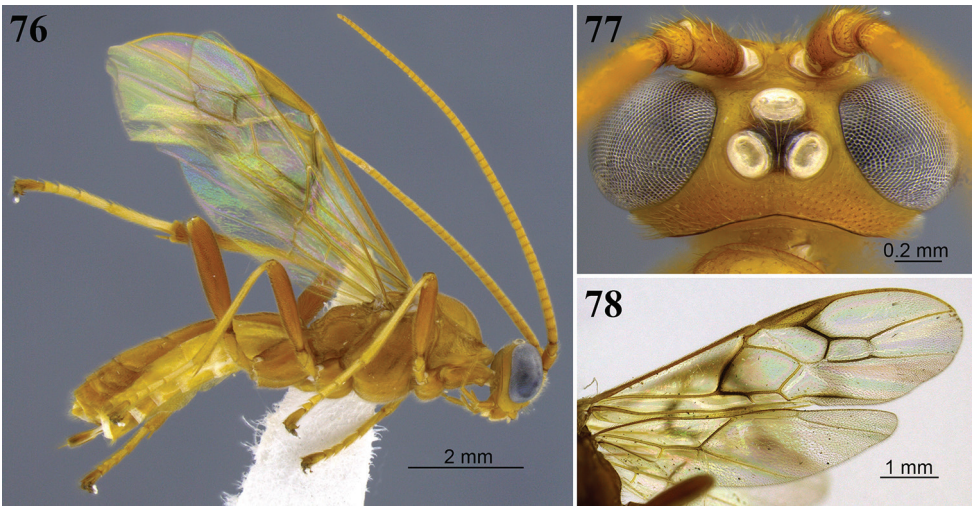

Figures 76–78. *Aleiodes santarosensis* sp. nov. **76** lateral habitus **77** head, dorsal view **78** wings.

Paratypes. 4 females, 12 males (UWIM), same as holotype; 2 females, 1 male (UWIM), same data except "6.VII.1997"; 1 female, 2 males (UWIM), same data except "27–30.VI.1997"; 1 male (UWIM), same data, except "… at Dorms UV Light, 3 June 1995 Dadelahi, Prie, Zitani"; 1 female (INBIO) "3km NO de Nacaome, 100m, P. N. Barra Honda, Prov. Guan. COSTA RICA, 3 a 30 mayo 1993 M. Reyes L-N 239000, 386000."

Description. Body length 6.8–8.3 mm. Fore wing length 6.0–6.9 mm.

Head (Fig. 77). In dorsal view eye length/temple 4.9–6.3. Eye height/head width 0.42–0.44. Eye height/minimum distance between eyes 1.3–1.4. OD/POL 3.8–5.2. OD/OOL 2.9–3.8. Frons excavated. Frons lateral carina absent. Occipital carina dorsally complete and nearly straight. Occiput in dorsal view nearly straight, not indented medially. Occipital carina ventrally meeting hypostomal carina. Mid-longitudinal crest at upper face present. Hypoclypeal depression/face width 0.35. Malar space/eye height 0.16. Face height/width 0.7. Clypeus height/width 0.75. Clypeus convex, granulate. Sculpture of head shiny granular-coriaceous. Face transversely rugose-striate around median crest.

Antenna. Antennal segments 51–54. Antenna/body length 1.1–1.2. Scape/pedicel length 2.0–2.1. Length of first/second flagellomere 1.1–1.2. Fourth flagellomere length/apical width 1.4–1.6. Tip of apical flagellomere pointed.

Mesosoma. Length/height ~ 1.6. Width of mesoscutum/width of head 0.7. Mesoscutum length/width 1.1–1.2. Pronotal collar/vertex 1.0–1.1. Prescutellar sulcus with 7–9 distinct carinae. Mesoscutum posterior border with distinct complete carina. Metanotum with mid-longitudinal carina complete, connecting to a carinate pit posteriorly. Metanotum mid-pit present, delimited by carinae. Mid-longitudinal carina of propodeum present at basal ~ 0.7, absent posteriorly. Ventral mid-line of mesopleuron set within shallow smooth sulcus; pit at ventral mid-line weakly indicated. Notauli

weakly indicated anteriorly, indistinctly crenulate. Sternaulus weakly indicated anteriorly, rugose. Sculpture of mesosoma mostly granulate. Pronotum granulate ventrally, pronotal groove mostly crenulate, short subventral longitudinal carina present. Mesopleuron rugose below subalar groove. Subalar groove sparsely crenulate. Mid-posterior region of mesoscutum rugose, with a short mid-longitudinal carina posteriorly, with irregularly carinate notauli. Mesoscutellar trough entirely costate. Metanotum mostly smooth, with one or two pairs of lateral carinae. Propodeum mostly rugose.

Wings. Fore wing: Stigma length/height 3.3–3.4. Vein r/2RS 1.25–1.45. Vein r/RS+Mb 1.2–1.6. Vein 3RSa/2RS ~ 1.7. Vein 3RSa/2M 0.85–0.89. Vein 3RSa/3RSb ~ 0.4. Vein 1CUa/1CUb 0.8–0.9. Vein 1CUa/2CUa 1.8–1.9. Vein 1cu-a inclivous. Vein 1M weakly curved basally, or weakly, evenly curved. Vein RS+Ma distinctly curved. Vein M+CU virtually straight. Vein 1-1A weakly sinuate at apex. Vein 1a absent. Second submarginal cell trapezoidal. Subbasal cell glabrous, with two parallel rows of short setae subapically. Basal cell mostly glabrous, setose below costal vein and around dark spot near vein 1M. Hind wing: Vein RS bent at basal 0.3, with vein r present. Marginal cell narrowest at base. Vein M+CU/1M 1.6–1.8. Vein M+CU/r-m 1.4. Vein m-cu present, spectral, or partly tubular. Vein m-cu position relative to vein r-m interstitial, or antefurcal. Vein 2-1A absent. Basal cell sparsely setose, bare posteriorly.

Hind legs. Femur length/width 4.6. Length of tibia/tarsi ~ 0.9. Length of basitarsus/tarsi 2–4 ~ 0.7. Sculpture of hind coxa dorsally granulate. Tarsal claws not pectinate. Metasoma. T1 length/apical width ~ 1.1. T2 length/apical width ~ 0.8. T3 length/apical width 0.5–0.6. Mid-longitudinal carina extending until basal ~ 0.7 of T3. Metasoma sculpture T1 rugose, T2 and most of T3 striate-rugose, or sculpture weaker at T3, or remainder terga granular-coriaceous. Ovipositor sheath/hind basitarsus 0.42–0.54. Apex of ovipositor sheaths truncate; apical point absent.

Color. Brownish yellow or brownish orange. Antenna entirely brownish yellow. Legs mostly brownish orange, tibia and tarsi whitish yellow except hind tibia gradually darkening from whitish yellow basally to brownish orange apically. Wings weakly tinged yellow, vein brownish yellow except fore wing veins 1M, 1CU, apex of 1-1A, 2CUb medially, r, and veins of second submarginal cell brown or dark brown. Ovipositor sheaths dark brown.

Male. Essentially as in female. Body length 6.7–7.8 mm; fore wing length 5.3–6.0 mm; antenna with 49–52 segments.

Diagnosis. *Aleiodes santarosensis* is a mainly brownish yellow species, with the whole antenna brownish yellow and whitish yellow tibia and tarsi 1–4 (Fig. 76). This is the only species in this study with tibia basally and tarsi 1–4 whitish yellow but without dark brown regions on apex of hind femur and tibia (Fig. 76). It is similar to *A. brevicarina*, from which is can be distinguished also by the large glabrous regions on the discal and basal cells of fore wing (Fig. 78). In contrast, these cells are mostly evenly setose in *A. brevicarina* (Fig. 32).

Distribution. Known only from localities in northwest Costa Rica.

Etymology. The name *santarosensis* refers to Santa Rosa National Park in Guanacaste Province of northwest Costa Rica, the type-locality of this species.

***Aleiodes taurus* Shimbori & Penteado-Dias, sp. nov.**
http://zoobank.org/EE216129-501C-4DFA-B1AD-DBD764182066
Figs 79–84

Type material. Holotype, female (DCBU #21814) "FAZ. CANCHIM SÃO CARLOS – SP luz, MATA, 19.X.1982 A.S. Soares col."

Description. Body length 7.7 mm. Fore wing length 6.4 mm.

Head (Fig. 80). In dorsal view eye length/temple 3.4–3.9. Eye height/head width 0.4. Eye height/minimum distance between eyes 1.1–1.2. OD/POL 2.2–2.5. OD/OOL 2.4–2.8. Frons excavated. Frons lateral carina present in addition to W-shaped carina. Occipital carina dorsally complete and nearly straight. Occiput in dorsal view nearly straight, not indented medially. Occipital carina ventrally meeting hypostomal carina. Mid-longitudinal crest at upper face present. Hypoclypeal depression/face width 0.37. Malar space/eye height 0.19. Face height/width 0.75. Clypeus height/width ~ 0.6. Clypeus convex, granulate. Sculpture of head vertex coarsely granulate, frons rugose. Face transversely rugose-striate at dorsal half, granulate medially.

Antenna. Antennal segments 30+ (antenna broken). Antenna/body length? (antenna broken). Scape/pedicel length 2.6. Length of first/second flagellomere 1.2. Fourth flagellomere length/apical width 1.7. Tip of apical segment of antenna missing.

Mesosoma. Length/height ~ 1.6. Width of mesoscutum/width of head 0.74. Mesoscutum length/width ~ 1.0. Pronotal collar/vertex 0.8. Prescutellar sulcus with entirely costate, lateral carina oblique and nearly reaching anterior border. Mesoscutum posterior border with distinct complete carina. Metanotum with complete mid-longitudinal carina, carinate posterior pit bisected by carina. Metanotum mid-pit present, delimited by carinae. Mid-longitudinal carina of propodeum present and basal 0.5 or less. Ventral mid-line of mesopleuron set within shallow smooth sulcus; pit at ventral mid-line present, shallow. Notauli present anteriorly, shallowly and weakly crenulate. Sternaulus weakly indicated anteriorly, rugose. Sculpture of mesosoma mostly granulate. Pronotum rugose laterally, pronotal groove crenulate laterally, with two parallel subventral carinae. Mesopleuron rugose below subalar groove. Subalar groove sparsely crenulate. Mid-posterior region of mesoscutum rugose, with a short mid-longitudinal carina posteriorly. Mesoscutellar trough entirely costate. Metanotum costate. Propodeum mostly rugose.

Wings. Fore wing: Stigma length/height 3.4. Vein r/2RS 1.5. Vein r/RS+Mb 1.4. Vein 3RSa/2RS 2.1. Vein 3RSa/2M 0.9. Vein 3RSa/3RSb 0.44. Vein 1CUa/1CUb 1.0. Vein 1CUa/2CUa 1.9. Vein 1cu-a nearly vertical. Vein 1M weakly curved basally. Vein RS+Ma distinctly curved. Vein M+CU virtually straight. Vein 1-1A nearly straight. Vein 1a absent. Second submarginal cell rectangular, slightly widening toward apex. Subbasal cell glabrous, with two parallel rows of short setae subapically, and a narrow patch of setae just below vein 1CUa. Basal cell with more or less large glabrous region posteriorly, sometimes with sparse setae; costal and apical regions evenly setose. Hind wing: Vein RS bent at basal 0.3, with vein r present. Marginal cell narrowest at base. Vein M+CU/1M 1.5. Vein M+CU/r-m 1.5. Vein m-cu present, spectral. Vein m-cu position relative to vein r-m just antefurcal. Vein 2-1A absent. Basal cell sparsely setose, bare posteriorly.

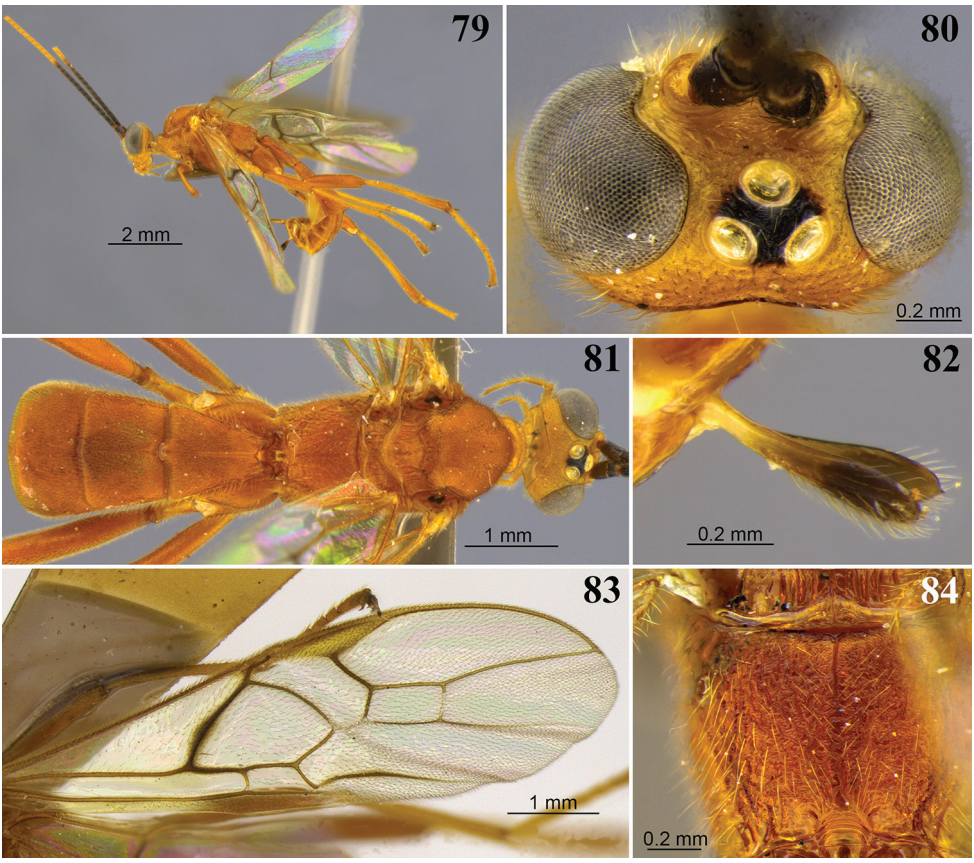

Figures 79–84. *Aleiodes taurus* sp. nov. **79** lateral habitus **80** head, dorsal view **81** dorsal habitus **82** ovipositor sheaths showing rounded ends with apical point **83** wings **84** propodeum, dorsal view.

Hind legs. Femur length/width 5.2. Length of tibia/tarsi ~ 0.9. Length of basitarsus/tarsi 2–4 0.65. Sculpture of hind coxa dorsally mostly shiny granular-coriaceous, finely striate apically. Tarsal claws not pectinate.

Metasoma. T1 length/apical width ~ 1.2. T2 length/apical width 0.7. T3 length/apical width 0.6. Mid-longitudinal carina extending until basal 0.7 of T3. Metasoma sculpture: T1, T2 and basal 0.7 of T3 rugose-costate, sculpture weaker at T3, remainder metasoma smooth. Ovipositor sheath/hind basitarsus 0.55. Apex of ovipositor sheaths roughly rounded; apical point present, distinct.

Color (Figs 79–84). Brownish orange. Head and pronotal collar yellow, stemmaticum black. Antenna with basal 12 or 13 flagellomeres black, apical segments brownish orange; pedicel black; scape dark brown to black, ventrally brownish orange. Base of tibiae and tarsi 1–4 slightly lighter than remainder legs. Wings subhyaline; stigma and most veins orange to yellow; vein 1M almost entirely dark brown, veins 1CUa, r, 2RS, and apex of 2CUb brown; infuscate areas around base of vein 1M and below apex of vein 1-1A. Ovipositor sheaths dark brown.

Male. Unknown.

Diagnosis. *Aleiodes taurus* is most similar to *A. gonodontivorus.* The main distinguishing characters are the differently shaped second submarginal cell, long and widening apically, with vein 3RSa 2.1 × longer than vein 2RS (Fig. 83), and the propodeum with very short longitudinal carina (Fig. 84) in *A. taurus*. In *A. gonodontivorus* the vein 3RSa is at most 1.7 × longer than 2RS (Fig. 44), and the longitudinal carina of propodeum is nearly complete.

Distribution. This species is known only from the type-locality in Brazil.

Etymology. The name is from the Latin word *taurus* meaning bull, being a reference to the collecting locality. The holotype was collected in a forest fragment at the research station of the Brazilian Agricultural Research Corporation - EMBRAPA, formerly a farm named Fazenda Canchim, in which a breed of beef cattle was developed, the Canchim, between 1940 and 1970. This area now comprises one of the largest remaining fragments of forest in the municipality of São Carlos.

Acknowledgments

We would like to thank the curators of the following collections for the loans of specimens for this research: Andrew Bennett, Canadian National Collection, Ottawa, Canada (CNCI); Carlos Roberto Ferreira Brandão, Museu de Zoologia da Universidade de São Paulo, São Paulo, Brazil (MZUSP); Gerardo Lamas and Lidia Sulca, Colección de Entomologia del Museo de Historia Natural de La Universidad Nacional Mayor de San Marcos (MUSM); Gabriel A. F. Melo, Coleção Entomológica Padre Jesus S. Moure, Departamento de Zoologia da Universidade Federal do Paraná (DZUP); Marcelo T. Tavares, Coleção de Insetos do Departamento de Ciências Biológicas da Universidade Federal do Espírito Santo (UFES); Instituto Nacional de Biodiversidad, Santo Domingo de Heredia, Costa Rica (INBIO); E. Kierych, Polish Academy of Sciences, Warsaw (PASW); Daniel H. Janzen, University of Pennsylvania, Philadelphia, USA (UPP); and Brian Farrell, Museum of Comparative Zoology, Harvard University, Cambridge, Massachusetts, USA (MCZC). Research funding and imaging equipment was provided by National Science Foundation grants DEB-10-20751 and DEB 14-42110 (Dimensions of Biodiversity Program). This study was financed in part by the Coordenação de Aperfeiçoamento de Pessoal de Nível Superior – Brasil (CAPES) – Finance Code 001. Additional research support for SRS was provided by McIntire-Stennis Grant Project number WYO-530-14, Studies of Parasitoid Wasps of Forest Ecosystems, and for EMS and AMPD by the INCT-HYMPAR (Instituto Nacional de Ciência e Tecnologia dos Hymenoptera Parasitoides) financed by FAPESP (São Paulo Research Foundation) and CNPq (National Council for Scientific and Technological Development). This work was also supported by Wyoming Agricultural Experiment Station funding to SRS provided through the USDA National Institute of Food and Agriculture, McIntire-Stennis project 1021111. Any opinions, findings, and conclusions expressed are those of the authors and do not necessarily reflect the views of the National Science Foundation.

References

Areekul-Butcher B, Quicke DLJ (2011) Revision of *Aleiodes* (*Hemigyroneuron*) parasitic wasps (Hymenoptera: Braconidae: Rogadinae) with reappraisal of subgeneric limits, descriptions of new species and phylogenetic analysis. Journal of Natural History 45(23–24): 1403–1476. https://doi.org/10.1080/00222933.2011.557557

Areekul-Butcher B, Smith MA, Sharkey MJ, Quicke DLJ (2012) A turbo-taxonomic study of Thai *Aleiodes* (*Aleiodes*) and *Aleiodes* (*Arcaleiodes*) (Hymenoptera: Braconidae: Rogadinae) based largely on COI barcoded specimens, with rapid descriptions of 179 new species. Zootaxa 3457: 1–232. https://www.biotaxa.org/Zootaxa/article/view/zootaxa.3457.1.1

Braet Y, van Achterberg C (2011) *Athacryvac* gen. n. from French Guiana (Hymenoptera: Braconidae: Rogadinae), with description of two new species. Tijdschrift voor Entomologie 154: 283–290. https://doi.org/10.1163/22119434-900000325

Fortier JC (2009) A revision of the *Tetrasphaeropyx* Ashmead lineage of the genus *Aleiodes* Wesmael (Hymenoptera: Braconidae: Rogadinae). Zootaxa 2256: 1–126. https://doi.org/10.11646/zootaxa.2256.1.1

Fortier JC, Shaw SR (1999) Cladistics of the *Aleiodes* lineage of the subfamily Rogadinae (Hymenoptera: Braconidae). Journal of Hymenoptera Research 8: 204–237. https://www.biodiversitylibrary.org/page/4490710#page/532/mode/1up

Garro LS, Shimbori EM, Penteado-Dias AM, Shaw SR (2017) Four new species of *Aleiodes* (Hymenoptera: Braconidae: Rogadinae) from the Neotropical Region. The Canadian Entomologist 149: 560–573. https://doi.org/10.4039/tce.2017.23

Harris RA (1979) A glossary of surface sculpturing. Occasional Papers in Entomology of the California Department of Food and Agriculture 28: 1–31.

Karlsson D, Ronquist F (2012) Skeletal morphology of *Opius dissitus* and *Biosteres carbonarius* (Hymenoptera: Braconidae), with a discussion of terminology. PLoS ONE 7 (4): e32573. https://doi.org/10.1371/journal.pone.0032573

Marsh PM, Shaw SR (1998) Revision of North American *Aleiodes* Wesmael (Part 3): the *seriatus* (Herrich-Schaeffer) species-group. Proceedings of the Entomological Society of Washington 100: 395–408. https://www.biodiversitylibrary.org/page/16150249

Marsh PM, Shaw SR (1999) Revision of the North American *Aleiodes* Wesmael (Part 5): The *melanopterus* (Erichson) Species-Group (Hymenoptera: Braconidae, Rogadinae). Journal of Hymenoptera Research 8(1): 98–108. https://www.biodiversitylibrary.org/page/4490531

Marsh PM, Shaw SR (2001) Revision of North American *Aleiodes* (part 6): the *gasterator* (Jurine) and *unipunctator* (Thunberg) species-group (Hymenoptera: Braconidae: Rogadinae). Proceedings of the Entomological Society of Washington 103: 291–307. https://www.biodiversitylibrary.org/page/16279537

Marsh PM, Shaw SR (2003) Revision of North American *Aleiodes* (part 7): the *compressor* Herrich-Schaeffer, *ufei* (Walley), *gressitti* (Muesebeck) and *procerus* Wesmael species-groups (Hymenoptera: Braconidae: Rogadinae). Proceedings of the Entomological Society of Washington 105: 698–707. https://www.biodiversitylibrary.org/page/16212241

Quicke DLJ (2012) We know too little about parasitoid wasp distributions to draw any conclusions about latitudinal trends in species richness, body size and biology. Public Library of Science One 7: e32101. https://doi.org/10.1111/j.1471-8286.2007.01678.x

Ratnasingham S, Hebert PDN (2007) BOLD: The Barcode of Life Data System (http://www.barcodinglife.org/). Molecular Ecology Notes 7(3): 355–364.

Sharkey MJ (1997) Key to New World subfamilies of the Braconidae. In: Wharton RA, Marsh PM, Sharkey MJ (Eds) Manual of the New World genera of the family Braconidae (Hymenoptera). International Society of Hymenopterists Special Publication, Washington, 39–63.

Sharkey MJ, Wharton RA (1997) Morphology and terminology. In: Wharton RA, Marsh PM, Sharkey MJ (Eds) Manual of the New World genera of the family Braconidae (Hymenoptera). International Society of Hymenopterists Special Publication, Washington, 19–37.

Shaw MR (1983) On[e] evolution of endoparasitism: the biology of some genera of Rogadinae (Braconidae). In: Gupta VK (Ed.) Studies on the Hymenoptera: a collection of articles on Hymenoptera commemorating the 70th birthday of Henry K. Townes. Contributions of the American Entomological Institute 20, 307–328.

Shaw MR (1994) Parasitoid host ranges. In: Hawkins BA, Sheehan W (Eds) Parasitoid community ecology. Oxford University Press, Oxford, 111–144.

Shaw MR, Huddleston T (1991) Classification and biology of braconid wasps. Handbooks for the Identification of British Insects, Volume 7, Part 11. Royal Entomological Society of London, London, 126 pp.

Shaw SR (1993) Systematic status of *Eucystomastax* Brues and characterization of the Neotropical species (Hymenoptera: Braconidae: Rogadinae). Journal of Hymenoptera Research 2(1): 1–11. https://www.biodiversitylibrary.org/page/4490140

Shaw SR (1997) Subfamily Rogadinae s.s. In: Wharton RA, Marsh PM, Sharkey MJ (Eds) Manual of the New World genera of the family Braconidae (Hymenoptera). International Society of Hymenopterists Special Publication, Washington, 403–412.

Shaw SR (2006) *Aleiodes* wasps of eastern forests: a guide to parasitoids and associated mummified caterpillars. Technology Transfer Series, Forest Health Technology Enterprise Team, Morgantown, 121 pp.

Shaw SR, Marsh PM, Fortier JC (1997) Revision of North American *Aleiodes* (Part 1): the *pulchripes* Wesmael species-group in the New World (Hymenoptera: Braconidae, Rogadinae). Journal of Hymenoptera Research 6: 10–35. https://www.biodiversitylibrary.org/page/4491455

Shaw SR, Marsh PM, Fortier JC (1998a) Revision of North American *Aleiodes* (Part 2): the *apicalis* (Brullé) species-group in the New World (Hymenoptera: Braconidae, Rogadinae). Journal of Hymenoptera Research 7: 62–73. https://www.biodiversitylibrary.org/page/4490550

Shaw SR, Marsh PM, Fortier JC (1998b) Revision of North American *Aleiodes* (Part 4): the *albitibia* Herrich-Schaeffer and *praetor* Reinhard species-groups (Hymenoptera: Braconidae: Rogadinae) in the New World. Proceedings of the Entomological Society of Washington 100: 553–565. https://www.biodiversitylibrary.org/page/16150407

Shaw SR, Marsh PM, Fortier JC (2006) Revision of North American *Aleiodes* Wesmael (Part 8): the *coxalis* (Spinola) Species-Group (Hymenoptera: Braconidae, Rogadinae). Zootaxa 1314: 1–30. https://doi.org/10.11646/zootaxa.1314.1.1

Shaw SR, Marsh PM, Talluto MA (2013) Revision of North American *Aleiodes* (Part 9): the *pallidator* (Thunberg) species-group with description of two new species (Hymenoptera: Braconidae, Rogadinae). Zootaxa 3608: 204–214. https://doi.org/10.11646/zootaxa.3608.3.4

Shimbori EM, Penteado-Dias AM (2011) Taxonomic contribution to the *Aleiodes melanopterus* (Erichson) species-group (Hymenoptera, Braconidae, Rogadinae) from Brazil. ZooKeys 142: 15–25. https://doi.org/10.3897/zookeys.142.1705

Shimbori EM, Shaw SR (2014) Twenty-four new species of *Aleiodes* Wesmael from the eastern Andes of Ecuador with associated biological information (Hymenoptera, Braconidae, Rogadinae). Zookeys 405: 1–81. https://doi.org/10.3897/zookeys.405.7402

Shimbori, EM, Shaw SR, Penteado-Dias AM (2015) A revision of the New World species of the *Aleiodes compressor* species group (Hymenoptera: Braconidae: Rogadinae). The Canadian Entomologist 147: 665–673. https://doi.org/10.4039/tce.2015.9

Shimbori, EM, Shaw, SR, Almeida LFV, Penteado-Dias, AM (2016) Eleven new species of *Athacryvac* Braet & van Achterberg from the Neotropical Region (Hymenoptera, Braconidae, Rogadinae). Zootaxa 4138 (1): 83–117. https://doi.org/10.11646/zootaxa.4138.1.3

Smith MA, Wood DM, Janzen DH, Hallwachs W, Hebert PDN (2007) DNA barcodes affirm that 16 species of apparently generalist tropical parasitoid flies (Diptera, Tachinidae) are not all generalists. Proceedings of the National Academy of Sciences 104(12): 4967–4972. https://doi.org/10.1073/pnas.0700050104

Smith MA, Rodriguez JJ, Whitfield JB, Deans AR, Janzen DH, Hallwachs W, Hebert PDN (2008) Extreme diversity of tropical parasitoid wasps exposed by iterative integration of natural history, DNA barcoding, morphology, and collections. Proceedings of the National Academy of Sciences 105(34): 12359–12364. https://doi.org/10.1073/pnas.0805319105

Townsend AC, Shaw SR (2009) Nine new species of *Aleiodes* Wesmael reared at Yanayacu Biological Station (Hymenoptera: Braconidae:Rogadinae) in eastern Ecuador. Journal of Insect Science 9: 1–37. https://doi.org/10.1673/031.009.3701

van Achterberg C (1991) Revision of the genera of the Afrotropical and W. Palaearctic Rogadinae Foerster (Hymenoptera: Braconidae). Zoologische Verhandelingen 273: 1–102. https://www.researchgate.net/publication/254893871

van Achterberg C (1993) Illustrated key to the subfamilies of the Braconidae (Hymenoptera: Ichneumonoidea). Zoologische Verhandelingen 283: 1–189. https://www.researchgate.net/publication/302989015

van Achterberg C, Shaw MR (2016) Revision of the western Palaearctic species of *Aleiodes* Wesmael (Hymenoptera, Braconidae, Rogadinae). Part 1: Introduction, key to species groups, outlying distinctive species, and revisionary notes on some further species. ZooKeys 639: 1–164. https://doi.org/10.3897/zookeys.639.10893

van Achterberg C, Shaw MR, Quicke DLJ (2020) Revision of the western Palaearctic species of *Aleiodes* Wesmael (Hymenoptera, Braconidae, Rogadinae). Part 2: Revision of the *A. apicalis* group. ZooKeys 919: 1–259. https://doi.org/10.3897/zookeys.919.39642

Yu D, van Achterberg C, Horstmann K (2012) Taxapad 2012–World Ichneumonoidea 2011. Taxonomy, biology, morphology and distribution. On USB Flash drive. www.taxapad.com, Ottawa, Ontario, Canada.

Zaldívar-Riverón A, Shaw MR, Sáez AG, Mori M, Belokoblylskij SA, Shaw SR, Quicke, DLJ (2008) Evolution of the parasitic wasp subfamily Rogadinae (Braconidae): phylogeny and evolution of lepidopteran host ranges and mummy characteristics. BMC Evolutionary Biology 8: 1–20. https://doi.org/10.1186/1471-2148-8-329

ZooKeys 964: 109–126 (2020)
doi: 10.3897/zookeys.964.47441
https://zookeys.pensoft.net

RESEARCH ARTICLE

A peer-reviewed open-access journal
ZooKeys
Launched to accelerate biodiversity research

A new species of *Periclistus* Foerster, 1869 from China and review of the tribe Diastrophini (Hymenoptera, Cynipoidea, Cynipidae)

Yin Pang[1*], Zhiwei Liu[1,2*], Cheng-Yuan Su[1], Dao-Hong Zhu[1]

1 *Institute of Evolutionary Ecology and Conservation Biology, Central South University of Forestry & Technology, Shaoshan Road South 498#, Changsha, Hunan 410004, China* **2** *Dept. of Biological Sciences, Eastern Illinois University, 600 Lincoln Ave, Charleston, IL 61920, USA*

Corresponding author: Zhiwei Liu (zliu@eiu.edu); Dao-Hong Zhu (daohongzhu@yeah.net)

Academic editor: A. Köhler | Received 19 October 2019 | Accepted 15 April 2020 | Published 27 August 2020

http://zoobank.org/1EFD1A95-A4D6-406F-A911-CA220052B4B4

Citation: Pang Y, Liu Z, Su C-Y, Zhu D-H (2020) A new species of *Periclistus* Foerster, 1869 from China and review of the tribe Diastrophini (Hymenoptera, Cynipoidea, Cynipidae). ZooKeys 964: 109–126. https://doi.org/10.3897/zookeys.964.47441

Abstract

A new species of cynipid gall wasps, *Periclistus orientalis* Pang, Liu & Zhu, **sp. nov.**, is herein described from Hunan, China in the tribe Diastrophini (Hymenoptera: Cynipoidea: Cynipidae). The phylogenetic relationship between *Periclistus* and all the other Diastrophini genera, except the recently described *Xestophanopsis* Pujade-Villar et al., 2019, was analyzed using a fragment of the mitochondrial COI gene and a fragment of the nuclear 28S gene. A taxonomic key to the known genera of Diastrophini and an updated taxonomic key to the known Eastern Palearctic species of *Periclistus* were provided. In addition, an updated checklist of the known species of the genus from the world is given.

Keywords

cynipid gall wasp, inquiline gall wasp, molecular phylogeny, Oriental, rose gall

Introduction

Inquiline gall wasps of Cynipidae (Hymenoptera: Cynipoidea) are guests living in the galls induced mostly by other cynipid wasps and occasionally by gall makers of other

* Contributed equally as the first authors.

taxonomic groups, including Cecidomyiidae (Diptera) (Wachi et al. 2011; Ide et al. 2018) and Cecidosidae (Lepidoptera) (Van Noort et al. 2007). According to phylogenetic studies using morphological data, they were considered to have evolved from a single gall-making ancestor that have lost the ability to make galls and were thus all grouped in one tribe, i.e., Synergini (Ritchie 1984; Ronquist 1994; Liljeblad and Ronquist 1998; Ronquist and Liljeblad 2001). However, a comprehensive study on the phylogenetic relationship within Cynipidae based on both morphology and molecular data concluded that inquiline cynipids may have multiple origins, resulting in a significantly revised classification of Cynipidae, particularly with regard to the inquiline members of the family (Ronquist et al. 2015).

Diastrophini is one of the newly established tribes in the updated classification by Ronquist et al. (2015) and currently comprises five genera of gall makers and inquilines exclusively associated with host plants of the Rosaceae family (Pujade-Villar et al. 2016) in the subfamily Rosoideae (Potter et al. 2007). The only species of the tribe that is not associated with a Rosaceae host is *Diastrophus smilacis* reared from *Smilax* sp. (Smilaceae) (Schick et al. 2003). Among the five genera included in Diastrophini, the genera *Diastrophus* Hartig, 1840 and *Xestophanes* Foerster, 1869 consist of gall makers only. *Diastrophus* is widely distributed in the Holarctic and has one known species from Mesoamerica (Nieves-Aldrey et al. 2013) and its members induce galls on species of *Rubus*, *Fragaria*, and *Potentilla* (Palaearctic and Nearctic) (Schick et al. 2003; Melika 2006; Abe et al. 2007) while *Xestophanes* is endemic to Europe in the western Palearctic and the two known species of the genus induce galls on *Potentilla* spp. (Nieves-Aldrey 1994, 2001; Melika 2006). Two other genera of the tribe, *Periclistus* Foerster, 1869 and *Synophromorpha* Ashmead, 1903, are inquilines, using, respectively, galls made by gall makers belonging to different cynipid tribes – species of *Synophromorpha* are associated with galls of *Diastrophus* (Schick et al. 2003) while species of *Periclistus* are associated with galls of *Diplolepis* and *Liebelia* (Cynipidae: Diplolepidini) formed on *Rosa* spp. (Ronquist and Liljeblad 2001; Ronquist et al. 2015). Both *Periclistus* and *Synophromorpha* have a Holarctic distribution (Ritchie 1984; Ritchie and Shorthouse 1987; Ronquist 1994; Ronquist et al. 2015; Pujade-Villar et al. 2015). Although *P. smilacis* Ashmead 1896 was reported to be reared from galls of *Diastrophus smilacis* Ashmead, 1896 in Florida, USA, which would also suggest that the species is associated with *Smilax* (Smilaceae), the record seemed to be incorrect (Burks 1979; Pujade-Villar et al. 2016, 2019). The fifth genus, *Xestophanopsis* Pujade-Villar et Wang, 2019, recently described from China is apparently a gall maker associated with Rosaceae host (Pujade-Villar et al. 2019), which needs to be confirmed with rearing data.

The genus *Periclistus* consists of 18 valid species found in the Holarctic region (Pujade et al. 2016; HOL 2018), including five species from the Eastern Palearctic (Pujade-Villar et al. 2016). In the present paper, we describe a new species of the genus from Hunan, China, which is also the first record of the genus from the Oriental region. In the recent study on the phylogeny, evolution and classification of cynipid gall wasps by Ronquist et al. (2015), the tribe Diastrophini was relatively well represented, including at least one species from each genus. The two included *Periclistus* species, i.e., *P. brandtii* and *P. pirata* are from the western Palearctic and the Nearctic, respectively. The new species was thus sequenced as a representative from the Eastern Palearctic + Oriental for one mitochondrial gene (COI) and one nuclear gene (28s) and included

in an updated phylogenetic analysis of the tribe to examine how the three species are related to each other and the underlying biogeographical implications.

In addition, we also updated the taxonomic key to the species of *Periclistus* Foerster, 1869 from the Eastern Palearctic by Pujade-Villar et al. (2019) and the Oriental region to include the new species and provided a key to the five currently recognized genera of the tribe Diastrophini to facilitate future work on the tribe.

Materials and methods

Galls collected from April through August were kept in plastic jars with moistened cotton and placed in fine meshed rearing cages. The rearing setup was placed on shelves in ambient environment in the lab and checked daily for emergence. Wasps were collected at emergence and preserved in 100% ethanol, and labeled vials were stored in ultralow freezer at -80 °C for long storage until being retrieved later for preparation for morphological studies or for DNA extraction in molecular studies.

Specimens for conventional morphological examination were air dried at room temperature before being mounted. Specimens mounted to pinned triangle card paper were photographed with Leica M205C microscope system equipped (Leica Inc., Germany) with Leica DMC6200 digital camera attached to a computer.

We follow Ronquist and Nordlander (1989) and Ronquist (1995) for structural terminology, Melika (2006) for measurement definitions, and Harris (1979) for surface sculpture descriptions. Abbreviations:

F1, F2 the first and second flagellomere, respectively,
LOL (lateral-frontal ocelli distance): the distance between anterior and lateral ocelli,
OOL (ocellar-ocular distance): the distance from the outer margin of a posterior ocellus to the inner margin of the compound eye, and
POL (post-ocellar distance): the distance between the inner margins of the posterior ocelli.

All type specimens are deposited in the Insect Collection, Central South University of Forestry and Technology (**CSUFT**), Changsha, Hunan, China.

Three individuals of the new species were used for DNA extraction. The insects were washed in sterile water before DNA extraction to avoid cross-contamination. Total DNA was extracted from each individual using SDS/proteinase K digestion and phenol-chloroform extraction method as previously described (Zhu et al. 2007). Extracted DNA pellets were air dried, resuspended in 50 µl sterile water, and then stored at 4 °C before being used for PCR and sequencing. For phylogenetic analysis, we chose a specific region of the cytochrome oxidase subunit I gene (COI), which was amplified using the primers HCO-2198 (5' TAA ACT TCA GGG TGA CCA AAA AAT CA 3') and LCO-1490 (5' GGT CAA CAA ATC ATA AAG ATA TTG G 3') (Folmer et al. 1994), and the ribosome gene 28S, which was amplified using the primers D2F (5' CGT GTT GCT TGA TAG TGC AGC 3') and D2R (5' TCA AGA CGG GTC CTG AAA GT

3') (Dowton and Austin 2001), or 28Sbout (5' CCC ACA GCG CCA GTT CTG CTT ACC 3') and 28SF (5'AGT CGT GTT GCT TTG ATA GTG CAG 3') primers (Rokas et al. 2002). These two gene fragments were chosen because of their suitability for recovering inter- and intrageneric phylogenies within the Hymenoptera in general and Cynipidae in particular (Rokas et al. 2002) as well as the availability of sequences of the two genes for a reasonable number of congeneric species from public gene sequence depositories. The PCR cycling conditions were: 5 min at 95 °C , followed by 35 cycles of 30 s at 95 °C , 1 min at 46 °C and 1 min at 72 °C, and a final elongation step of 5 min at 72 °C for COI and 5 min at 95 °C, followed by 35 cycles of 30 s at 95 °C, 1 min at 56 °C and 1 min at 72 °C, and a final elongation step of 5 min at 72 °C for 28S. Amplified PCR products were sent to Invitrogen (Shanghai, China) for sequencing. The COI and 28S gene sequences were retrieved from GenBank (https://www.ncbi.nlm.nih.gov/genbank/) for three species of *Diastrophus*, as well as one species for *Synophromorpha*, *Xestophanopsis*, and *Periclistus* respectively. In addition, sequences of the two genes were also acquired from GenBank or by sequencing for *Dryocosmus liui* as outgroup. The final dataset consists of nine species including outgroup (Table 1). Multiple sequence alignment was performed using ClustalW (Thompson et al. 1994) implemented in Mega 7.0 (Kumar et al. 2016) using default parameters. Aligned sequences were then visually edited in Mega 7.0 and trimmed, resulting in a final aligned length of 1133 bp nucleotides, consisting of 670 bps for COI and 490 bps or 1106 bps for 28S.

The final dataset was subjected to Mega 7.0 for evaluation of best-fit nucleotide substitution model (Nei and Kumar 2000) using Maximum Likelihood (ML) method with default settings except that we used "very strong" branch swap filter. Phylogenetic analysis was conducted using MrBayes 3.2.6 x64 for Windows (Ronquist et al. 2012) (Bayesian Inference method, BI), assuming a generalized time-reversible (GTR) model with gamma distributed rate variation across sites (+G) based on best fit nucleotide substitution model evaluation described above. For Bayesian analysis, two independent runs were performed with the default priors and MCMC parameters except the following: nst = 6, rates = gamma, MCMC runs comprised 10 million generations sampled at every 1,000 generations with 30% burn-in time. Convergence was achieved

Table 1. List of species included in phylogenetic analysis of Diastrophini relationship based on mitochondrial COI and nDNA 28S. Most sequences were retrieved from GenBank, except for those in bold, which were acquired by sequencing in the present study. Abbreviations for generic names: *Dr – Dryocosmus*, *Di – Diastrophus*, *Sy – Synophromorpha*, *Xe – Xestophanes*, and *Pe – Periclistus*; for geographical distributions: WP = Western Palearctic, EP = Eastern Palearctic, O = Oriental, and N = Nearctic.

Species	Distribution	COI #	28S #	Reference
Di. rubi	WP	DQ012640	DQ012598	Liljeblad (2002)
Di. potentillae	N	AY368914	AY368940	Liljeblad (2002)
Di. turgidus	N	AY368913	AY368939	Liljeblad (2002)
Sy. sylvestris	N	AY368911	AY368937	Liljeblad (2002)
Xe. potentillae	WP	AY368912	AY368938	Liljeblad (2002)
Pe. brandtii	WP	AF395181	AF395152	Rokas et al. (2002)
Pe. pirata	N	DQ012649	DQ012606	Liljeblad (2002)
Pe. orientalis	O	**MN633410**	**MN633411**	Present study
Dr. liui	EP	MG754067	**MN633412**	Pang et al. (2018), present study

as being diagnosed by the average standard deviation of split frequencies between the two independent runs (<0.01) and PSRF values (1 with < 1% deviation). The final tree from both analyses was rooted with *Dryocosmus liui* based on published phylogeny of Cynipidae (Ronquist et al. 2015).

Taxonomy

Diastrophini Ronquist et al., 2015

Key to genera

1 Vertex and mesoscutum (Fig. 7) variously sculptured, imbricate to coriaceous. Mesopleuron usually longitudinally striae (Figs 15, 19) and occasionally shining smooth (Fig. 8) **2**

– Vertex and mesoscutum smooth, devoid of sculpture (Figs 12, 13). Mesopleuron usually completely smooth without sculpture, and occasionally with very reduced diagonal fine striae **3**

2 Vertex and mesoscutum mildly to roughly coriaceous, but always entirely punctate setigenous (Figs 5–8, 14, 15). Inquilines of *Diplolepis* and *Liebelia* galls formed on *Rosa* spp. Holarctic..... ***Periclistus***

– Vertex and mesoscutum mostly mildly coriaceous and scarcely punctate setigenous (Figs 16, 19). Inquilines of *Diastrophus* galls on *Rubus* spp. Holarctic..... ***Synophromorpha***

3 Abdominal terga 3–8 free in both sexes (Fig. 17). Galls mostly on *Rubus* spp., but also on *Fragaria* and *Potentilla*. Mostly Holarctic, with one species from Mesoamerica in Nearctic..... ***Diastrophus***

– Abdominal terga 3+4 fused in females (Fig. 18); free in males..... **4**

4 Antenna of female with 11 flagellomeres, F1 equal or longer than F2; radial cell at most 3.5 times as long as wide, have a weak tarsal tooth. Galls on *Potentilla* spp. Western Palearctic..... ***Xestophanes***

– Antenna of female with 10 flagellomeres, F1 shorter than F2; radial cell at least 4.0 times as long as broad; tarsal claw with a strong basal lobe. Host plant unknown. Eastern Palearctic..... ***Xestophanopsis***

Periclistus Forster, 1869

***Periclistus orientalis* Pang, Liu & Zhu, sp. nov.**
http://zoobank.org/77D32C97-1A16-4FE6-9A17-EC87B42749EB
Figures 1–11

Type materials. ***Holotype*:** ♀ (CSUFT), China, Hunan Province, Zhuzhou City, 27.83N, 113.13E, reared in 2011-V-10-20 from galls collected in 2011-IV, leg. Xiao-Hui Yang; ***Paratypes*:** 4♀♀, 2♂♂ (CSUFT), collection data and locality same as holotype.

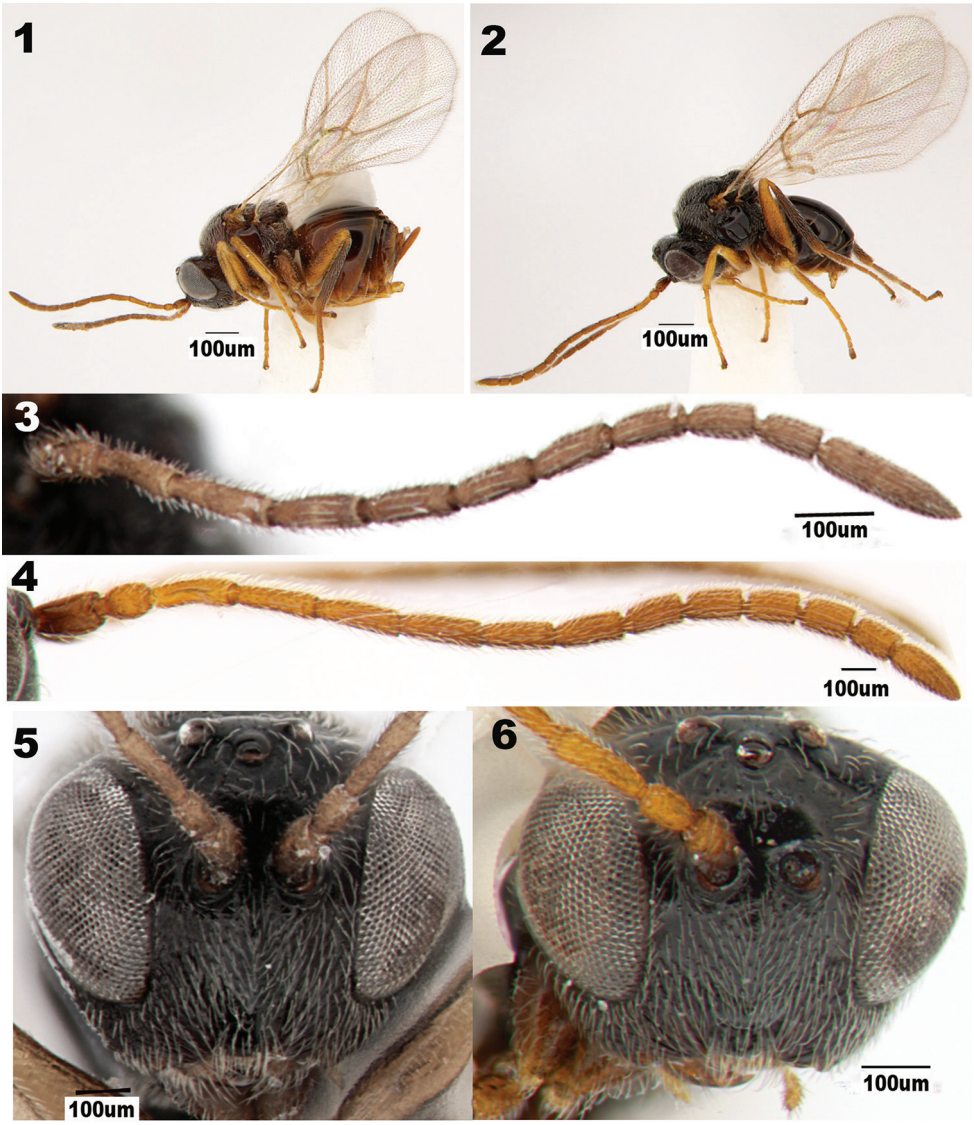

Figures 1–6. *Periclistus orientalis* sp. nov. **1** general habitus (♀) **2** general habitus (♂) **3** antenna (♀) **4** antenna (♂) **5** head in anterior view (♀) **6** head in anterior view (♂).

Etymology. The species epithet is derived from Latin *orient*, meaning east, to suggest the type locality from the Oriental region.

Diagnosis. *Periclistus orientalis* can be distinguished from the other congeneric species in the Eastern Palearctic using the taxonomic key provided herein. Below we provide more detailed comparison of the new species with the two very similar species, i.e., *P. setosus* and *P. capillatus*.

Periclistus orientalis sp. nov. is similar to *P. setosus*, but differs from the latter in the lower face with striae radiating from clypeus reaching eyes and antennal socket in the

new species, whereas in *P. setosus* striae of lower face not reaching eyes and antennal socket (Fig. 5); notauli distinctly present in posterior one third of scutum and medial sulcus absent in the new species, whereas complete and distinctly in *P. setosus* (Wang et al., 2012) (Fig. 7); lateral surface of pronotum entirely coriaceous with evenly distributed dense setigerous punctures (Fig. 8) in the new species, but in the latter lateral surface of pronotum glabrous, with sparse setigerous punctures ventrolaterally. The new species is also similar to *P. capillatus* Belizin, 1968. It differs from *P. capillatus* in the mesoscutum glabrous with piliferous punctures and dense appressed pubescence in the new species, whereas with piliferous points and sparse pubescence in *P. capillatus* (Fig. 7); notauli distinctly present in posterior one third of scutum and medial sulcus absent in the new species, whereas incomplete or very weakly impressed anteriorly in *P. capillatus* (Fig. 7); fused metasomal tergites T2+T3 anterolaterally with a patch of sparse white setae, mostly smooth except for minute punctures on laterally posterior half and a narrow band of punctures along posterior margin, whereas in the latter metasomal tergites fused (T2+T3) smooth, with an anterolateral patch of white setae, and the subsequent segments glabrous with micropunctures (Figs 1, 9).

Description. Female: ***Body*** length 2.7–2.8mm ($N = 5$).

Coloration. Head completely black. Antenna uniformly light brown. Front and middle legs reddish brown, except coxa and claw black; hind legs black, except tarsomeres 1 and 5 reddish brown. Mandible and maxilla reddish brown, labial palpi light brown. Mesosoma black; metasoma mostly reddish brown in anterior half, and dark in dorsal half. Ventral spine of hypopygium reddish brown.

Antenna filiform with ten flagellomeres, slightly tapering toward apex; pedicel 1.67 times as long as broad; relative lengths of scape, pedicel and F1-F10: 9:5:10:10:10:9:8:8:7:6:6:13 (Fig. 3).

Head coriaceous, with sparse setae, 2.0 times as broad as long in dorsal view, 1.24 times as wide as high and slightly broader than mesosoma in dorsal view. Gena delicately coriaceous and not broadened behind eyes. Malar space 0.27 times as high as height of eye. Lower face with striae radiating from clypeus and reaching eyes and antennal socket, entirely densely punctate with white, long, and appressed setae; median area slightly elevated, delicately coriaceous, lateral carinae bordering median area complete from clypeus to antennal socket and about as strong as radiating striae on lateral areas of lower face. Clypeus inversely trapezoid, ventral margin straight, and delicately coriaceous with dense long setae; anterior tentorial pits indistinct; epistomal sulcus and clypeo-pleurostomal lines indistinct. Transfacial distance longer than height of eye; distance between inner margin of eye and outer rim of antennal torulus slightly longer than distance between antennal toruli, all larger than diameter of torulus (Fig. 5). Ratios of POL/OOL, POL/LOL, and LOL/OOL1.3, 1.8 and 0.7, respectively. Frons, vertex and gena behind eyes, and postgena with sparse setigerous punctures; setae long and white. Frons coriarious and smooth, with scattered punctures. Vertex smooth and evenly punctate with long setae (Fig. 7).

Mesosoma longer than high in lateral view and with white setae. Pronotum median length nearly one third of length of outer lateral margin; anterior lateral depressions medially separated broadly from each other, laterally open, continuing to a dis-

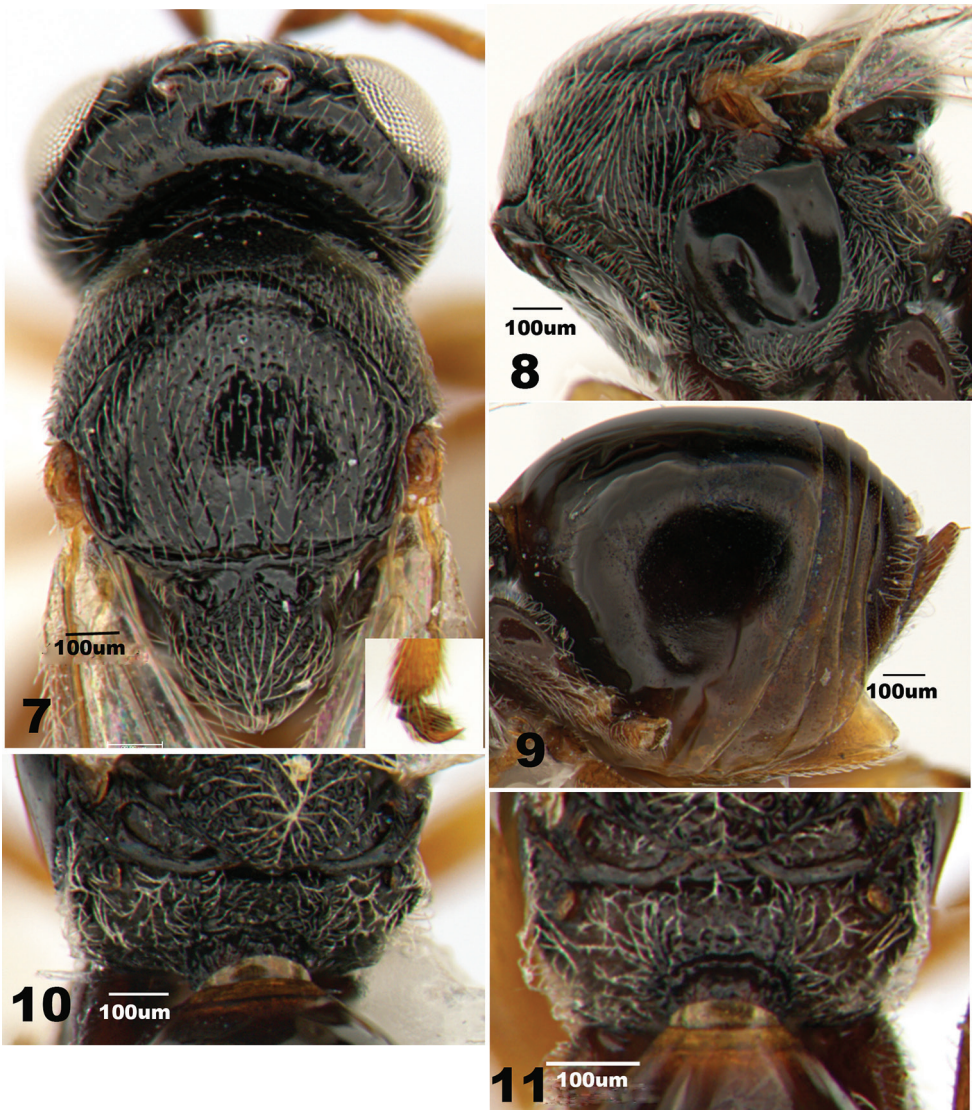

Figures 7–11. *Periclistus orientalis* **7** head and mesosoma in dorsal view (♀, similar in ♂) **8** mesosoma in lateral view (♀) **9** metasoma in lateral view (♀) **10** propodeum in dorsal view (♀) **11** propodeum in dorsal view (♂).

tinct furrow; posterior rim of anterior lateral depressions extending dorsally to reach posterior margin of pronotum, distinctly separating anterior plate from lateral pronotal areas. Anterior plate of pronotum delicately coriaceous, posteriorly with shallowly punctate and sparsely setose (Fig. 7); lateral pronotal areas coriaceous, entirely densely punctate with appressed long setae, without glabrous ventral nude area (Fig. 8). Mesoscutum smooth and shiny, slightly broader than long, distinctly depressed anteriorly, with evenly dispersed piliferous punctures; anteroadmedian signum absent, notauli distinctly present in posterior one third of scutum, medial sulcus absent, parapsidal

signa present in posterior half and absent anteriorly (Fig. 7). Scutellar foveae large, deeply impressed, glabrous, separated by a broad median carina (Fig. 7). Mesoscutellum about as broad as long, rugose and foveolate with sparse, appressed setae (Fig. 7). Mesopleuron distinctly higher than broad, glabrous and shining, devoid of striation and pubescence, except for pubescence along ventral margin (Fig. 8); mesopleural triangle glabrous, not separated from rest of mesopleuron by a ventral carina. Metapleural sulcus reaching mesopleuron in upper one fourth of its height; metapleuron rugulose with long setae; metanotum slightly overhanging. Lateral propodeal carinae distinct and evenly curved outwards; median propodeal area rugose foveolate; lateral propodeal areas with dense setae (Fig. 10).

Forewing with distinct veins R+Sc, R1+Sc, R1, M, M+Cu1, Cu1, Cu1b, Cu1a, 2r and Rs+M; areolet distinct and large; radial cell closed, 3.3 times as long as wide; all visible veins dark brown (Fig. 1).

Metasoma nearly as long as head and mesosoma combined, distinctly longer than height in lateral view, distinctly punctate posteriorly. Metasomal tergites 2+3 with some setae ventrally. Prominent part of ventral spine of hypopygium very short (Fig. 9).

Male: Similar to female, but different as follows. Antenna with 12 flagellomeres, pedicel 2.5 times as long as broad. F1 strongly curved medially. Relative lengths of scape, pedicel and F1-F12: 7:5:13:12:7:7:6:6:5:5:5:5:4:7 (Fig. 4). Second and third metasomal tergites not fused, separated by a suture (Fig. 2).

Biology. All specimens were reared from galls collected from *Rosa multiflora*, and the galls were very similar in morphology to those made by *Diplolepis japonica*: fleshy and spherical with pointed spikes on top, pinkish green to greenish yellow in color, and located on rachis or central vein of leaflets of both upper and under sides (Fig. 20). Nonetheless, the identity of the host gall maker remains reclusive since our rearing yielded no specimen of the putative gall maker. The galls were collected from April through August, and specimens of *P. orientalis* emerged in early May from galls collected in April.

Distribution. Known from Zhuzhou City, Hunan Province, China.

The known species of *Periclistus* in the Eastern Palearctic can be identified using the following taxonomic key modified from Pujade-Villar et al. (2016) to accommodate the new species.

Taxonomic Key to Eastern Palearctic species of *Periclistus* Foerster, 1869

1 Forewing with a small clouded macula posterior to anterior margin near apex of radial cell; radial cell of forewing long, ca 4.0 times as long as wide, and open distally **2**

– Forewing hyaline; radial cell of forewing short, ca 3.0 times as long as wide, and partially closed or closed with inconspicuous submarginal vein **3**

2 Notauli present anteriorly, weakly impressed; and metasoma reddish brown (Distribution: Japan: Honshu, Shikoku and Kyushu) ..... ***P. natalis***

– Notauli absent; and metasoma dark brown (Distribution: Japan: (Honshu, Shikoku and Kyushu) ..... ***P. quinlani***

3 Notauli completely absent. (Distribution: China: Qinghai) ...***P. qinghainensis***
– Notauli present, complete or incomplete **4**
4 Fronts and vertex without fine piliferous punctures; F1 slightly shorter than F2; notauli incomplete, absent to very weakly impressed in anterior 2/3 to 3/4 of scutum. (Distribution: Russia: Primorie (in the Far East) and China: Henan, Shaanxi) ..... ***P. capillatus***
– Fronts and vertex with fine piliferous punctures; F1 is equal to F2 in length; notauli complete **5**
5 Lower face with striae radiating from clypeus not reaching eyes and antennal socket; notauli complete and deeply impressed throughout, narrow anteriorly and relatively broadened posteriorly; lateral surface of pronotum glabrous, with sparse setigerous punctures ventrolaterally. (Distribution: China: Zhejiang, Fujian) ..... ***P. setosus***
– Lower face with striae radiating from clypeus reaching eyes and antennal socket; notauli distinctly present in posterior one third of scutum and medial sulcus absent; lateral surface of pronotum entirely coriaceous with evenly distributed dense setigerous punctures (Fig. 8). (Distribution: China: Hunan).. ..... ***P. orientalis***

Discussion

The Diastrophini tribe consists of gall inducers and inquilines of galls, which are all associated with Rosaceae plants belonging to the supertribe Rosodae (Potter et al. 2007), except for the newly described monotypic genus *Xestophanopsis*, whose biology is not yet known (Pujade-Villar et al. 2019). The major morphological difference between the gall-maker and inquiline genera of the tribe is the lack of any kind of sculpture on upper face, vertex, and mesoscutum in the gall maker genera, a feature also shared by *Xestophanopsis*. The genus *Diastrophus* is unique compared to the other genera of the tribe in having metasomal terga 2 and 3 free in female (Fig. 17), not fused as in the other genera of the tribe while *Xestophanes* differs from all other genera of the tribe by having a rather reduced basal lobe on tarsal claw, rather than a well-developed one (Melika 2006, Ritchie 1984, Pujade-Villar et al. 2019). *Xestophanes* is further separated from *Xestophanopsis* by having eleven flagellomeres in female antenna, rather than having ten as in the latter (Pujade-Villar et al. 2019). On the other hand, the two inquilinous genera, *Synophromorpha* and *Periclistus*, are morphologically very similar. Ritchie and Shorthouse (1987), in their revision of *Synophromorpha*, listed several diagnostic features separating *Periclistus* from the former, including mesoscutum coriaceous; notauli weaker, not percurrent, and not broadened posteriorly or with anterior pits; ventral margin of subalar triangle with row of setigerous punctures; radial cell closed; male A3 usually strongly notched and broadened distally. However, these differences are either hard to define and become less obvious when the eastern Asian *Periclistus* (Fig. 7) species are included in the comparison (Abe 1998). Abe (1998) also mentioned that the

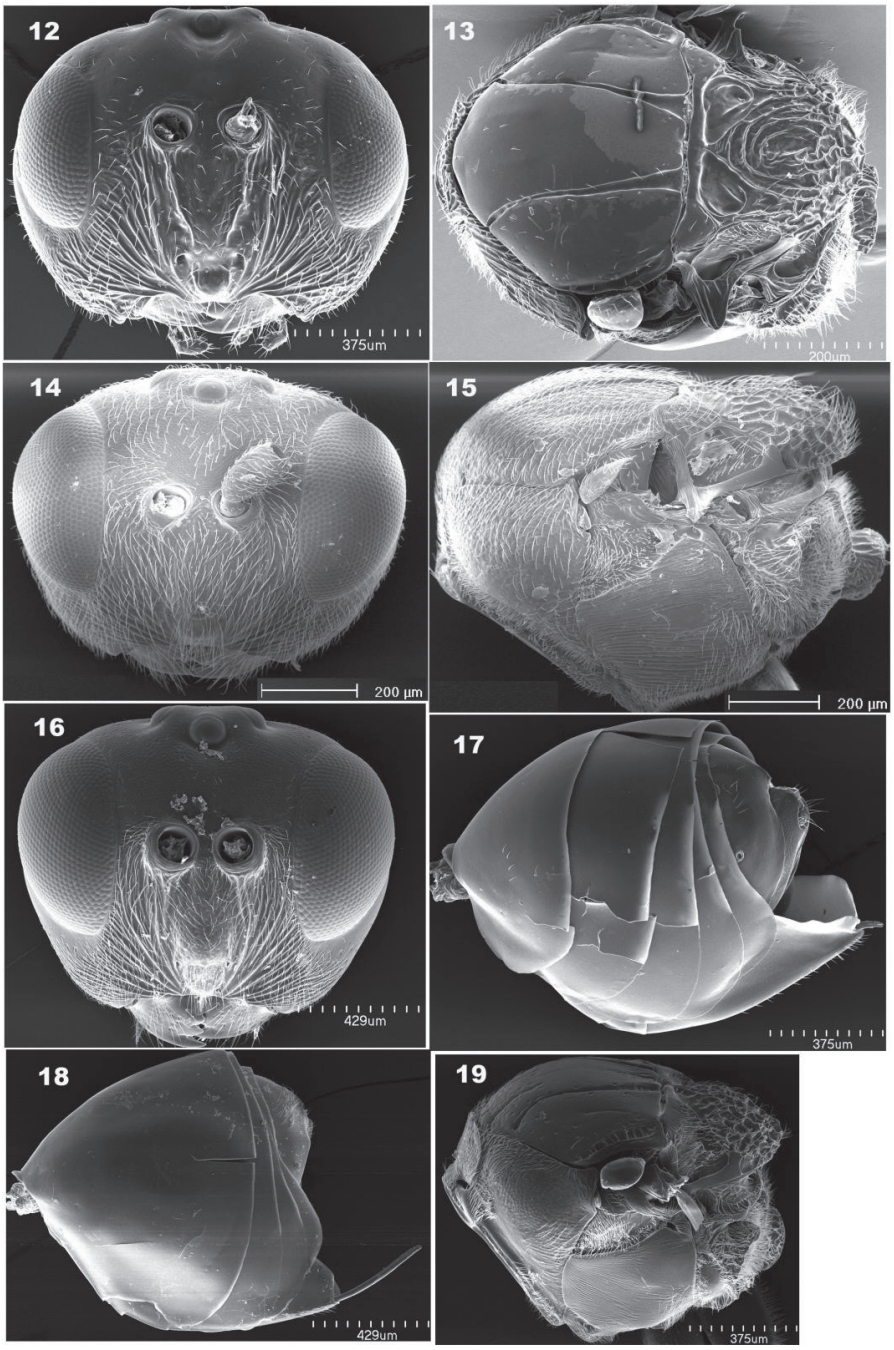

Figures 12–19. SEM images of representative Diastrophini species **12** *Diastrophus nebulosus* head in anterior view (♀) **13** *Diastrophus nebulosus* mesosoma in dorsal view (♀) **14** *Periclistus brandtii* head in anterior view (♀) **15** *Periclistus brandtii* mesosoma in lateral view (♀) **16** *Synophromorpha sylvestris* head in anterior view (♀) **17** *Diastrophus nebulosus* metasoma in lateral view (♀) **18** *Xestophanes potentillae* metasoma in lateral view (♀) **19** *Synophromorpha sylvestris* mesosoma in lateral view (♀).

Figure 20. Galls on *Rosa multiflora*, from which specimens of *Periclistus orientalis* were reared.

two genera differ in how the mesoscutellum extended posteriorly, but we have observed no difference regarding this feature by comparing *P. brandtii* (Fig. 15) and *S. sylvestris* (Fig. 19). Biologically, the two genera have different host plant and host gall associations – all *Synophromorpha* species with known host data are guests in the galls made by *Diastrophus* species on *Rubus* plants (Ritchie and Shorthouse 1987; Abe 1998; Wachi et al. 2013) while all *Periclistus* species with available host data are guests of galls made by *Diplolepis* spp. and *Liebelia* spp. (Diplolepidini, Cynipidae) on *Rosa* plants (Ritchie 1984; Ronquist and Liljeblad 2001; Ronquist et al. 2015; Pujade-Villar et al. 2016). Therefore, it was considered more suitable to retain these two genera as separate despite their close morphological affinity (Abe 1998). Our phylogenetic analysis and genetic distance comparison, although based on limited molecular data available, provide support for this proposition. Phylogenetically the two genera do not form a monophyletic clade (Fig. 21; Ronquist et al. 2015). The pairwise COI sequence distance between *Sy. sylvestris* and *P. pirata*, and *P. orientalis* are 19% and 20%, respectively, which are considerably higher than those between *Sy. sylvestris* and species of the gall making genera of the Diastrophini tribe (Table 2). Furthermore, the two genera seem to be reliably separated morphologically as well, by the general lack of setae and weaker sculpture on head, lateral sides of pronotum, mesoscutum and mesopleuron in *Synophromorpha* (Figs 16, 19) as compared to *Periclistus* (Figs 5–8, 14, 15).

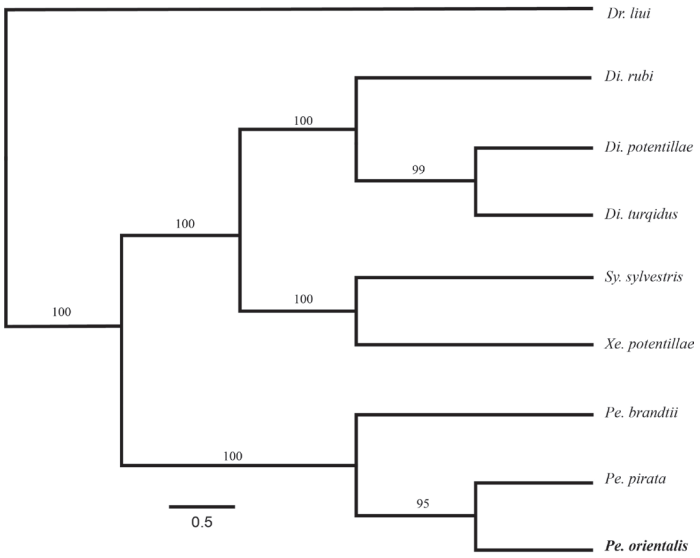

Figure 21. Phylogenetic relationship of Diastrophini species based on COI and 28S sequences resolved using with MrBayes 3.2.6 (Ronquist et al. 2012). Two independent MCMC runs were run with the following parameters: 10 million gens, nst = 6, rates = gamma, sample frequency = 1/1,000, burn-in = 30%, and otherwise default. The length of the branches is drawn to scale of genetic distance and the number over branches is posterior probability. Abbreviations for generic names: *Dr* – *Dryocosmus*, *Di* – *Diastrophus*, *Sy* – *Synophromorpha*, *Xe* – *Xestophanes*, and *Pe* – *Periclistus*.

Table 2. Pair-wise COI sequence distance between four Diastrophinii genera, *Periclistus* (*Pe.*), *Diastrophus* (*Di.*), *Xestophanes* (*Xe.*), and *Synophromorpha* (*Sy.*). *Xestophanopsis* is not included in the comparisons because of lack of data and specimens.

	Di. potentillae	***Di. turgidus***	***Di. rubi***	***Pe. orientalis***	***Pe. pirata***	***Pe. brandtii***	***Sy. sylvestris***	***Xe. potentillae***
Di. potentillae								
Di. turgidus	0.13							
Di. rubi	0.12	0.10						
Pe. orientalis	0.23	0.25	0.22					
Pe. pirata	0.21	0.21	0.19	**0.17**				
Pe. brandtii	0.19	0.21	0.17	**0.15**	**0.12**			
Sy. sylvestris	0.13	0.14	0.11	0.20	0.19	0.14		
Xe. potentillae	0.14	0.09	0.10	0.19	0.17	0.15	0.07	
Dr. liui	0.22	0.22	0.24	0.28	0.24	0.22	0.19	0.18

Key: numbers in bold indicate pairs of congeners of *Periclistus*; numbers in grey block indicate pairs between a *Periclistus* species and a species of another genus.

There exists confusion about the number of valid known species in *Periclistus*, ranging from 14 (Penzes et al. 2012; Pujade-Villar et al. 2016) to 18 (HOL, the Hymenoptera Online database, 2018). Apparently, the latter was uninformed of the fact that several species have been transferred to other genera since the initial descriptions. Below we provide an update of species list for the genus, including the species described and recombination published since Penzes et al. (2012). Information and sources on

detailed distribution, host gall making species, and host plants are found in Ritchie (1984) and summarized in Penzes et al. (2012). *Periclistus idoneus* Belizin, 1973 was subsequently transferred to *Aulacidea* by Pujade-Villar et al. (2016) and thus is not included herein (* denotes synonymy and recombination suggested by Ritchie (1984), NA – Nearctic, PA – Palearctic, and O – Oriental).

1. *P. arefactus* McCracken & Egbert, 1922	NA
2. *P. brandtii* (Ratzeburg, 1831)	PA
3. *P. californicus* Ashmead, 1896	NA
4. *P. caninae* (Hartig, 1840)	PA
5. *P. capillatus* Belizin, 1968	PA
6. *P. mongolicus* Belizin, 1973	PA
7. *P. natalis* Taketani & Yasumatzu, 1973	PA
8. *P. obliquus* Provancher, 1888*	NA
9. *P. orientalis* sp. nov.	O
10. *P. piceus* Fullaway, 1911	NA
11. *P. pirata* (Osten-Sacken, 1863)	NA
12. *P. qinghainensis* Pujade-Villar et al., 2015	EP
13. *P. quinlani* Taketani & Yasumatzu, 1973	PA
14. *P. semipiceus* (Harris, 1841)*	NA
15. *P. smilacis* Ashmead, 1896*	NA

Ritchie (1984), in his dissertation on inquiline Cynipidae, conducted an extensive revision of the genus *Periclistus*, and proposed synonymy and recombination for several species (indicated in the above list with *) in the genus, including the transfer of *P. semipiceus* to *Diplolepis* and *P. obliquus* Provancher to *Eumayria*, and considered *P. smilacis* a junior synonym of *P. pirata*. In addition, six species were also described as new in the dissertation (named by Ritchie and Shorthouse). Unfortunately, the work has not been published and therefore are not considered valid taxonomic changes until future publication.

Within *Periclistus*, the new species is easily grouped together with its congeners from the Eastern Palearctic in that they all have entirely smooth and shiny mesopleuron without striae, mesoscutum smooth and moderately punctate setigerous (Pujade-Villar et al. 2015), suggesting that the Eastern Palearctic species may form a monophyletic lineage, which nonetheless needs to be tested based on formal phylogenetic analysis.

With the inclusion of *P. orientalis* in our analysis based on COI and 28S sequences, the resulting phylogenetic tree (Fig. 21) is consistent with the multiple gene tree of Ronquist et al. (2015) regarding the Diastrophini. In our result, *P. orientalis* as a representative species from the Eastern Palearctic + Oriental is shown to be more closely related to the eastern Nearctic *P. pirata* than with *P. brandtii* from the western Palearctic, which may suggest the Eastern Asia-Eastern North America disjunct distribution frequently observed in flowering plants (Xiang et al. 1998; Wen 1999) and other organismal groups, including insects (Nordlander et al. 1996; Ren et al. 2019). However,

the suggestion should be taken with caution since we only sampled one single species from each region, and future phylogenetic analysis with more dense species sampling is needed to test this hypothesis.

Acknowledgements

The project was supported by a grant from the Forestry Science and Technology Research Project of the State Forestry Administration of China No. 2014-03 (D-H Zhu) and a grant from the National Key Research and Development Program of China (No. 2016YFE0128200) (D-H Zhu).

References

Abe Y (1998) Palaearctic occurrence of the genus Synophromorpha (Hymenoptera: Cynipidae) confirmed on the basis of a new species from Japan. Insect Systematics and Evolution 29: 25–28. https://doi.org/10.1163/187631298X00168

Abe Y, Melika G, Stone GN (2007) The diversity and phylogeography of cynipid gallwasps (Hymenoptera: Cynipidae) of the Oriental and Eastern Palearctic regions, and their associated communities. Oriental Insects 41: 169–212. https://doi.org/10.1080/00305316.2007.10417504

Burks BD (1979) Superfamily Cynipoidea. In: Krombein KV, Hurd Jr PD, Smith DR, Burks BD (Eds) Catalog of Hymenoptera in America North of Mexico (Vol. 1). Symphyta and Apocrita. Smithsonian Institution Press, Washington, 1045–1107.

Csóka G, Stone GN, Melika G (2005) Biology, Ecology and evolution of gall-inducing Cynipidae. In: Raman A, Schaefer CW, Withers TM (Eds) Biology, Ecology and Evolution of Gallinducing Arthropods. Science Publishers, Inc. Enfield. New Hampshire, 569–636.

Dowton M, Austin AD (2001) Simultaneous analysis of 16S, 28S, COI and morphology in the Hymenoptera: Apocrita–evolutionary transitions among parasitic wasps. Biological Journal of the Linnean Society 74(1): 87–111. https://doi.org/10.1111/j.1095-8312.2001.tb01379.x

Folmer O, Black M, Hoeh W, Lutz R, Vrijenhoek R (1994) DNA primers for amplification of mitochondrial cytochrome c oxidase subunit I from diverse metazoan invertebrates. Molecular Marine Biology and Biotechnology 3: 294–299. https://doi.org/10.4028/www.scientific.net/DDF.7.460

Förster A (1869) Ueber die Gallwespen. Verhandlungen der Kaiserlich-Königlichen Zoologisch-Botanischen Gesellschaft in Wien 19: 327–370.

Harris R (1979) A glossary of surface sculpturing. State of California, Department of Food and Agriculture. Occasional Papers in Entomology 28: 1–31.

HOL (2018) Hymenoptera Online (HOL). [Online] https://hol.osu.edu/index.html?id=322955 [accessed 4 December 2018]

Ide T, Kusumi J, Miura K, Abe Y (2018) Gall inducers arose from inquilines: Phylogenetic position of a gall-inducing species and its relatives in the inquiline tribe Synergini (Hyme-

noptera: Cynipidae). Annals of the Entomological Society of America 111: 6–12. https://doi.org/10.1093/aesa/sax065

Kumar S, Stecher G, Tamura K (2016) MEGA7: Molecular Evolutionary Genetics Analysis version 7.0 for bigger datasets. Molecular Biology and Evolution 33: 1870–1874. https://doi.org/10.1093/molbev/msw054

Liljeblad J (2002) Phylogeny and evolution of gall wasps. PhD Thesis, Stockholm University, Sweden.

Liljeblad J, Ronquist F (1998) A phylogenetic analysis of higher-level gall wasp relationships (Hymenoptera:Cynipidae). Systematic Entomology 23: 229–252. https://doi.org/10.1046/j.1365-3113.1998.00053.x

Melika G (2006) Gall Wasps of Ukraine. Cynipidae. – Vestnik zoologii (supplement) 21(1): 1–300.

Nei M, Kumar S (2000) Molecular Evolution and Phylogenetics. Oxford University Press, New York, 333 pp.

Nieves-Aldrey J (1994) Revision of West-European genera of the tribe Aylacini Ashmead (Hymenoptera, Cynipidae). Journal of Hymenoptera Research 3: 175–206.

Nieves-Aldrey J (2001) Hymenoptera, Cynipidae. In: Ramos M, Alba Tercedor J, Bellés i Ros X, Gosálbez i Noguera J, Guerra Sierra A, Macpherson Mayol E, Martín Piera F, Serrano Marino J, Templado González J (Eds) Fauna Ibérica (Vol. 16). Museo Nacional de Ciencias Naturales, CSIC, Madrid, 636 pp.

Nieves-Aldrey, J, Rodriguez P, Medianero E (2013) Description of a new species of *Diastrophus* (Hymenoptera: Cynipidae: "Aylacini") from Colombia: the first herb gall wasp native to the Neotropical region. Annals of the Entomological Society of America 106: 719–728. https://doi.org/10.1603/AN13033

Nordlander G, Liu Z, Ronquist F (1996) Phylogeny and biogeography of the family Ibaliidae (Hymenoptera: Cynipoidea). Systematic Entomology 21: 151–166. https://doi.org/10.1046/j.1365-3113.1996.d01-4.x

Pang Y, Su CY, Zhu DH (2018) Discovery of a new species of *Dryocosmus* Giraud, 1859 (Hymenoptera: Cynipidae: Cynipini) on *Castanopsis tibetana* from China. Zootaxa 4403: 99–110. https://doi.org/10.11646/zootaxa.4403.1.5

Pénzes Zs, Melika G, Bozsoki Z, Bihari P, Mikó I, Tavakoli M, Pujade-Villar J, Fehér B, Fülöp D, Szabó K, Sipos B, Somogyi K, Stone GN (2009) Systematic re-appraisal of the gall-usurping wasp genus *Synophrus Hartig*, 1873 (Hymenoptera: Cynipidae:Synergini). Systematic Entomology 34: 1–25. https://doi.org/10.1111/j.1365-3113.2009.00482.x

Pénzes Zs, Tang CT, Bihari P, Bozsó M, Schwéger S, Melika G (2012) Oak associated inquilines (Hymenoptera, Cynipidae, Synergini). Tiscia Monograph Series 11: 1–66.

Potter D, Eriksson T, Evans RC, Oh S, Smedmark JEE, Morgan DR, Kerr M, Robertson KR, Arsenault M, Dickinson TA, Campbell CS (2007) Phylogeny and classification of Rosaceae. Plant Systematics and Evolution 266(1): 5–43. https://doi.org/10.1007/s00606-007-0539-9

Pujade-Villar J, Melika G (2005) *Synergus castanopsidis* (Beutenmüller, 1918) and Synergus mexicanus Gillette, 1896, two conflictive cynipid inquilines species from America (Hymenoptera, Cynipidae: Synergini). Boletín de la Sociedad Entomológica Aragonesa 37: 215–218.

Pujade-Villar J, Wang YP, Guo R, Chen XX (2016) Revision on Palaearctic species of *Periclistus* Förster with description of a new species and its host plant gall (Hymenoptera, Cynipidae). ZooKeys 596: 65–75. https://doi.org/10.3897/zookeys.596.5945

Pujade-Villar J, Wang Y, Liu Z, Chen X, He J, Ferrer-Suay M (2019) Discovery of *Xestophanopsis* gen. n. from China and taxonomic revision of two species misplaced in *Ceroptres* Hartig, 1840 (Hymenoptera, Cynipoidea: Cynipidae). Entomologica Fennica 30(3): 126–137. https://doi.org/10.33338/ef.84149

Ren Z, von Dohlen CD, Harris AJ, Dikow RB, Su X, Wen J (2019) Congruent phylogenetic relationships of *Melaphidina* aphids (Aphididae: Eriosomatinae: Fordini) according to nuclear and mitochondrial DNA data with taxonomic implications on generic limits. PLoS ONE 14(2): e0213181. https://doi.org/10.1371/journal.pone.0213181

Ritchie AJ (1984) A review of the higher classification of the inquiline gall wasps (Hymenoptera: Cynipidae) and a revision of the Nearctic species of *Periclistus* Forster. Ph.D. dissertation, Carleton University, Ottawa. https://doi.org/10.1016/0005-2744(67)90229-X

Ritchie AJ, Shorthouse JD (1987) Revision of the genus *Synopromorpha* Ashmead (Hymenoptera: Cynipidae). Canadian Entomologist 119: 215–230. https://doi.org/10.4039/Ent119215-3

Rokas A, Nylander JAA, Ronquist F, Stone GN (2002) A maximum likelihood analysis of eight phylogenetic markers in gall wasps (Hymenoptera: Cynipidae); implications for insect phylogenetic studies. Molecular Phylogenetics and Evolution 22: 206–219. https://doi.org/10.1006/mpev.2001.1032

Ronquist F (1994) Evolution of parasitism among closely related species: phylogenetic relationships and the origin of inquilinism in gall wasps (Hymenoptera, Cynipidae). Evolution 48: 241–266. https://doi.org/10.1111/j.1558-5646.1994.tb01310.x

Ronquist F (1995) Phylogeny and early evolution of the Cynipoidea (Hymenoptera). Systematic Entomology 20: 309–335. https://doi.org/10.1111/j.1365-3113.1995.tb00099.x

Ronquist F, Liljeblad J (2001) Evolution of the gall wasp-host plant association. Evolution 55: 2503–2522. https://doi.org/10.1111/j.0014-3820.2001.tb00765.x

Ronquist F, Nieves-Aldrey J, Buffington ML, Liu Z, Liljeblad J, Nylander JAA (2015) Phylogeny, Evolution and Classification of Gall Wasps: the plot thickens. PLoS ONE 10: e0123301. https://doi.org/10.1371/journal.pone.0123301

Ronquist F, Nordlander G (1989) Skeletal morphology of an archaic cynipoid, *Ibalia rufipes* (Hymenoptera: Ibaliidae). Entomologica Scandinavica, Supplementum (Sweden) 33: 1–60.

Ronquist F, Teslenko M, Vander-Mark P, Ayres DL, Darling A, Höhna S, Larget B, Liu L, Suchard MA, Huelsenbeck JP (2012) MrBayes 3.2: efficient Bayesian phylogenetic inference and model choice across a large model space. Systematic Biology 61: 539–542. https://doi.org/10.1093/sysbio/sys029

Schick K, Liu Z, Goldstein P (2003) Phylogeny, historical biogeography, and macroevolution of host use among *Diastrophus* gall wasps (Hymenoptera: Cynipidae). Proceedings of the Entomological Society of Washington 105(3): 715–732.

Schwéger S (2016) Eastern Palearctic oak cynipid inquilines (Hymenoptera: Cynipidae: Synergini) and associated gall wasps (Hymenoptera: Cynipidae: Cynipini). PhD thesis, University of Szeged, Hungary.

Taketani A, Yasumatsu K (1973) Description and some biological notes of two new species of the genus *Periclistus* Förster from Japan. Esakia 8: 1–11.

Thompson JD, Higgins DG, Gibson TJ (1994) CLUSTAL W: improving the sensitivity of progressive multiple sequence alignment through sequence weighting, position-specific gap

penalties and weight matrix choice. Nucleic Acids Research 22: 4673–4680. https://doi.org/10.1093/nar/22.22.4673

Van Noort S, Stone GN, Whitehead VB, Nieves-Aldrey J (2007) Biology of *Rhoophilus loewi* (Hymenoptera: Cynipoidea: Cynipidae), with implications for the evolution of inquilinism in gall wasps. Biological Journal of the Linnean Society 90: 153–172. https://doi.org/10.1111/j.1095-8312.2007.00719.x

Wachi N, Ide T, Abe Y (2011) A new inquiline species of *Saphonecrus* (Hymenoptera: Cynipidae: Synergini) associated with cecidomyiid galls on oak trees in Japan. Annals of the Entomological Society of America 104: 369–373. https://doi.org/10.1603/AN10187

Wachi N, Ide T, Abe Y (2013) Eastern Palearctic occurrence of *Diastrophus* (Hymenoptera: Cynipidae: Aylacini) on *Rubus* bushes, with description of a new species. Annals of the Entomological Society of America 106: 288–293. https://doi.org/10.1603/AN12114

Wang Y, Liu Z, Chen X (2012) Eastern Palaearctic cynipid inquilines–the genus *Ceroptres* Hartig, 1840 with descriptions of two new species (Hymenoptera: Cynipidae: Cynipinae). Annals of the Entomological Society of America 105(3): 377–385. https://doi.org/10.1603/AN11017

Wen J (1999) Evolution of Eastern Asian and Eastern North American Disjunct Distributions in Flowering Plants. Annual Review of Ecology and Systematics 30: 421–455. https://doi.org/10.1146/annurev.ecolsys.30.1.421

Xiang QY, Soltis DE, Soltis PS (1998) The Eastern Asian and Eastern and Western North American floristic disjunction: congruent phylogenetic patterns in seven diverse genera. Molecular Phylogenetics and Evolution 10: 178–190. https://doi.org/10.1006/mpev.1998.0524

Zhu DH, He YY, Fan YS, Ma MY, Peng DL (2007) Negative evidence of parthenogenesis induction by *Wolbachia* in a gall wasp species, *Dryocosmus kuriphilus*. Entomologia Experimentalis and Applicata 124: 279–284. https://doi.org/10.1111/j.1570-7458.2007.00578.x

ZooKeys 964: 127–141 (2020)
doi: 10.3897/zookeys.964.53947
https://zookeys.pensoft.net

RESEARCH ARTICLE

A peer-reviewed open-access journal
ZooKeys
Launched to accelerate biodiversity research

Identification of *Delia* spp. (Robineau-Desvoidy) (Diptera, Anthomyiidae) and its cruciferous hosts in Mexico

Ricardo Meraz-Álvarez[1], Néstor Bautista-Martínez[1], Carlos Patricio Illescas-Riquelme[2], Héctor González-Hernández[1], Jorge Manuel Valdez-Carrasco[1], Jade Savage[3]

1 *Colegio de Postgraduados, Posgrado en Fitosanidad-Entomología y Acarología, Carretera México-Texcoco Km. 36.5, Montecillo, Texcoco 56230, Estado de México, México* **2** *Centro de Investigación en Química Aplicada, Blvd. Enrique Reyna Hermosillo No.140 C.P. 25294 Saltillo, Coahuila, México* **3** *Biological Sciences, Bishop's University, Sherbrooke, Quebec, J1M 1Z7, Canada*

Corresponding author: Néstor Bautista-Martínez (nestor@colpos.mx)

Academic editor: Marc De Meyer | Received 8 May 2020 | Accepted 15 July 2020 | Published 27 August 2020

http://zoobank.org/7FE783A4-DF0F-4AED-A4E6-FD1199B98A7A

Citation: Meraz-Álvarez R, Bautista-Martínez N, Illescas-Riquelme CP, González-Hernández H, Valdez-Carrasco JM, Savage J (2020) Identification of *Delia* spp. (Robineau-Desvoidy) (Diptera, Anthomyiidae) and its cruciferous hosts in Mexico. ZooKeys 964: 127–141. https://doi.org/10.3897/zookeys.964.53947

Abstract

Soil pests of cruciferous crops in Mexico have been gaining importance in recent years; such is the case of *Delia* spp. (Robineau-Desvoidy) (Diptera, Anthomyiidae), of which, to date, there are no studies on the correct identification of associated species, as well as the range of hosts. In an integrated pest management program, it is essential to know this information to design and implement adequate phytosanitary measures. Plants infested by *Delia* spp. were collected in the states of Guanajuato, Puebla, and Mexico from June to November 2017 and March to December 2018 in commercial plantations of cruciferous crops (*Brassica oleracea* L. var. *italica*, *botrytis* and *capitata*), *B. napus* L., and *Raphanus sativus* L.) as well as some cruciferous weeds (*R. raphanistrum* L., *Sisymbrium irio* L., *B. campestris* L., *Capsella bursa-pastoris* L., and *Lepidium virginicum* L.) in the edges of these crops. The two species found in this study, *Delia planipalpis* (Stein) and *Delia platura* (Meigen), identified using male genitalia was corroborated by molecular techniques. Both species emerged from all the sampled hosts, except for *C. bursa-pastoris* and *L. virginicum*. The association of the two species in cruciferous crops and weeds, provides valuable information for the management of these insects not only in cruciferous crops but other ones that are strongly attacked by *D. platura*.

Keywords
Male genitalia, molecular identification, soil pests, root damage, root maggots, weeds, wild hosts

Introduction

The family Anthomyiidae, commonly called root maggots (Huckett 1965), is a large group of flies of the dipteran clade Muscoidea which also includes house flies (Muscidae), latrine flies (Fannidae), and dung flies (Scathophagidae) (Ding et al. 2015; Kutty et al. 2019). The larvae are mainly phytophagous or saprophagous. They have been found in stems, roots, floral heads, and foliage of live plants as well as plants in process of decomposition. Some are scavengers or coprophagous in excrement of birds and other animals. Others are tenants, diners, or parasites in nests of bees, solitary wasps, rodents, and land turtles. They are also found on beaches where they feed on seaweeds and near freshwater ponds, or streams (Huckett 1987; Smith 1989). They can also be omnivorous; certain species are known to be endoparasitoids of grasshoppers and kleptoparasitoids in hymenopteran nests (Suwa 1974; Gilbert and Jervis 1998), and there are predators of simulid larvae (Ackland and Werner 2006).

According to Michelsen (2014), nearly 2 000 species are known worldwide, but undoubtedly there are more waiting to be described (Smith 1989). Although they are distributed the world over, this family is better represented in temperate regions, especially in the Holarctic region. Almost 600 species belonging to 50 to 60 genera are known in the Nearctic region and a similar number is known in the Palaearctic region (Huckett 1987; Smith 1989).

From an economic standpoint, some species are phytophagous and feed on live plant tissues (Hill 1987) of food crops, ornamentals, weeds (Huckett 1987), and forest trees (Suwa 1974; Turgeon and Sweeney 1993). Some family members are significant agricultural pests, particularly those that belong to the genus *Delia* (Robineau-Desvoidy), such as *D. radicum* (Linnaeus), *D. platura* (Meigen), *D. planipalpis* (Stein), *D. florilega* (Zetterstedt), *D. floralis* (Fallén), and *D. antiqua* (Meigen) (Savage et al. 2016). Also included are cereal sprout flies (*D. coarctata* (Fallen), *D. arambourgi* (Seguy), *D. flavibasis* (Stein)) (Macharia and Mueke 1986), and miners (*D. echinata* (Seguy), *D. cardui* (Meigen), and *D. brunnescens* (Zetterstedt)) (Hill 1987). Certain *Delia* species have a relatively small range of hosts. *Delia radicum* and *D. antiqua*, for example, attack only plants of the family Brassicaceae and *Allium* spp., respectively. However, *D. platura* and *D. florilega* have a wide range of hosts including species of Brassicaceae and *Allium* spp. in decomposing process as well as legumes, Cucurbitaceae, and some cereals (Howard 1994). In general, they attack a larger diversity of plant species than their common name indicates (Brooks 1951).

The damage *Delia* spp. cause to vegetables, cereals, ornamentals, and forest species is considerable. An example of this is *D. radicum*, one of the most studied species and considered the primary pest of several crops of the Brassicaceae family in temperate

latitudes (35–60°N) of North America, Europe and Asia (Dixon et al. 2014). In Canada, where most of the provinces raise crucifers such as cabbage, cauliflower, broccoli, and rutabaga (*Brassica napus* var. napobrassica (L.) Rchb.), the problem becomes acute because there are few authorized pesticides, such as diazinon and chlorpyrifos (van Herk et al. 2017). Additionally, resistance to chlorpyrifos is confirmed in areas where rutabaga is cultivated (Blackshaw et al. 2012) and where there are high concentrations of pesticide residue in aquifers (Joseph and Zarate 2015).

In Mexico, 67.7% of the total income from export of produce is earned by 20 crops, among which is broccoli, cultivated mainly in Guanajuato (24 886 ha), Puebla (2 772 ha), and Michoacán (2 225 ha). Mexico is considered the fifth world producer of broccoli and cauliflower (SIAP 2018). In the main crucifer-producing regions, the economically important pests are diamondback moth (*Plutella xylostella* (Linnaeus)) (Lepidoptera, Plutellidae), cabbage looper (*Trichoplusia ni* (Hübner)) (Lepidoptera, Noctuidae), cabbage worm (*Copitarsia decolora* (Guenée)), and cabbage aphid (*Brevicoryne brassicae* (Linnaeus)) (Hemiptera, Aphididae). Contamination by several biological stages of these pests, as well as their excretions, affects the quality or health of the produce. There are also other secondary pests that, if they are not adequately managed, can have a negative impact on yield and quality of the harvest (Barrios-Díaz et al. 2004; Suárez-Vargas et al. 2006; Santoyo-Juárez and Martínez 2011; Bujanos-Muñiz et al. 2013a, 2013b).

In recent years in different regions of the country, major outbreaks of root maggot (*Delia* spp.) have occurred in crucifers. However, the identification of these insects has not been sufficiently supported, and identification has only been to the genus level. There are reports from the state of Guanajuato which mentioned flies of the genus *Hylemia* (= *Delia*) associated with maize and beans, as well as with crucifers (Marín-Jarillo 2001). In the region of Acatzingo, Puebla, in the 2000 spring-summer crop cycle, the pest was detected in a cabbage crop and identified as *Hylemia* sp. (= *Delia*) (Barrios-Díaz et al. 2004).

Because integrated management of any pest requires reliable diagnosis and, given the economic importance, the difficulty of identifying this group of insects and the lack of research to date in the country, this study posed the following objectives: to identify the *Delia* species complex associated with broccoli (*B. oleracea* var. *italica*), cabbage (*B. oleracea* var. *capitata*), and cauliflower (*B. oleracea* var. *botrytis*) crops principally and to determine their range of cruciferous hosts as well as the type of damage they cause.

Materials and methods

Delia species for identification were collected in cultivated and wild crucifers from June 2017 to December 2018 in the states of Guanajuato, Puebla, and Mexico. The crops included in the collections were broccoli (*B. oleracea* var. *italica*), cabbage (*B. oleracea* var. *capitata*), and cauliflower (*B. oleracea* var. *botrytis*), as well as turnip (*B. napus* L.), radish (*Raphanus sativus* L.), and other wild crucifers such as wild radish (*Raphanus*

raphanistrum L.), field mustard (*Brassica campestris* L.), London rocket (*Sisymbrium irio* L.), shepherd's purse (*Capsella bursa-pastoris* L.), and Virginia pepperweed (*Lepidium virginicum* L.) For the cultivated crucifers, 10–15 plants with symptoms of wilting were selected in each lot, as well as less developed contiguous plants and some apparently health plants. Wild crucifer plants were selected at random within and on the outer edges of commercial crops; these plants generally did not show wilting symptoms, and the sample size varied from 5 to 20 plants, depending on their abundance in the crop as a consequence of weed control. The plants on which *Delia* larvae were detected were extracted intact together with the soil adhered to the roots. Later, all the plants collected from the same farm were grouped and placed into 2–3 L plastic bags and labeled with locality, date, and host, separating cultivated from wild hosts. The age of the crops from which infested material was collected ranged from 20 to 70 days after transplant to the field. In the case of wild crucifers, the specimens collected ranged in maturity from seedlings to plants with flowers and seeds. The material was transported to the Laboratory of Agricultural Entomology of the Colegio de Postgraduados, Campus Montecillo, Texcoco, State of Mexico, and confined. The samples were kept in a rearing chamber at a temperature of 26±2 °C, 60±20% relative humidity, and photoperiod of 12:12 (light:dark) until adult emergence. As the adults emerged, they were separated by sex and morphotype for each sample.

Species identification

Morphological identification of the specimens (including the traits of the male genitalia) was conducted in the Laboratory of Agricultural Entomology of the Colegio de Postgraduados, Campus Montecillo. The keys and illustrations by Darvas and Szappanos (2003) and Savage et al. (2016) were used to differentiate sexes and to identify species; the distance between the eyes (holoptic males and dichoptic females) and the chaetotaxy of the hind femur were used. Images were taken with a Photomicroscope III Carl Zeiss (Carl Zeiss, Germany). To confirm the identity of the collected species, DNA barcodes (Hebert et al. 2003) were used. DNA was extracted from the mitochondrial gene of the cytochrome c oxidase subunit I (COI) (Folmer et al. 1994) of 25 adult specimens (19 males and six females) and amplified. The sequences of this material can be consulted in Barcode of Life Data System (BOLD) (http://www.barcodinglife.org) in the public database *Delia* of Mexico (https://doi.org/10.5883/ds-domex) and all sequences were deposited in GenBank (accession numbers MT888006–MT888030). The sequences of at least 550 base pairs were grouped using the BOLD aligner. Intraspecific and interspecific distances were calculated in BOLD using the distance model Kimura 2 parameters (K2P) (Kimura 1980).

The specimens are deposited in the National Center for Phytosanitary Reference, Division of Plant Health, SENASICA, Tecámac, State of Mexico. Adult and larval specimens were also provided to the entomological collection of the Colegio de Postgraduados, Campus Montecillo. Moreover, the specimens used for molecular identification are in the insect collection of Bishop's University, Quebec, Canada.

Results

Tables 1 and 2 show the number of emerged adults in each of the samples collected in cultivated and wild cruciferous, respectively. *Delia planipalpis* and *D. platura* emerged from both cultivated and wild hosts. The number of adults of *D. planipalpis* was greater than *D. platura* in 89% and 88% of the cases, respectively. Both species emerged from all the hosts except from *C. bursa-pastoris* and *L. virginicum* where no damage from larvae of *Delia* spp. was observed when these were collected.

Discussion

The specimens were identified as *Delia planipalpis* (Stein) and *Delia platura* (Meigen) (Fig. 1) using male genitalia as the principal reference since they are the fundamental identification tool for species of the family Anthomyiidae (Darvas and Szappanos 2003). The extracted male genitalia of *D. planipalpis* and *D. platura* male genitalia are similar to those illustrated by Wang et al. (2014), Savage et al. (2016), and Darvas and Szappanos (2003). In addition, there are morphological differences that are highly useful in separating these two species. In the terminalia of *D. planipalpis*, the short, armored cercus with radially arranged setae does not extend beyond the tip of the surstylus, whose arms are thinner at the basal and apical parts than in the middle. The setae of the epandrium are short and sparse. In contrast, the cercus in *D. platura* is elongated and oval, with numerous setae directed toward the front and upward; in length the setae can reach the tip or extend beyond the tip of the surstylus arms, and extend approximately to mid-length of the surstylus between the arms, which tend to be narrower at the apex and have short setae on the lateral margins. In *D. planipalpis* abdominal sternite V lacks the pair of setae at the apex of each of the arms, as in *D. platura* (Fig. 2).

The results of the DNA barcodes were congruent with the morphology and also indicated that all the specimens sequenced for *D. platura* belong to BOLD:AAA3453, one of the two different barcode index numbers (BIN) for this species. This population is found almost exclusively in the New World (Savage et al. 2016). The material of each species formed a compact cluster in the phylogenetic tree (Fig. 3), with each belonging to a different BIN (Ratnasingham and Hebert 2013). The greatest interspecific distance was 10.49% and the greatest intraspecific distance was 0.34% for *D. planipalpis* and 0% for *D. platura*.

This is the first report of species-level identifications of *Delia* in commercial crucifer crops and wild hosts in Mexico. It is supported by images of adult male genitalia and corroborated by COI gene sequence data. However, there are also external morphological traits that are very useful for initial diagnosis, such as the array of setae along the hind femurs of males and females (Savage et al. 2016) and chaetotaxy in general. Nevertheless, identification based solely on chaetotaxy has generally not been sufficient and is often the cause of confusion in the literature;

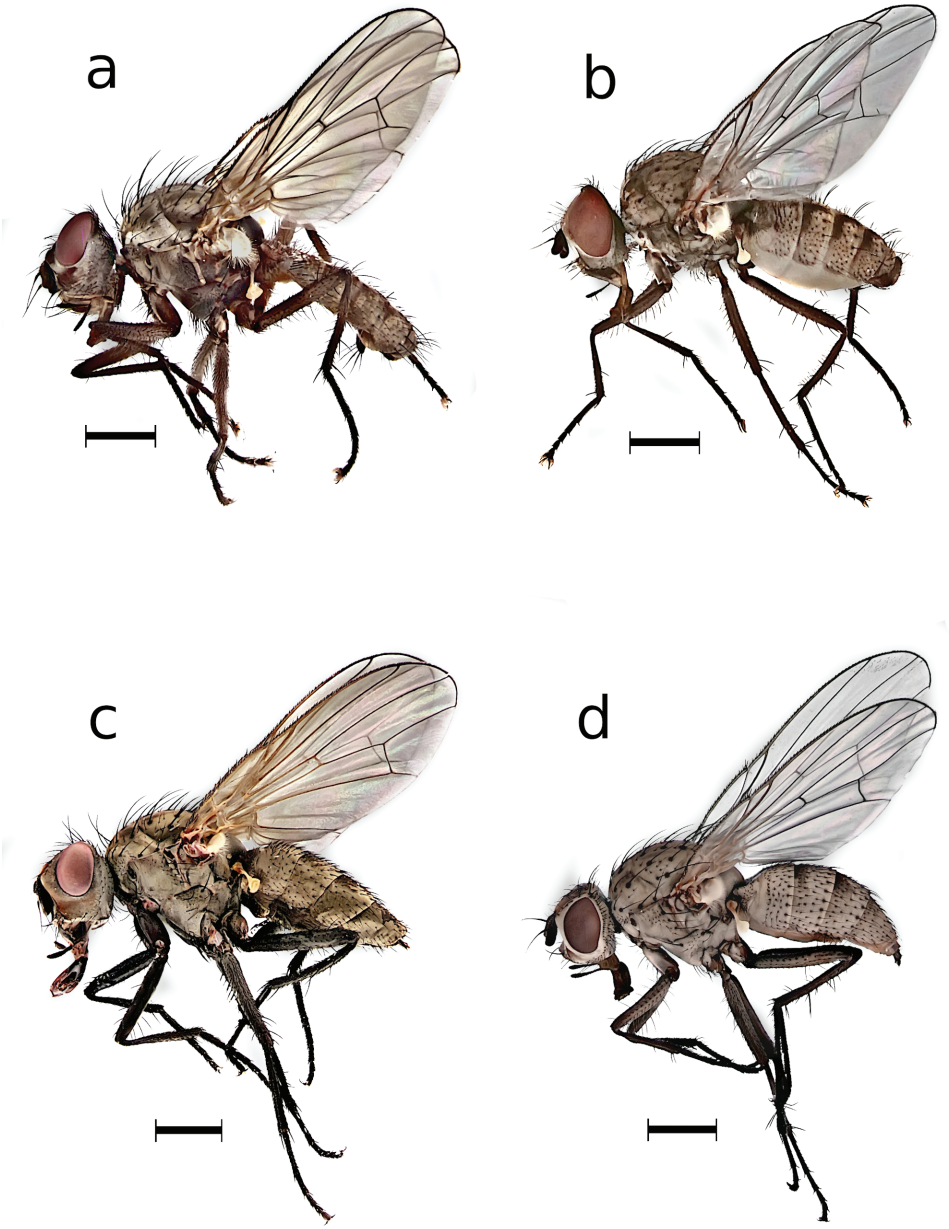

Figure 1. a male *Delia planipalpis* **b** male *Delia platura* **c** female *Delia planipalpis* **d** female *Delia platura*. Scale bars: 1 mm.

there are many questionable records (Darvas and Szappanos 2003). It is possible to separate the two species identified here because all their biological stages exhibit morphological differences, unlike other species whose immature states are morphologically indistinguishable. For example, in some regions, *D. planipalpis* is confused with *D. radicum*, and *D. platura* is confused with *D. florilega* (Savage et al. 2016),

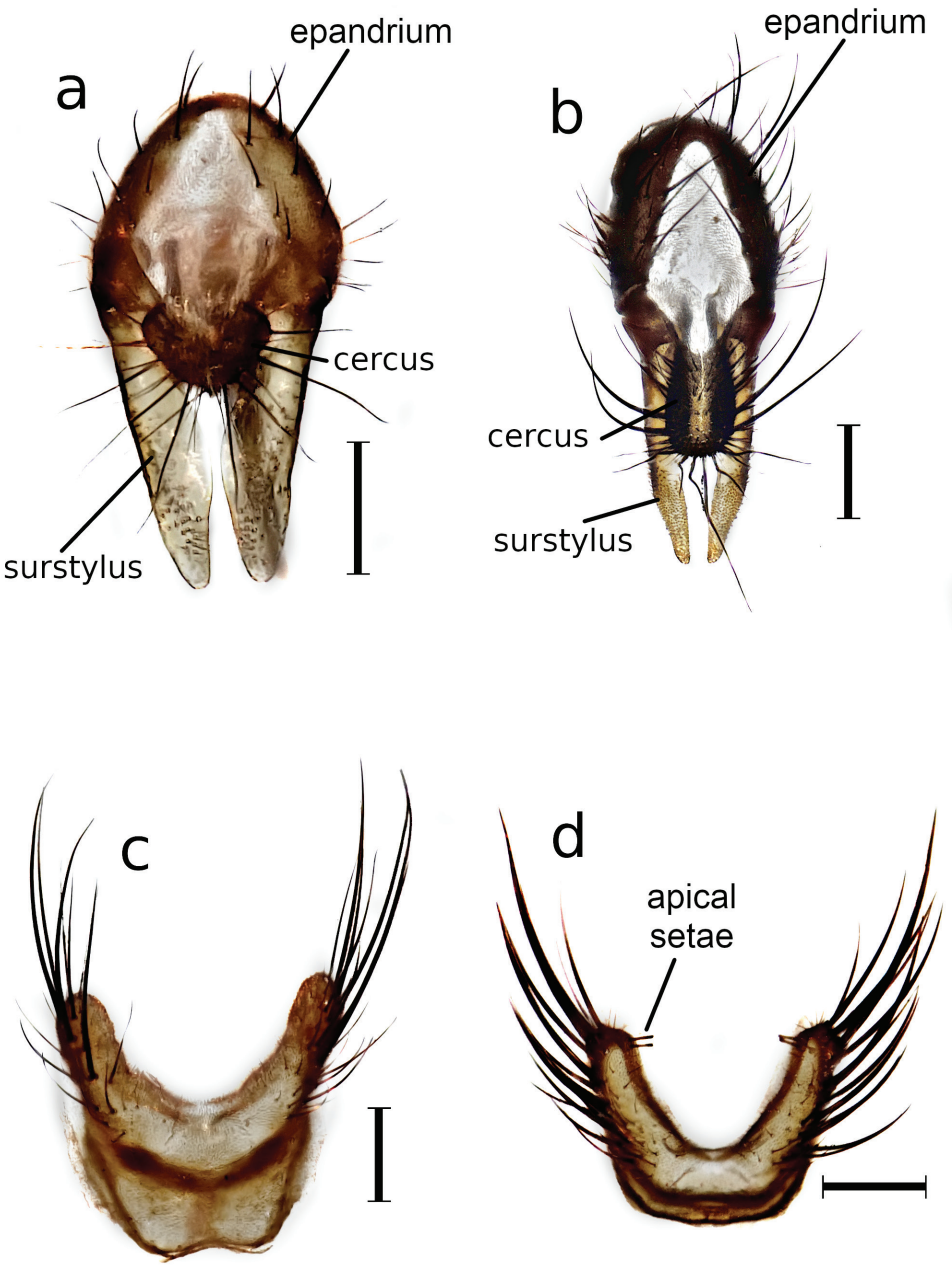

Figure 2. Male genitalia. **a** terminalia of *Delia planipalpis* **b** terminalia of *D. platura* **c** abdominal sternite V of *D. planipalpis* **d** abdominal sternite V of *D. platura*. Scale bars: 200 nm.

and thus, the presence of one species might be overlooked because of a mistaken identification. In general, the family Anthomyiidae is considered a taxonomically complex insect group because the traits used to differentiate sexes and species are not always constant (Colyer and Hammond 1968).

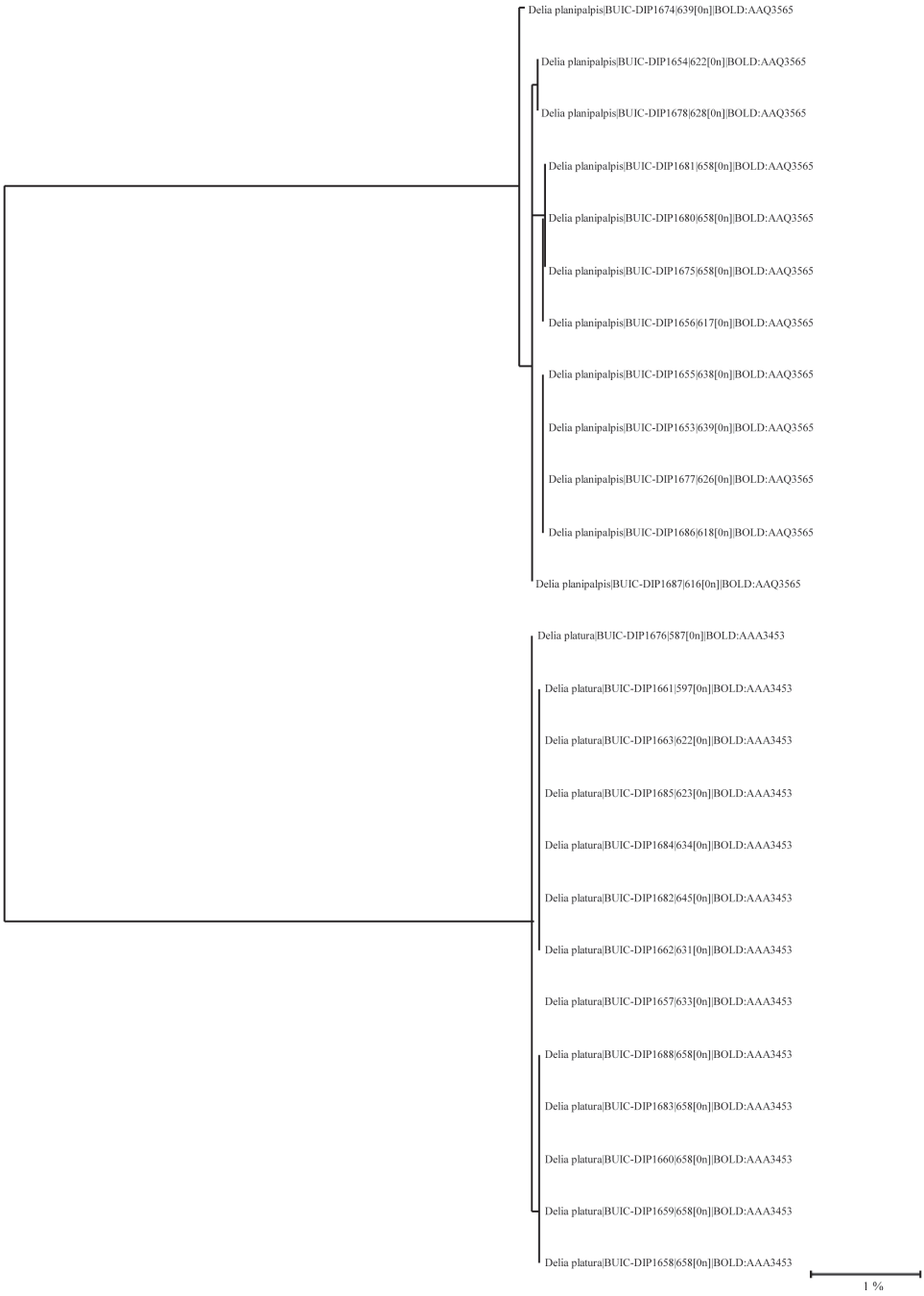

Figure 3. Phylogenetic tree (based on the K2P distance model) for 25 COI sequences (minimum 550 bpm, 0 bp ambiguous) of *Delia* specimens. The line includes species name, sample identification by BOLD, sex, and barcode index number (BIN).

For this reason, it is understandable that little or no research on this insect group has been done in Mexico; even the most common *Delia* pest is difficult to identify without adequate training. Furthermore, the challenge becomes greater when dealing with females or immature specimens that lack the characteristics for diagnosis (Savage et al. 2016). Females cannot be identified without an appropriate key (Darvas and Szappanos 2003). Finally, few people work with this type of pest, which results in national collections with vague identifications and a scarcity of well-preserved specimens that could contribute to the knowledge of their distribution, hosts, and dates of appearance, among other data.

Delia planipalpis and *D. platura* emerged in both cultivated (Table 1) and only from wild (Table 2) hosts *R. raphanistrum*, *B. campestris*, and *S. irio*. This coincides with information presented by Savage et al. (2016), who mentioned that *D. platura* is generally found in infestations together with other species of *Delia* and their association depends on the host. For example, in bean seed in Canada, it is associated with the seed-infesting fly *D. florilega*. In our study, more *D. planipalpis* adults emerged than *D. platura* in cultivated (Table 1) and wild (Table 2) crucifers; *D. planipalpis* is

Table 1. Number of *Delia planipalpis* and *D. platura* adults emerged in cultivated crucifers.

Collection site	Crop	*Delia planipalpis*			*Delia platura*			Collection date
		♀♀	♂♂	Total	♀♀	♂♂	Total	
San Felipe Tenextepec, Tepeaca, Puebla 19°01'39.80"N, 97°52'12.28"W	Cauliflower	3	5	8	2	1	3	31-V-2017
	Broccoli	1	2	3	1	3	4	
	Broccoli	16	12	28	0	0	0	25-VIII-2017
	Turnip	15	9	24	1	0	1	13-IV-2018
	Broccoli	4	1	5	0	0	0	12-VII-2018
	Broccoli	4	9	13	0	0	0	8-XI-2018
San Mateo Parra, Tepeaca, Puebla 18°59'35.98"N, 97°51'43.20"W	Broccoli	2	2	4	1	0	1	12-VII-2017
Guadalupe Calderón, Tepeaca, Puebla 18°57'27.35"N, 97°50'43.51"W	Cauliflower	0	3	3	0	1	1	12-VII-2017
Acatzingo, Puebla 18°58'30.72"N, 97°47'53.55"W	Cabbage	2	4	6	3	0	3	12-VII-2017
		25	17	42	11	15	26	18-X-2017
		0	0	0	2	4	6	13-IV-2018
Tepeaca, Puebla 19°00'04.9"N, 97°53'12.8"W	Cabbage	5	7	12	0	0	0	29-IX-2018
	Cabbage	12	12	24	0	2	2	22-XI-2018
Los Reyes, Tepeaca, Puebla 18°57'27.18"N, 97°50'50.24"W	Radish	19	35	54	1	1	2	6-XII-2018
Montecillo, Texcoco, Estado de México 19°28'10"N, 98°54'00.81"W	Radish	1	0	1	0	0	0	27-IV-2018
	Radish	4	2	6	3	1	4	11-V-2018
	Radish	5	3	8	3	2	5	19-V-2018
Dolores Hidalgo, Guanajuato 21°09'52"N, 100°57'18"W	Broccoli	4	3	7	1	0	1	8-V-2018
San Luis de la Paz Guanajuato 21°19'23"N, 100°33'22"W	Broccoli	6	4	10	2	1	3	6-IV-2018
San Diego de la Unión, Guanajuato 21°24'30.4"N, 100°45'19.3"W	Broccoli	7	4	11	1	1	2	25-X-2018
	Broccoli	13	11	24	0	0	0	4-XII-2018

Table 2. Number of *Delia planipalpis* and *D. platura* adults emerged in wild crucifers.

Collection site	Host	*Delia planipalpis*			*Delia platura*			Collection date
		♀♀	♂♂	Total	♀♀	♂♂	Total	
Acatzingo, Puebla 18°58'30.72"N, 97°47'53.55"W	*R. raphanistrum*	2	1	3	0	0	0	12-VII-2017
	S. irio	3	1	4	0	1	1	12-VII-2017
	R. raphanistrum	21	20	41	0	1	1	22-XI-2018
San Felipe Tenextepec, Puebla 19°01'39.80"N, 97°52'12.28"W	*R. raphanistrum*	0	0	0	1	2	3	12-VII-2017
	R. raphanistrum	20	37	57	2	6	8	8-XI-18
Los Reyes, Tepeaca, Puebla 18°57'27.18"N, 97°50'50.24"W	*R. raphanistrum*	21	23	44	0	0	0	6-XII-2018
Montecillo, Texcoco, Estado de México 19°28'10"N, 98°54'00.81"W	*R. raphanistrum*	3	1	4	11	8	19	26-III-2018
	C. bursa-pastoris	0	0	0	0	0	0	26-III-2018
	S. irio	5	3	8	1	3	4	29-III-2018
	B. campestris	7	2	9	0	0	0	29-III-2018
	R. raphanistrum	3	5	8	1	2	3	1-IV-2018
	L.virginicum	0	0	0	0	0	0	1-IV-2018
	B. campestris	1	0	1	1	0	1	3-IV-2018
	C. bursa-pastoris	0	0	0	0	0	0	1-IV-2018
	L. virginicum	0	0	0	0	0	0	1-IV-2018
	S. irio	2	5	7	0	0	0	11-IV-2018
	R. raphanistrum	0	0	0	1	0	1	16-IV-2018
	B. campestris	17	10	27	2	1	3	27-IV-2018
	S. irio	1	2	3	2	0	2	6-V-2018
	S. irio	0	2	2	0	0	0	6-V-2018
	R. raphanistrum	6	7	13	0	0	0	20-X-2018
	C. bursa-pastoris	0	0	0	0	0	0	20-X-2018
	L. virginicum	0	0	0	0	0	0	20-X-2018

catalogued as a phytophagous species that mainly attacks radish (Kelleher 1958), unlike *D. platura* that is phytophagous only under certain circumstances causing damage to roots and often appears in small numbers in conjunction with other phytophagous species (Brooks 1951). In this respect, combined infestations have been reported of *D. platura*/*D. antiqua* (Finlayson 1956) and *D. platura*/*D. florilega* (Savage et al. 2016) in onion. Finch (1989) mentions that *D. platura* is not a primary species and only invades seeds when the seed coat has been infested by pathogens before germinating.

Damage

Female *Delia* spp. oviposit at the base of the plant stem and in the surrounding soil. Once the larva emerges, it feeds on external tissue of the stem before penetrating it or the basal leaves. The level of damage caused by *Delia* spp. larvae is in function of plant age: between 10 and 30 days after transplant, the damaged plants exhibit symptoms similar to those caused by water deficit (Fig. 4a, b), and they may die or have delayed growth with consequentially poor-quality inflorescence. *Delia* spp. larvae in *B. oleracea* (var. *italica*, *capitata*, and *botrytis*) crops are generally found at the base of the plant feeding on the root crown, damaging the main stem and the root system and causing the plant's death or notably delaying its growth. Moreover, galleries resulting from larva feeding can be seen in the main

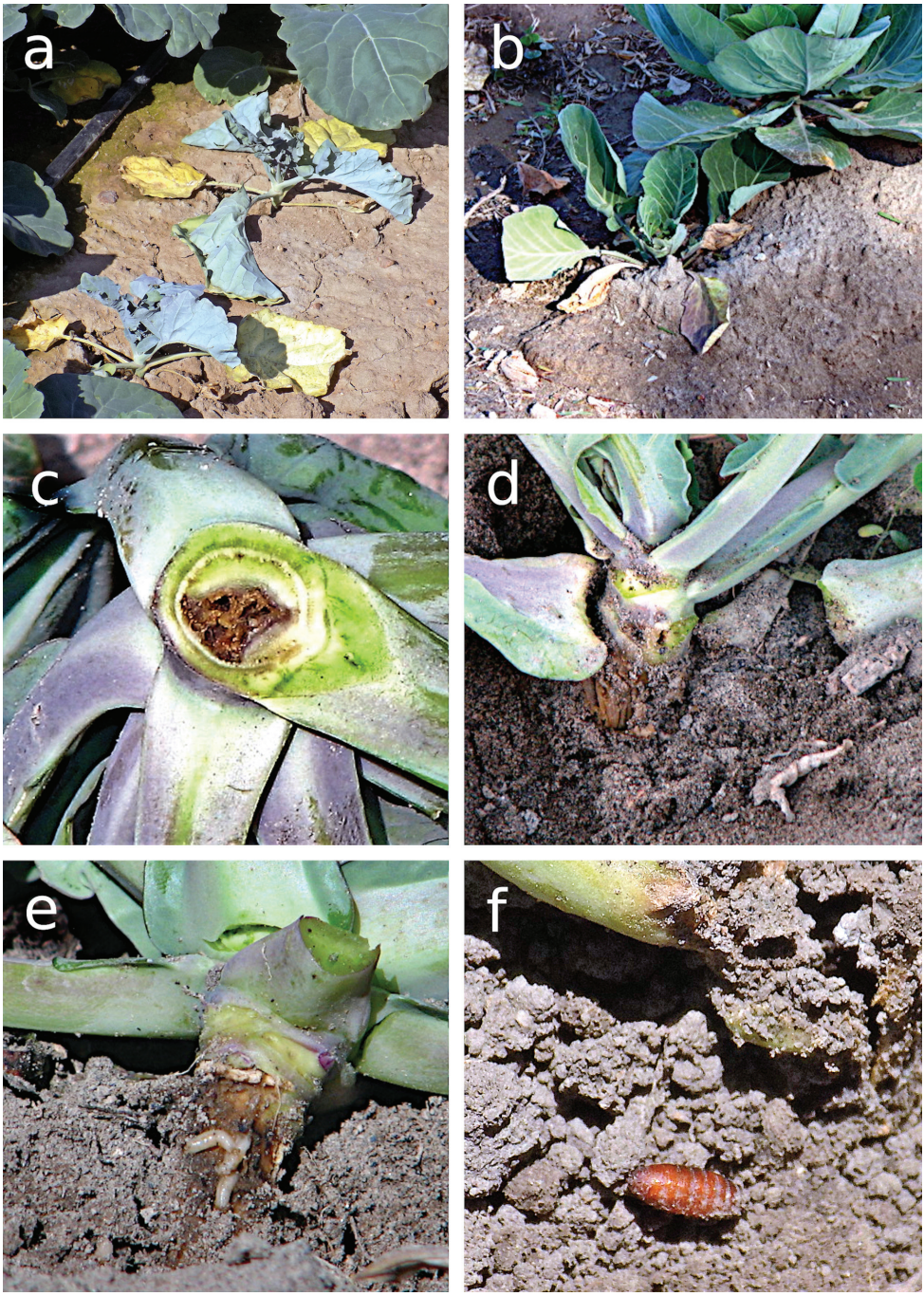

Figure 4. Damage caused by *Delia planipalpis* and *D. platura*. **a** broccoli plants damaged by *Delia* spp. larvae **b** cabbage plant with yellow wilted basal leaves **c** main stem of a cabbage plant with galleries **d** cabbage plant with holes where larvae exited **e** *Delia* spp. larvae feeding superficially on the stem of a cabbage plant **f** *Delia* spp. pupa at the site where plant was extracted.

stem as well as orifices through which third instar larvae exit to pupate in the soil (Fig. 4c, d). Pupae can be observed at the site where the attacked plant is extracted (Fig. 4f) and in the substrate adhered to the roots. Older plants, more than 30 days after transplant, can tolerate the damage caused by feeding larvae, reflecting plant vigor. According to Wheatley and Finch (1984), crops that grow vigorously can bear large populations without showing symptoms, although attacked plants will be smaller, and the quality of the final product will be poorer. This occurs when *Delia* spp. larvae feed superficially on the external tissues of the main stem (Fig. 4e) and penetrate basal leaves, which become yellow and wilted (Fig. 4b).

In a broccoli field nearing harvest time, damage caused by third instar *D. planipalpis* larvae was observed at the base of the upper stratum leaves, very close to the floret. With this damage, the leaves will fall off, and under conditions of high relative humidity, other insects and saprophagous organisms enter.

Another type of damage caused in radish and turnip is the formation of galleries in the edible part. It is common that the damage in these hosts begins in the plant core and continues into the harvestable part. Although this type of damage does not generally cause plant death, the produce is not suitable for commercial sale. Death of radish plants occurs when infestations are high, or the plants are still small.

During field observations, we were able to confirm the presence of adult *D. planipalpis* and *D. platura* on the edges of the crop fields. However, this is not necessarily indicative of significant damage to the crop caused by larvae. Savage et al. (2016) mention that some *Delia* species can be highly abundant as adults, but they are rarely involved in crop damage. In a cabbage field close to harvest we observed adults on the periphery of the crop; they likely came from neighboring crucifer crops and wild crucifers of the area. These observations coincide with Hawkes (1972), who reported that adult *Erioischia brassicae* (Bouché) (= *Delia radicum* L.), once they locate the crop, remain on the edges during the morning and in the afternoon move into the crop to oviposit and finally return to the edges of the crop at sunset.

Conclusions

Two species of *Delia* were identified, *Delia planipalpis* and *D. platura*, which were found associated with broccoli (*B. oleracea* var. *italica*), cabbage (*B. oleracea* var. *capitata*), and cauliflower (*B. oleracea* var. *botrytis*), as well as in radish (*R. sativus*) and turnip (*B. napus*). The extent of damage caused by *Delia* spp. larvae depends on plant age and crop type. For example, in *B. oleracea*, *Delia* spp. can cause plant death, delay growth, or make the produce unfit for commercialization because of damage caused to the harvestable part, as also for *R. sativus* and *B. napus*.

Delia planipalpis and *D. platura* larvae generally feed on the same plant and pupate in the soil near the plant root or in the same germination substrate that remains adhered to the roots. In the wild crucifers *R. raphanistrum*, *B. campestris*, and *S. irio*, which are alternate hosts, it is also common to find both *Delia* species feeding on the same plant. However, they do not cause plant death, even in the seedling stage.

Given the field observations, it is likely that *D. planipalpis* is the species that first invades healthy plants and, as damage by the feeding larvae progresses, *D. platura* is later attracted by the volatiles emitted by the plant. Nevertheless, study is needed to determine the possible volatile compounds emitted during decomposition of plant tissue caused as by the feeding of *D. planipalpis* larvae and to identify the moment when *D. platura* arrives. This kind of basic information is useful to design specific phytosanitary measures to control *D. planipalpis*, not only on cruciferous crops, but even on other crops that are strongly attacked by *D. platura* in some regions of Mexico.

References

Ackland DM, Werner D (2006) Description of a new species of *Alliopsis* Schnabl & Dziedzicki (Diptera, Anthomyiidae) from Armenia and Georgia that is predaceous on black fly larvae (Diptera, Simuliidae). Zoology in the Middle East 39: 81–88. https://doi.org/10.1080/09397140.2006.10638186

Barrios-Díaz B, Alatorre-Rosas R, Bautista-Martínez, Calyecac-Cortero GH (2004) Identificación y fluctuación poblacional de plagas de col (*Brassica oleracea* var. *Capitata*) y sus enemigos naturales en Acatzingo, Puebla. Agrociencia 38: 239–248.

Blackshaw, RP, Vernon RS, Prasad R (2012) Reduction of *Delia radicum* attack in field brassicas using a vertical barrier. Entomologia Experimentalis et Applicata 144: 145–156. https://doi.org/10.1111/j.1570-7458.2012.01271.x

Brooks AR (1951) Identification of the root maggots (Diptera: Anthomyiidae) attacking cruciferous garden crops in Canada, with notes on biology and control. The Canadian Entomologist 83: 109–120. https://doi.org/10.4039/Ent83109-5

Bujanos-Muñiz R, Marín-Jarillo JA, Díaz-Espino LF, Herrera-Vega R (2013a) Control de plagas del cultivo de brócoli en la región del Bajío, México: el cuadro básico de recomendación de insecticidas. SAGARPA, INIFAP, Centro de Investigación Regional Centro. Campo Experimental Bajío. Guanajuato, México, 26 pp.

Bujanos-Muñiz R, Marín-Jarillo JA, Díaz-Espino LF, Gámez-Vázquez AJ, Ávila-Perches MA, Herrera-Vega R, Dorantes-González JRA, Gámez-Vázquez FP (2013b) Manejo integrado de la palomilla dorso de diamante *Plutella xylostella* en la región del Bajío, México. SAGARPA, INIFAP, Centro de Investigación Regional Centro. Campo Experimental Bajío, Guanajuato, 40 pp.

Colyer CN, Hammond CO (1968) Flies of the British Isles. Warne, London/New York, 383 pp.

Darvas B, Szappanos A (2003) Male and female morphology of some central European *Delia* (Anthomyiidae) pests. Acta Zoologica Academiae Scientiarum Hungaricae 49: 87–101.

Ding S, Li X, Wang N, Cameron SL, Mao M, Wang Y, Xi Y, Yang D (2015) The phylogeny and evolutionary timescale of Muscoidea (Diptera: Brachycera: Calyptratae) inferred from mitochondrial genomes. PLoS ONE 10 (7): e0134170. https://doi.org/10.1371/journal.pone.0134170

Dixon P, Cass L, Vincent C, Olfert O (2014) Implementation and adoption of integrated pest management in Canada: Insects. In: Peshin R, Pimentel D (Eds) Integrated Pest Man-

agement: Experiences with Implementation. Springer, Dordrecht, 221–252. https://doi.org/10.1007/978-94-007-7802-3_9

Finch S (1989) Ecological considerations in the management of *Delia* pest species in vegetable crops. Annual. Review of Entomology 34: 117–137. https://doi.org/10.1146/annurev.en.34.010189.001001

Finlayson DG (1956) Maggots and puparia in stems and seed balls of onions at harvest. Journal of Economic Entomology 49: 460–462. https://doi.org/10.1093/jee/49.4.460

Folmer O, Black M, Hoeh W, Lutz R, Vrijenhoek R (1994) DNA primers for amplification of mitochondrial cytochrome c oxidase subunit I from diverse metazoan invertebrates. Molecular Marine Biology and Biotechnology 3: 294–299.

Gilbert F, Jervis M (1998) Functional, evolutionary and ecological aspects of feeding-related mouthpart specializations in parasitoid flies. Biological Journal of the Linnean Society 63: 495–535. https://doi.org/10.1111/j.1095-8312.1998.tb00327.x

Hawkes C (1972) The diurnal periodicity and cycle of behaviour of the adult cabbage root fly (*Erioischia brassicae*). Annals of Applied Biology 70: 109–118. https://doi.org/10.1111/j.1744-7348.1972.tb04695.x

Hebert PD, Cywinska A, Ball SL, deWaard JR (2003) Biological identifications through DNA barcodes. Proccedings of the Royal Society B: Biological Sciences 270: 313–321. https://doi.org/10.1098/rspb.2002.2218

Hill DS (1987) Agricultural Insect Pests of Temperate Regions and their Control. Cambridge University Press, Cambridge/London, 659 pp.

Howard R, Garland JA, Seaman WL (1994) Disease and Pests of vegetable Crops in Canada. An Illustrated compendium. The Canadian Phytopathological Society and yhe Entomological Society of Canada, Ottawa, 1021 pp.

Huckett HC (1965) The Muscidae of Northern Canada, Alaska, and Greenland (Diptera). Memoirs of the Entomological Society of Canada Vol. 97: 1–369. https://doi.org/10.4039/entm9742fv

Huckett HC (1987) Anthomyiidae. In: McAlpine JF, Peterson BV, Shewell GE, Teskey HJ, Vockeroth DM (Eds) Manual of Neartic Diptera Vol. 2. Monograph No. 28. Research Branch, Agriculture Canada, Ottawa, 1099–1114.

Joseph SV, Zarate J (2015) Comparing efficacy of insecticides against cabbage maggot (Diptera: Anthomyiidae) in the laboratory. Crop Protection 77: 148–156. https://doi.org/10.1016/j.cropro.2015.07.022

Kelleher JS (1958) Life-history and ecology of *Hylemya planipalpis* (Stein) (Diptera: Anthomyiidae), a root maggot attacking radish in Manitoba. The Canadian Entomologist 90: 675–680. https://doi.org/10.4039/Ent90675-11

Kimura M (1980) A simple method for estimating evolutionary rate of base substitutions through comparative studies of nucleotide sequences. Journal of Molecular Evolution 16: 111–120. https://doi.org/10.1007/BF01731581

Kutty SN, Meusemannb K, Baylesse KM, Marinho MAT, Pont AC, Zhou X, Misof B, Wiegmann BM, Yeates D, Cerretti P, Meier R, Pape T (2019) Phylogenomic analysis of Calyptratae: resolving the phylogenetic relationships within a major radiation of Diptera. Cladistics 35: 605–622. https://doi.org/10.1111/cla.12375

Macharia M, Mueke JM (1986) Resistance of barley varieties to barley fly *Delia flavibasis* Stein (Diptera: Anthomyiidae). International Journal of Tropical Insect Science 7: 75–77. https://doi.org/10.1017/S1742758400003143

Marín-Jarillo JA (2001) Insectos plagas de maíz. Guía para su identificación. SAGARPA. INIFAP. Campo experimental Bajío. Folleto técnico No. 1. Celaya, Guanajuato, México, 29 pp.

Michelsen V (2014) Checklist of the family Anthomyiidae (Diptera) of Finland. ZooKeys 441: 369–382. https://doi.org/10.3897/zookeys.441.7527

Ratnasingham S, Hebert PDN (2013) A DNA-based registry for all animal species: the Barcode Index Number (BIN) System. PLoS ONE 8: e66213. https://doi.org/10.1371/journal.pone.0066213

Santoyo-Juárez JA, Martínez-Alvarado CO (2011) Tecnología de producción de brócoli. Fundación Produce Sinaloa A. C. SAGARPA, Gobierno del Estado de Sinaloa, México, 29 pp.

Savage J, Fortier AM, Fournier F, Bellavance V (2016) Identification of *Delia* pest species (Diptera: Anthomyiidae) in cultivated crucifers and other vegetable crops in Canada. Canadian Journal of Arthropod Identification 29: 1–40.

SIAP (2018) Servicio de Información Agroalimentaria y Pesquera. https://www.gob.mx/siap/acciones-y-programas/produccion-agricola-33119 [Accessed on: 2019-7-19]

Smith KGV (1989) An introduction to the immature stages of British flies: Diptera larvae, with notes on eggs, puparia and pupae. Handbooks for the Identification of British Insects. Royal Entomological Society 10: 1–280.

Suárez-Vargas AD, Bautista-Martínez N, Valdez-Carrasco J, Angulo-Ormeño A, Alatorre-Rosas R, Vera-Graziano J, Equihua-Martínez A, Pinto VM (2006) Fluctuación poblacional de *Copitarsia decolora* (Gueéne) y su asociación con crucíferas comerciales. Agrociencia 40: 501–509.

Turgeon JJ, Sweeney JD (1993) Hosts and distribution of spruce cone maggots (*Strobilomyia* spp.) (Diptera: Anthomyiidae) and first record of *Strobilomyia appalachensis* Michelsen in Canada. The Canadian Entomologist 125: 637–642. https://doi.org/10.4039/Ent125637-4

Suwa M (1974) Anthomyiidae of Japan (Diptera). Insecta Matsumurana 4: 1–247.

van Herk WG, Vernon RS, Waterer DR, Tolman JH, Lafontaine PJ, Prasad RP (2017) Field evaluation of insecticides for control of cabbage maggot (Diptera: Anthomyiidae) in rutabaga in Canada. Journal of Economic Entomology 110: 177–185. https://doi.org/10.1093/jee/tow238

Wang QK, Yang YZ, Liu MQ, Zhang D (2014) Fine structure of *Delia platura* (Meigen) (Diptera: Anthomyiidae) revealed by scanning electron microscopy. Microscopy Research and Technique 77: 619–630. https://doi.org/10.1002/jemt.22380

Wheatley GA, Finch S (1984) Effects of oilseed rape on the status of insect pests of vegetable brassicas. In: Proceedings of the British Crop Protection Conference-Pests and Diseases 2: 807–814.

ZooKeys 964: 143–159 (2020)
doi: 10.3897/zookeys.964.55703
https://zookeys.pensoft.net

RESEARCH ARTICLE

A peer-reviewed open-access journal
ZooKeys
Launched to accelerate biodiversity research

Revision of *Nagiella* Munroe (Lepidoptera, Crambidae), with the description of a new species from China

Xiao-Qiang Lu[1], Xi-Cui Du[1]

1 *College of Plant Protection, Southwest University, Chongqing, China*

Corresponding author: Xi-Cui Du (duxicui@hotmail.com)

Academic editor: Colin Plant | Received 22 June 2020 | Accepted 4 August 2020 | Published 27 August 2020

http://zoobank.org/CB14C568-5B55-487E-94A3-AE980C2E839B

Citation: Lu X-Q, Du X-C (2020) Revision of *Nagiella* Munroe (Lepidoptera, Crambidae), with the description of a new species from China. ZooKeys 964: 143–159. https://doi.org/10.3897/zookeys.964.55703

Abstract

The genus *Nagiella* was studied using morphological and DNA barcode data. *Nagiella bispina* **sp. nov.** is described as a new species, and *N. hortulatoides* Munroe is recorded in China for the first time. The diagnosis of this genus is revised, and the genitalia description of *N. quadrimaculalis* (Kollar and Redtenbacher) and *N. inferior* (Hampson) are given in English for the first time. *Nosophora incomitata* (Swinhoe) **stat. rev.** is removed from the synonym of *N. quadrimaculalis*. Photographs of the habitus and genitalia as well as COI DNA Barcode data of these four species are provided.

Keywords

DNA barcodes, Maximum Likelihood analysis, morphology, Pyraloidea, Spilomelinae

Introduction

Nagiella Munroe, 1976 is the objective replacement name of *Nagia* Walker, 1866, with *N. desmialis* Walker, 1866 as the type species. Swinhoe (1894) described two species of *Nagia* and mentioned that *Nagia quadrimaculalis* (Kollar & Redtenbacher, 1844) = *Nagia desmialis*. However, Hampson (1899) regarded *Nagia* as a synonym of *Syllepte* Hübner, 1823 and his opinion was followed by some researchers (Shibuya 1928, 1929; Klima 1931, 1939a). Munroe (1976) proposed that *Nagiella* and *Syllepte* were different in genitalia and type of maculation and mentioned that the type species, *N. desmialis*,

was generally considered a synonym of *Scopula quadrimaculalis*. Munroe's opinion was followed by some researchers (Kirti and Sodhi 2001; Rose 2002; Ullah et al. 2017). In addition, *Nagiella* was regarded as a synonym of *Pleuroptya* Meyrick, 1890 (= *Patania* Moore, 1888) (Kirpichnikova 1987; Leraut 1997), and *Scopula quadrimaculalis* and *Sylepta inferior* were placed in *Pleuroptya* for a long time (Inoue 1982; Wang and Speidel 2000; Bae et al. 2008; Du 2009; Heppner 2012; Sasaki and Yamanaka 2013). Ullah et al. (2017) regarded *Nagiella* as a valid genus and published one cryptic species of it. Mally et al. (2019) placed *Nagiella* in Agroterini Acloque, 1897 based on morphological characteristics.

To date, four species of *Nagiella* have been identified worldwide, and they have been recorded in the Palaearctic and Oriental realms. These species are all distributed in China, with *N. hortulatoides* Munroe, 1976 being recorded in China for the first time in this study. *Nagiella inferior* and *N. quadrimaculalis* are widely distributed in the Palaearctic and Oriental realms (Wang 1980; Inoue 1982; Bae et al. 2008; Du 2009; Sasaki and Yamanaka 2013), with the latter species also recorded from Central Africa (Ghesquière 1942). In addition to China, *N. hortulatoides* is distributed in Myanmar. *Nagiella occultalis* Misbah & Yang in Ullah et al. 2017 is only distributed in China (Ullah et al. 2017). In this study, one new species, *Nagiella bispina*, is described based on morphological and DNA barcode data, and the diagnosis of this genus is revised.

Materials and methods

Taxon sampling

The specimens were collected by light trap at night and killed by ethyl acetate or ammonium hydroxide. The specimens are deposited in the College of Plant Protection, Southwest University, Chongqing, China (SWUCPP) and the Institute of Zoology, Chinese Academy of Sciences, Beijing (IOZ). Information on the specimens from which the DNA Barcode region of the COI gene was sequenced is shown in Table 1. In total, 24 sequences were analysed in this study, with eight being from the BOLD database (Ratnasingham and Hebert 2007; http://v4.boldsystems.org/). The sequences obtained from our laboratory have been uploaded to BOLD.

Genitalia preparation mainly follows Li and Zheng (1996). Images of the adults were captured with a digital camera (Nikon P7700), and images of the genitalia were captured with a digital camera (Leica DFC 450) attached to a digital microscope (Leica M205 A).

DNA extraction, PCR amplification, and sequencing

In total, all five species of *Nagiella* were included for PCR analysis and DNA sequencing (Table 1). Total DNA from legs of fresh or dry specimens was extracted using the TIANGEN DNA Kit following the manufacturer's instructions, and the 658-base pair (bp) barcode region of COI was amplified using the LepF1/LepR1 primers (Hajiba-

Table 1. Sample information for the *Nagiella* and outgroup specimens included in the study.

Species	Sequence ID	Location (China)	BOLD Accession NO. er
N. hortulatoides Munroe, 1976	LXQ180100	Yunnan	DULU001-19
	LXQ180099	Yunnan	DULU002-19
	LXQ180217	Yunnan	DULU003-19
N. inferior (Hampson, 1899)	LXQ180251	Hubei	DULU004-19
	LXQ180127	Yunnan	DULU005-19
	Pyr000509	Shanxi	CNPYD509-10
	Pyr000508	Shanxi	CNPYD508-10
N. quadrimaculalis (Kollar & Redtenbacher, 1844)	XD1405327	Sichuan	GBMIN79565-17
	XD1402131	Hainan	DULU006-19
	XD1402129	Hubei	DULU007-19
	Pyr002264	Shaanxi	CNPYB413-16
	Pyr002266	Shaanxi	CNPYB415-16
	Pyr000498	Hubei	CNPYD498-10
N. occultalis Misbah & Yang in Ullah et al. 2017	Pyr002290	Shaanxi	CNPYB439-16
	Pyr002397	Shaanxi	CNPYB407-16
	Pyr000499	Hubei	CNPYD499-10
N. bispina sp. nov.	LXQ180091	Guangdong	DULU008-19
	LXQ180092	Guangdong	DULU009-19
Patania balteata (Fabricius, 1798)	XD1405399	Sichuan	GBGL38467-19
	XD1405300	Sichuan	GBMIN79548-17
	XD1405441	Sichuan	GBGL38468-19
P. chlorophanta (Butler, 1878)	XD1404265	Guangxi	GBMIN79550-17
	XD1404239	Guangxi	GBMIN79549-17
	XD1401035	Guangxi	GBMIN79551-17

baei et al. 2006). PCR products were sent to Sangon Biotechnology Co., Ltd. (Shanghai, China) for sequencing using the aforementioned primers.

Data analysis

All COI sequences were aligned by MEGA 7.0 (Kumar et al. 2016) and adjusted visually after being translated into amino acid sequences. Intraspecific and interspecific genetic divergence values were quantified based on the Kimura 2-parameter (K2P) distance model (Kimura 1980). Phylogenetic analysis was performed based on Maximum Likelihood (ML) with the GTR GAMMA model of nucleotide substitution, and with 1000 bootstrap replicates (Stamatakis et al. 2008). *Patania balteata* and *P. chlorophanta* were chosen as the outgroup species as they were members of the same tribe (Agroterini), but not congeneric with *Nagiella*.

Results

DNA sequence analysis

Overall, 24 COI sequences, including six of the outgroup species, were analysed. The dataset contained no obvious pseudogenes, indicating the correct target gene sequence was amplified and sequenced.

Five monophyletic clades for *Nagiella* were observed in the resulting phylogenetic tree (Fig. 1). The pairwise genetic distances within and between these lineages are given in Table 2. The average intraspecific genetic distance ranged from 0.00 to 0.02%, while the average interspecific genetic distance ranged from 3.30 to 9.46%. The maximum intraspecific COI genetic distance was much less than the minimum interspecific distance. The monophyla observed in the phylogenetic analysis were in full congruence with our morphological hypotheses for the investigated species (Fig. 1).

Taxonomy

Nagiella Munroe, 1976

Nagia Walker, 1866: 1320 (preocc.). Type species: *Nagia desmialis* Walker, 1866, by monotypy.

Nagiella Munroe, 1976: 876. Type species: *Nagia desmialis* Walker, 1866, by monotypy (of *Nagia* Walker, 1866).

Diagnosis. Frons rounded. Labial palpus broad, obliquely upturned and curved, compressed, third joint extremely minute, short and stout (Fig. 2). Male antenna with ventral cilia. Legs smooth. Fore wings near rectangular at the tips; length of cell ap-

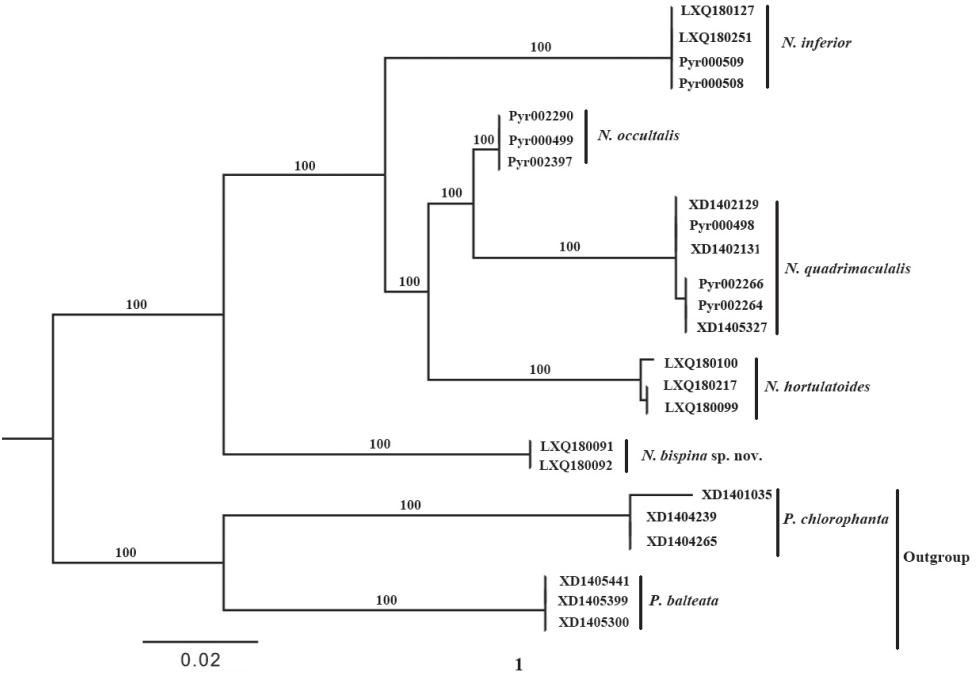

Figure 1. Phylogenetic hypothesis of relationships among five species of *Nagiella* inferred from a Maximum likelihood (ML) analysis of the DNA barcode data, with *Patania balteata* and *P. chlorophanta* as outgroup species.

Table 2. Kimura 2-parameter genetic distances in percent, calculated within (in bold) and between species of *Nagiella*.

	1	2	3	4	5
1 *N. hortulatoides* (*N* = 3)	**0.20**				
2 *N. inferior* (*N* = 4)	6.87	**0.00**			
3 *N. quadrimaculalis* (*N* = 6)	4.87	6.68	**0.09**		
4 *N. occultalis* (*N* = 3)	4.00	5.16	3.30	**0.00**	
5 *N. bispina* sp. nov. (*N* = 2)	8.95	9.46	8.80	7.57	**0.00**

proximately half of wing; R from cell at approximately two-thirds; Rs_2 anastomosed with Rs_3 approximately three-fifths beyond cell; Rs_1 closely approximated to Rs_2+Rs_3; Rs_4 curved towards Rs_2+Rs_3 at base; discocellulars arcuately incurved; M_2, M_3 and CuA_1 from posterior angle of the cell uniformly at the base; CuA_2 from three-fourths below the cell. Hindwing with length of cell one-third of wing; Sc+R anastomosed with Rs approximately one-fourth beyond the cell; M_2, M_3 and CuA_1 separately from posterior angle of the cell; CuA_2 from two-thirds below the cell; discocellulars incurved (Fig. 3). Male genitalia: Uncus short and wide; gnathos present in most species; valva lingulate, posterior margin with long setae cluster in most species; clasper near base, developed and pointed to sacculus; phallus cylindrical, cornuti absent in most species. Female genitalia: Apophyses anteriores longer than apophyses posteriores, rhomboidally expanded near base; ductus seminalis from the ductus bursae; corpus bursae oval, with signum.

Remarks. According to Munroe (1976) and Ullah et al. (2017), *Nagiella* can be differentiated from its similar genera by its short and wide uncus, developed gnathos, broader valva with stout setae subapically, large oblique clasper and absence of cornuti, as well as by the type of wing maculation. In *N. bispina* sp. nov., however, the gnathos is absent, the valva costa has no stout setae, and cornuti are present. Other morphological and DNA barcode data of this new species indicate it as a member of the genus. Therefore, the diagnosis of *Nagiella* was revised based on previous studies and our research, including supplementation of the wing venation.

Key to species of *Nagiella* based on morphology and genitalia

1 Wings white, forewing with discoidal spot round .....***N. hortulatoides***
– Wings brown, forewing with discoidal spot squarish.....**2**
2 Gnathos absent, phallus with a hook-shaped cornutus....***N. bispina* sp. nov.**
– Gnathos present, phallus without cornutus.....**3**
3 Uncus with setae on distal half; gnathos stubby, finger-like or tuberculiform .....***N. inferior***
– Uncus without setae; gnathos slender, finger-like **4**
4 Forewing with white spot between orbicular spot and discoidal spot proportionally narrowed or elongate; uncus with distal margin slightly concave.....***N. occultalis***
– Forewing with white spot between orbicular spot and discoidal spot nearly square or rectangular; uncus with distal margin truncate...***N. quadrimaculalis***

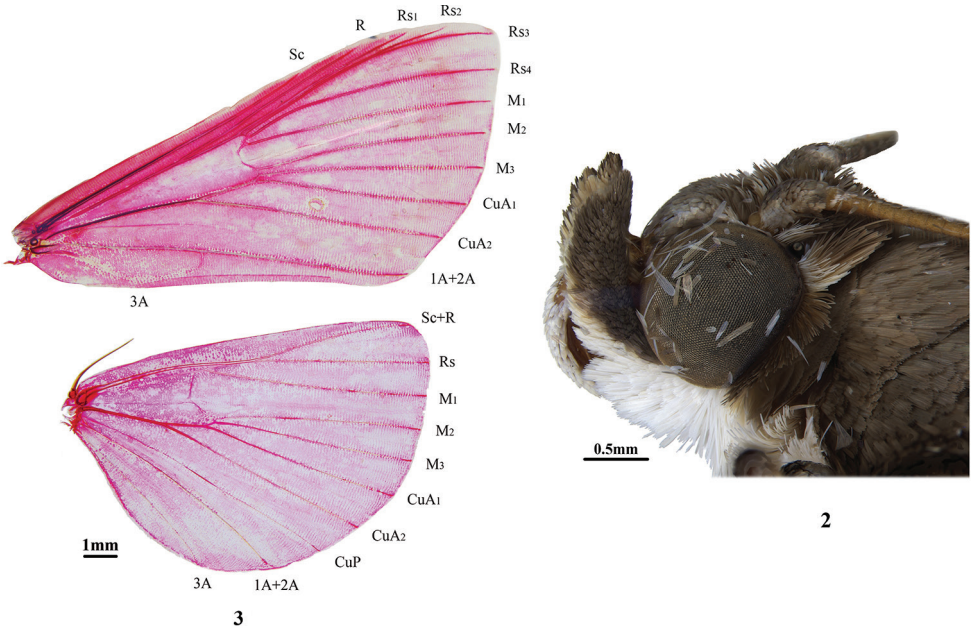

Figures 2, 3. Head and wing venation of *Nagiella quadrimaculalis* (Kollar & Redtenbacher, 1844). Wing slide no. LXQ20001, male.

Nagiella hortulatoides Munroe, 1976

Figures 4, 9

Nagiella hortulatoides Munroe, 1976: 876, figs 2, 14, 19.

Material examined. China, Yunnan: 10 ♂♂, Honghe Prefecture, Huanglian Mountain, 900 m, 27.V.2018, leg. Xiao-Qiang Lu & Xi-Cui Du. Genitalia slide no.: LXQ18170 ♂, LXQ18187 ♂, LXQ18311 ♂.

Diagnosis. Adult (Fig. 4): Frons, palpi, basal antenna, most of vertex black. Thorax orange with blackish-fuscous spot. Wings white, light orange at base, maculation grey, with terminal line white, discontinuous. Forewing with orbicular spot and discoidal spot round, a large elongate elliptical spot from base to orbicular spot below cell; grey terminal area broad, with inside concave between M_1 and CuA_2. Hindwing with discoidal spot round; grey terminal area broad, with inside slightly concave between M_2 and CuA_2. Abdomen with first and second segment orange with three black spots, the rest grey. Male genitalia (Fig. 9): Uncus trapezoidal. Gnathos slender, finger-like. Valve elongate lingulate, posterior margin with clusters of long setae near middle and terminal, clasper thickly finger-like. Female genitalia: Corpus bursae with a round signum (Munroe 1976).

Distribution. China (Yunnan), Myanmar (Munroe 1976).

Remarks. This species is recorded for the first time in China.

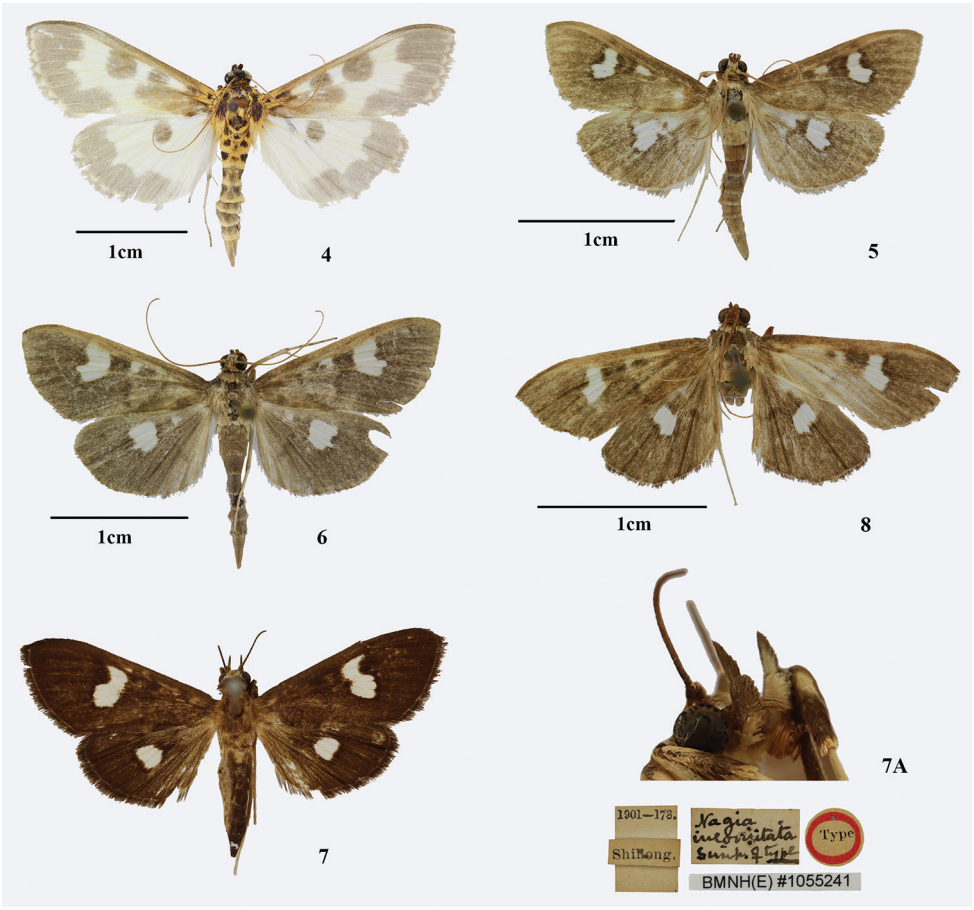

Figures 4–8. Habitus of *Nagiella* species **4** *N. hortulatoides* male **5** *N. inferior* male **6** *N. quadrimaculalis* male **7** *Nagia incomitata* Swinhoe 1894 female, type, BMNH Pyr., London. **7A** head **8** *Nagiella bispina* sp. nov. male, holotype.

Nagiella inferior (Hampson, 1899)

Figures 5, 10, 13

Sylepta [sic] *inferior* Hampson, 1899: 724.
Botys quadrimaculalis Motschulsky, 1861: 37.
Nagiella inferior: Munroe, 1976: 876.
Pleuroptya inferior: Inoue, 1982: 343.

Material examined. China, Liaoning: Huanren County, Laotuding, 28.VII.2012, leg. Dan-Dan Zhang & Li-Jun Yang (SYSU); Gansu: 1 ♂, Kangxian County, Baiyun Mountain, 1200 m, 3.VII.2018, leg. Xiao-Qiang Lu & Xi-Cui Du; Shanxi: 1 ♂, Jincheng

City, Manghe, 725 m, 28.VI.2018, leg. Xiao-Qiang Lu & Xi-Cui Du; Shaanxi: Ningxia County, Xunyangba Town, 1400 m, 4.VIII.2014, leg. Jiu-Yang Luo & Kai-Li Liu; 3 ♂♂, Taibai County, Huangbaiyuan Town, 1200 m, 19.VIII.2014, leg. Kai-Li Liu; 6 ♂♂, 1 ♀, Baojilong County, 900 m, 6.VII.2018, leg. Xiao-Qiang Lu & Xi-Cui Du; Hubei: 15 ♂♂, Dabie Mountain, Taohua Village, 590 m, 25–28.VI.2014, leg. Li-Jun Xu; 2 ♂♂, Xiangyang City, Maqian Town, 1100 m, 19.VI.2018, leg. Xiao-Qiang Lu & Xi-Cui Du; Zhejiang: 1 ♂, Jiulong Mountain, 50 m, 4.VIII.2011, leg. Xiao-Bing Fu; 9 ♂♂, Tianmu Mountain Nature Reserve, 400 m, 25–28.VII.2011, leg. Xi-Cui Du & Xiao-Bing Fu; 4 ♂♂, Qingliangfeng Nature Reserve, 300 m, 18–22.V.2012, leg. Xiao-Bing Fu**;** Tibet: Motuo County, Didong Village, 840 m, 15.VIII.2006, leg. Fu-Qiang Chen (IOZ); Chongqing: 1 ♂ Jingfoshan Nature Reserve, 679 m, 15.IX.2018, leg. Xi-Cui Du; 1 ♂, Hechuan Farm, 230 m, 3.VII.2009, leg. Xi-Cui Du; 6 ♂♂, Chengkou County, Dongan Village, xingtian Village, 1300 m, 26.VI.2013, leg. Gui-Qing He & Li-Jun Xu; Sichaun: 4 ♂♂, Tongjiang County, Nuoshui River Scenic Area, 700 m, 5.VII.2013, leg. Gui-Qing He & Dan Xu; 1 ♂, Nanjiang County, Guangwu Mountain, 900 m, 10.VII.2013, leg. Gui-Qing He & Li-Jun Xu; 1 ♂, 2 ♀♀, Huagaoxi Nature Reserve, Guandou Village, 763 m, 11.X.2014, leg. Li-Jun Xu & Dan Xu; Guizhou: 1 ♂, Kuankuoshui, Baishao, 800 m, 12.VIII.2010, leg. Xi-Cui Du; 1 ♂, Maolan Nature Reserve, Lanei Village, 806 m, 24.VII.2015, leg. Dan Xu; Yunnan: 2 ♂♂, Honghe Prefecture, Ma'andi, 1300 m, 14.V.2015, leg. Xue-Li Wei; 2 ♂♂, Xishuangbannadaizu Prefecture, Menglun Town, 620 m, 17.V.2018, leg. Xiao-Qiang Lu & Xi-Cui Du; Guangxi: 1 ♂, Longzhou, Nonggang, 188 m, 26.VII.2011, leg. Gui-Qing He; 1 ♂, Jingxiu, Shengtang Mountain, 600 m, 28.VIII. 2011, leg. Li-Yang Jun; 1 ♂, Jinzhong Mountain, Miaozhai, 1450 m, 31.VII.2014, leg. Xue-Li Wei & Chao Ran; 3 ♂♂, Cenwanglaoshan, Longdaping, 1290 m, 10.VIII.2014, leg. Xue-Li Wei & Chao Ran; 1♂, Hechi, Jiuwanshan, 1600 m, 23.VII.2015, leg. Ji-Ping Wan; Hainan: Wuzhi Mountain, 795 m, 20.V.2014, leg. Li-Jun Xu & Xu Dan. Genitalia slide no.: XLJ13114 ♂, XLJ14053 ♂, XLJ14219 ♂, LXQ18284 ♂, LXQ18291 ♂, LXQ18303 ♂, XLJ14220 ♀, XLJ14239 ♀.

Diagnosis. Adult (Fig. 5): Wings brown. Forewing length 10.0–12.5 mm (wingspan 22.0–28.0 mm); a small white spot between the orbicular spot and discoidal spot; a large white subreniform spot between the discoidal spot and postmedial line, up to Rs_2+Rs_3 and down to CuA_1; antemedial and postmedial line unclear. Hindwing with a large white irregular quadrilateral spot between the discoidal spot and postmedial line, dentated between M_2 and M_3. Male genitalia (Fig. 10): Uncus trapezoidal, distal half with setae. Gnathos stubby, fingerlike or tuberculiform. Clasper thin, fingerlike. Female genitalia (Fig. 13): Signum round, very small.

Male genitalia (Fig. 10). Uncus trapezoidal, slightly concave terminally, distal half with setae. Gnathos stubby, finger-like or tubercle-like. Valva elongate lingulate, slightly narrowed, terminal with a crowd of long setae, posterior margin with a cluster of long setae near the middle and slightly concave distally; clasper thin, finger-like, constricted near middle. Saccus conical, broad. Juxta semi-circular. Phallus longitudinally wrinkled distally.

Female genitalia (Fig. 13). Apophyses anteriores ca. twice the length of apophyses posteriores. Ductus bursae ca. twice the length of corpus bursae; ductus seminalis from the middle of ductus bursae. Corpus bursae oval, with a very small leaflike signum.

Distribution. China (Liaoning, Gansu, Shanxi, Shaanxi, Henan, Hubei, Zhejiang, Jiangsu, Jiangxi, Tibet, Sichuan, Chongqing, Guizhou, Yunnan, Guangdong, Guangxi, Hainan, Fujian, Taiwan), Korea, Japan, India, Russia (far east) (Hampson 1899; Inoue 1982; Du 2009).

Nagiella quadrimaculalis (Kollar & Redtenbacher, 1844)

Figures 6, 11, 14

Scopula quadrimaculalis Kollar & Redtenbacher, 1844: 492.
Nagia desmialis Walker, 1866: 1320.
Omiodes quadrimaculalis: Meyrick, 1890: 441.
Botys quadrimaculalis: Snellen, 1890: 589.
Sylepta [sic] *quadrimaculalis*: Hampson, 1896: 336.
Sylepta [sic] *desmialis*: Swinhoe, 1906: 293.
Nagiella quadrimaculalis: Munroe, 1976: 876.
Pleuroptya quadrimaculalis: Inoue, 1982: 343.

Material examined. China, Gansu: 4 ♂♂, 3 ♀♀, Kangxian County, Baiyun Mountain, 1200 m, 3.VII.2018, leg. Xiao-Qiang Lu & Xi-Cui Du; Shanxi: 4 ♂♂, Lishanxiachuan Nature Reserve, 1560 m, 26.VII.2012, leg. Gui-Qing He; Shaanxi: 11 ♂♂, Ningshan County, Yangjuba Town, 1400 m, 4.VIII.2014, leg. Hai-Li Yu & Jiu-Yang Luo; 7 ♂♂, 8 ♀♀, Yang County, 3500 m, 15.VIII.2017, leg. Jian-Yue Qiu & Hao Xu; 7 ♂♂, 1 ♀, Taibai County, Huangbaiyuan, 1291 m, 16.VII.2018, leg. Qing-Ming Liu; Henan: 33 ♂♂, Neixiangbaotianman Nature Reserve, Luotiofeng, 1300 m, 8.VI.2017, leg. Jian-Yue Qiu & Hao Xu; Hubei: 28 ♂♂, 3 ♀, Dabie Mountain, Taohua Village, 590 m, 20.VII.2010, leg. Li-Jun Xu; 4 ♂♂, Luotian County, Qingguantai, 580 m, 1.VII.2014, leg. Jiu-Yang Luo; 11 ♂♂, Changyang County, Hejiaping, 800 m, 18.VI.2018, leg. Xiao-Qiang Lu & Xi-Cui Du; 4 ♂♂, Wufenghou River, 1100 m, 26, VII.2018, leg. Jian-Yue Qiu & Hao Xu; Hunan: 7 ♂♂, Shimen County, Huping Mountain, Dadongping, 1400 m, 8.VI.2017, leg. Jian-Yue Qiu & Hao Xu; 5 ♂♂, Sangzhi County, tianping Mountain, 1400 m, 15.VII.2018, leg. Jian-Yue Qiu & Hao Xu; 6 ♂♂, 2 ♀♀, Yizhang County, Mangshan Nature Reserve, 1000 m, 2.VIII.2018, leg. Jian-Yue Qiu & Hao Xu; Zhejiang: 10 ♂♂, Tianmu Mountain Nature Reserve, 400 m, 26–29.VII.2011, leg. Xiao-Bing Fu & Xi-Cui Du; 11 ♂♂, 3 ♀♀, Qingliang Mountain, Shunxiwu, 300 m, 18–21.V.2012, leg. Xiao-Bing Fu; Jiangxi: 1 ♂, 1 ♀, Jinggangshan City, Xiaoxidong, 625 m, 30.V.2011, leg. Jin-Wei Li; Chongqing: 18 ♂♂, 10 ♀♀, Jingfo Mountain Nature Reserve, 1700 m, 12.VII.2010, leg. Xi-Cui Du & Sheng-wen Shi; 10 ♂♂, Simian Mountain Nature Reserve, 1120 m, 19.VII. 2010, leg. Xi-Cui Du & Li-fang Song; 3 ♂♂, Simian Mountain Nature Reserve, 1200 m, 15–19. VII. 2012,

leg. Gui-Qing He & Li-Jun Xu; 13 ♂♂, 1 ♀, Chengkou County, Xingtian Village, 1300 m, 1.VII.2013, leg. Gui-Qing He & Li-Jun Xu; Sichuan: 4 ♂♂, 1 ♀, Luding County, Hailuogou, 3478 m, 4.VII.2012, leg. Jin-Wei Li; 19 ♂♂, Nanjiang County, Guangwu Mountain, 700 m, 3.VII.2013, leg. Gui-Qing He & Li-Jun Xu; 21 ♂♂, 14 ♀♀, Xuyong County, huagaoxi Nature Reserve, 621 m, 26–30.VIII.2013, leg. Dan Xu & Xue-Li Wei; 19 ♂♂, 3 ♀♀, An'zi River Nature Reserve, 1690 m, 4.VIII.2015, leg. Xi-Cui Du; Guizhou: 11 ♂♂, 1 ♀, Kuankuoshui Nature Reserve, 800 m, 10–17. VIII.2010, leg. Xi-Cui Du; 5 ♂♂, Libo County, An'xiang, 1345 m, 22.VII.2015, leg. Ji-Ping Wan; Yunnan: 1 ♂, 1 ♀, Ninglang County, Xichuan, 2400 m, 20.VII.2013, leg. Gui-Qing He; 19 ♂♂, 2 ♂♂, Malipo County, Daxichang, 1465 m, 7.VI.2015, leg. Man-Fei Tao; Dawei Mountain Nature Reserve, 2700 m, 27.V.2018, leg. Xiao-Qiang Lu & Xi-Cui Du; 10 ♂♂, Huanglian Mountain Nature Reserve, 900 m, 23.VI.2018, leg. Xiao-Qiang Lu & Xi-Cui Du; 15 ♂♂, 1 ♀, Xihuangbanna Prefecture, Menglun Town, 620 m, 17.V.2018, leg. Xiao-Qiang Lu & Xi-Cui Du; Guangdong: 27 ♂♂, 15 ♀♀, Nanlingbabao Mountain Nature Reserve, 1070 m, 22.VIII.2010, leg. Xi-Cui Du; 2 ♂♂, 1 ♀, Shixing County, Baling Nature Reserve, 496 m, 29.V.2017, leg. Yong-Hong Duan (SYSU); Guangxi: 22 ♂♂, Hechi City, Jiuwan Mountain, 1600 m, 26.VII.2015, leg. Ji-Ping Wan; 4 ♂♂, Guilin City, Maoer Mountain Nature Reserve, 1100 m, 23.VII.2015, leg. Kai-Li Liu & Jing-Xia Zhao; 9 ♂♂, Rongshui County, Peixiu Village, 1900 m, 24.VIII.2015, leg. Ji-Ping Wan; 12 ♂♂, Cenwanglao Mountain, Dalongping, 1290 m, 4.VIII.2014, leg. Xue-Li Wei & Chao Ran; Fujian: 8 ♂♂, Wuyi Mountain Nature Reserve, Tongmu Village, 758 m, 20.VIII.2016, leg. Kai Chen & Yong-Hong Duan (SYSU). Genitalia slide no.: XLJ13123 ♂, XLJ13158 ♂, XLJ13215 ♂, XLJ14029 ♂, XLJ14056 ♂, XLJ14075 ♂, XLJ14076 ♂, XLJ14133 ♂, XLJ14229 ♂, LXQ19304 ♂, LXQ19305 ♂, LXQ18308 ♂, LXQ18310 ♂, XLJ13124 ♀, XLJ13159 ♀, XLJ13216 ♀, XLJ114012 ♀, XLJ14030 ♀, LXQ18306 ♀.

Diagnosis. Adult (Fig. 6): Wings brown. Forewing length 12.0–20.0mm (wingspan 26.0–43.0 mm); a small white spot between the orbicular spot and discoidal spot; a large white sub-reniform spot between the discoidal spot and postmedial line, up to Rs_2+Rs_3 and down to CuA_1; antemedial and postmedial line unclear. Hindwing with a large white irregular quadrilateral spot between the discoidal spot and postmedial line, dentated between M_2 and M_3. Male genitalia (Fig. 11): Uncus trapezoidal. Gnathos slender, finger-like. Clasper thickly finger-like. Female genitalia (Fig. 14): Signum small, round.

Male genitalia (Fig. 11). Uncus trapezoidal. Gnathos slender, finger-like. Valva elongate lingulate, with apex narrowed, posterior margin with a cluster of long setae near the middle; clasper thickly finger-like. Saccus conical, broad. Juxta peach-shaped. Phallus longitudinally wrinkled distally.

Female genitalia (Fig. 14). Apophyses anteriores ca. twice the length of apophyses posteriores. Ductus bursae ca. twice the length of corpus bursae, distinctly narrowed near the base; ductus seminalis from approximately one third of the ductus bursae. Corpus bursae oval, with a small round signum.

Distribution. China (Heilongjiang, Liaoning, Gansu, Shanxi, Shaanxi, Henan, Hebei, Hubei, Shandong, Hunan, Zhejiang, Jiangxi, Tibet, Sichuan, Chongqing, Guizhou, Yunnan, Guangdong, Guangxi, Hainan, Fujian, Taiwan), Korea, Japan, Indonesia, India (Sikkim), Nepal, Russia (far east), Malaysia (Walker 1866; Inoue 1982; Du 2009).

Host. *Rhus chinensis* Mill (Anacardiaceae) (Fan and Piao 2013).

Remarks. In addition to *Rhus chinensis* Mill, another host, *Metaplexis japonica* Makino (Apocynaceae), was recorded by Fan and Piao (2013) in the same article according to Yoshiyasu (1991). However, we found *M. japonica* was recorded by Yoshiyasu (1991) as the host of *Glyphodes quadrimaculalis* (Bremer and Grey 1853) but not of *N. quadrimaculalis* (Kollar and Redtenbacher). *Rhus chinensis* Mill is the only host of *N. quadrimaculalis* (Kollar and Redtenbacher) known so far.

Swinhoe (1894) stated that *Nagia incomitata* was between *Nagia quadrimaculalis* and *N. flavispila*, but quite different to either. But *N. incomitata* was regarded as a synonym of *N. quadrimaculalis* because they were similar in habitus (Bae et al. 2008). We investigated the original description and type specimen of *N. incomitata* Swinhoe, 1894, and compared them with the description and photographs of *N. quadrimaculalis* (Kollar and Redtenbacher 1844; Du 2009; Sasaki and Yamanaka 2013). The third segment of labial palpus of the former is slender and pointed distally (Fig. 7A), the forewing has no small white spot between the orbicular spot and discoidal spot, and the large white spot beyond the cell is down to the CuA_2 (Fig. 7); while the third segment of labial palpus of the latter is stubby and blunt distally (Fig. 2), the forewing has a small white spot between the orbicular spot and discoidal spot, and the large white spot beyond the cell is down to the CuA_1 (Fig. 6). Therefore, *N. incomitata* is not a synonym of *N. quadrimaculalis*. *Nagia incomitata* was transferred to *Chalcidoptera* Butler, 1887 by Swinhoe (1901) after stating previously that it did not belong into *Nagia* (Swinhoe 1900). Hampson (1896), on the other hand, considered it a synonym of *Nosophora chironalis* (Walker, 1859), which he later revised (Hampson 1903) by reinstating it as *Nosophora incomitata*, with the junior synonym *Nosophora triguttalis* Warren, 1896. In the same publication on page 216, Hampson (1903) synonymised the males of *N. incomitata* with *Sylepta* [sic] *quadrimaculalis*. For the time being (i.e., until the type material has been investigated), we conclude as Hampson (1903), Klima (1939b), and Mandal and Bhattacharya (1980), who considered *incomitata* a species of *Nosophora*.

Nagiella occultalis Misbah & Yang in Ullah et al. 2017

Nagiella occultalis Misbah & Yang in Ullah et al. 2017: 70. Figs 2A, 3, 4A, B.

Note. Description of the habitus and genitalia was provided by Ullah et al. (2017).

Distribution. China (Shaanxi, Hubei) (Ullah et al. 2017).

***Nagiella bispina* sp. nov.**
http://zoobank.org/EA3EDE34-1DEA-4FA7-B5A9-70F596B3B2DE
Figures 8, 12, 15, 15A

Type material. ***Holotype.*** ♂, pinned, with genitalia on a separate slide. China, Guangdong: Nanling, Babao Mountain Nature Reserve, 24.98N, 113.03E, 1070 m, 23.VIII.2010, leg. Xi-Cui Du, genitalia slide no. XLJ14011 ♂. ***Paratypes.*** China, Guangdong: 1 ♂, 1 ♀, same data as holotype. Genitalia slide no.: XLJ14009 ♀, XLJ14134 ♂.

Diagnosis. This species is very similar to *N. quadrimaculalis* externally, but can be distinguished from the latter by its rather short and wide uncus with distal margin round, gnathos absent, clasper thick thorn-like, phallus with a hook-shaped cornutus; ductus bursae ca. the same length as corpus bursae with two thorn-like signa (Fig. 15A). In *N. quadrimaculalis*, the uncus is trapezoidal, gnathos is slender and finger-like, clasper is thickly finger-like, and phallus exhibits no cornuti; ductus bursae is ca. twice the length of corpus bursae and corpus bursae has a small round signum (Fig. 14).

Description. Adult (Fig. 8). Body brown tinged with copper-colour. Forewing length 11.5–13.5 mm (wingspan 26.0–30.0 mm). Frons, vertex, antenna and maxillary palpus brown. Male antenna with ventral cilia ca. half as long as the diameter of flagellomere. Labial palpus with first and second segments white ventrally, the rest brown. Thorax and abdomen brown dorsally, off-white ventrally. Legs off-white, fore tibia brown distally. Wings brown. Forewing with antemedial line excurved, unclear; orbicular spot and discoidal spot dark brown, the latter squarish; a small white spot between the orbicular spot and discoidal spot; a large white sub-reniform spot between the discoidal spot and postmedial line, up to Rs_2+Rs_3 and down to CuA_1; postmedial line unclear, from ca. 2/3 of the costa, along outer edge of the large white spot, excurved from M_2 to CuA_2, then incurved and nearly vertical to the inner margin below the posterior angle of cell; cilia lightly brown with white basal line. Hindwing with discoidal spot dark brown, short band; a large white irregular quadrilateral spot between the discoidal spot and postmedial line, dentated between M_2 and M_3; postmedial line unclear, along outer edge of the large white spot, lightly excurved from M_2 to CuA_2, then incurved and nearly vertical to the inner margin below the posterior angle of cell; cilia lightly brown with white basal line. Abdomen with each segment white distally.

Male genitalia (Fig. 12). Uncus rather short and wide, with distal margin round. Gnathos absent. Valva lingulate, slightly widened; clasper thick thorn-like, with a cluster of long setae at the base. Saccus conical. Juxta near diamond. Phallus with a thick hook-shaped cornutus.

Female genitalia (Fig. 15, 15A). Apophyses anteriores ca. twice the length of apophyses posteriores. Ductus bursae ca. the same length as corpus bursae, expanded and sclerotized near the middle; antrum slightly sclerotized; ductus seminalis from expanded part. Corpus bursae oval; two thorn-like signa of different sizes, surrounded by dense microspines.

Etymology. The specific name, *bispina*, is derived from the Latin *bi* (meaning two or double) and *spina* (meaning spine or thorn) in reference to the two thorn-like signa.

Distribution. China (Guangdong).

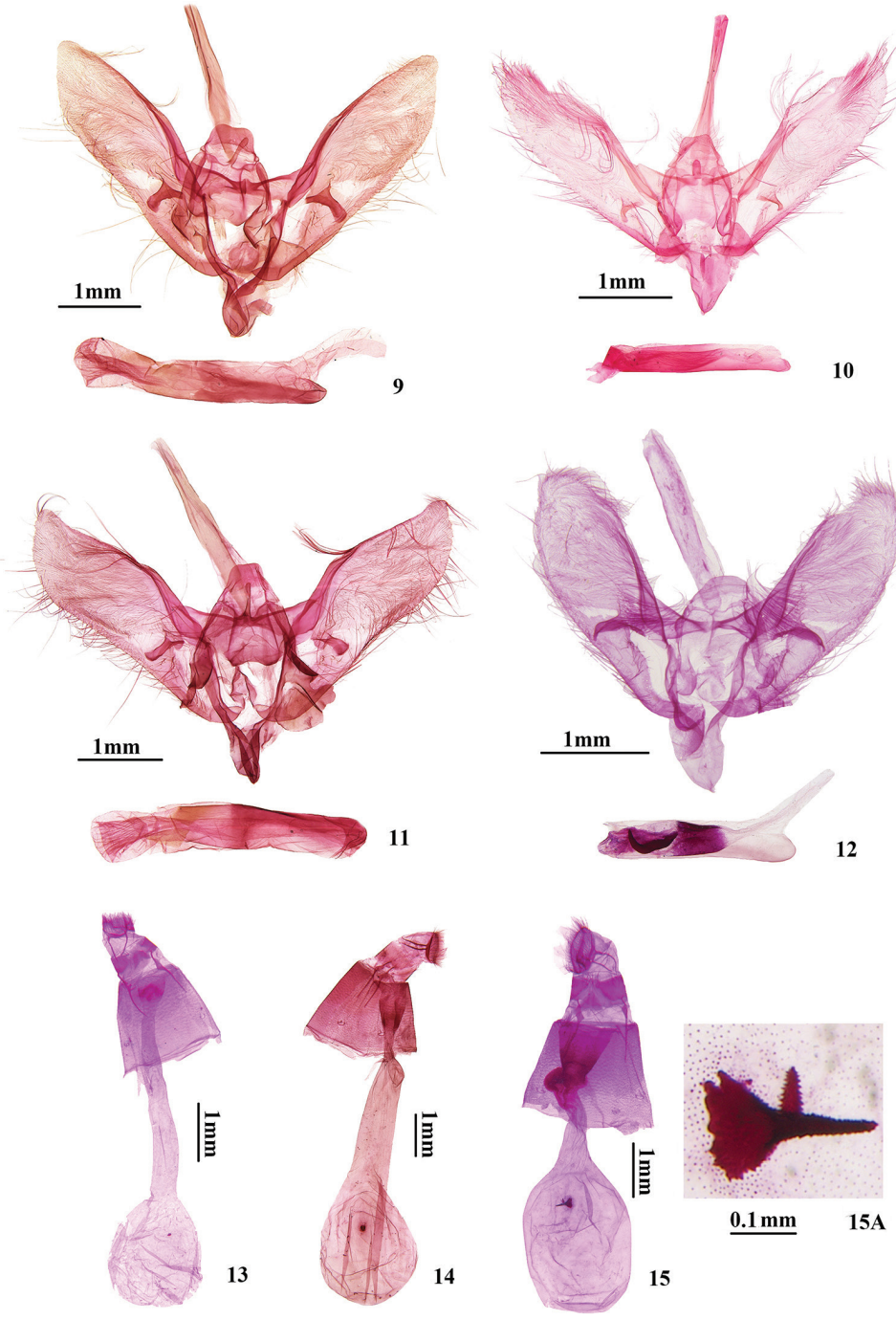

Figures 9–15. Genitalia of *Nagiella* species **9** *N. hortulatoides*: male, genitalia slide no. LXQ18311 **10, 13** *N. inferior*: **10** male, genitalia slide no. LXQ18291 **13** female, genitalia slide no. XLJ14239 **11, 14** *N. quadrimaculalis*: **11** male, genitalia slide no. LXQ18310 **14** female, genitalia slide no. LXQ18306 **12, 15** *N. bispina* sp. nov.: **12** male, holotype, genitalia slide no. XLJ14011 **15** female, paratype, slide no. XLJ14009 **15A** signa.

Acknowledgements

We are grateful to Li-Jun Xu and Dan Xu for their preliminary work on this genus. We are also grateful to Dr. Dan-Dan Zhang (School Of Life Science, Sun Yat-Sen University) for providing specimens, to the Institute of Zoology (Chinese Academy of Sciences, Beijing) for the loan of specimens, and to Geoff Martin (the Natural History Museum, London) for providing the corresponding author with access to examine specimens. Our sincere appreciation is given to Dr. Richard Mally (University Museum of Bergen, Norway) for his elaborative revision and instructive suggestions, and to Dr. Colin Plant for his important linguistic corrections for our manuscript. We also give our thanks to the anonymous Elsevier language editor for reviewing our manuscript. This study was funded by the National Natural Sciences Foundation of China (No. 31772500) and by Chongqing Research Program of Basic Research and Frontier Technology (No. cstc2018jcyjAX0544).

References

Bae YS, Byun BK, Paek MK (2008) Pyralid moths of Korea (Lepidoptera: Pyraloidea). Korea National Arboretum, Samsungad, Seoul, 426 pp.

Butler AG (1878) Illustrations of Typical Specimens of Lepidoptera Heterocera in the Collection of the British Museum. Printed by order of the Trustees, London, 62 pp. [20 pls.]

Butler AG (1887) Descriptions of new species of Heterocerous Lepidoptera (Pyralites) from the Solomon Islands. Annals and Magazine of Natural History, including Zoology, Botany and Geology, London (ser. 5) 20: 114–124. https://doi.org/10.1080/00222938709460019

Du XC (2009) Spilomelinae. In: Li HH, Ren YD, Zhang DD, Du XC, Li WC, You P (Eds) Insect fauna of Henan (Lepidoptera: Pyraloidea). Science Press, Beijing, 237–305. [359–363, 397–408, 433–440] https://doi.org/10.1080/00305316.2008.10417555

Fabricius JC (1798) Supplementum Entomologiae Systematicae. Proft et Storch, Hafniae. 572 pp. [1–52, emendanda.]

Fan LH, Piao MH (2013) Larval descriptions for four species in the genus *Pleuroptya* (Lepidoptera: Crambidae: Spilomelinae) from China, with notes on biology, Entomotaxonomia 35(1): 45–52.

Ghesquière J (1942) Catalogues raisonnés de la Faune Entomologique du Congo Belge. Lépidoptères, Microlépidoptères (deuxième partie). Annales du Musée Royal du Congo Belge (Sér. C – Zoologie), Tervuren (sér. 3 (2)) 7(2): 121–240. [pl. 6.]

Hajibabaei M, Janzen DH, Burns JM, Hallwachs W, Hebert PDN (2006) DNA barcodes distinguish species of tropical Lepidoptera. Proceedings of the National Academy of Sciences of the United States of America 4(103): 968–971. https://doi.org/10.1073/pnas.0510466103

Hampson GF (1896) Moths. The Fauna of British India, including Ceylon and Burma, London 4, 594 pp.

Hampson GF (1899) A revision of the moths of the subfamily Pyraustinae and family Pyralidae. Part I. Proceedings of the Zoological Society of London 1898 (4): 590–761. [pls 49–50.]

Hampson GF (1903) The moths of India. Supplementary paper to the volumes in "The fauna of British India." Series II. Part IX, X. The Journal of the Bombay Natural History Society 15: part IX: 19–37; part X: 206–226. [pl. C.]

Heppner JB (2012) Taiwan Lepidoptera Catalog. Supplement 1 corrections and additions. Lepidoptera Novae 5(1): 1–84.

Hübner J (1823) Zuträge zur Sammlung exotischer Schmettlinge [sic]: bestehend in Bekundigung einzelner Fliegmuster neuer oder rarer nichteuropäischer Gattungen. Augsburg, 1–40. [pls [36]–[69].]

Inoue H (1982) Pyralidae. In: Inoue H et al. (Eds) Moths of Japan. Kodansha, Tokyo, 1: 307–404, 2: 223–254.

Kimura M (1980) A simple method for estimating evolutionary rates of base substitutions through comparative studies of nucleotide sequences. Journal of Molecular Evolution 16: 111–120. https://doi.org/10.1007/BF01731581

Kirpichnikova VA (1987) Obsor roda *Pleuroptya* Meyr. (Lepidoptera, Pyralidae) fauny Dalnego Wostoka. In: Ler PA, Kirpichnikova VA, Kononenko VS (Eds) Lepidoptera of the Soviet Far East. Far East Scientific Centre, Vladivostok, 54–60. [126]

Kirti JS, Sodhi JS (2001) A systematic list of Pyraustinae of northeastern India (Pyralidae: Lepidoptera). Zoos' Print Journal 16(10): 607–614. https://doi.org/10.11609/JoTT.ZPJ.16.10.607-14

Klima A (1931) Pyralidae: Subfamily: Pyraustinae I. In: Bryk F (Eds) Lepidopterorum Catalogus. Dr. W. Junk, s' Gravenhage 89: 186–224.

Klima A (1939a) Pyralididae: Subfamily: Pyraustinae II. In: Bryk F (Eds) Lepidopterorum Catalogus. Dr. W. Junk, s' Gravenhage 94: 225–384. https://doi.org/10.5962/bhl.title.124016

Klima A (1939b) Pyralididae: Subfamily: Pyraustinae I. In: Bryk F (Eds) Lepidopterorum Catalogous. Dr. W. Junk, s' Gravenhage 89: 3–224. https://doi.org/10.5962/bhl.title.124016

Kollar V, Redtenbacher L (1844) Aufzählung und Beschreibung der von Freiherrn Carl v. Hügel auf seiner Reise durch Kaschmir und das Himaleyagebirge gesammelten Insecten. Hallbergersche Verlagshandlung, Stuttgart, 395–564.

Kumar S, Stecher G, Tamura K (2016) MEGA7: Molecular Evolutionary Genetics Analysis Version 7.0 for bigger datasets. Molecular Biology and Evolution 33(7): 1870–1874. https://doi.org/10.1093/molbev/msw054

Leraut PJA (1997) Liste systématique et synonymique des Lépidoptères de France, Belgique et Corse (deuxième édition). Alexanor, Paris, supplement: 7–526.

Li HH, Zheng ZM (1996) Methods and techniques of specimens of Microlepidoptera. Journal of Shaanxi Normal University (natural science edition) 24(3): 63–70.

Mally R, Hayden JE., Neinhuis C, Jordal BH, Nuss M (2019) The phylogenetic systematics of Spilomelinae and Pyraustinae (Lepidoptera: Pyraloidea: Crambidae) inferred from DNA and morphology. Senckenberg Gesellschaft fur Naturforschung 77(1): 141–204. https://doi.org/10.26049/ASP77-1-2019-07

Mandal DK, Bhattacharya DP (1980) On the Pyraustinae (Lepidoptera: Pyralidae) from the Andaman, Nicobar and Great Nicobar islands, Indian ocean. Records of the Zoological Survey of India 77: 293–342.

Meyrick E (1890) On the classification of the Pyralidina of the European fauna. Transactions of the Entomological Society of London: 429–492. https://doi.org/10.1111/j.1365-2311.1890.tb02704.x

Moore F (1888) Descriptions of new Indian lepidopterous insects from the collection of the late Mr. W.S. Atkinson. Heterocera (continued) (Pyralidae, Crambidae, Geometridae, Tortricidae, Tineidae). In: Hewitson WC, Moore F (Eds) Descriptions of new Indian Lepidopterous Insects from the Collection of the Late Mr. W.S. Atkinson 3. Asiatic Society of Bengal/ Taylor & Francis, Calcutta / London, 199–299. [pls 6–8.]

Motschulsky VI (1861) Insectes du Japon. Etudes entomologiques, réd. par Victor de Motschulsky, Helsingfors 9: 4–39.

Munroe EG (1976) New genera and species of Pyraustinae (Lepidoptera: Pyralidae), mainly from the collection of the British Museum (Natural History). The Canadian Entomologist 108: 873–884. https://doi.org/10.4039/Ent108873-8

Ratnasingham S, Hebert PDN (2007) BOLD: The Barcode of Life Data System (www.barcodinglife.org). Molecular Ecology Notes 7(3): 355–364. https://doi.org/10.1111/j.1471-8286.2007.01678.x

Rose HS (2002) An inventory of the moth fauna (Lepidoptera) of Jatinga, Assam, India. Zoos' Print Journal, India 17(2): 707–721. https://doi.org/10.11609/JoTT.ZPJ.17.2.707-21

Sasaki A, Yamanaka H (2013) Spilomelini. In: Nasu Y, Hirowatari T, Kishida Y (Eds) The Standard of Moths in Japan IV. Gakken Education Publishing, Tokyo, 74–84. [415–478.]

Shibuya J (1928) The systematic study on the formosan Pyralidae. Journal of the Faculty of Agriculture, Hokkaido Imperial University 22: 217–229.

Shibuya J (1929) On the known and unrecorded species of the Japanese Pyraustinae (Lepid.). Journal of the Faculty of Agriculture, Hokkaido Imperial Universitym 25: 182–183.

Snellen PCT (1890) A catalogue of the Pyralidina of Sikkim collected by Henry J. Elwes and the late Otto Möller, with notes by H. J. Elwes. Transactions of the Entomological Society of London: 557–647. [pls 19–20.] https://doi.org/10.1111/j.1365-2311.1890.tb03031.x

Stamatakis A, Hoover P, Rougemont J (2008) A rapid bootstrap algorithm for the RAxML Web Servers. Systematic Biology 57: 758–771. https://doi.org/10.1080/10635150802429642

Swinhoe C (1894) New Pyrales from the Khasia Hills. Annals and Magazine of Natural History, including Zoology, Botany and Geology, London (ser. 6) 14(81): 197–210. https://doi.org/10.1080/00222939408677791

Swinhoe C (1900) Noctuina, Geometrina and Pyralidina. In: Swinhoe C, Walsingham L, Durrant JH (Eds) Catalogue of eastern and Australian Lepidoptera Heterocera in the Collection of the Oxford University Museum. Part II. Clarendon Press, Oxford, 540 pp. [pls 1–8.]

Swinhoe C (1901) New genera and species of Eastern and Australian moths. Annals and Magazine of Natural History, including Zoology, Botany and Geology, London (ser. 7) 8: 16–27. https://doi.org/10.1080/03745480109443321

Swinhoe C (1906) New and little-known species of Heterocera from the East. Annals and Magazine of Natural History, including Zoology, Botany and Geology, London (ser. 7) 17: 283–297. [379–383.] https://doi.org/10.1080/00222930608562524

Ullah M, Yang ZF, Qiao PP, Zhang YL (2017) A new cryptic species of *Nagiella* Munroe from China revealed by DNA barcodes and morphological evidence (Lepidoptera, Crambidae, Spilomelinae). ZooKeys 679: 65–76. https://doi.org/10.3897/zookeys.679.11960

Walker F (1859) Pyralides. List of the Specimens of Lepidopterous Insects in the Collection of the British Museum, London 18: 509–798.

Walker F (1865) Supplement 4. List of the Specimens of Lepidopterous Insects in the Collection of the British Museum, London 34: 1121–1533.

Warren W (1896) New species of Pyralidae from the Khasia Hills. Annals and Magazine of Natural History, including Zoology, Botany and Geology, London (ser. 6) 18: 107–119. [163–177, 214–232.] https://doi.org/10.1080/00222939608680418

Wang HY, Speidel W (2000) Pyraloidea (Pyraloidea, Crambidae). Guide Book to Insects in TaiWan (19). Shu Shan Books, Taipei, 295 pp.

Wang PY (1980) Economic Insect Fauna of China (Lepidoptera: Pyralidae). Science Press, Beijing, 229 pp.

Yoshiyasu Y (1991) New host record and feeding habit *Glyphodes quadrimaculalis* (Lepidoptera, Pyralidae). Japanese Journal of Entomology 59(4): 1–774.

ZooKeys 964: 161–161 (2020)
doi: 10.3897/zookeys.964.57515
https://zookeys.pensoft.net

CORRIGENDA

A peer-reviewed open-access journal
ZooKeys
Launched to accelerate biodiversity research

Corrigendum: *Echinotermes biriba*, a new genus and species of soldierless termite from the Colombian and Peruvian Amazon (Termitidae, Apicotermitinae). ZooKeys 748: 21–30. https://doi.org/10.3897/zookeys.748.24253

Daniel Castro[1], Rudolf H. Scheffrahn[2], Tiago F. Carrijo[3]

1 *Instituto Amazónico de Investigaciones Científicas SINCHI, Avenida Vásquez Cobo Calles 15 y 16, Leticia, Amazonas, Colombia* **2** *Fort Lauderdale Research and Education Center, Institute for Food and Agricultural Sciences, University of Florida, 3205 College Avenue, Davie, Florida 33314, USA* **3** *Centro de Ciências Naturais e Humanas, Universidade Federal do ABC, Rua Arcturus 03, Jardim Antares, 09606-070, São Bernardo do Campo, SP, Brazil*

Corresponding author: Daniel Castro (danielkaz80@gmail.com)

Academic editor: E. Cancello | Received 11 August 2020 | Accepted 16 August 2020 | Published 27 August 2020

http://zoobank.org/AC0E63D8-B49C-4BF0-AF06-22BEA86901F2

Citation: Castro D, Scheffrahn RH, Carrijo TF (2020) Corrigendum: Echinotermes biriba, a new genus and species of soldierless termite from the Colombian and Peruvian Amazon (Termitidae: Apicotermitinae). ZooKeys 748: 21–30. https://doi.org/10.3897/zookeys.748.24253. ZooKeys 964: 161–161. https://doi.org/10.3897/zookeys.964.57515

Our recent description of *Echinotermes biriba* (Castro et al. 2018) does not clearly define the type repositories as we only give the acronyms "CATAC" and "UF". The holotype and paratype workers are deposited in the Colección de artrópodos terrestres de la Amazonía Colombiana of the SINCHI Institute in Leticia, Amazonas, Colombia (**CATAC**). Additional paratype workers are deposited in the University of Florida Termite Collection at Fort Lauderdale Research and Education Center, Davie, Florida, United States (**UF**).

References

Castro D, Scheffrahn, RH, Carrijo TF (2018) *Echinotermes biriba*, a new genus and species of soldierless termite from the Colombian and Peruvian Amazon (Termitidae, Apicotermitinae). ZooKeys 748: 21–30. https://doi.org/10.3897/zookeys.748.24253